

**THE ROLE OF THE ANDROGEN RECEPTOR PATHWAY IN
PROSTATE CANCER PROGRESSION**

Rute Marques

The research described in this thesis was performed in the Department of Urology of the Erasmus Medical Center and was financially supported by the Netherlands Organization for Scientific Research (NWO), through ZonMW grant 903-46-187.

The publication of this thesis was financially supported by (in alphabetical order):

5gfrUNYbYVW

BD Biosciences

Erasmus University Rotterdam

GlaxoSmithKline

Novartis Pharma Nederland

Sanofi-Aventis

Stichting Urologisch Wetenschappelijk Onderzoek (SUWO)

Stichting Wetenschappelijk Onderzoek Prostaatcancer (SWOP)

Cover and lay-out: R.B. Marques and Optima Grafische Communicatie

Printing: Optima Grafische Communicatie, Rotterdam

ISBN: 978-90-8559-555-7

© Copyright R.B. Marques, Rotterdam 2009

THE ROLE OF THE ANDROGEN RECEPTOR PATHWAY IN PROSTATE CANCER PROGRESSION

De rol van de androgeenreceptor cascade in de
progressie van prostaatkanker

Proefschrift

ter verkrijging van de graad van doctor aan de
Erasmus Universiteit Rotterdam
op gezag van de rector magnificus
Prof.dr. H.G. Schmidt
en volgens besluit van het College voor Promoties

De openbare verdediging zal plaatsvinden op
woensdag 2 september 2009
om 11.30 uur

door

Rute Barbosa Marques
geboren te Espinho, Portugal



PROMOTIECOMMISSIE

Promotor: Prof.dr. C.H. Bangma

Overige leden: Prof.dr.ir. J. Trapman
Dr. P.M.J.J. Berns
Dr. G. van der Pluijm

Copromotor: Dr.ir. G.W. Jenster

CONTENTS

| | page |
|--|------|
| List of abbreviations | |
| Chapter 1 - General introduction and scope of the thesis | 7 |
| 1.1. Introduction | 9 |
| 1.2. Normal prostate | 9 |
| 1.3. Prostate cancer development | 10 |
| 1.4. Prostate cancer diagnosis | 11 |
| 1.5. Prostate cancer therapy | 12 |
| 1.6. The AR pathway in normal prostate homeostasis | 13 |
| 1.7. The AR pathway in prostate cancer development and progression | 15 |
| 1.8. Model systems for prostate cancer investigation | 18 |
| 1.9. Scope of the thesis | 19 |
| 1.10. References | 21 |
| Chapter 2 - The human PC346 xenograft and cell line panel: a model system for prostate cancer progression | 27 |
| Chapter 3 - Androgen receptor modifications in prostate cancer cells upon long-term androgen ablation and antiandrogen treatment | 47 |
| Chapter 4 - Gene expression profile of the androgen receptor pathway in androgen-responsive versus hormone-refractory PC346 prostate cancer cells | 67 |
| Chapter 5 - Bypassing the androgen receptor pathway in PC346 hormone-refractory prostate cancer cells | 107 |
| Chapter 6 - General discussion | 157 |
| Summary | 179 |
| Samenvatting | 181 |
| Acknowledgements | 185 |
| Curriculum vitae | 187 |
| List of publication | 189 |

LIST OF ABBREVIATIONS

| | |
|--------------|--|
| ACSL3 | acyl-CoA synthetase long-chain family member 3 |
| AD | androgen-dependent |
| AI | androgen-independent |
| AR | androgen receptor |
| BCL2 | B-cell CLL/lymphoma 2 |
| BPH | benign prostatic hyperplasia |
| CGH | comparative genomic hybridization |
| DHT | dihydrotestosterone |
| DKK3 | dickkopf homolog 3 |
| DNA | deoxyribonucleic acid |
| EGF | epidermal growth factor |
| ENDOD1 | endonuclease domain containing 1 |
| ERG | v-ets erythroblastosis virus E26 oncogene homolog (avian) |
| ETV1 | ets variant 1 |
| FCS | fetal calf serum |
| FGF | fibroblast growth factor |
| GAPDH | glyceraldehyde 3-phosphate dehydrogenase |
| HGF | hepatocyte growth factor |
| HNPC | hormone-naïve prostate cancer |
| HRPC | hormone-refractory prostate cancer |
| IGF1 | Insulin-like growth factor 1 |
| IL6 | interleukin 6 (interferon, beta 2) |
| JAK/STAT | Janus kinase/ signal transducer and activator of transcription 1 |
| KGF | keratinocyte growth factor |
| MAPK | mitogen-activated protein kinase |
| MCCC2 | methylcrotonoyl-Coenzyme A carboxylase 2 |
| MTT | 3-(4,5-dimethylthiazol-2-yl)-2,5-diphenyltetrazoliumbromide |
| OH-flutamide | hydroxyflutamide |
| PAP | prostate acid phosphatase |
| PBGD | porphobilinogen deaminase |
| PI3K | phosphoinositide-3-kinase |
| PIN | prostatic intraepithelial neoplasia |
| PCa | prostate cancer |
| PCR | polymerase chain reaction |
| PSA | prostate specific antigen |
| PTEN | phosphatase and tensin homolog |
| R1881 | 17-methyltrienolone |
| RNA | ribonucleic acid |
| TMPRSS2 | transmembrane protease, serine 2 |
| TP53 | tumor protein p53 |
| TURP | transurethral resection of the prostate |
| TWIST1 | twist homolog 1 |
| VAV3 | vav 3 guanine nucleotide exchange factor |
| Wt | wild-type |

Chapter 1

**General Introduction and
Scope of the Thesis**

1.1. Introduction

Prostate adenocarcinoma is the most frequently diagnosed non-cutaneous male malignancy in the Western countries. In The Netherlands, 9516 men were diagnosed with prostate cancer in 2006, of which 1 out of 4 may die as a result of the disease [1]. If one considers the frequency of latent cancers estimated from autopsy studies, the numbers can be as high as 30% of men in their sixties, indicating that the prostate epithelial cells are particularly susceptible to malignant transformation [2]. Nevertheless, only a fraction of these latent tumors will eventually manifest itself clinically. At present, diagnosis of the disease at an early stage is essential for the successful eradication of the cancer, as no curative treatment exists for advanced metastasized tumors. However, the early detection of prostate tumors carries the risk of over-treating cancers that pose no threat to the patient, aggravated by the fact that these treatments often have severe side effects. Present challenges in prostate cancer research are the identification of prognostic markers that, at an early stage, can distinguish the indolent tumors from those that will progress and become life threatening, and the development of targeted therapies for advanced disease. To achieve this, a thorough knowledge of the intrinsic mechanisms for prostate cancer onset and progression is essential.

1.2. Normal prostate

The prostate is an exocrine male reproductive organ whose function is to produce prostatic fluid, rich in sugars, proteins and enzymes that make up 30% of the semen and regulate the liquidity of the ejaculate and the motility of the sperm. The normal human prostate is about 3 cm in diameter, has the shape of a chestnut and is located immediately below the bladder neck, surrounding the urethra. It can be divided into three anatomic regions: the transition zone, consisting of two pear-shaped lobes located peri-urethrally; the central zone, located behind the proximal prostatic urethra, surrounding the ejaculatory ducts; and the peripheral zone, which contains more than 70% of the normal prostate gland and envelopes the previous zones (Fig. 1) [3]. The peripheral and the transition zones have similar glandular structures composed of small, round acini embedded in a loose stroma with randomly oriented smooth muscle fibers. However, the transitional zone has a more compact stroma and is the site of origin of benign prostatic hyperplasia (BPH), whereas the peripheral zone is more prone to malignant transformation. The central zone has a different embryonic origin than the other two zones, and unlike those, it has large irregular acini with extensive intraluminal folds and a dense stromal compartment. The acini and ducts of the glandular tissue are lined by a double layer of epithelial cells [4]. The luminal secretory cells of the inner layer have a cuboidal shape and produce a variety of proteins and enzymes, such as prostate acid phosphatase (PAP) and prostate specific antigen (PSA), which are released into the seminal fluid [5]. A continuous outer layer of flattened non-secretory basal cells separates the epithelium from the basement membrane. Neuroendocrine cells can also be found, scattered throughout the glands, mostly in or just above the basal cell layer. Although the exact function of the basal cell compartment is not clear, it is thought to harbor a stem cell population responsible for the renewal of the basal, luminal and the neuroendocrine cells [6,7]. Other investigators argue that basal cells have ultrastructural features of active differentiated cells and produce enzymes capable of converting

adrenal steroid precursors into active androgens, suggesting a regulatory role on the maintenance of the luminal compartment [8,9]. But while the biological function of the basal cell layer is uncertain, its value in the diagnosis of prostate cancer is unquestionable, as the progressive loss of the basal epithelial cells is a histological marker for malignant transformation of the gland [10,11].

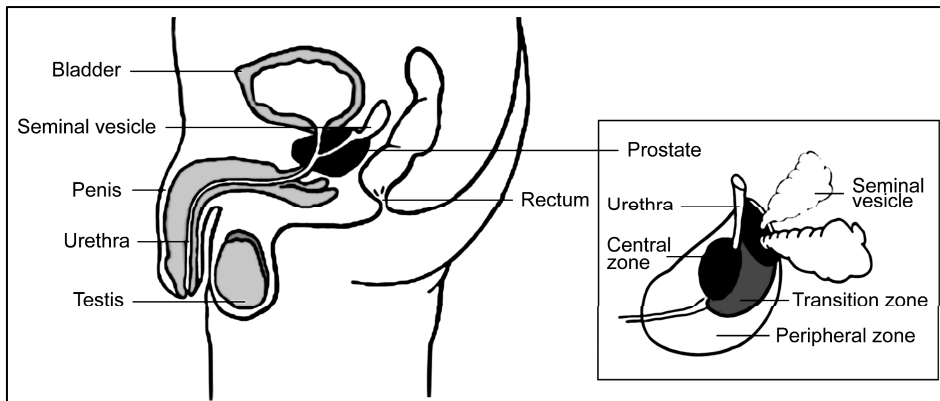


Figure 1 - Schematic representation of the prostate anatomy. The prostate is a chestnut shaped gland located immediately below the bladder neck, and can be divided into three anatomic regions: the transitional zone, the central zone and the peripheral zone.

1.3. Prostate cancer development

The origin of prostate cancer is still the subject of intense research. In 1996, Bonkhoff *et al.* suggested that the basal cells, being the compartment with the highest proliferative activity, were the most likely to suffer malignant transformation [12]. The authors proposed the stem cell model for prostate cancer pathogenesis, which postulates the existence of an androgen-independent stem cell population within the basal cell compartment. This stem cell population would be the source of prostate cancer, the proliferating cells then partly differentiating into secretory luminal cells and neuroendocrine cells, giving rise to all the cell lineages observed in prostate tumors [12,13]. The alternative hypothesis is that the luminal epithelial cells are the origin of prostate cancer. This hypothesis is based on the observations that (i) the basal cell compartment is absent in prostate adenocarcinomas [10,11]; (ii) unlike basal cells, most prostate tumor cells express androgen-receptor (AR), PAP and PSA [14]; and (iii) under certain conditions, luminal cells are also capable of self-renewal [15].

The oncogenic events that underlie prostate cancer development are matter of extensive investigation. It has been estimated that the accumulation of roughly a half-dozen independent genetic aberrations are necessary for the gradual progression from benign gland to malignant tumors [16,17]. Prostate cancer progression can be divided in five stages: pre-malignant, locally confined, infiltrating, metastatic and hormone-refractory disease. High-grade prostatic intraepithelial neoplasia (PIN) is widely assumed as the precursor lesion of locally confined prostate cancer. Much evidence

corroborates this theory: (i) PIN can be found in men early in their fifties, thus preceding the onset of cancer; (ii) its incidence increases with age; (iii) like prostate tumors, it is preferentially located in the peripheral zone of the prostate and, (iv) it is often found in close proximity with invasive carcinoma [18]. Furthermore, high-grade PIN shows many morphological and genetic aberrations found in locally confined disease. High-grade PIN is characterized by a cellular proliferation within the prostatic ducts and acini, with these cells presenting a large nucleus, prominent nucleoli and increased cytoplasmatic density. The basal cell layer may be disrupted and fragmented, but the benign architecture of the gland is still preserved [18]. Organ-confined prostate cancer is characterized by the complete absence of the basal cell layer, with the tumor growth invading the adjacent stroma but without penetrating through the prostatic capsule. In locally advanced cancer, the tumor penetrates the capsule and infiltrates surrounding tissues, such as the seminal vesicles, rectum or the bladder neck [19]. Tumors that transgress the prostatic boundaries are more aggressive and likely to progress into metastatic disease [20]. Besides local and distant lymph-nodes, the most common sites of prostate cancer metastasis are the bone, lung and liver [21]. At this stage, patients are offered systemic hormonal-therapy, but despite an initial improvement, these tumors eventually become resistant to therapy and recur as hormone-refractory disease. Hormonal-therapy and the mechanisms of hormone-refractory growth will be discussed below.

1.4. Prostate cancer diagnosis

Until 15 years ago prostate cancer was frequently detected at an advanced stage of the disease, when the patient presented himself to the physician with lower urinary tract symptoms, micturation problems and/or metastasis related complains. At that time, palpation via digital rectal examination (DRE) was the only method to examine the prostatic gland. Nowadays, DRE by itself is considered to be a rather ineffective tool as it is limited to bigger palpable tumors, which border the rectal wall. The introduction of transrectal ultrasonography (TRUS) has allowed for the visualization of the entire prostate gland and for the detection of impalpable tumors. However, by far not all prostatic adenocarcinomas are visible by ultrasonography and this technique is mainly used for measuring the volume of the prostate and for guiding needle biopsies [22]. In the mid 1980s, a test changed the course of prostate cancer history: the measurement of serum concentration of PSA [23,24]. PSA is a protein produced almost exclusively by the luminal epithelial cells of the prostate. Aberrations in the glandular architecture at the tumor site leads to leakage of PSA, which eventually enters the blood stream through diffusion. The serum PSA test allows for the detection of prostate tumors at very early stages, and since its introduction it has resulted in a dramatic increase in the documented incidence of prostate adenocarcinoma worldwide. In addition to its use in the detection of prostate cancer, the PSA test is also used in the follow up of tumor recurrences in patients who underwent therapy. However, increased serum concentrations of PSA are not specific for prostate cancer. Basically, any abnormality of the prostate gland, such as benign prostatic hyperplasia (BPH), infection/inflammation (prostatitis), as well as ageing, can lead to an increase in PSA. Due to the lack of specificity of PSA screening, many patients undergo unnecessary biopsies or treatment

for indolent tumors [24,25,26]. Furthermore, the reference serum PSA cutoff of 4 ng/ml fails to detect about 20% of high-grade prostate tumors, but lowering this cutoff to 3 ng/ml could result in a negative biopsy rates as high as 70% to 80%. In 2005, the Prostate Cancer Prevention Trial concluded that there is no PSA cutoff that retains simultaneously high sensitivity and specificity [27]. In an attempt to enhance the diagnostic and prognostic potential of PSA, multiple adaptations of the PSA test have been developed. These include measurements of PSA density (PSA level divided by the volume of the prostate), PSA velocity (rate at which PSA increases over time) and free/total PSA (percentage of free PSA in relation to PSA bound to serum proteins). Finally, to differentiate cancer from other prostate disorders, PSA testing must be combined with physical examination [28]. Upon an increased PSA value and/or suspicious DRE, the final diagnosis will always be established by histological examination of needle biopsies.

Due to the limitations of PSA tests and to the invasive nature of the needle biopsy procedure, the development of novel diagnostic and prognostic markers for prostate cancer has become an urgent and challenging enterprise. Recently, α -methylacyl-CoA racemase (AMACR), kallikrein 2 (KLK2), annexin 3, hepsin, prostate cancer antigen 3 (PCA3/DD3), early prostate cancer antigen (ECPA), TMPRSS2:ERG/ETV1 gene fusions, urokinase plasminogen activator and receptor (uPA/uPAR), among others, have emerged as candidate biomarkers [28,29]. Independent large-scale trials still have to prove whether or which of these markers can be applied clinically in the detection and management of prostate cancer.

1.5. Prostate cancer hormonal therapy

The detection of prostate cancer at early stages of the disease allows for a curative treatment of these patients. There are three main options for organ-confined disease: active surveillance, radical prostatectomy and radiotherapy. When choosing the treatment modality, the clinician must take into account the life expectancy of the patient, the characteristics of the tumor and the side effects of the treatment on the quality of life of the patient. In this perspective, an eighty-year old man, with an indolent tumor and limited life expectancy, is preferentially directed into a clinical surveillance program, whereas a sixty-year old patient with clinically localized disease is more likely to receive curative therapy.

Unfortunately, if regional or distant metastasis are present, the cancer is no longer curable and only palliative treatment may be offered [23]. Since, in 1941, Charles Huggins and his team first discovered that castration inhibited the growth of prostate tumors, androgen ablation became the mainstay therapy for advanced disease [30]. Hormonal therapy for prostate cancer consists of the surgical or pharmacological castration of the patient, by bilateral orchidectomy or administration of LHRH agonists, respectively, both leading to a decrease in testosterone production [31]. However, these approaches do not inhibit the production of adrenal androgens or *de novo* steroidogenesis by the tumor cells themselves. The novel drug abiraterone is a inhibitor of CYP17A1, a key enzyme in the biosynthesis of androgens [32]. In phase I and II clinical trials, abiraterone was capable of reducing testosterone production bellow castration levels and showed strong antitumor activity, which is now being evaluated in

phase III trials. Antiandrogens supplementation is often given to prevent an initial testosterone flare, associated with the commencement of LHRH therapy [33]. Furthermore, antiandrogens are also used to block the effect of adrenal androgens, which in the absence of testosterone may play a role in activating the androgen receptor [33]. Most common antiandrogens used in the treatment of advanced prostate cancer are flutamide, bicalutamide, nilutamide and cyproterone acetate [33,34]. Unfortunately, although the great majority of the patients will respond well to the hormonal therapy, these tumors will eventually recur as hormone-refractory disease within 1-3 years [35,36]. This condition has a very poor prognosis with a median survival time of 5-10 months. Recently, a new generation of antiandrogenic drugs, RD162 and MDV3100, showed promising results in second-line treatment of castration-resistant tumors and are entering phase III trials [37].

1.6. The AR pathway in normal prostate homeostasis

Androgens are also known as the male sex hormones, as they play a central role in the development of the male phenotype during fetal life and puberty, and control male fertility and sexual behavior in adults. Testosterone and 5 α -dihydrotestosterone (DHT) are essential for the normal development and maintenance of the prostate. Prostate organogenesis initiates at around 10 weeks of gestation and is strictly dependent on androgens, as the outgrowth of the prostatic buds from the urogenital sinus and differentiation of prostatic epithelium will not occur in the absence of androgens. During puberty, testosterone production by the Leydig cells of the testis is switched on, driving the final growth and maturation of the adult prostate. In adult life, androgens remain essential for the maintenance of prostate structure and function, while androgen ablation leads to prostate involution and preferential loss of luminal epithelial cells [38,39].

The actions of androgens are mediated by the AR, a transcription factor of the steroid receptor family. The AR gene is located on the X chromosome at q11.2-q12, spans almost 100 Kb and contains 8 exons that encode a protein with an apparent molecular mass of 110-114 kDa. The structure of the androgen receptor, which is conserved over the other members of the steroid receptors family, is typically divided in three functional domains (Fig. 2) [40,41,42]. The N-terminal domain (NTD), the largest domain of the AR, is encoded by exon 1 and contains the transactivation function of the receptor. The DNA-binding domain (DBD) is responsible for the sequence specific interaction of the receptor with DNA. It is encoded by exons 2 and 3 and also contains sequences involved in AR homodimerization. The ligand-binding domain (LBD), which is encoded by exons 4 to 8, contains the androgen binding function and also plays a role in receptor dimerization [43]. Curiously, truncation of the LBD results in a constitutively active receptor [44]. The DBD and the LBD are linked by a stretch of about 50 amino acids, called the hinge-region. The nuclear localization signal (NLS) that targets the nuclear translocation of the receptor is located in this region.

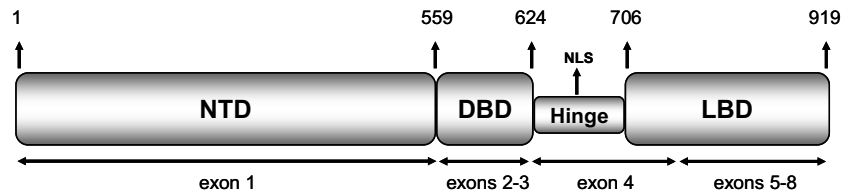


Figure 2 - Schematic representation of the androgen receptor structure. The AR is composed of three functional domains: the N-terminal domain (NTD), the DNA-binding domain (DBD) and the ligand-binding domain (LBD). A nuclear localization signal (NLS), located in the hinge region, targets nuclear translocation upon hormone binding. Amino acid and exon numbering are indicated above and under, respectively.

The AR is highly expressed in the luminal layer of glandular epithelia of male accessory sex organs, breast and skin, and surrounding smooth muscle, fibroblasts and accepted model for the intracellular action mesenchymal stromal cells. Other AR expressing tissues include skeletal muscle, vascular endothelium, brain, bone and hair follicles [45]. Consequently, these are also the tissues primarily affected by alterations in AR signaling, which associate with impairments in male virilisation and fertility, spinal and bulbar muscular atrophy, osteoporosis, acne, hair loss (alopecia) and cardiovascular disease [46]. The currently accepted model for the intracellular actions of androgens in the prostate is depicted in Figure 3.

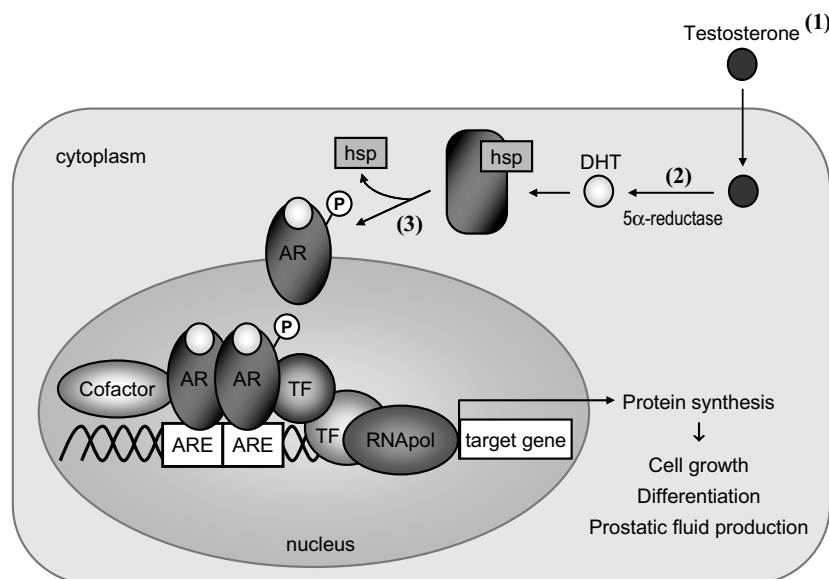


Figure 3 - The AR signaling pathway in the prostate. Sites of therapeutical intervention practiced currently are marked with numbers: (1) chemical/surgical castration can be used to reduce the levels of circulating testosterone; (2) conversion of testosterone to its fully active metabolite DHT can be targeted with inhibitors of 5 α -reductase enzyme; (3) AR antagonists can be used to compete with DHT and testosterone for binding to the AR. TF: transcription factors. RNA pol: RNA polymerase; ARE: androgen response elements; hsp: heat-shock proteins.

Testosterone is synthesized in the testis under the control of luteinizing hormone (LH) from the pituitary. It enters the target cells by diffusion and, in the cytoplasm of some cell types, is converted by 5 α -reductases to the more potent metabolite DHT. Upon AR binding, the receptor will undergo a conformational change, dissociate from chaperone heat-shock proteins and translocate to the nucleus. The active form of the receptor then binds as a homodimer to specific Androgen Response Elements (AREs) in the promoters/enhancers of target genes. Here, the AR interacts with specific nuclear cofactors, including co-activators or co-repressors, and the general transcription machinery, regulating expression of genes involved in the proliferation, differentiation and maintenance of the prostate [43,47,48]. The expression pattern of androgen-regulated genes is cell-type specific and changes with the developmental stage. During embryonic development androgens induce the expression of growth factors in mesenchymal stroma cells, which in turn indirectly stimulate the proliferation of prostatic epithelial cells that do not yet express the AR. In the adult prostate, secretory luminal cells, as well as the stromal cells, do express the AR, but at this stage the role of androgens is no longer to promote growth but rather to maintain the structure, differentiation state and secretory function of the gland [38]. In adult prostatic luminal cells, androgens regulate the expression of genes involved in the production and secretion of the components of prostatic fluid. These include genes encoding secreted proteins, such as PAP and PSA, but also genes involved in the metabolism of proteins, steroids, lipids and polyamines [49]. Furthermore, androgens inhibit epithelial cell death, since castration results in prostatic involution and nearly complete loss of these cells through apoptosis. Besides their role in normal prostate development and homeostasis, androgens may also fuel the growth of prostate tumors. The first indication that prostate adenocarcinomas were androgen-dependent came from Huggins *et al.* over six decades ago [30]. In a revolutionary experiment, the authors showed that prostate tumors shrank upon castration, setting the basis for hormonal therapy.

1.7. The AR pathway in prostate cancer development and progression

Only in atypical situations will androgens stimulate proliferation of adult prostatic epithelial cells, for instance during regeneration after castration/injury or in the case of malignant transformed cells. The fact that androgens stimulate the proliferation of prostate cancer epithelial cells has puzzled investigators for decades. The recent discovery that over 60% of the prostate tumors harbor a fusion between the TMPRSS2 gene and an ETS gene family member has shed light into this enigma [50]. TMPRSS2 is an androgen-regulated gene expressed in normal and malignant prostate epithelial cells, whereas ETS family members are transcription factors that regulate expression of growth and development related genes. ETS factors are normally not expressed in prostate epithelial cells, but fusions with 5' untranslated region of the TMPRSS2 gene provide androgen-responsive promotor/enhancer elements that drive robust expression of these potential oncogenes. In fact, the ETS factor most frequently fused in prostate cancer is the ERG oncogene, which is also involved in chromosomal translocations in Ewing sarcoma, myeloid leukemia and cervical carcinoma [51,52,53]. Up to date, fusions with ERG, ETV1, ETV4 and ETV5 factors have been detected in prostate cancer but TMPRSS2:ERG gene fusions are by far the most common, perhaps because both

genes are located in the same orientation within the same chromosomal locus (21q22.3) [54,55]. Following the discovery of TMPRSS2, additional 5' fusion partners have been identified, including SLC45A3, ACSL3, HERV-K_22q11.3, HNRPA2B1, C15orf21, KLK2, CANT1, FLJ35294 and DDX5, most of which are prostate-specific and androgen-regulated [55,56,57]. These findings suggest that deregulation of ETS oncogenes through fusions with androgen-responsive genes may be a possible explanation for the androgen-regulated growth of prostate adenocarcinomas. However, the biological role of aberrant ETS factors expression is still controversial, since prostate specific expression of ERG or ETV1 in mice induced PIN but not cancer [56,58]. Furthermore, *in vitro* overexpression of these proto-oncogenes did not affect proliferation but promoted cell migration and invasion. Finally, recent studies have shown that aberrant ERG expression cooperated with PTEN loss to promote progression from PIN to invasive adenocarcinomas, setting another piece in this puzzle [59,60,61].

Androgen ablation therapy of patients with disseminated disease offers no more than a temporary tumor remission and relieve of the symptoms, as the cancer will eventually become resistant and relapse. Theoretically, androgen-dependent prostate cancer cells have two possible mechanisms for surviving and growing under androgen-depleted conditions: to sensitize the AR pathway to the low androgen concentrations or to bypass the AR pathway by invoking alternative survival and growth pathways (Fig. 4) [62].

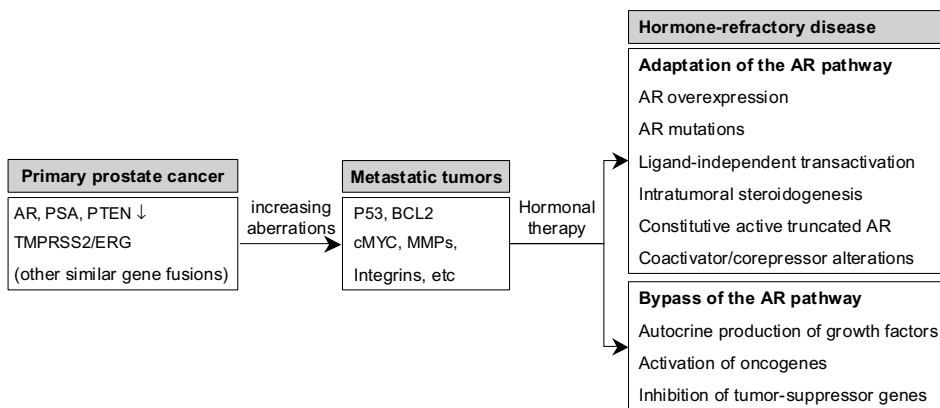


Figure 4 - The AR pathway in prostate cancer progression. Two strategies to overcome hormonal therapy: to adapt the AR pathway or to invoke alternative survival and growth pathways

Immunohistochemical analysis of prostate biopsies showed that the great majority of the androgen-independent cancers express the AR, often at higher levels than in primary tumors [63,64,65]. This observation suggests that the AR pathway may still be functionally active in hormone-refractory disease. AR gene amplification is observed approximately 30% of the hormone-refractory tumors and has been proposed to confer a growth advantage under androgen ablation conditions [65,66,67]. Other

modifications of the AR pathway that may induce hormone-refractory growth include activating AR mutations, intratumoral steroidogenesis, ligand-independent activation by cross-talk with other signaling pathway, constitutively active AR isoforms and alterations in AR co-regulators [62,68,69]. Many AR mutations have been discovered in prostate cancer that alter ligand specificity and receptor activity, the most widely known and intensely studied being the T877A mutation [70]. This mutation results in a threonine to alanine substitution in the ligand-binding domain of the AR, enabling receptor binding and activation by numerous non-androgenic compounds, including AR antagonists such as flutamide or cyproterone acetate [71]. This and similar AR mutations are relatively rare in hormone-naïve disease, but its frequency is much increased in recurrent tumors after hormonal therapy [72,73,74]. Also, two mutations (E231G and K580R) were recently identified that lead to increased AR basal activity and by itself were enough to produce prostate cancer in transgenic mouse models, implicating the AR as a potential oncogene [75,76]. A growing list of AR mutations is available in the AR Mutation Database (<http://www2.mcgill.ca/androgendb/>) [77]. Recent reports suggest that prostate tumors may be able to synthesize androgens *de novo* and/or to convert adrenal steroids into testosterone and DHT [78,79]. These studies showed an increased expression of steroidogenic enzymes, associated with elevated intratumoral androgen levels, in hormone-refractory metastasis. In this manner, local androgen production by prostate cancer cells may permit tumors to circumvent the depletion of circulating androgens. Cumulative evidence shows that the AR may also be activated in the absence of androgenic ligands, by cross-talk with Ras/MAPK, PI3/AKT and JAK/STAT pathways [80,81]. Activation of these pathways by numerous signaling factors, such as IL6, IGF1, KGF or EGF, can induce AR phosphorylation, consequent homodimerization, nuclear translocation and stimulation of AR target genes (Fig. 5A) [82]. Another potential mechanism for maintaining the AR pathway in the absence of ligand is the expression of constitutively active AR isoforms, lacking the C-terminal LBD domain. These constitutively active isoforms may arise from alternative splicing variants, truncating mutations or proteolytic cleavage, all of which have been recently detected in hormone-refractory samples [83,84,85]. The control of AR function also involves interaction of the receptor with a number of co-factors that regulate AR transcriptional activity. Alterations in ARA55, ARA70, SRC1 or TIF2 co-activators, as well as NCOR1 and NCOR2 co-repressors, among others, have been described in hormone-refractory disease [86,87]. However, these reports are often conflicting and further studies are necessary to elucidate the precise role of AR coregulators in prostate cancer progression. The mechanisms of AR pathway adaptation during prostate cancer progression will be further discussed in Chapters 3 and 4.

As an alternative to adapt the AR pathway, tumor cells may become truly androgen-independent, escaping the demand for androgens and an active receptor. To effectively bypass the AR pathway, cancer epithelial cells must be able to survive the apoptotic signals triggered by androgen ablation and invoke alternative growth pathways. This may be achieved by autocrine production of growth factors or its receptors, by activation of oncogenes and/or by deactivation of tumor suppressor genes.

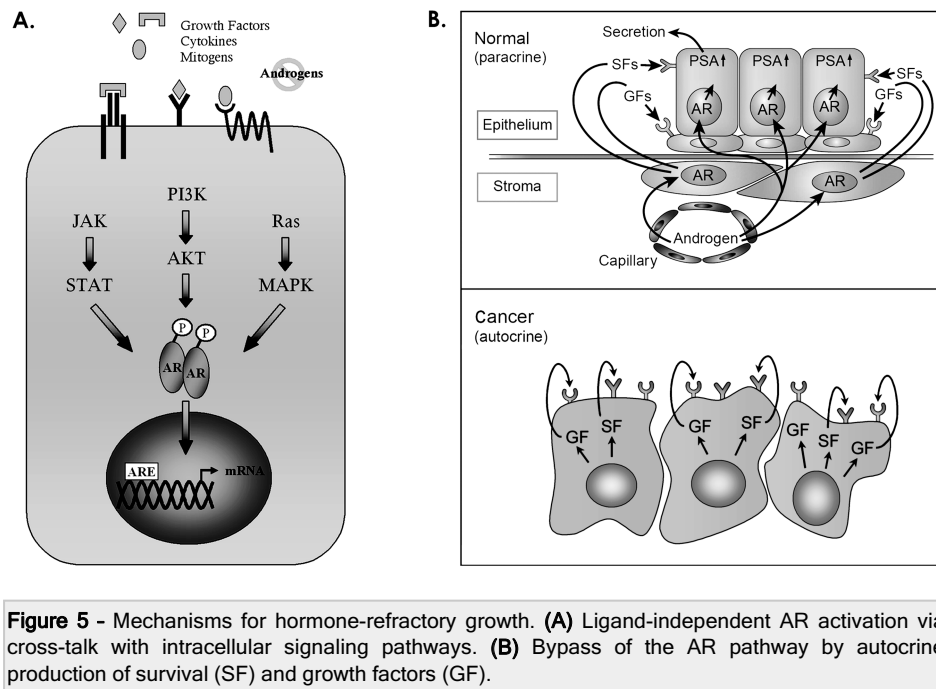


Figure 5 - Mechanisms for hormone-refractory growth. **(A)** Ligand-independent AR activation via cross-talk with intracellular signaling pathways. **(B)** Bypass of the AR pathway by autocrine production of survival (SF) and growth factors (GF).

Programmed cell death (apoptosis) and cell division are part of cell renewal and differentiation in benign cells. But the balance between these two processes is shifted during prostate malignancy (and other cancers) towards cell growth and proliferation. The cell cycle regulators MYC, RB and EZH2, as well as key regulators of apoptosis, such as TP53, PTEN (pro-apoptotic) or BCL2 (anti-apoptotic), have all been reported to be deregulated in prostate cancer [88,89]. Survival and growth of prostate epithelial cells are also regulated in paracrine manner by soluble factors secreted by stromal cells in response to androgens, including IGF1, KGF, FGF family members, EGF, HGF, TGF β , IL6, among others [90]. A switch to autocrine production of these growth factors by epithelial cells may be a potential mechanism to circumvent AR signaling (Fig. 5B). Chapter 5 of this thesis will address the various means to bypass the AR pathway.

1.8. Model systems in prostate cancer investigation

To investigate the mechanisms whereby prostate cancer develops and progresses, identify disease markers and potential therapeutical targets or to test novel drugs, the use of prostate cancer model systems is essential for basic research. The ideal model would reproduce the characteristics of the different stages of prostate cancer in humans, from initiation to metastasis, including hormone-refractory disease. But in practice, this ideal model system does not exist and researchers must meticulously choose, from the available human and animal derived systems, the model that best suits the particular question addressed. Animal model systems include transgenic and knockout mice,

hormonally/carcinogenically induced prostate cancer in rats and spontaneous prostate cancer in dogs. These model systems have the advantages of allowing the study of the initiation events in prostate carcinogenesis and the testing of (dietary) prevention programs. Eventually, the results of animal models must be extrapolated and validated in human derived systems, such as mouse xenografts or *in vitro* cell lines. In the xenograft models, human prostate tissue is transplanted and propagated in immune-deficient mice. These systems allow the maintenance of human prostate tumors *in vivo*, being particularly suitable for the study of tumor progression, biomarker identification and the testing of novel therapies. The major limitation of human model systems (xenografts and cell lines) is that these are derived from established prostate tumors and, therefore, cannot replicate prostate cancer initiation. *In vitro* cell line cultures offer unlimited sample amounts and extra experimental flexibility, being used for long-term hormonal manipulations and in the basal research of oncogenes, tumor suppressor genes and signaling pathways. Due to the technical difficulties in establishing permanent *in vitro* cultures of human prostate carcinomas, the number of cell lines available is very limited and the vast majority of the *in vitro* studies are based on the three cell lines and its derivatives: LNCaP, PC3 and DU145. Although undoubtedly valuable, these “classical” cell lines have serious limitations: the LNCaP cell line used as prototype for androgen-responsive disease, expresses a mutated (T877A) AR, showing altered hormone response properties; whereas PC3 and DU145, unlike most prostate tumors, do not express AR or PSA [71,91]. Therefore, in our laboratory added efforts were set into the generation of xenograft and *in vitro* cell lines representing different disease stages, among which the PC346 model used in this manuscript. A review of currently available human prostate cancer cell lines and xenografts is presented in Chapter 2.

1.9. Scope of the thesis

Activation of the AR by androgens is responsible for the normal development and maintenance of the prostate but also sustains its malignant outgrowth. Whether the AR pathway is still driving prostate cancer survival and growth in patients under androgen blockade is a clinically relevant issue. With this project we seek for a better understanding of the involvement of the AR pathway in the progression of androgen-dependent prostate cancer into androgen-independence. It is our hypothesis that androgen-dependent tumors have two possible strategies for growing in a low-androgen environment: to sensitize the AR pathway to the lowered androgen concentrations and/or to bypass the AR pathway by invoking alternative survival and growth pathways.

To assess our hypothesis we made use of an *in vitro* panel of human prostate cancer cell lines, the PC346 progression model. PC346C, PC346DCC, PC346Flu1 and PC346Flu2 are a panel of prostate cancer cell lines derived from the transurethral resection of the prostate of a non-progressive patient. The PC346C cell line was directly produced from the PC346P xenograft. The other mentioned cell lines were derived from the parental PC346C by long-term culture on androgen-depleted medium (PC346DCC) or in androgen-depleted medium supplemented with hydroxyflutamide (PC346Flu1 and PC346Flu2). Chapter 2 summarizes the establishment and characterization of the

PC346 progression model and compares it to other available human prostate cancer cell lines and xenografts.

The first aim of this study was to assess whether the *in vitro* long-term hormone depletion would select for modifications in the AR pathway and how these modifications could affect cell growth and androgen response. To characterize the AR status, cell growth and hormone-responsiveness of the PC346 cell lines, the AR was sequenced and quantified, its activity determined by reporter assays, and hormone-responsiveness was assessed by growth assays upon stimulation with androgens and antiandrogens. This work is described in Chapter 3, where we address how changes in the AR pathway may result in an adaptive advantage for progression of prostate tumors. Furthermore, we show that the cell lines developed for this project are a representative model system to investigate the role of AR signaling in prostate cancer progression.

In Chapter 4 we focus on the hypothesis that prostate cancer cells achieve androgen-independence by adapting their AR pathway to the androgen-depleted conditions. We used microarray technology to compare the expression pattern of androgen-regulated genes between the androgen-responsive and androgen-independent PC346 cell lines, in an attempt to: (i) establish the gene expression program regulated by the AR in these cell lines; (ii) establish whether the AR is still functional in the androgen-independent sublines; (iii) identify the mechanism(s) by which the AR pathway may be adjusted to the low androgen/high antiandrogen levels; (iv) identify androgen-regulated genes that could possibly be used in the diagnosis/prognosis of prostate cancer or as a therapeutic target.

The final aim of this project was to explore whether the AR pathway was still active in the androgen-independent cells under androgen-deprived conditions and to identify putative alternative growth/survival pathways. To accomplish this, the androgen-independent sublines, cultured in their respective androgen-deprived selection medium, were compared with the parental androgen-responsive PC346C (supplemented with androgens), by using expression microarrays (Chapter 5). By further comparing the differentially expressed genes in the AI sublines versus the androgen-responsive PC346C, with the androgen-regulated genes established in Chapter 4, we intend to: (i) assess whether the AR pathway is “ON” or “OFF” in the AI sublines; (ii) identify putative alternative growth/survival pathways; (iii) select and validate a set of non-androgen-regulated genes that could drive prostate cancer growth. To guide the selection of these genes, the microarray data produced in this study was linked to an assortment of publicly available gene expression databases on human prostate tumors, xenografts and cell lines, using the SRS platform [92]. This allowed access to a comprehensive collection of data leading to crucial clues on how the AR pathway evolves and how putative oncogenes and tumor suppressors are regulated in prostate cancer progression.

1.10. References

1. Ferlay J, Autier P, Boniol M, Heanue M, Colombet M, et al. (2007) Estimates of the cancer incidence and mortality in Europe in 2006. *Ann Oncol* 18: 581-592.
2. Delongchamps NB, Singh A, Haas GP (2006) The role of prevalence in the diagnosis of prostate cancer. *Cancer Control* 13: 158-168.
3. Whittaker R Instant Anatomy. Available at: <http://www.instantanatomy.net>.
4. McNeal JE (1988) Normal histology of the prostate. *Am J Surg Pathol* 12: 619-633.
5. Mann T (1974) Secretory function of the prostate, seminal vesicle and other male accessory organs of reproduction. *J Reprod Fertil* 37: 179-188.
6. Schalken JA, van Leenders G (2003) Cellular and molecular biology of the prostate: stem cell biology. *Urology* 62: 11-20.
7. Bonkhoff H, Remberger K (1998) Morphogenetic concepts of normal and abnormal growth in the human prostate. *Virchows Arch* 433: 195-202.
8. El-Alfy M, Pelletier G, Herno LS, Labrie F (2000) Unique features of the basal cells of human prostate epithelium. *Microsc Res Tech* 51: 436-446.
9. El-Alfy M, Luu-The V, Huang XF, Berger L, Labrie F, et al. (1999) Localization of type 5 17beta-hydroxysteroid dehydrogenase, 3beta-hydroxysteroid dehydrogenase, and androgen receptor in the human prostate by in situ hybridization and immunocytochemistry. *Endocrinology* 140: 1481-1491.
10. Wojno KJ, Epstein JI (1995) The utility of basal cell-specific anti-cytokeratin antibody (34 beta E12) in the diagnosis of prostate cancer. A review of 228 cases. *Am J Surg Pathol* 19: 251-260.
11. O'Malley FP, Grignon DJ, Shum DT (1990) Usefulness of immunoperoxidase staining with high-molecular-weight cytokeratin in the differential diagnosis of small-acinar lesions of the prostate gland. *Virchows Arch A Pathol Anat Histopathol* 417: 191-196.
12. Bonkhoff H, Remberger K (1996) Differentiation pathways and histogenetic aspects of normal and abnormal prostatic growth: a stem cell model. *Prostate* 28: 98-106.
13. Lam JS, Reiter RE (2006) Stem cells in prostate and prostate cancer development. *Urol Oncol* 24: 131-140.
14. Dhom G, Seitz G, Wernert N (1988) Histology and immunohistochemistry studies in prostate cancer. *Am J Clin Oncol* 11 Suppl 2: S37-42.
15. van der Kwast TH, Tetu B, Suburu ER, Gomez J, Lemay M, et al. (1998) Cycling activity of benign prostatic epithelial cells during long-term androgen blockade: evidence for self-renewal of luminal cells. *J Pathol* 186: 406-409.
16. Brothman AR, Maxwell TM, Cui J, Deubler DA, Zhu XL (1999) Chromosomal clues to the development of prostate tumors. *Prostate* 38: 303-312.
17. Hughes C, Murphy A, Martin C, Sheils O, O'Leary J (2005) Molecular pathology of prostate cancer. *J Clin Pathol* 58: 673-684.
18. Epstein JI (2009) Precursor lesions to prostatic adenocarcinoma. *Virchows Arch* 454: 1-16.
19. Schroder FH, Hermanek P, Denis L, Fair WR, Gospodarowicz MK, et al. (1992) The TNM classification of prostate cancer. *Prostate Suppl* 4: 129-138.
20. Wheeler TM, Dilliglugil O, Kattan MW, Arakawa A, Soh S, et al. (1998) Clinical and pathological significance of the level and extent of capsular invasion in clinical stage T1-2 prostate cancer. *Hum Pathol* 29: 856-862.
21. Bubendorf L, Schopfer A, Wagner U, Sauter G, Moch H, et al. (2000) Metastatic patterns of prostate cancer: an autopsy study of 1,589 patients. *Hum Pathol* 31: 578-583.
22. Lee F, Littrup PJ (1992) The role of digital rectal examination, transrectal ultrasound, and prostate specific antigen for the detection of confined and clinically relevant prostate cancer. *J Cell Biochem Suppl* 16H: 69-73.
23. Frydenberg M, Stricker PD, Kaye KW (1997) Prostate cancer diagnosis and management. *Lancet* 349: 1681-1687.
24. Lilja H, Ulmert D, Vickers AJ (2008) Prostate-specific antigen and prostate cancer: prediction, detection and monitoring. *Nat Rev Cancer* 8: 268-278.

25. Schroder FH, Hugosson J, Roobol MJ, Tammela TL, Ciatto S, et al. (2009) Screening and prostate-cancer mortality in a randomized European study. *N Engl J Med* 360: 1320-1328.
26. Andriole GL, Grubb RL, 3rd, Buys SS, Chia D, Church TR, et al. (2009) Mortality results from a randomized prostate-cancer screening trial. *N Engl J Med* 360: 1310-1319.
27. Schroder FH, Carter HB, Wolters T, van den Bergh RC, Gosselaar C, et al. (2008) Early detection of prostate cancer in 2007. Part 1: PSA and PSA kinetics. *Eur Urol* 53: 468-477.
28. Steuber T, O'Brien MF, Lilja H (2008) Serum markers for prostate cancer: a rational approach to the literature. *Eur Urol* 54: 31-40.
29. Sardana G, Dowell B, Diamandis EP (2008) Emerging biomarkers for the diagnosis and prognosis of prostate cancer. *Clin Chem* 54: 1951-1960.
30. Huggins C, Hodges CV (2002) Studies on prostatic cancer: I. The effect of castration, of estrogen and of androgen injection on serum phosphatases in metastatic carcinoma of the prostate. 1941. *J Urol* 168: 9-12.
31. Sharifi N, Gulley JL, Dahut WL (2005) Androgen deprivation therapy for prostate cancer. *Jama* 294: 238-244.
32. Reid AH, Attard G, Barrie E, de Bono JS (2008) CYP17 inhibition as a hormonal strategy for prostate cancer. *Nat Clin Pract Urol* 5: 610-620.
33. Galbraith SM, Duchesne GM (1997) Androgens and prostate cancer: biology, pathology and hormonal therapy. *Eur J Cancer* 33: 545-554.
34. Wirth MP, Hakenberg OW, Froehner M (2007) Antiandrogens in the treatment of prostate cancer. *Eur Urol* 51: 306-313; discussion 314.
35. Crawford ED, Eisenberger MA, McLeod DG, Spaulding JT, Benson R, et al. (1989) A controlled trial of leuprolide with and without flutamide in prostatic carcinoma. *N Engl J Med* 321: 419-424.
36. Eisenberger MA, Blumenstein BA, Crawford ED, Miller G, McLeod DG, et al. (1998) Bilateral orchiectomy with or without flutamide for metastatic prostate cancer. *N Engl J Med* 339: 1036-1042.
37. Tran C, Ouk S, Clegg NJ, Chen Y, Watson PA, et al. (2009) Development of a Second-Generation Antiandrogen for Treatment of Advanced Prostate Cancer. *Science*.
38. Cunha GR, Ricke W, Thomson A, Marker PC, Risbridger G, et al. (2004) Hormonal, cellular, and molecular regulation of normal and neoplastic prostatic development. *J Steroid Biochem Mol Biol* 92: 221-236.
39. Gnanapragasam VJ, Robson CN, Leung HY, Neal DE (2000) Androgen receptor signalling in the prostate. *BJU Int* 86: 1001-1013.
40. Brinkmann AO, Klaasen P, Kuiper GG, van der Korput JA, Bolt J, et al. (1989) Structure and function of the androgen receptor. *Urol Res* 17: 87-93.
41. Chang CS, Kokontis J, Liao ST (1988) Molecular cloning of human and rat complementary DNA encoding androgen receptors. *Science* 240: 324-326.
42. Chang CS, Kokontis J, Liao ST (1988) Structural analysis of complementary DNA and amino acid sequences of human and rat androgen receptors. *Proc Natl Acad Sci U S A* 85: 7211-7215.
43. Brinkmann AO, Blok LJ, de Ruiter PE, Doesburg P, Steketee K, et al. (1999) Mechanisms of androgen receptor activation and function. *J Steroid Biochem Mol Biol* 69: 307-313.
44. Jenster G, van der Korput HA, Trapman J, Brinkmann AO (1995) Identification of two transcription activation units in the N-terminal domain of the human androgen receptor. *J Biol Chem* 270: 7341-7346.
45. Ruizeveld de Winter JA, Trapman J, Vermey M, Mulder E, Zegers ND, et al. (1991) Androgen receptor expression in human tissues: an immunohistochemical study. *J Histochem Cytochem* 39: 927-936.
46. Bagatell CJ, Bremner WJ (1996) Androgens in men--uses and abuses. *N Engl J Med* 334: 707-714.
47. Eder IE, Culig Z, Putz T, Nessler-Menardi C, Bartsch G, et al. (2001) Molecular biology of the androgen receptor: from molecular understanding to the clinic. *Eur Urol* 40: 241-251.
48. Bolton EC, So AY, Chaivorapol C, Haqq CM, Li H, et al. (2007) Cell- and gene-specific regulation of primary target genes by the androgen receptor. *Genes Dev* 21: 2005-2017.

49. DePrimo SE, Diehn M, Nelson JB, Reiter RE, Matese J, et al. (2002) Transcriptional programs activated by exposure of human prostate cancer cells to androgen. *Genome Biol* 3: RESEARCH0032.
50. Tomlins SA, Rhodes DR, Perner S, Dhanasekaran SM, Mehra R, et al. (2005) Recurrent fusion of TMPRSS2 and ETS transcription factor genes in prostate cancer. *Science* 310: 644-648.
51. Simpson S, Woodworth CD, DiPaolo JA (1997) Altered expression of Erg and Ets-2 transcription factors is associated with genetic changes at 21q22.2-22.3 in immortal and cervical carcinoma cell lines. *Oncogene* 14: 2149-2157.
52. Shimizu K, Ichikawa H, Tojo A, Kaneko Y, Maseki N, et al. (1993) An ets-related gene, ERG, is rearranged in human myeloid leukemia with t(16;21) chromosomal translocation. *Proc Natl Acad Sci U S A* 90: 10280-10284.
53. Ida K, Kobayashi S, Taki T, Hanada R, Bessho F, et al. (1995) EWS-FLI-1 and EWS-ERG chimeric mRNAs in Ewing's sarcoma and primitive neuroectodermal tumor. *Int J Cancer* 63: 500-504.
54. Kumar-Sinha C, Tomlins SA, Chinnaiyan AM (2008) Recurrent gene fusions in prostate cancer. *Nat Rev Cancer* 8: 497-511.
55. Han B, Mehra R, Dhanasekaran SM, Yu J, Menon A, et al. (2008) A fluorescence in situ hybridization screen for E26 transformation-specific aberrations: identification of DDX5-ETV4 fusion protein in prostate cancer. *Cancer Res* 68: 7629-7637.
56. Tomlins SA, Laxman B, Dhanasekaran SM, Helgeson BE, Cao X, et al. (2007) Distinct classes of chromosomal rearrangements create oncogenic ETS gene fusions in prostate cancer. *Nature* 448: 595-599.
57. Attard G, Clark J, Ambrosine L, Mills IG, Fisher G, et al. (2008) Heterogeneity and clinical significance of ETV1 translocations in human prostate cancer. *Br J Cancer* 99: 314-320.
58. Tomlins SA, Laxman B, Varambally S, Cao X, Yu J, et al. (2008) Role of the TMPRSS2-ERG gene fusion in prostate cancer. *Neoplasia* 10: 177-188.
59. King JC, Xu J, Wongvipat J, Hieronymus H, Carver BS, et al. (2009) Cooperativity of TMPRSS2-ERG with PI3-kinase pathway activation in prostate oncogenesis. *Nat Genet* 41: 524-526.
60. Carver BS, Tran J, Gopalan A, Chen Z, Shaikh S, et al. (2009) Aberrant ERG expression cooperates with loss of PTEN to promote cancer progression in the prostate. *Nat Genet* 41: 619-624.
61. Squire JA (2009) TMPRSS2-ERG and PTEN loss in prostate cancer. *Nat Genet* 41: 509-510.
62. Jenster G (1999) The role of the androgen receptor in the development and progression of prostate cancer. *Semin Oncol* 26: 407-421.
63. van der Kwast TH, Schalken J, Ruizeveld de Winter JA, van Vroonhoven CC, Mulder E, et al. (1991) Androgen receptors in endocrine-therapy-resistant human prostate cancer. *Int J Cancer* 48: 189-193.
64. Ruizeveld de Winter JA, Janssen PJ, Sleddens HM, Verleun-Mooijman MC, Trapman J, et al. (1994) Androgen receptor status in localized and locally progressive hormone refractory human prostate cancer. *Am J Pathol* 144: 735-746.
65. Brown RS, Edwards J, Dogan A, Payne H, Harland SJ, et al. (2002) Amplification of the androgen receptor gene in bone metastases from hormone-refractory prostate cancer. *J Pathol* 198: 237-244.
66. Koivisto P, Kononen J, Palmberg C, Tammela T, Hyytinen E, et al. (1997) Androgen receptor gene amplification: a possible molecular mechanism for androgen deprivation therapy failure in prostate cancer. *Cancer Res* 57: 314-319.
67. Linja MJ, Savinainen KJ, Saramaki OR, Tammela TL, Vessella RL, et al. (2001) Amplification and overexpression of androgen receptor gene in hormone-refractory prostate cancer. *Cancer Res* 61: 3550-3555.
68. Grossmann ME, Huang H, Tindall DJ (2001) Androgen receptor signalling in androgen-refractory prostate cancer. *J Natl Cancer Inst* 93: 1687-1697.
69. Devlin HL, Mudryj M (2009) Progression of prostate cancer: multiple pathways to androgen independence. *Cancer Lett* 274: 177-186.

70. Veldscholte J, Ris-Stalpers C, Kuiper GG, Jenster G, Berrevoets C, et al. (1990) A mutation in the ligand binding domain of the androgen receptor of human LNCaP cells affects steroid binding characteristics and response to anti-androgens. *Biochem Biophys Res Commun* 173: 534-540.
71. Veldscholte J, Berrevoets CA, Ris-Stalpers C, Kuiper GG, Jenster G, et al. (1992) The androgen receptor in LNCaP cells contains a mutation in the ligand binding domain which affects steroid binding characteristics and response to antiandrogens. *J Steroid Biochem Mol Biol* 41: 665-669.
72. Culig Z, Hobisch A, Hittmair A, Cronauer MV, Radmayr C, et al. (1997) Androgen receptor gene mutations in prostate cancer. Implications for disease progression and therapy. *Drugs Aging* 10: 50-58.
73. Taplin ME, Rajeshkumar B, Halabi S, Werner CP, Woda BA, et al. (2003) Androgen receptor mutations in androgen-independent prostate cancer: Cancer and Leukemia Group B Study 9663. *J Clin Oncol* 21: 2673-2678.
74. Bergerat JP, Ceraline J (2009) Pleiotropic functional properties of androgen receptor mutants in prostate cancer. *Hum Mutat* 30: 145-157.
75. Han G, Buchanan G, Ittmann M, Harris JM, Yu X, et al. (2005) Mutation of the androgen receptor causes oncogenic transformation of the prostate. *Proc Natl Acad Sci U S A* 102: 1151-1156.
76. Shi XB, Xue L, Tepper CG, Gandour-Edwards R, Ghosh P, et al. (2007) The oncogenic potential of a prostate cancer-derived androgen receptor mutant. *Prostate* 67: 591-602.
77. Gottlieb B, Beitel LK, Wu JH, Trifiro M (2004) The androgen receptor gene mutations database (ARDB): 2004 update. *Hum Mutat* 23: 527-533.
78. Montgomery RB, Mostaghel EA, Vessella R, Hess DL, Kalhorn TF, et al. (2008) Maintenance of intratumoral androgens in metastatic prostate cancer: a mechanism for castration-resistant tumor growth. *Cancer Res* 68: 4447-4454.
79. Stanbrough M, Bubley GJ, Ross K, Golub TR, Rubin MA, et al. (2006) Increased expression of genes converting adrenal androgens to testosterone in androgen-independent prostate cancer. *Cancer Res* 66: 2815-2825.
80. Wang Y, Kreisberg JI, Ghosh PM (2007) Cross-talk between the androgen receptor and the phosphatidylinositol 3-kinase/Akt pathway in prostate cancer. *Curr Cancer Drug Targets* 7: 591-604.
81. Culig Z (2004) Androgen receptor cross-talk with cell signalling pathways. *Growth Factors* 22: 179-184.
82. Zhu ML, Kyprianou N (2008) Androgen receptor and growth factor signalling cross-talk in prostate cancer cells. *Endocr Relat Cancer* 15: 841-849.
83. Hu R, Dunn TA, Wei S, Isharwal S, Veltri RW, et al. (2009) Ligand-independent androgen receptor variants derived from splicing of cryptic exons signify hormone-refractory prostate cancer. *Cancer Res* 69: 16-22.
84. Ceraline J, Cruchant MD, Erdmann E, Erbs P, Kurtz JE, et al. (2004) Constitutive activation of the androgen receptor by a point mutation in the hinge region: a new mechanism for androgen-independent growth in prostate cancer. *Int J Cancer* 108: 152-157.
85. Libertini SJ, Tepper CG, Rodriguez V, Asmuth DM, Kung HJ, et al. (2007) Evidence for calpain-mediated androgen receptor cleavage as a mechanism for androgen independence. *Cancer Res* 67: 9001-9005.
86. Brooke GN, Parker MG, Bevan CL (2008) Mechanisms of androgen receptor activation in advanced prostate cancer: differential co-activator recruitment and gene expression. *Oncogene* 27: 2941-2950.
87. Chmelar R, Buchanan G, Need EF, Tilley W, Greenberg NM (2007) Androgen receptor coregulators and their involvement in the development and progression of prostate cancer. *Int J Cancer* 120: 719-733.
88. Lee EC, Tenniswood M (2004) Programmed cell death and survival pathways in prostate cancer cells. *Arch Androl* 50: 27-32.
89. Gurumurthy S, Vasudevan KM, Rangnekar VM (2001) Regulation of apoptosis in prostate cancer. *Cancer Metastasis Rev* 20: 225-243.

90. Berry PA, Maitland NJ, Collins AT (2008) Androgen receptor signalling in prostate: effects of stromal factors on normal and cancer stem cells. *Mol Cell Endocrinol* 288: 30-37.
91. Chlenski A, Nakashiro K, Ketels KV, Korovaitseva GI, Oyasu R (2001) Androgen receptor expression in androgen-independent prostate cancer cell lines. *Prostate* 47: 66-75.
92. Veldhoven A, de Lange D, Smid M, de Jager V, Kors JA, et al. (2005) Storing, linking, and mining microarray databases using SRS. *BMC Bioinformatics* 6: 192.

Chapter 2

The Human PC346 Xenograft and Cell Line Panel: a Model System for Prostate Cancer Progression

Rute B. Marques¹, Wytske M. van Weerden¹, Sigrun Erkens-Schulze¹,
Corrina M. de Ridder¹, Chris H. Bangma¹, Jan Trapman², Guido Jenster¹

¹Department of Urology and ²Department of Pathology,
Josephine Nefkens Institute, Erasmus Medical Center,
PO Box 1738, 3000 DR, Rotterdam, The Netherlands

European Urology (2006) 49: 245-257

ABSTRACT

Objective: Prostate cancer (PCa) model systems that reflect the different disease stages are essential for studying the development and progression of PCa and for testing new treatment modalities. This review summarizes the establishment and characterization of the PC346 progression model, and compares it to other human PCa cell lines and xenografts available.

Methods: The PC346 model was derived from the transurethral resection of a primary prostate tumor. Tumor samples were subcutaneously implanted into athymic mice, resulting in the development of a series of xenografts, from which *in vitro* cell cultures were established.

Results: The PC346 panel includes sublines with hormone-response characteristics that range from androgen-sensitive to androgen-independent growth. *In vivo* and *in vitro* selection of androgen-sensitive lines under androgen-depleted conditions replicated the clinically relevant relapse phenomenon, and resulted in a series of modifications in the androgen-receptor (AR) pathway: AR mutation, overexpression and downregulation.

Conclusions: The PC346 panel reproduces many biological characteristics of the different phases of clinical PCa and the most common AR modifications observed in hormone-refractory tumors, being a valuable addition to the limited collection of model systems currently available.

INTRODUCTION

The understanding of prostate cancer (PCa) basic biology and the development and testing of novel therapies require the use of suitable model systems. An ideal model system should mimic the characteristics of different stages of prostate cancer in humans, from cancer initiation, progression, hormone-refractory disease and metastasis. There are different types of PCa models: animal systems, such as transgenic and knockout mice, hormonally/ carcinogenically induced PCa in rats and spontaneous dog models; or systems derived from (human) prostate tissue, such as xenografts and *in vitro* cell lines [1]. This review will focus on the latter, xenografts and *in vitro* culture models established from human prostate tumors, in particular the development and characterization of the PC346 model.

Xenografts are models in which human prostate tissue is transplanted into an animal, generally an immune-deficient mouse. In this way, human prostate tumors can be propagated *in vivo* for indefinite periods of time, allowing the study of tumor progression under different experimental conditions and the testing of novel therapies. Although xenografts resemble more closely the *in vivo* situation of the patient, *in vitro* cultures offer more experimental flexibility, a higher control over environmental variables and unlimited sample amounts. On the other hand, *in vitro* cell lines lack the interaction with the prostate environment and miss the effect of stromal/epithelial interactions and vascularization. These model systems are useful and complementary for defining the role of hormones in PCa progression and the signaling pathways involved in hormone-refractory cell proliferation. A wide variety of *in vivo* and *in vitro* models are necessary to represent the different characteristics and progression of human PC. Unfortunately, due to the poor growth of human prostate tissue *in vitro* and *in vivo*, the number of xenografts and cell lines available is limited. Furthermore, many of the available systems were established from metastatic lesions or represent the advanced-stage hormone-refractory state of the disease, whereas models for the androgen-dependent state are rare [2, 3]. Until the mid nineties, researchers were restricted to the “classical” *in vitro* PC-3, DU145 and LNCaP, but extensive efforts during the past decade have led to a considerable increase in the collection of xenografts and cell lines available (Table 1). Traditionally, PCa xenografts have been grafted and propagated subcutaneously. Recently, Wang and associates showed that subrenal grafting of human prostate tissue resulted in more efficient tumor-take and short-term recovery than subcutaneous grafting, probably due to the high degree of vascularity of the site [4]. Besides the higher tumor-take rate, subrenal grafting resulted in better histopathological differentiation and could also be used with benign and low-grade tumor tissues, which are generally very difficult to grow subcutaneously. Although the authors have proved that the prostate tissue could be efficiently grafted, maintained and recovered from the subrenal compartment, they have not addressed whether these xenografts could be serially transplanted as permanent lines. Furthermore, the subrenal site has a limited xenograft carrying capacity, and the grafting surgery and follow up of tumor growth are technically complex. Despite the need for further optimization, subrenal grafting is a promising technique that will hopefully help boost the development of novel xenograft models.

Table 1 - Overview of established xenografts and *in vitro* culture models for human prostate cancer.

| Name | Year | Origin | Androgen response | AR expression | PSA expression | AR sequence |
|---|------|--------------------------------------|-------------------|---------------|----------------|----------------|
| Prostate Cancer Xenografts | | | | | | |
| PC-EW [5] | 1984 | Lymph node | AD | Yes | Yes | Wt |
| PC82 [6] | 1980 | Primary | AD | Yes | Yes | Wt |
| PC133 [3] | 1981 | Bone | AI | No | No | n/a |
| PC135 [3] | 1982 | Primary | AI | No | No | n/a |
| PC295 [7] | 1996 | Lymph node | AD | Yes | Yes | Wt |
| PC310 [7] | 1996 | Primary | AD | Yes | Yes | Wt |
| PC324 [7] | 1996 | Primary | AI | No | No | n/a |
| PC339 [7] | 1996 | Primary | AI | No | No | n/a |
| PC374 [7] | 1996 | Skin | AI | No | No | n/a |
| PC346P* [7] | 1996 | Primary | AS | Yes | Yes | Wt |
| PC346B [3] | 2000 | Primary | AS | Yes | Yes | Wt |
| CWR21 [8] | 1993 | Primary | n/a | n/a | n/a | n/a |
| CWR22 [8, 9] | 1993 | Primary | AD | Yes | Yes | H874Y |
| CWR31 [8] | 1993 | Primary | n/a | n/a | n/a | n/a |
| CWR91 [8] | 1993 | Primary | n/a | n/a | n/a | n/a |
| LuCaP 23.1 [10] | 1996 | Lymph node | AS | Yes | Yes | n/a |
| LuCaP 23.8 [10] | 1996 | Lymph node | AS | Yes | Yes | n/a |
| LuCaP 23.12 [10] | 1996 | Liver | AS | Yes | Yes | n/a |
| LuCaP 35 [11] | 2003 | Lymph node | AS | Yes | Yes | Wt |
| LuCaP 41[12-14] | 1999 | Primary | AS | Yes | Yes | n/a |
| LuCaP 49 [15] | 2002 | Lymph node, small cell carcinoma | AI | No | No | n/a |
| LuCaP 58 [12-14] | 1999 | Lymph node | AS | Yes | Yes | n/a |
| LuCaP 69 [12-14] | 1999 | Bowel | n/a | Yes | Yes | Wt |
| LuCaP 70 [12-14] | 1999 | Liver | n/a | Yes | Yes | n/a |
| LuCaP 73 [12-14] | 1999 | Pelvis | AI/AS | Yes | Yes | n/a |
| LAPC-3 [16] | 1997 | Primary | AI | Yes | Yes | Wt |
| LAPC-4 [16] | 1997 | Lymph node | AD | Yes | Yes | Wt |
| LAPC-9 [17] | 1999 | Bone | AS | Yes | Yes | Wt |
| MDA PCa-31 [1] | 1998 | Liver | n/a | Yes | Yes | n/a |
| MDA PCa-40 [1] | 1998 | Liver | n/a | No | No | n/a |
| MDA PCa-43 [1] | 1998 | Adrenal | n/a | Yes | Yes | n/a |
| MDA PCa-44 [1] | 1998 | Skin | n/a | No | No | n/a |
| TEN12 [18] | 2004 | Primary | AD/AS | Yes | Yes | Wt |
| BM18 [19] | 2005 | Bone | AD | Yes | Yes | n/a |
| Prostate Cancer <i>In Vitro</i> Cell Lines | | | | | | |
| PC-3 [20] | 1978 | Bone | AI | No | No | n/a |
| DU 145 [21] | 1978 | Brain | AI | No | No | n/a |
| LNCaP [22] | 1980 | Lymph node | AD/AS | Yes | Yes | T877A |
| 1013L [23] | 1980 | Primary, transitional cell carcinoma | AI | No | No | n/a |
| UM-SCP-1 [24] | 1984 | Primary, squamous cell carcinoma | AI | No | No | n/a |
| ARCaP [25] | 1996 | Ascites | AI/AS | Yes | Yes | Wt |
| MDA PCa 1** | 1996 | Ascites | AI | No | No | n/a |
| MDA PCa 2a [26] | 1997 | Bone | AI/AS | Yes | Yes | L701H, T877A |
| MDA PCa 2b [26] | 1997 | Bone | AI/AS | Yes | Yes | L701H, T877A |
| LAPC-4 [16] | 1997 | Lymph node | AD | Yes | Yes | Wt |
| 22Rv1 [27] | 1999 | Primary, CWR22R xenograft | AI/AS | Yes | No | H874Y, 2xExon3 |
| PC346C [3] | 2000 | Primary, PC346P xenograft | AS | Yes | Yes | Wt |
| PSK-1 [28] | 2000 | Primary, small cell carcinoma | AI | No | No | n/a |
| CWR-R1 [29] | 2001 | Primary, CWR22R xenograft | AI/AS | Yes | No | H874Y |
| DuCaP [11] | 2001 | Dura mater | AI/AS | Yes | Yes | Wt |
| VCaP [30] | 2001 | Vertebra | AI/AS | Yes | Yes | Wt |

This table includes a list of original xenografts and *in vitro* cultures, but not their derivative sublines, artificially immortalized lines or lines previously reported as cross-contaminants. AD: androgen-dependent; AI: androgen-independent; AS: androgen-sensitive; Wt: *wil- type* sequence; n/a: not available. *The PC346P xenograft has also been previously referred to as PC346. ** MDA PCa 1 was derived from the same patient as the ARCaP cell line. The LuCaP series has been extended with xenografts LuCaP 77, 81, 86.2, 92.1, 93, 96, 105 and 115 [31]. To date, no detailed information has been published on the origin, androgen responsiveness and AR status of these lines, which therefore were not included in this table.

PC346 is a progression model designed to study the mechanisms of androgen-independent outgrowth, which inevitably follows endocrine therapy of patients. The PC346 panel consists of five xenografts and six cell lines, which represent different phases of clinical PC, from androgen-responsive growth, through tumor relapse, to androgen independence. In this article we will review the establishment and characterization of the complete PC346 panel, including the most recent additions.

Origin of the PC346 tumor model

A Caucasian 68 years old male was diagnosed with bladder cancer and advanced prostate adenocarcinoma, presenting 17 ng/ml serum PSA. He had negative scans for both bone and lymph node metastasis (T4N0M0), and underwent four weeks treatment with cyproterone acetate prior to a transurethral resection (TUR) of the prostate. The tumor was dissected from surrounding tissue and small pieces of solid tumor tissue (approximately 30 mm³) were subcutaneously implanted in both shoulders of male athymic NMRI nude mice (Naval Medical Research Institute, Bethesda, Maryland, USA). Two samples of the TUR material were propagated in parallel, giving rise to two distinct lines, PC346P and PC346B, from which a panel of five xenografts and six *in vitro* cell cultures was established (Fig. 1). Histologically, the primary patient material (Gleason score 9) and resulting xenografts show a low degree of differentiation, with lack of glandular structures (Fig. 2A).

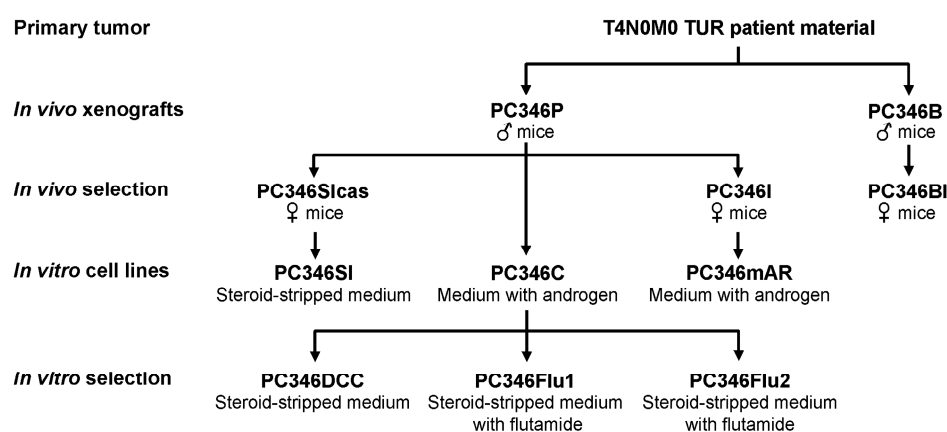
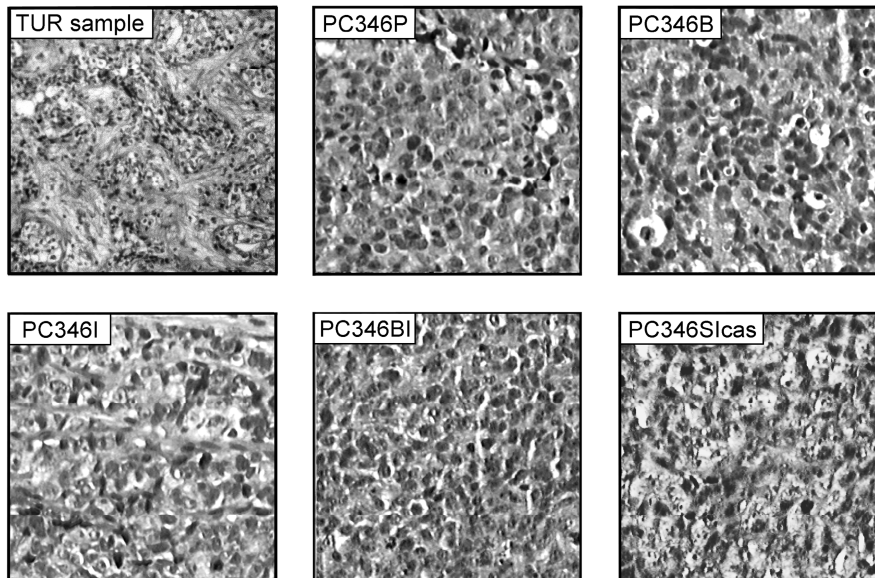


Figure 1 - Development of the PC346 human prostate cancer progression model

A.



B.

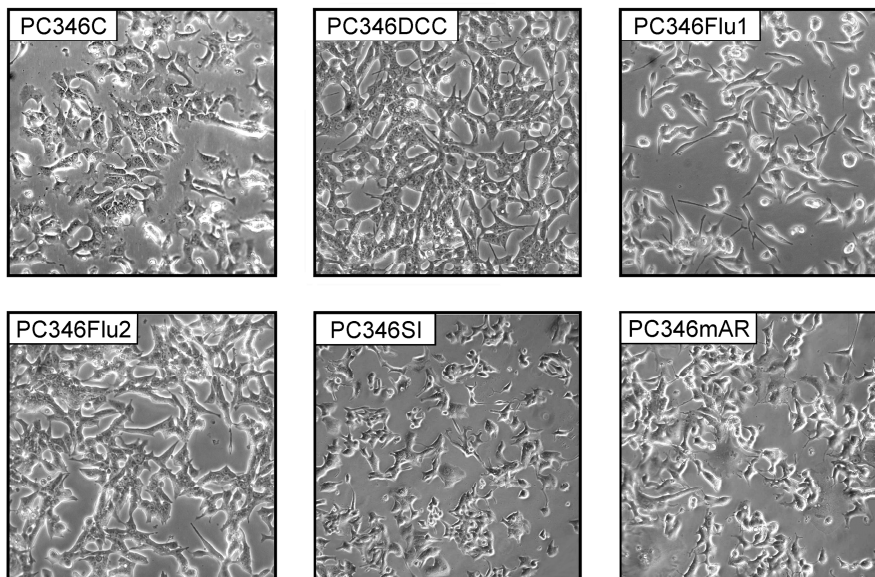


Figure 2 - Morphological characteristics of PC346 xenografts and cell lines. **(A)** Hematoxylin-eosin stained sections from formaldehyde-fixed, paraffin-embedded patient TUR material and derived xenografts (original amplification 100x). **(B)** Phase contrast microscopic photographs of the *in vitro* cell cultures (200x).

Establishment and growth characteristics of PC346 xenografts

The parental PC346P and PC346B tumors show similar growth characteristics in intact male mice: a high (85-90%) take rate of the transplants, 3-8 weeks lag-phase and an average doubling-time of about 10 days (Table 2). Both these xenografts are being propagated in intact male NMRI nude mice for over 50 passages and, to date, tumor growth characteristics have remained constant. These xenografts were originally identified as androgen-dependent, since tumor transplantation into female or castrated male mice rarely resulted in tumor development [7]. The tumors that did develop had a prolonged lag-phase and a 2-4 fold reduction in growth rate (Table 2). Furthermore, roughly half of these tumors eventually regressed and disappeared within a few months, and the remaining tumors would not survive subsequent re-transplantations in female or castrated males. This posed great difficulties to the development of androgen-independent (AI) sublines, and called for a more elaborate selection approach.

The AI sublines PC346I and PC346BI were derived from PC346P and PC346B, respectively, by initially transplanting these tumors in female mice supplemented with testosterone (through a subcutaneous silastic implant [32]). After 50 days, once the tumors were established and growing, the testosterone implant was removed and some tumors showed a regression followed by regrowth. These regrowing tumors were subsequently passaged into non-supplemented female mice. Only two of these recurrent tumors were able to grow in female mice: the PC346I and PC346BI xenografts (Fig. 1). PC346I and PC346BI tumors grow equally well in female and male mice, showing AI growth characteristics with no significant response to castration (Table 2).

For the androgen-sensitive PC346P and PC346B xenografts, androgen ablation of established tumors (300-800 mm³) yielded considerably different results from those of castration prior to transplantation. Castration of mice bearing PC346P tumors, resulted in variable responses, including tumor regression (in one third of the cases), tumor retardation followed by growth relapse, and continued growth (Fig. 3A). Despite this high variation, the growth rate of PC346P is significantly decreased upon castration (Fig. 3B). Interestingly, established PC346B tumors, did not significantly respond to castration of the tumor-bearing mice (Fig. 3B). These results indicate that both PC346P and PC346B are androgen-responsive but not strictly dependent on androgens for growth. The fact that PC346P and PC346B, two xenografts derived from the same tumor, respond in a different way to castration, suggests heterogeneity in the original patient material. Indeed, tumor heterogeneity is not a novel finding nor is it exclusive to prostate carcinomas [33].

In 1981 Isaacs *et al.* hypothesized that prostate tumors contained a mixture of cells with different androgen sensitivities, and that the transition to androgen-independence involved the "clonal expansion" of AI cells already present prior to the androgen ablation treatment [34]. This hypothesis is supported by Craft *et al.*, who used serial dilution and fluctuation analysis of the LAPC-9 xenograft model to show that AI cells were already present in the original tumor at a frequency of about 1 per 10⁵-10⁶ androgen-dependent cells [17]. Moreover, the fact that prostate carcinomas are often multifocal, with two or more histologically but also genetically distinct tumors within the prostate, further corroborates the multiclonal character of prostate carcinomas [35-37]. An alternative hypothesis for the transition to the AI state is that PCa cells adapt to the

altered hormonal environment by changing gene expression. In reality, the transition to androgen-independence is a complex process that probably involves both clonal selection, and adaptative upregulation of growth promoting or downregulation of apoptotic genes [38]. The diverse assortment of PC346 lines provides a valid model system to help elucidate this phenomenon.

After copious attempts, we recently produced a hormone-refractory subline of PC346P by direct transplantation into female mice: the PC346SIcas xenograft. In female mice, this xenograft has a 75% tumor-take rate, 4-10 weeks lag-phase and a doubling-time of 10 days. As with PC346I and PC346BI, tumor-take and growth rates of PC346SIcas were not significantly different between castrated and sham-castrated male mice, indicating that the subline is androgen-independent (Table 2).

Table 2 - Tumor development of PC346 xenografts in male, castrated male and female mice.

| | Males | | | Castrated males | | | Females | | |
|----------------|---------|-------|------------|-----------------|-------|-------------|---------|--------|-------------|
| | TT | LP | TD | TT | LP | TD | TT | LP | TD |
| PC346P | 89 ± 4% | 25-45 | 8.1 ± 0.5 | 16 ± 9% | 37-79 | 32.0 ± 7.7 | 10 ± 5% | 67-116 | 19.5 ± 3.0 |
| PC346B | 87 ± 5% | 19-62 | 12.1 ± 2.6 | 8 ± 5% | 30-52 | 56.4 ± 22.0 | 10 ± 6% | 56-122 | 25.8 ± 11.5 |
| PC346I | 83 ± 7% | 23-35 | 10.5 ± 1.4 | 81 ± 7% | 29-55 | 8.5 ± 0.8 | 71 ± 7% | 30-49 | 10.1 ± 1.0 |
| PC346BI | 86 ± 8% | 19-32 | 11.8 ± 1.6 | 80 ± 12% | 19-35 | 11.2 ± 2.1 | 82 ± 7% | 18-52 | 11.0 ± 0.8 |
| PC346SI | 93 ± 3% | 30-51 | 10.6 ± 1.7 | 90 ± 3% | 28-58 | 12.4 ± 0.8 | 75 ± 8% | 34-69 | 10.1 ± 1.7 |

TT, tumor take, percentage of tumors that develop after transplantation. LP, lag phase: time (days) till tumor volume reaches 100 mm³. TD, tumor-doubling time.

Establishment and growth characteristics of PC346 *in vitro* cell lines

Efforts to generate *in vitro* cultures from the various PC346 xenografts culminated in the development of PC346C, PC346mAR and PC346SI, from the PC346P, PC346I and PC346SIcas xenografts, respectively (Fig. 1). Unfortunately, until now we have been unable to establish permanent *in vitro* lines from PC346B and PC346BI. The PC346C cell line, like its parental xenograft PC346P, is androgen-responsive: it grows slowly in steroid-stripped medium, is 2-3 fold stimulated by the synthetic androgen R1881 and is not stimulated by the antiandrogen hydroxyflutamide (Fig. 4).

To mimic *in vitro* the endocrine therapy applied to patients with advanced metastatic PC, we continuously cultured (>2 years) PC346C in androgen-depleted conditions, producing the PC346DCC, PC346Flu1 and PC346Flu2 sublines [39]. PC346DCC was derived from passage 45 of PC346C by culturing in steroid-stripped medium. The flutamide-resistant PC346Flu1 and PC346Flu2 sublines were produced from passage 45 and 75 of PC346C, respectively, by culturing in steroid-stripped medium supplemented with 1 μM of hydroxyflutamide. The resulting AI sublines not only show distinct morphologic features (Fig. 2B), but also different hormone response properties. PC346DCC grows well in the absence of androgens and is unresponsive to either R1881 or hydroxyflutamide (Fig. 4). PC346Flu1 grows optimally in steroid-stripped medium or in medium supplemented with hydroxyflutamide, being inhibited by physiologic concentrations of androgens. PC346Flu2 and PC346mAR share similar hormone responses. These lines are stimulated by both R1881 and hydroxyflutamide,

raising the question whether the AR is mutated. Finally, the PC346SI is, like PC346DCC, unresponsive to hormonal stimulation.

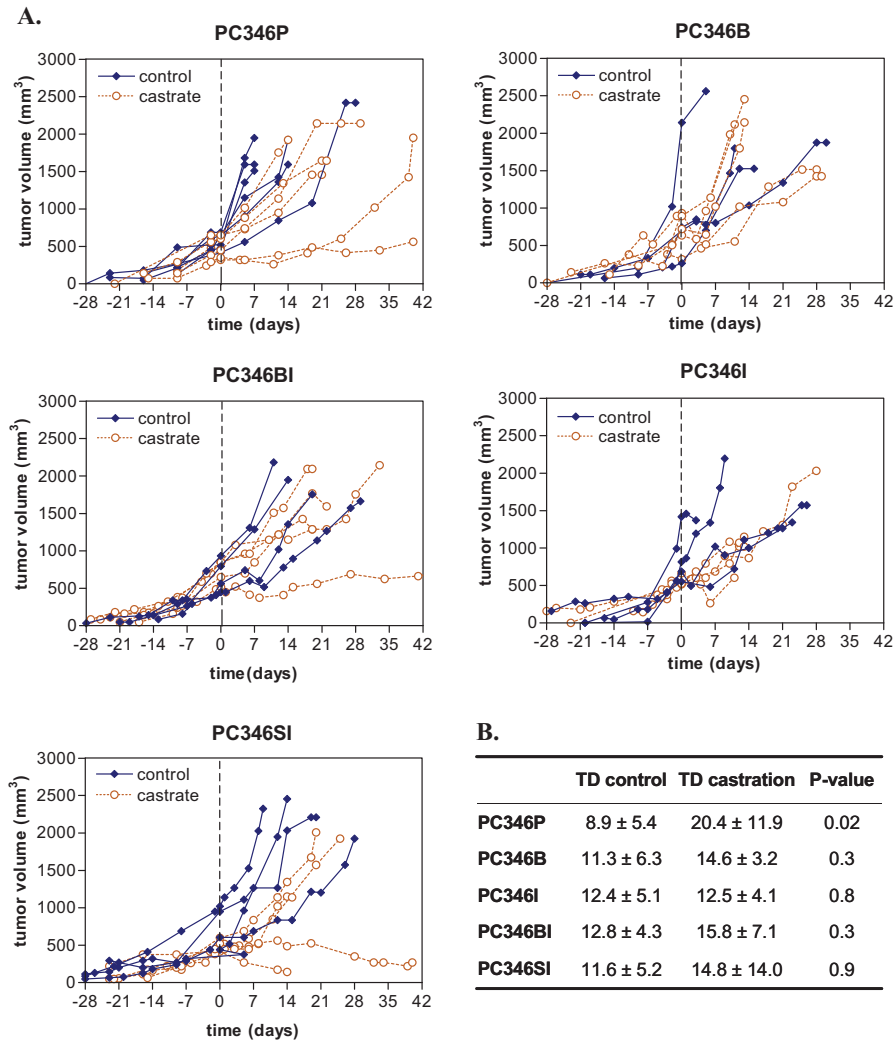


Figure 3 - Response of PC346 xenografts to castration. Tumors were subcutaneously implanted into the shoulders of 6-8 weeks old male NMRI nu/nu mice, and tumor volume was measured weekly with calipers. **(A)** tumor growth in castrated male mice (—○—), compared to control sham-operated animals (—◆—). Mice were castrated when tumor volume reached 300-800 mm³; vertical, dashed line at t₀ indicates the time point of castration. Tumor volume is plotted for each individual animal. **(B)** effect of castration on tumor-doubling time (TD) of xenografts. The growth rates were determined by linear regression of the tumor volume (in semi-logarithmic scale) over time, and the TD calculated from the 1/slope of tumor volume rise; p-values were determined by Mann-Whitney statistical test.

Status of the AR pathway in the PC346 panel

The progression of human prostate cancer during endocrine therapy is characterized by an inevitable transition from androgen responsiveness towards androgen independence. Androgen regulation through testosterone and dihydrotestosterone is mediated by the androgen receptor (AR), a member of the steroid receptor family and a key transcription factor for genes involved in the proliferation, maintenance and differentiation of the prostate [40]. AR expression is present in the vast majority of primary prostate tumors, hormone-refractory cancers and metastasis [41, 42], and the AR pathway may still be actively implicated in the growth of androgen-independent cancer cells.

The PC346 panel of xenografts and *in vitro* cell lines constitutes an excellent tool to further study the role of the AR in the progression to AI PC. To assess the status of the AR pathway in the different lines, we quantified the AR and the AR-target gene PSA by western blotting. Additionally, exons 2-8 of the AR gene were checked for mutations by SSCP analysis and sequencing.

Western blot analysis revealed that, despite the very low levels of AR protein in PC346SIcas, PC346DCC and PC346mAR, all xenografts and cell lines expressed the receptor (Fig. 5). The PC346I xenograft and PC346Flu1 cell line overexpress the receptor in comparison to their respective androgen-responsive parental lines, PC346P and PC346C. Conversely, PC346BI and PC346DCC have downregulated AR expression upon selection under androgen-depleted conditions. PSA protein was also detected in all lines, although at extremely low levels in PC346DCC. The cellular localization of AR protein was assessed by immunocytochemistry. AR expression in PC346C, PC346Flu1, PC346Flu2 and PC346mAR cells, cultured in their respective selection medium, was localized in the nucleus. PC346DCC showed cytoplasmic AR expression, which was extremely low but above background staining of the negative control (no primary antibody). As observed in the western blot, PC346Flu1 showed increased AR expression compared to the other *in vitro* lines. PC346SI revealed a heterogeneous expression pattern, for the most part localized in the cytoplasm, but some positive nuclei were also present. In the androgen-sensitive xenografts PC346P and PC346B, propagated in intact male mice, the AR was mainly localized in the nucleus. In the androgen-independent xenografts PC346I and PC346BI, which were propagated in castrated mice, a stronger cytoplasmic staining was observed, together with some positive nuclei (Fig. 6). When the cell lines and xenografts were grown in the presence of androgens, nuclear staining was always predominant, also for the AR positive AI lines (data not shown).

Sequence analysis of the AR gene revealed a *wild-type* receptor in PC346P, PC346B, PC346BI and PC346SIcas xenografts, and in PC346C, PC346Flu1 and PC346SI cell lines. A Thr to Ala substitution at codon 877 in the steroid-binding domain was found in the PC346I xenograft and in two cell lines: PC346mAR and PC346Flu2. A novel mutation was detected in codon 311 of PC346DCC AR, resulting in Lys to Arg substitution [39]. However, AR reporter assays show no evidence of altered transactivation properties of this mutated receptor, which responds to R1881 and hydroxyflutamide like the *wild-type* AR (wtAR).

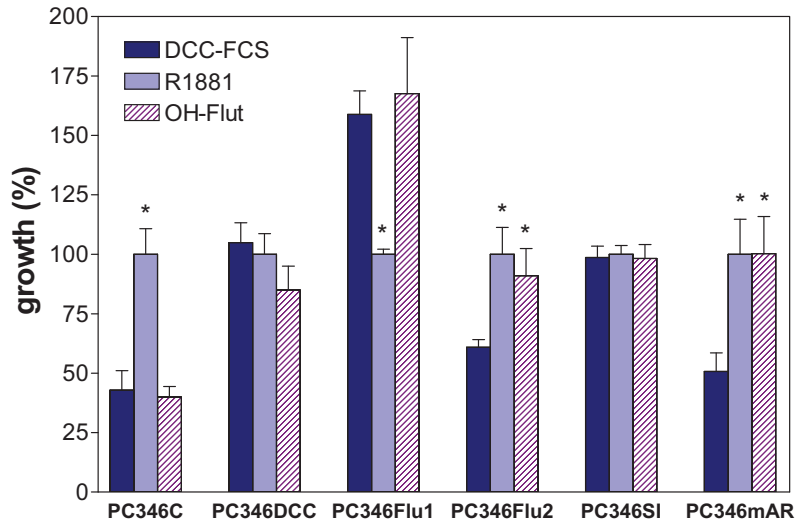


Figure 4 - Hormone sensitivity of PC346 in vitro cell lines. Cell growth was assessed after 10 days stimulation with 0.1 nM R1881 (R1881), 1 μ M hydroxyflutamide (OH-Flut) or vehicle (DCC-FCS), using a MTT assay described previously [39]. Growth in the presence of 0.1 nM R1881 was set at 100 % and the results are expressed as mean + SEM of at least three independent experiments. *p < 0.05 by non-parametric Mann-Whitney test.

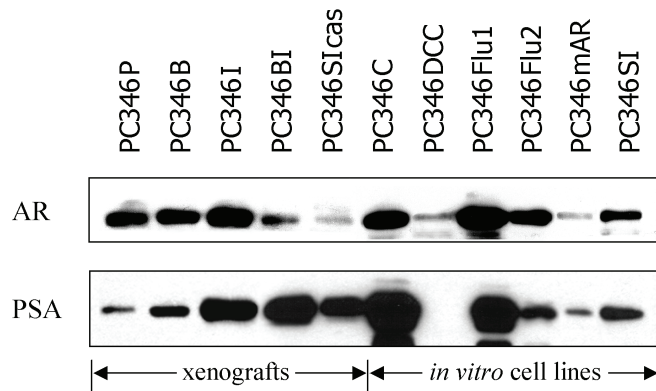


Figure 5 - Western blotting analysis of AR and PSA protein expression. Western blotting was performed on 10 μ g total protein extract, using rabbit polyclonal antibodies sp197 anti-human AR [67] and anti-human prostate-specific antigen (DakoCytomation BV, The Netherlands), as described previously [68]. For the protein isolation, the androgen-independent PC346I, PC346BI, and PC346SIcas xenografts were propagated in castrated male mice, while the parental androgen-sensitive lines PC346P and PC346B were propagated in intact males. Each *in vitro* cell line was cultured in its respective selection medium: PC346C and PC346mAR on medium supplemented 0.1 nM of R1881; PC346DCC and PC346SI on steroid-stripped medium; PC346Flu1 and PC346Flu2 on steroid-stripped medium supplemented with 1 μ M OH-flutamide.

Theoretically, androgen-dependent PCa cells have two possible strategies to evade androgen ablation and/or antiandrogen therapy: to adapt the AR pathway, or to invoke an alternative survival/growth pathway [43, 44]. Our observations with the PC346 AI sublines suggest that the AR pathway may still be important and functionally active in most hormone-refractory cancers. Indeed, other groups have observed in patient material increased AR levels in relapsed tumors in comparison to primary tumors [45, 46], while AR gene amplification has been reported in up to 30% of recurrent cancers [13, 47, 48]. It has been proposed that higher receptor levels could lead to sensitization to residual androgen concentrations and broadened ligand-specificity [49] or to constitutive ligand-independent activation [50]. Recently, Han *et al.* reported a somatic AR mutation (E251G), which is able to convert the receptor into a potent oncogene sufficient to cause invasive and metastatic PCa in transgenic mice [51]. This new data suggests that the AR may be a proto-oncogene and that alteration of the normal AR signaling can facilitate transformation and progression. Additionally, AR point mutations that alter the activity and binding-specificity of the receptor have been clinically associated with disease progression [52, 53]. The T877A mutation was the first AR mutation described in PC. It was first reported in the LNCaP cell line and is known to widen ligand-specificity of the receptor to estrogens, progestins, adrenal androgens and even to synthetic antiandrogens such as flutamide or cyproterone acetate [54]. The detection of the T877A mutation in the PC346mAR and PC346Flu2 cell lines was consistent with the results of the *in vitro* proliferation assay, which showed growth stimulation in presence of either R1881 or hydroxyflutamide. It is striking that the same mutation has been found in three lines of the panel: PC346I, PC346mAR and PC346Flu2. PC346mAR was established *in vitro* from the PC346I xenograft, which explains the presence of the mutation in the cell line. Codon 877 of the AR gene is in fact a known mutation “hotspot” in hormone-refractory PC, justifying the idea that the T877A mutation may have arisen independently in PC346I and PC346Flu2 [55-57]. To further investigate the origin of the T877A mutation in the PC346 model, we performed allele-specific oligo (ASO) hybridization, a sensitive technique capable of identifying 1 mutated cell out of 99 cells with *wild-type* AR. ASO blotting did not detect the T877A mutation in the patient’s TUR material nor in any other xenograft but PC346I, where it became detectable after 2 subsequent passages in female mice. The fact that the mutation is not present in the other AI xenografts and that the original PC346P has retained its hormone response properties, suggests that it may have occurred spontaneously, being selected for by propagation in female mice. Nevertheless, we cannot exclude that cells with mutated AR were already present in the patient, representing less than 1% of an originally heterogeneous cell population. To assess the stability of the *in vitro* cultures and exclude that the AR mutations arose due to genomic instability, these were previously analyzed using Genome-wide Comparative Genomic Hybridization (CGH) microarrays [39]. We found few chromosomal abnormalities, most of them present in every cell line, indicating that they originated prior to the development of the sublines. Only four chromosomal modifications detected in the androgen-independent sublines were not present in the parental PC346C, loss of chromosome Y and gain of 18 in PC346Flu2, loss of 8p in PC356DCC and gain of 11 in PC346mAR, which confirms the relative genomic stability of the sublines [39].

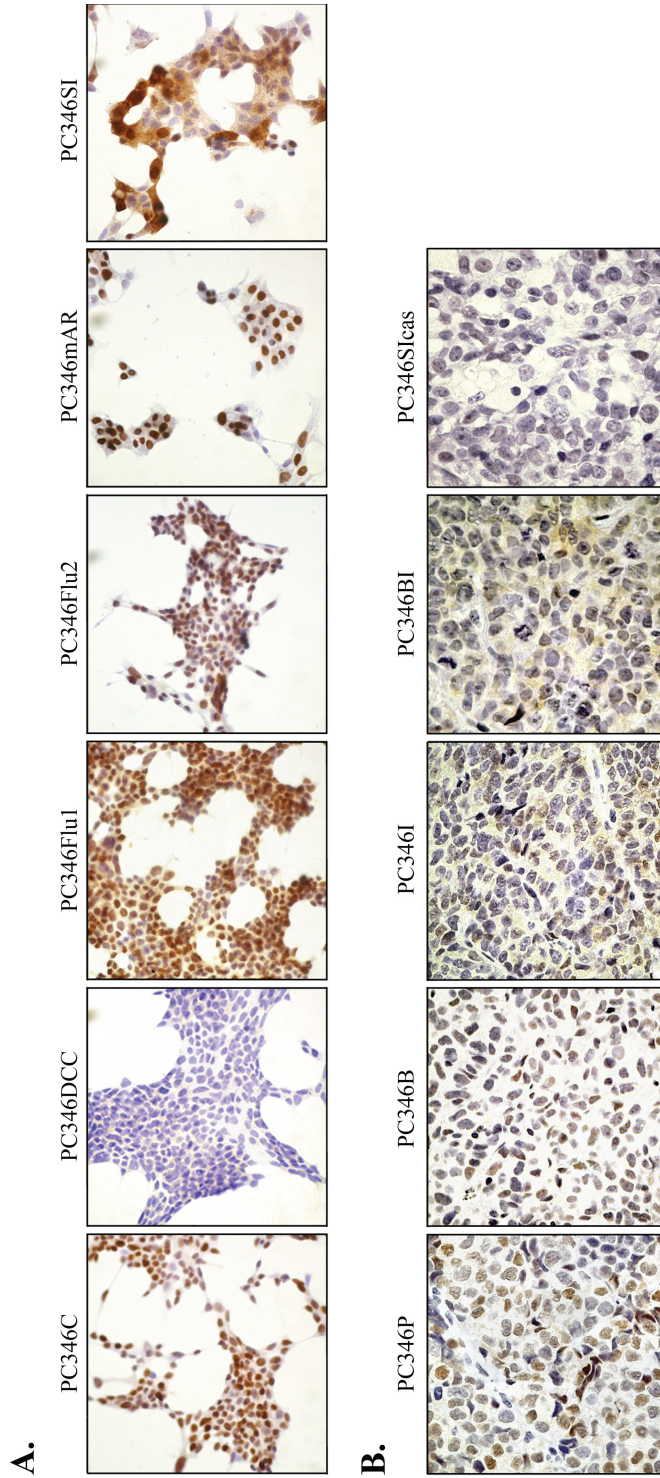


Figure 6 - Androgen receptor immunocytochemistry of the PC346 *in vitro* cell lines (A) and xenografts (B). Each line was cultured under the selection conditions described in figure 5. Specimens were incubated with anti-AR monoclonal primary antibodies AR441 (NeoMarkers) for the xenografts and F39.4.1 [69] for the *in vitro* lines, stained with diaminobenzidine (DAB) and counter-stained with hematoxylin.

The PC346BI, PC346SI and PC346DCC express low levels of AR and PSA, and are unresponsive to hormonal manipulations, suggesting that they may have bypassed the AR pathway. The mechanisms for bypassing the AR pathway are not yet fully known, but may involve autocrine production of growth-stimulatory factors [58], activation of oncogenes [59] and/or downregulation of apoptotic signals [60, 61].

The androgen-responsive characteristics and the status of the AR pathway in the PC346 panel are summarized in Table 3.

Table 3 - Overview of the PC346 panel: AR status, PSA expression and androgen-responsiveness

| | AR status | | PSA expression | Hormone response |
|-----------------|------------|----------------------|----------------|------------------|
| | Expression | Sequence (exons 2-8) | | |
| PC346P xeno | + | wt | + | ++ |
| PC346B xeno | + | wt | + | ++ |
| PC346I xeno | ++ | T877A | ++ | - |
| PC346BI xeno | -/+ | wt | ++ | - |
| PC346Sicas xeno | -/+ | wt | + | - |
| PC346C cells | + | wt ^a | ++ | ++ |
| PC346DCC cells | -/+ | K311R ^a | - | - |
| PC346Flu1 cells | ++ | wt ^a | ++ | + ^b |
| PC346Flu2 cells | + | T877A ^a | + | + |
| PC346mAR cells | -/+ | T877A | -/+ | + |
| PC346SI cells | + | wt | + | - |

^a For these cell lines, exon 1 of the AR gene was previously analysed by automatic sequencing [39].

^b Proliferation of PC346Flu1 is inhibited by androgens at physiologic concentrations (Fig. 4).

Comparison to other xenograft and cell line model systems for human prostate cancer

PC346P and PC346B are among the very few PCa xenografts exhibiting androgen-sensitive growth characteristics and wtAR expression. Although these tumors rarely develop in female and castrated male mice, castration of mice bearing established PC346P tumors resulted in variable responses, including tumor regression, tumor retardation followed by growth relapse, or continued growth. Interestingly, established PC346B tumors did not significantly respond to castration. This is in contrast to the strictly androgen-dependent xenografts PC82, PC295 and PC310 previously established in our laboratory [3, 7, 62], which do not develop in females or castrated males and show complete regression after castration of tumor-bearing animals without tumor relapse.

The LAPC-4 [16] and LuCaP-23 [10] xenograft models have been reported to show a response to castration very similar to our results with PC346P xenograft. In contrast to PC346P, LuCaP-23 tumors seem less dependent on androgens, since tumors do develop and grow in castrated mice. CWR22 [9] and LAPC-9 [17] also show recurrent growth after androgen ablation, but with a considerably longer (3-6 months) time to relapse. The LAPC and LuCaP models were derived from metastatic lesions of

patients with hormone-refractory disease, while CWR22 expresses the rare H874Y mutant AR [63], therefore raising the question whether these are representative models for the hormone-naïve stage of PC. In contrast, PC346P is derived from a primary tumor of a non-progressive patient and is androgen-sensitive, although with a heterogeneous response to castration.

The number of *in vitro* PCa cell line models is limited, and most of them represent the late-stage hormone-refractory phenotype. Until recently, the majority of the *in vitro* studies were based on the “classical” LNCaP, PC3 and Du145 cell lines. Although most prostate tumors are AR-positive, PC3 [20] and Du145 [21] show little or no AR and PSA expression [64]. Also, the androgen-responsive LNCaP cell line, often used as a model for androgen-dependent disease, has altered hormone-response properties due to the expression of a mutated AR [65]. Over the past decade, a few novel PCa cell lines have become available, among which ARCaP, VCaP, DuCaP, LAPC-4, MDA PCa 2a/b and CWR22Rv1 [66]. Of all these cell lines, the lymph node derived LAPC-4 is the only one that presents truly androgen-dependent characteristics [66]. Therefore, the androgen-sensitive PC346C cell line, derived from a primary tumor and expressing *wild-type* AR, is a unique and valuable contribution to the available *in vitro* models.

CONCLUSIONS

The PC346 model consists of a panel of six cell lines and five xenografts that recapitulates the relapse phenomenon observed in patients upon endocrine therapy: after an initial response to androgen ablation, tumors ultimately resume growth in an androgen-independent manner. By *in vivo* and *in vitro* hormonal manipulations of the androgen-sensitive PC346P, PC346B and PC34C, we established a set of AI sublines, which reproduce the most common AR modifications observed in hormone-refractory disease: downregulation, overexpression and mutation. This unique panel of xenografts and cell lines constitutes a valuable PCa progression model for basic and translational research.

ACKNOWLEDGMENTS

We thank Karin Hermans for the sequencing and Single Strand Conformation Polymorphism (SSCP) analysis of the AR gene, Dr. Hein van der Poel for the allele-specific oligo (ASO) hybridization, and Denie Zonruiter and Suzanne Reneman for biotechnical assistance in the animal care and propagation of the xenografts.

This study was supported by the Netherlands Organization for Scientific Research (NWO; 903-46-187), the Dutch Cancer Society (KWF; NKB97-1479) and the Foundation for Scientific Urological Research (SUWO; 00-037).

REFERENCES

1. Navone NM, Logothetis CJ, von Eschenbach AC and Troncoso P. Model systems of prostate cancer: uses and limitations. *Cancer Metastasis Rev* 1998. 17(4): 361-71.
2. Van Bokhoven A, Varella-Garcia M, Korch C, Johannes WU, Smith EE, Miller HL, Nordeen SK, Miller GJ and Lucia MS. Molecular characterization of human prostate carcinoma cell lines. *Prostate* 2003. 57(3): 205-25.
3. van Weerden WM and Romijn JC. Use of nude mouse xenograft models in prostate cancer research. *Prostate* 2000. 43(4): 263-71.
4. Wang Y, Revelo MP, Sudilovsky D, Cao M, Chen WG, Goetz L, Xue H, Sadar M, Shappell SB, Cunha GR and Hayward SW. Development and characterization of efficient xenograft models for benign and malignant human prostate tissue. *Prostate* 2005. 64(2): 149-59.
5. Hoehn W, Wagner M, Riemann JF, Hermanek P, Williams E, Walther R and Schruaffer R. Prostatic adenocarcinoma PC EW, a new human tumor line transplantable in nude mice. *Prostate* 1984. 5(4): 445-52.
6. Hoehn W, Schroeder FH, Reimann JF, Joebis AC and Hermanek P. Human prostatic adenocarcinoma: some characteristics of a serially transplantable line in nude mice (PC 82). *Prostate* 1980. 1(1): 95-104.
7. van Weerden WM, de Ridder CM, Verdaasdonk CL, Romijn JC, van der Kwast TH, Schroeder FH and van Steenbrugge GJ. Development of seven new human prostate tumor xenograft models and their histopathological characterization. *Am J Pathol* 1996. 149(3): 1055-62.
8. Pretlow TG, Wolman SR, Micale MA, Pelley RJ, Kursh ED, Resnick MI, Bodner DR, Jacobberger JW, Delmoro CM, Giaconia JM and et al. Xenografts of primary human prostatic carcinoma. *J Natl Cancer Inst* 1993. 85(5): 394-8.
9. Nagabhushan M, Miller CM, Pretlow TP, Giaconia JM, Edgehouse NL, Schwartz S, Kung HJ, de Vere White RW, Gumerlock PH, Resnick MI, Amini SB and Pretlow TG. CWR22: the first human prostate cancer xenograft with strongly androgen-dependent and relapsed strains both in vivo and in soft agar. *Cancer Res* 1996. 56(13): 3042-6.
10. Ellis WJ, Vessella RL, Buhler KR, Bladou F, True LD, Bigler SA, Curtis D and Lange PH. Characterization of a novel androgen-sensitive, prostate-specific antigen-producing prostatic carcinoma xenograft: LuCaP 23. *Clin Cancer Res* 1996. 2(6): 1039-48.
11. Lee YG, Korenchuk S, Lehr J, Whitney S, Vessella R and Pienta KJ. Establishment and characterization of a new human prostatic cancer cell line: DuCaP. *In Vivo* 2001. 15(2): 157-62.
12. Buhler KR, Quinn JE, Whitney SC, Lin DW, Ellis WJ, Corey E, Liu AY, True LD, Lange PH, Vessella RL, Macoska JA and Bruchovsky N. Progression to androgen-independent LNCaP human prostate tumors: cellular and molecular alterations. *J Urol* 1999. 161(4S): 58.
13. Linja MJ, Savinainen KJ, Saramaki OR, Tammela TL, Vessella RL and Visakorpi T. Amplification and overexpression of androgen receptor gene in hormone-refractory prostate cancer. *Cancer Res* 2001. 61(9): 3550-5.
14. Laitinen S, Karhu R, Sawyers CL, Vessella RL and Visakorpi T. Chromosomal aberrations in prostate cancer xenografts detected by comparative genomic hybridization. *Genes Chromosomes Cancer* 2002. 35(1): 66-73.
15. True LD, Buhler K, Quinn J, Williams E, Nelson PS, Clegg N, Macoska JA, Norwood T, Liu A, Ellis W, Lange P and Vessella R. A neuroendocrine/small cell prostate carcinoma xenograft-LuCaP 49. *Am J Pathol* 2002. 161(2): 705-15.
16. Klein KA, Reiter RE, Redula J, Moradi H, Zhu XL, Brothman AR, Lamb DJ, Marcelli M, Beldegrun A, Witte ON and Sawyers CL. Progression of metastatic human prostate cancer to androgen independence in immunodeficient SCID mice. *Nat Med* 1997. 3(4): 402-8.
17. Craft N, Chhor C, Tran C, Beldegrun A, DeKernion J, Witte ON, Said J, Reiter RE and Sawyers CL. Evidence for clonal outgrowth of androgen-independent prostate cancer cells from androgen-dependent tumors through a two-step process. *Cancer Res* 1999. 59(19): 5030-6.

18. Harper ME, Goddard L, Smith C and Nicholson RI. Characterization of a transplantable hormone-responsive human prostatic cancer xenograft TEN12 and its androgen-resistant sublines. *Prostate* 2004. 58(1): 13-22.
19. McCulloch DR, Opeskin K, Thompson EW and Williams ED. BM18: A novel androgen-dependent human prostate cancer xenograft model derived from a bone metastasis. *Prostate* 2005. 65(1): 35-43.
20. Kaighn ME, Narayan KS, Ohnuki Y, Lechner JF and Jones LW. Establishment and characterization of a human prostatic carcinoma cell line (PC-3). *Invest Urol* 1979. 17(1): 16-23.
21. Stone KR, Mickey DD, Wunderli H, Mickey GH and Paulson DF. Isolation of a human prostate carcinoma cell line (DU 145). *Int J Cancer* 1978. 21(3): 274-81.
22. Horoszewicz JS, Leong SS, Chu TM, Wajsman ZL, Friedman M, Papsidero L, Kim U, Chai LS, Kakati S, Arya SK and Sandberg AA. The LNCaP cell line--a new model for studies on human prostatic carcinoma. *Prog Clin Biol Res* 1980. 37: 115-32.
23. Williams RD. Human urologic cancer cell lines. *Invest Urol* 1980. 17(5): 359-63.
24. Grossman HB, Wedemeyer G, Ren L and Carey TE. UM-SCP-1, a new human cell line derived from a prostatic squamous cell carcinoma. *Cancer Res* 1984. 44(9): 4111-7.
25. Zhou HY, Chang SM, Chen BQ, Wang Y, Zhang H, Kao C, Sang QA, Pathak SJ and Chung LW. Androgen-repressed phenotype in human prostate cancer. *Proc Natl Acad Sci U S A* 1996. 93(26): 15152-7.
26. Navone NM, Olive M, Ozen M, Davis R, Troncoso P, Tu SM, Johnston D, Pollack A, Pathak S, von Eschenbach AC and Logothetis CJ. Establishment of two human prostate cancer cell lines derived from a single bone metastasis. *Clin Cancer Res* 1997. 3(12 Pt 1): 2493-500.
27. Sramkoski RM, Pretlow TG, 2nd, Giaconia JM, Pretlow TP, Schwartz S, Sy MS, Marengo SR, Rhim JS, Zhang D and Jacobberger JW. A new human prostate carcinoma cell line, 22Rv1. *In Vitro Cell Dev Biol Anim* 1999. 35(7): 403-9.
28. Kim CJ, Kushima R, Okada Y and Seto A. Establishment and characterization of a prostatic small-cell carcinoma cell line (PSK-1) derived from a patient with Klinefelter syndrome. *Prostate* 2000. 42(4): 287-94.
29. Gregory CW, Johnson RT, Jr., Mohler JL, French FS and Wilson EM. Androgen receptor stabilization in recurrent prostate cancer is associated with hypersensitivity to low androgen. *Cancer Res* 2001. 61(7): 2892-8.
30. Korenchuk S, Lehr JE, L MC, Lee YG, Whitney S, Vessella R, Lin DL and Pienta KJ. VCaP, a cell-based model system of human prostate cancer. *In Vivo* 2001. 15(2): 163-8.
31. Koochekpour S, Zhuang YJ, Beroukhim R, Hsieh CL, Hofer MD, Zhou HE, Hiraiwa M, Pattan DY, Ware JL, Luftig RB, Sandhoff K, Sawyers CL, Pienta KJ, Rubin MA, Vessella RL, Sellers WR and Sartor O. Amplification and overexpression of prosaposin in prostate cancer. *Genes Chromosomes Cancer* 2005. 44(4): 351-64.
32. van Steenbrugge GJ, Groen M, de Jong FH and Schroeder FH. The use of steroid-containing Silastic implants in male nude mice: plasma hormone levels and the effect of implantation on the weights of the ventral prostate and seminal vesicles. *Prostate* 1984. 5(6): 639-47.
33. Heppner GH. Tumor heterogeneity. *Cancer Res* 1984. 44(6): 2259-65.
34. Isaacs JT and Coffey DS. Adaptation versus selection as the mechanism responsible for the relapse of prostatic cancer to androgen ablation therapy as studied in the Dunning R-3327-H adenocarcinoma. *Cancer Res* 1981. 41(12 Pt 1): 5070-5.
35. Macintosh CA, Stower M, Reid N and Maitland NJ. Precise microdissection of human prostate cancers reveals genotypic heterogeneity. *Cancer Res* 1998. 58(1): 23-8.
36. Cheng L, Song SY, Pretlow TG, Abdul-Karim FW, Kung HJ, Dawson DV, Park WS, Moon YW, Tsai ML, Linehan WM, Emmert-Buck MR, Liotta LA and Zhuang Z. Evidence of independent origin of multiple tumors from patients with prostate cancer. *J Natl Cancer Inst* 1998. 90(3): 233-7.
37. Bostwick DG, Shan A, Qian J, Darson M, Maihle NJ, Jenkins RB and Cheng L. Independent origin of multiple foci of prostatic intraepithelial neoplasia: comparison with matched foci of prostate carcinoma. *Cancer* 1998. 83(9): 1995-2002.

38. So A, Gleave M, Hurtado-Col A and Nelson C. Mechanisms of the development of androgen independence in prostate cancer. *World J Urol* 2005. 23(1): 1-9.
39. Marques RB, Erkens-Schulze S, de Ridder CM, Hermans KG, Waltering K, Visakorpi T, Trapman J, Romijn JC, van Weerden WM and Jenster G. Androgen receptor modifications in prostate cancer cells upon long-term androgen ablation and antiandrogen treatment. *Int J Cancer* 2005. 117(2): 221-9.
40. Gelmann EP. Molecular biology of the androgen receptor. *J Clin Oncol* 2002. 20(13): 3001-15.
41. van der Kwast TH, Schalken J, Ruizeveld de Winter JA, van Vroonhoven CC, Mulder E, Boersma W and Trapman J. Androgen receptors in endocrine-therapy-resistant human prostate cancer. *Int J Cancer* 1991. 48(2): 189-93.
42. Ruizeveld de Winter JA, Janssen PJ, Sleddens HM, Verleun-Mooijman MC, Trapman J, Brinkmann AO, Santerse AB, Schroder FH and van der Kwast TH. Androgen receptor status in localized and locally progressive hormone refractory human prostate cancer. *Am J Pathol* 1994. 144(4): 735-46.
43. Jenster G. The role of the androgen receptor in the development and progression of prostate cancer. *Semin Oncol* 1999. 26(4): 407-21.
44. Culig Z, Steiner H, Bartsch G and Hobisch A. Mechanisms of endocrine therapy-responsive and -unresponsive prostate tumours. *Endocr Relat Cancer* 2005. 12(2): 229-44.
45. Gregory CW, He B, Johnson RT, Ford OH, Mohler JL, French FS and Wilson EM. A mechanism for androgen receptor-mediated prostate cancer recurrence after androgen deprivation therapy. *Cancer Res* 2001. 61(11): 4315-9.
46. Henshall SM, Quinn DI, Lee CS, Head DR, Golovsky D, Brenner PC, Delprado W, Stricker PD, Grygiel JJ and Sutherland RL. Altered expression of androgen receptor in the malignant epithelium and adjacent stroma is associated with early relapse in prostate cancer. *Cancer Res* 2001. 61(2): 423-7.
47. Koivisto P, Kononen J, Palmberg C, Tammela T, Hyytinen E, Isola J, Trapman J, Cleutjens K, Noordzij A, Visakorpi T and Kallioniemi OP. Androgen receptor gene amplification: a possible molecular mechanism for androgen deprivation therapy failure in prostate cancer. *Cancer Res* 1997. 57(2): 314-9.
48. Brown RS, Edwards J, Dogan A, Payne H, Harland SJ, Bartlett JM and Masters JR. Amplification of the androgen receptor gene in bone metastases from hormone-refractory prostate cancer. *J Pathol* 2002. 198(2): 237-44.
49. Chen CD, Welsbie DS, Tran C, Baek SH, Chen R, Vessella R, Rosenfeld MG and Sawyers CL. Molecular determinants of resistance to antiandrogen therapy. *Nat Med* 2004. 10(1): 33-9.
50. Huang ZQ, Li J and Wong J. AR possesses an intrinsic hormone-independent transcriptional activity. *Mol Endocrinol* 2002. 16(5): 924-37.
51. Han G, Buchanan G, Ittmann M, Harris JM, Yu X, Demayo FJ, Tilley W and Greenberg NM. Mutation of the androgen receptor causes oncogenic transformation of the prostate. *Proc Natl Acad Sci U S A* 2005. 102(4): 1151-6.
52. Taplin ME, Rajeshkumar B, Halabi S, Werner CP, Woda BA, Picus J, Stadler W, Hayes DF, Kantoff PW, Vogelzang NJ and Small EJ. Androgen receptor mutations in androgen-independent prostate cancer: Cancer and Leukemia Group B Study 9663. *J Clin Oncol* 2003. 21(14): 2673-8.
53. Culig Z, Hobisch A, Hittmair A, Cronauer MV, Radmayr C, Bartsch G and Klocker H. Androgen receptor gene mutations in prostate cancer. Implications for disease progression and therapy. *Drugs Aging* 1997. 10(1): 50-8.
54. Veldscholte J, Ris-Stalpers C, Kuiper GG, Jenster G, Berrevoets C, Claassen E, van Rooij HC, Trapman J, Brinkmann AO and Mulder E. A mutation in the ligand binding domain of the androgen receptor of human LNCaP cells affects steroid binding characteristics and response to anti-androgens. *Biochem Biophys Res Commun* 1990. 173(2): 534-40.
55. Gaddipati JP, McLeod DG, Heidenberg HB, Sesterhenn IA, Finger MJ, Moul JW and Srivastava S. Frequent detection of codon 877 mutation in the androgen receptor gene in advanced prostate cancers. *Cancer Res* 1994. 54(11): 2861-4.

56. Suzuki H, Akakura K, Komiya A, Aida S, Akimoto S and Shimazaki J. Codon 877 mutation in the androgen receptor gene in advanced prostate cancer: relation to antiandrogen withdrawal syndrome. *Prostate* 1996. 29(3): 153-8.
57. Buchanan G, Greenberg NM, Scher HI, Harris JM, Marshall VR and Tilley WD. Collocation of androgen receptor gene mutations in prostate cancer. *Clin Cancer Res* 2001. 7(5): 1273-81.
58. Russell PJ, Bennett S and Stricker P. Growth factor involvement in progression of prostate cancer. *Clin Chem* 1998. 44(4): 705-23.
59. Catz SD and Johnson JL. BCL-2 in prostate cancer: a minireview. *Apoptosis* 2003. 8(1): 29-37.
60. Vlietstra RJ, van Alewijk DC, Hermans KG, van Steenbrugge GJ and Trapman J. Frequent inactivation of PTEN in prostate cancer cell lines and xenografts. *Cancer Res* 1998. 58(13): 2720-3.
61. Gurumurthy S, Vasudevan KM and Rangnekar VM. Regulation of apoptosis in prostate cancer. *Cancer Metastasis Rev* 2001. 20(3-4): 225-43.
62. van Weerden WM, van Kreuningen A, Elissen NM, Vermeij M, de Jong FH, van Steenbrugge GJ and Schroder FH. Castration-induced changes in morphology, androgen levels, and proliferative activity of human prostate cancer tissue grown in athymic nude mice. *Prostate* 1993. 23(2): 149-64.
63. Tan J, Sharief Y, Hamil KG, Gregory CW, Zang DY, Sar M, Gumerlock PH, deVere White RW, Pretlow TG, Harris SE, Wilson EM, Mohler JL and French FS. Dehydroepiandrosterone activates mutant androgen receptors expressed in the androgen-dependent human prostate cancer xenograft CWR22 and LNCaP cells. *Mol Endocrinol* 1997. 11(4): 450-9.
64. Chlenski A, Nakashiro K, Ketels KV, Korovaitseva GI and Oyasu R. Androgen receptor expression in androgen-independent prostate cancer cell lines. *Prostate* 2001. 47(1): 66-75.
65. Veldscholte J, Berrevoets CA, Ris-Stalpers C, Kuiper GG, Jenster G, Trapman J, Brinkmann AO and Mulder E. The androgen receptor in LNCaP cells contains a mutation in the ligand binding domain which affects steroid binding characteristics and response to antiandrogens. *J Steroid Biochem Mol Biol* 1992. 41(3-8): 665-9.
66. van Bokhoven A, Caires A, Maria MD, Schulte AP, Lucia MS, Nordeen SK, Miller GJ and Varella-Garcia M. Spectral karyotype (SKY) analysis of human prostate carcinoma cell lines. *Prostate* 2003. 57(3): 226-44.
67. Kuiper GG, de Rooter PE, Trapman J, Boersma WJ, Grootegoed JA and Brinkmann AO. Localization and hormonal stimulation of phosphorylation sites in the LNCaP-cell androgen receptor. *Biochem J* 1993. 291 (Pt 1): 95-101.
68. Jenster G, de Rooter PE, van der Korput HA, Kuiper GG, Trapman J and Brinkmann AO. Changes in the abundance of androgen receptor isoforms: effects of ligand treatment, glutamine-stretch variation, and mutation of putative phosphorylation sites. *Biochemistry* 1994. 33(47): 14064-72.
69. Zegers ND, Claassen E, Neelen C, Mulder E, van Laar JH, Voorhorst MM, Berrevoets CA, Brinkmann AO, van der Kwast TH, Ruizeveld de Winter JA and et al. Epitope prediction and confirmation for the human androgen receptor: generation of monoclonal antibodies for multi-assay performance following the synthetic peptide strategy. *Biochim Biophys Acta* 1991. 1073(1): 23-32.

Chapter 3

Androgen Receptor Modifications in Prostate Cancer Cells Upon Long-Term Androgen Ablation and Antiandrogen Treatment

Rute B. Marques¹, Sigrun Erkens-Schulze¹, Corrina M. de Ridder¹, Karin G. Hermans², Kati Waltering³, Tapio Visakorpi³, Jan Trapman², Johannes C. Romijn¹, Wytske M. van Weerden¹, Guido Jenster¹

¹Department of Urology and ²Department of Pathology, Josephine Nefkens Institute, Erasmus Medical Center, PO Box 2040, 3000 CA, Rotterdam, The Netherlands. ³Laboratory of Cancer Genetics, University of Tampere and Tampere University Hospital, FIN-33014 Tampere, Finland

International Journal of Cancer 2005; 17(2): 221-229

ABSTRACT

To study the mechanisms whereby androgen-dependent tumors relapse in patients undergoing androgen blockade, we developed a novel progression model for prostate cancer (PCa). The PC346C cell line, established from a transurethral resection of a primary tumor, expresses *wild-type (wt)* androgen-receptor (AR) and secretes prostate-specific antigen (PSA). Optimal proliferation of PC346C requires androgens and is inhibited by the antiandrogen hydroxyflutamide. Orthotopic injection in the dorsal-lateral prostate of castrated athymic nude mice did not produce tumors, whereas fast tumor growth occurred in sham-operated males. Three androgen-independent sublines were derived from PC346C upon long-term *in vitro* androgen deprivation: PC346DCC, PC346Flu1 and PC346Flu2. PC346DCC exhibited androgen-insensitive growth, which was not inhibited by flutamide. AR and PSA were detected at very low levels, coinciding with a background AR activity in a reporter assay, which suggests that these cells have bypassed the AR pathway. PC346Flu1 and PC346Flu2 were derived by culture in steroid-stripped medium supplemented with hydroxyflutamide. PC346Flu1 strongly up-regulated AR expression and showed 10-fold higher AR activation than the parental PC346C. PC346Flu1 proliferation was inhibited *in vitro* by R1881 at concentrations ≥ 0.1 nM, consistent with a slower tumor growth rate in intact males than in castrated mice. PC346Flu2 carries the well-known T877A AR mutation, causing the receptor to become activated by diverse nonandrogenic ligands including hydroxyflutamide. Array-based Comparative Genomic Hybridization revealed little change between the various PC346 lines. The common alterations include gain of chromosomes 1, 7 and 8q and loss of 13q, which are frequently found in prostate cancer. In conclusion, by *in vitro* hormone manipulations of a unique androgen-dependent cell line expressing *wt*AR, we successfully reproduced common AR modifications observed in hormone-refractory prostate cancer: downregulation, overexpression and mutation.

INTRODUCTION

The androgens testosterone and dihydrotestosterone (DHT) are essential for the normal development and maintenance of the prostate but also sustain its malignant outgrowth. The actions of androgens are mediated by the androgen-receptor (AR), a member of the steroid receptor family and a chief regulatory transcription factor for genes involved in the proliferation and differentiation of the prostate [1]. As prostate cancer (PCa) development is initially dependent on androgens, androgen ablation, often supplemented with antiandrogens, is the mainstay therapy for metastasized disease [2]. Despite the initial success of this therapy, in most cases the cancer will relapse within 1-3 years as an incurable hormone-refractory condition.

The mechanisms whereby androgen-dependent tumors can survive and grow in patients under androgen blockade are not yet fully understood. Theoretically, androgen-dependent PCa cells have two possible strategies for growing in a low-androgen environment: to sensitize the AR pathway for high activity under low androgen concentrations or to bypass the AR pathway by invoking alternative survival and growth pathways [3,4].

Experimental observations suggest that the AR pathway may still be functionally active in hormone-refractory cancer. Immunohistochemical staining of tumor biopsies showed that the AR is expressed in most of the prostate cancers, often at higher levels in relapsed tumors than in primary tumors [5,6]. AR gene amplification has been reported in up to 30% of recurrent tumors [7,8,9]. How AR upregulation might confer a growth advantage under androgen ablation conditions is still not fully understood. In a recent study, Chen *et al* showed that increased levels of AR were sufficient to induce hormone-refractory growth in otherwise hormone-sensitive LNCaP and LAPC4 cells, which was in turn dependent on a functional ligand-binding domain [10]. It has been proposed that higher receptor levels could lead to sensitization for residual androgen concentrations and broadened ligand-specificity [10] or to constitutive ligand-independent activation [11]. Additionally, AR point mutations that alter the activity and binding specificity of the receptor have been clinically associated with disease progression. The first AR mutation described in PCa was the T877A mutation present in the LNCaP cell line, which widens ligand-specificity to estrogens, progestins, adrenal androgens and even to synthetic antiandrogens such as flutamide or cyproterone acetate [12]. Since then, AR sequence analysis has been carried out in numerous clinical samples, and a growing list of reported mutations can be found in the AR Mutation Database (<http://ww2.mcgill.ca/androgendb/>) [13]. Several findings suggest that the AR can also be activated in a ligand-independent fashion by cross-talk with polypeptide growth factor or cytokine signal transduction pathways [14]. Finally, alterations in the expression of various AR coregulators have been found in PCa cells and account for an additional mechanism to modulate AR activity [15,16,17].

All mechanisms discussed above depend on a functional AR pathway. Alternatively, androgen-dependent PCa cells may become truly androgen-independent, bypassing the need for the presence of androgens or the expression of the receptor. To effectively bypass the AR pathway, cells must be able to survive the apoptotic signal normally induced by androgen ablation and invoke alternative growth pathways. This hypothesis is supported by the high frequency of alterations in the anti-apoptotic Bcl-2

oncogene and in the pro-apoptotic PTEN tumor-suppressor gene in androgen-independent PCa [18,19,20,21,22]. Furthermore, several growth factors, which are normally regulated in a paracrine manner by nondiseased prostate stromal cells, are found to be upregulated in hormone-refractory cancer, concomitant with a switch to autocrine production by epithelial cancer cells [23].

To investigate the mechanisms regulating the proliferation of malignant cells in hormone-refractory disease, we developed a novel progression model for prostate cancer. The PC346C cell line was intentionally established from a primary tumor to represent the situation in hormone-naïve patients. It expresses wild-type AR and shows androgen-dependent growth characteristics. From PC346C, three androgen-independent sublines were derived by long-term culture in steroid-stripped medium either alone, PC346DCC, or supplemented with the antiandrogen flutamide, PC346Flu1 and PC346Flu2. These androgen-independent sublines show distinctive growth and hormone-sensitivity properties, providing an interesting model system to study the role of the AR and other pathways in androgen-independent growth.

MATERIAL AND METHODS

Reagents and cell lines

The basis culture medium used in the maintenance of PC346 cell lines consisted of DMEM-F12 (Cambrex BioWhitaker, Belgium) medium supplemented with 2% foetal calf serum (FCS; PAN Biotech GmbH, Aidenbach, Germany), 1% insulin-transferrin-selenium (Gibco BRL), 0.01% bovine serum albumin (Boehringer Mannheim, Germany), 10 ng/ml epidermal growth factor (Sigma-Aldrich), penicillin/streptomycin antibiotics (100 U/ml penicillin, 100 µg/ml streptomycin; BioWhitaker, Belgium); plus the following additions: 100 ng/ml fibronectin (Harbor Bio-Products, Tebu-bio, The Netherlands), 20 µg/ml fetuine (ICN Biomedicals, The Netherlands), 50 ng/ml cholera toxin, 0.1 mM phosphoethanolamine, 0.6 ng/ml triiodothyronine and 500 ng/ml dexametason (all from Sigma). For the MTT assays and transfections a simplified version of this medium was used, containing dextran-coated charcoal (DCC) treated FCS and without the additions.

The parental PC346C cell line was derived from the transurethral resection (TUR) of the prostate of a patient, which had negative scans for both bone and lymph node metastasis, and underwent four weeks treatment with Androcur® prior to the operation. This prostatic carcinoma specimen was initially implanted subcutaneously in male NMRI nu/nu mice (Taconic, M&B, Denmark), yielding the androgen-dependent PC346 xenograft [24,25]. The permanent *in vitro* PC346C cell line was subsequently established from the twelfth mouse passage of the PC346 xenograft. Cells were grown in T25 Primaria™ tissue culture flasks (BD Biosciences Benelux N.V, The Netherlands) at 37°C under 5% CO₂ humidified atmosphere, in the medium described above supplemented with 0.1 nM of R1881 (NEN, Boston MA, USA).

To mimic *in vitro* the endocrine therapy applied to patients with advanced metastatic PCa, we continuously cultured (>2 years) PC346C in androgen deprived conditions, producing the androgen independent sublines: PC346DCC, PC346Flu1 and PC346Flu2. PC346DCC was derived from passage 45 of PC346C by culturing in DCC-stripped medium. The flutamide resistant PC346Flu1 and PC346Flu2 sublines were

produced from passage 45 and 75 of PC346C, respectively, by culturing in DCC-stripped medium supplemented with 1 μ M of hydroxyflutamide (OH-flutamide, Schering-Plough Research Institute, New Jersey, USA).

Growth assays

To determine the effects of androgens and antiandrogens on cell proliferation, we performed a growth assay based on the enzymatic reduction of the tetrazolium salt MTT (3-[4,5-dimethylthiazol-2-yl]-2,5-diphenyl-tetrazoliumbromide; AppliChem, Belgium) by metabolically active cells. Cell growth was determined as described previously [26], with a few modifications. Briefly, 10^4 cells were seeded per well of 96-well microtiter plates, in 100 μ l of steroid-stripped medium (without additions). Cells were allowed to attach for 24 h, after which 8 wells were assayed immediately to establish t_0 . To the remaining wells, 100 μ l of culture medium was added either alone or supplemented with increasing concentrations of R1881 (ranging from 1 pM to 1 nM) or OH-flutamide (0.1 nM to 10 μ M); cells were then incubated for 7 or 10 days. At the end of the incubations, 30 μ l (15 μ l for t_0) of 5 mg/ml MTT was added to each well and cells were further incubated for 4 h at 37°C. After carefully removing the medium, we added to each well 100 μ l buffered DMSO (8 volumes of DMSO for 1 volume of buffer 0.1 M glycine, 0.1 M NaCl, pH 10.5), and determined the absorbance at 570 nm with a BIO-RAD 550 microplate reader. Wells containing medium alone served as blanks. The results were expressed as mean \pm SEM of at least three independent experiments, each with 8 replicate wells per cell line per hormonal condition.

Sequencing and FISH analysis of AR gene

Genomic DNA from the parental and derivative cell lines was isolated using the Puregene Genomic DNA Isolation kit (Gentra Systems, Minneapolis, USA), according to the manufacturer's protocol. Exons 1 to 8 of the AR were amplified by PCR in 12 portions using primers described previously [27], and automatically sequenced with ABI Prism Genetic Analyzer (Applied Biosystems). AR gene copy number was analyzed by fluorescence *in situ* hybridization (FISH) as described by Linja *et al* [7].

AR and PSA immunoblots

Cells were lysed in RIPA buffer (100 mM Tris-HCl pH 7.4, 5 mM EDTA, 1% Triton X-100, 1% desoxycholate, 0.1% SDS) with protease inhibitors. Protein concentrations were determined by a Bradford assay (BioRad) and 10 μ g of protein was loaded in sample buffer on a 30% SDS-polyacrylamide gel as described previously [28]. Gels were blotted onto a nitrocellulose membrane and the proteins of interest were visualized by chemiluminescence using the F39.4.1 anti-AR [29] or ER-Pr8 anti-PSA [30] mouse monoclonal antibodies and goat-anti-mouse secondary antibody conjugated with horseradish peroxidase (DakoCytomation BV, The Netherlands).

Quantitative TaqMan real-time PCR

Total RNA from two different passages of each cell line was isolated with RNAzol B reagent (Campro Scientific, Veenendaal, The Netherlands) according to the manufacturer's protocol. The RNA samples were further purified through RNeasy

columns (Qiagen), and the quality of the RNA was checked by 1 % agarose gel electrophoresis.

cDNA was synthesized from 2 µg total RNA: the samples were initially incubated with 10 ng/µl Oligo(dT)₁₂₋₁₈ primer (Invitrogen) for 10 min at 70°C, in 22 µl volume and chilled on ice. 8 µl 5x first-strand buffer (Invitrogen), 4 µl 100 mM DTT, 2 µl 10 mM dNTP mix, 20 U RNasin ribonuclease inhibitor (Promega) and 400 U MMLV-reverse transcriptase (Invitrogen) were then added, followed by 1h incubation at 37°C. Reverse transcriptase was inactivated by heating to 95°C for 10 min, and samples were stored at -20°C. Additionally, 0.5 µg RNA of each PC346 cell lines was pooled to produce the standard cDNA to be used in the calibration curve.

TaqMan real-time PCR analysis was performed in duplicate for each sample / standard on a 96-well Optical Reaction Plate with Barcode (Applied Biosystems), using an ABI Prism 7700 Sequence Detection System (PE Applied Biosystems). Amplification was performed in 40 µl reaction mixture, containing 1x Taqman buffer A (Applied Biosystems), 4 mM MgCl₂, 250 µM dNTPs mix, 2 ng/µl of each primer, 5 pmol FAM-labeled probe (Eurogentec, Belgium), 1U AmpliTaq Gold DNA polymerase (Applied Biosystems) and 8 µl of cDNA sample /standard. Primers and probes: AR forward, 5'-CATCAAGGAAGCTCGATCGT-3'; AR reverse, 5'-GAACTGATGCAGCTCTCTC-3'; AR probe, 5'-ACATCCTGCTCAAGACGCTCCT-3'; PSA forward, 5'-CCCTCAGAAGGT GACCA-3'; PSA reverse, 5'-ACCACCTTGGTGTACAGG-3'; PSA probe, 5'-TATCAC GTCATGGGGCAGTG-3'; RNA polymerase II forward, 5'-GATCGGAAGCACATGACT-3'; RNA polymerase II reverse, 5'-CTGTGGCAAGTGCATGTA-3'; RNA polymerase II probe, 5'-AAGATGCAAGAGGAGGAAGAGGT-3'. Gene specificity of the primers and probes was checked by BLAST queries and intron-spanning primers were chosen to avoid amplification of contaminating DNA. GAPDH primers and probe were purchased as kit Human GAPD (GAPDH) Endogenous Control (VIC probe) from Applied Biosystems. For each gene, a standard curve was constructed from serial dilutions of the reverse-transcribed PC346 RNA pool, which was then used to determine the quantity of target message from the threshold cycle (Ct) value. Two housekeeping genes were used as endogenous controls: RNA polymerase II and GAPDH. AR and PSA quantities for each sample were normalized against the average of the two internal controls. The results are presented for each cell line as the average relative quantity of the two passages analyzed ± SEM.

AR transactivation assays

PC346C and PC346Flu1 cells were seeded in 24-well plates at a density of 1×10^5 cells/well. To bring AR activity down to basal levels before the transfection, cells were androgen-starved in charcoal-stripped serum for 2 days. For the transfections, we added per well: 30 µl serum-free minimum medium containing 1 µl Fugene 6 (Boehringer Mannheim, Germany), 0.125 µg pEF4-LacZ control plasmid (Invitrogen BV, The Netherlands) and 0.125 µg (ARE)₂-TATA-Luc reporter plasmid [31] (previously referred to as ARE₂-E1b-luciferase), in a final volume of 500 µl. After overnight incubation, cells were stimulated for 24 h with 1 nM R1881, 1 µM OH-flutamide or 1 nM R1881 + 1 µM OH-flutamide. The next morning, cells were lysed in Reporter Lysis Buffer (Promega Benelux BV, The Netherlands) and the luciferase and galactosidase activities were measured as described previously [32]. The assay was performed in triplicate, each

experiment with 4 replicate wells per cell line per hormonal condition. Luciferase activity was normalized to the β -galactosidase control and the results are presented as the luciferase activity relative to PC346C basal activity in steroid-stripped medium.

Mouse tumor take assays

Orthotopic injections were performed on 6-8 weeks old male athymic nude NMRI nu/nu mice (Taconic, M&B, Denmark) as described previously [33], with some minor modifications. Briefly, cells in the exponential growth phase were harvested by trypsination, resuspended in PBS and 10^6 cells (in 20 μ l) were injected into one of the dorsal-lateral lobes of the prostate. Bilateral castration was performed one week prior to tumor cell injection using standard surgical techniques. Tumor growth was measured weekly by transrectal ultrasonography as described previously [34]. Tumor volume was calculated from formula $V = (\pi/6)(d_1 \times d_2)^{3/2}$, with d_1 and d_2 being two perpendicular tumor diameters. Mice were sacrificed when the tumor size reached 1500 mm³ or when showing signs of suffering from tumor burden. At the end of the experiment blood samples were collected for plasma PSA determination, as previously described [34]. The experiment was performed in two parts: first PC346Flu1 was tested and compared to the parental PC346C (10 castrated and 10 sham-operated mice were used per cell line); secondly, PC346DCC and PC346Flu2 were tested together with another group of the parental line (8 castrated and 8 sham-operated mice per cell line). Since there was no significant difference between the two PC346C groups, these results were analyzed together. All experiments were performed in agreement with The Netherlands' Experiments on Animals Act (1977) and the European Convention for Protection of Vertebrate Animals used for Experimental Purposes (Strasbourg, 18 March 1986). Approval was obtained from the Experimental Animal Committee (DEC). Tumor doubling times (TD) were determined by linear regression of 2Log-transformed tumor volume over time, using the previously described SAS procedure PROC MIXED (version 8.2, SAS Institute Inc., Cary, NC, USA) [35]. Doubling times were calculated from the 1/slope of tumor volume rise.

Genome-wide Comparative Genomic Hybridization (CGH) Arrays

For these experiments we used 1 Mb spaced genome-wide BAC arrays, containing a total of 3659 BAC clones robotically spotted in triplicate onto CMT-GAPS-coated slides (Ultra Gaps, Corning, Schiphol-Rijk, The Netherlands). These arrays were produced in the Department of Human Genetics, University Medical Center Nijmegen, The Netherlands, as described previously [36]. Probe labeling, array hybridization, image processing and data analysis were performed as previously described [36]. Briefly, 500 ng of the cell lines genomic DNA was labeled by random priming with Cy3-dUTP (Amersham Biosciences), combined with 500 ng Cy5-dUTP-labeled reference DNA and hybridized onto the genome-wide BAC arrays using a GeneTAC Hybridization Station (Genomic Solutions, Cambridgshire, UK). After scanning, Cy3 to Cy5 ratios were determined, log₂-transformed and normalized per array subgrid by Lowess regression with the software package SAS version 8.0 (SAS Institute). Thresholds for copy number gain and loss were set at log₂ Cy3/Cy5 ratio of +0.3 and -0.3, respectively.

RESULTS

Growth characteristics and hormone sensitivity of the PC364 cell line panel

The parental PC346C cell line showed androgen-responsive growth characteristics. PC346C proliferation was optimal in the presence of 0.1 nM of R1881 (Fig. 1A), which stimulated growth about 5-fold after 10 days incubation (Fig. 1B). This growth-stimulatory effect of R1881 was inhibited by 1 μ M OH-flutamide. In steroid-stripped (DCC) medium, the proliferation of PC346C was clearly impaired but cells could still survive and slowly divide (Fig. 1A). Long-term culture (>2 years) of the androgen-responsive PC346C cell line under androgen-deprived conditions resulted in the PC346DCC subline. PC346DCC exhibited true androgen-independent characteristics, with rapid proliferation in steroid-stripped medium and unresponsiveness to either R1881 or OH-flutamide. The flutamide-resistant PC346Flu1 and PC346Flu2 sublines were derived from PC346C by culturing in androgen-depleted medium supplemented with 1 μ M OH-flutamide. PC346Flu1 proliferated optimally under low androgen concentration, and growth inhibition was observed at R1881 concentrations \geq 0.1 nM ($P=0.05$), the optimal growth concentration for the parental line (Fig. 1B). Like PC346C, PC346Flu2 showed 2-fold growth stimulation with 0.1 nM R1881, but proliferated faster than the parental cell line in androgen-depleted medium. PC346Flu2 cells were not inhibited by OH-flutamide, which instead seemed to act as a growth agonist ($P=0.05$).

Sequencing and FISH analysis of the AR gene

AR sequencing revealed a *wild-type* AR in the parental PC346C and the PC346Flu1 subline. AR mutations were detected in both PC346DCC and PC346Flu2 sublines. In PC346DCC the K311R AR mutation was found, which has not been previously described in the literature. The T877A mutation was present in the PC346Flu2 subline. This mutation, which was originally reported for the LNCaP cell line, is well known for broadening AR specificity to diverse nonandrogenic steroids such as estrogens, progestins, adrenal androgens, and even the synthetic antiandrogen flutamide [12]. FISH analysis revealed that PC346C and all derivative sublines contain one copy of AR gene (data not shown).

AR and Prostate-Specific Antigen (PSA) expression

To assess the status of the AR pathway, expression of AR and the androgen-regulated PSA were analyzed by western blot and quantitative TaqMan RT-PCR. Western blot analysis showed that in PC346DCC the AR was downregulated to very low levels, concomitant with a decreased PSA expression (Fig. 2A). In contrast, AR protein expression in PC346Flu1 was upregulated by about 4-fold relative to the parental PC346C. PC346Flu2 showed AR protein levels identical to those observed in PC346C, although mRNA quantity seemed to be reduced (Fig. 2B). All cell lines expressed the prostate differentiation marker PSA when cultured in their respective selection medium. The highest PSA level was found for the androgen-dependent PC346C but it must be noted that its growth medium contained 0.1 nM R1881, in contrast to the selection medium for PC346Flu1 and PC346Flu2, which was supplemented with OH-flutamide. In general, TaqMan RT-PCR quantification confirmed the findings from the western blot analysis, revealing upregulation of PC346Flu1 AR mRNA and very low levels of AR and PSA mRNA in PC346DCC.

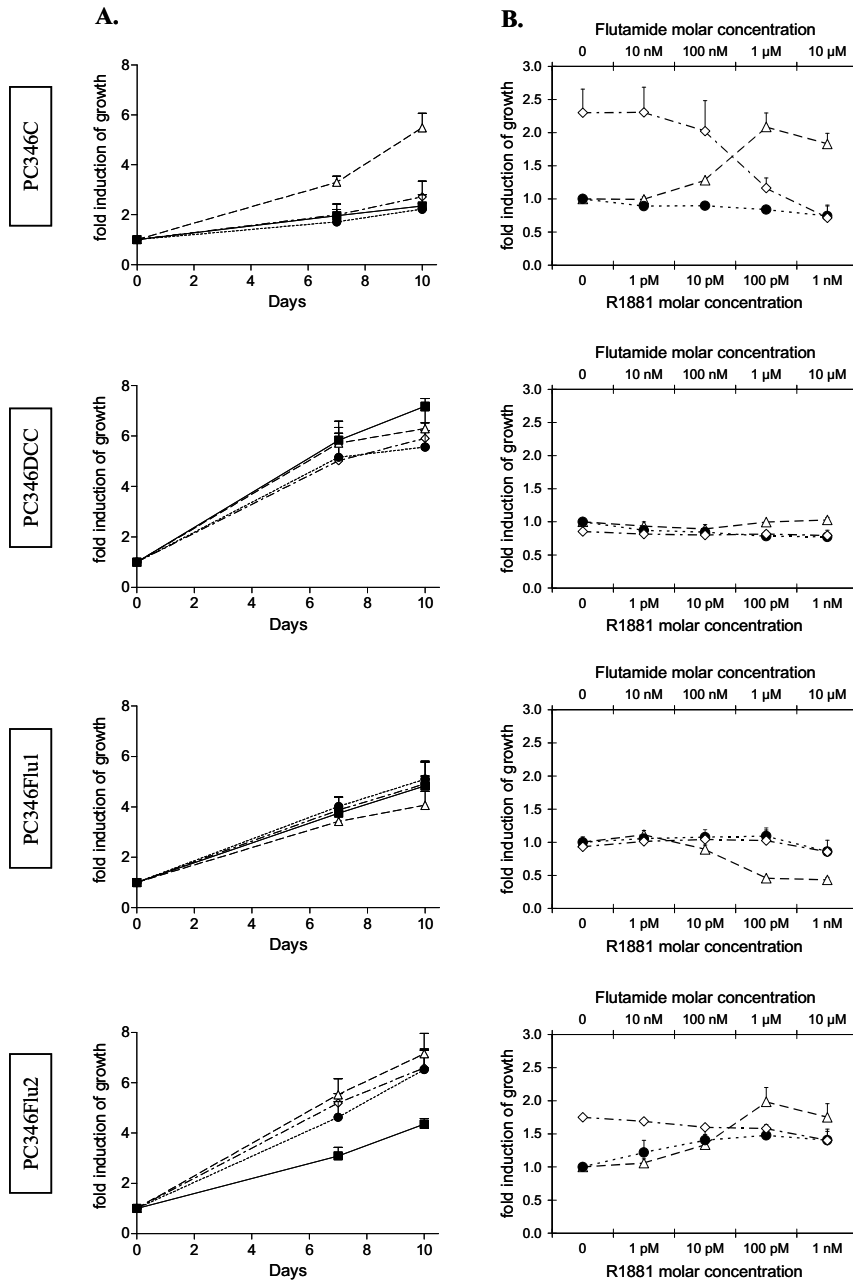


Figure 1 - Growth characteristics and hormone sensitivity of PC346 cell lines. **A**, PC346C, PC346DCC, PC346Flu1, PC346Flu2 cells were incubated in charcoal stripped-medium (■) supplemented with 0.1 nM R1881 (Δ), 1 μM OH-flutamide (●) or 1 μM OH-flutamide + 0.1 nM R1881 (◊). Cell number was measured by MTT assay on days 0, 7 and 10. Results are presented as fold increase in cell number relative to day 0. **B**, Cells were incubated for 10 days with increasing concentrations of R1881 (Δ; lower x-axis), OH-flutamide (●; upper x-axis)

or 0.1 nM R1881 with increasing concentrations of OH-flutamide (\diamond). Cell number was measured by MTT assay and results are presented as fold increase in cell number relative to no hormone addition. Values (\pm SEM) represent the mean of at least three independent experiments each carried out in 8 replicates.

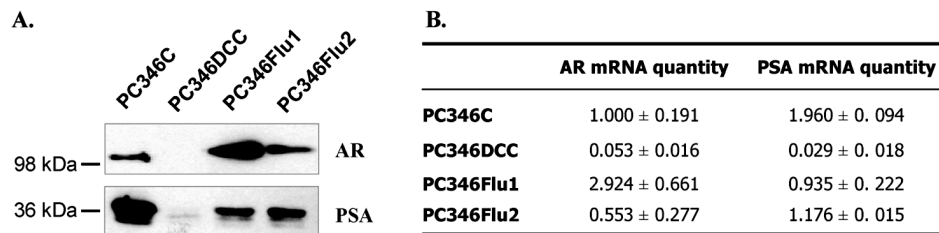


Figure 2 - Expression of AR and PSA in the parental and derivative cell lines. Each cell line was cultured in its respective selection medium: PC346C on medium supplemented with 2 % FCS and 0.1 nM of R1881, PC346DCC on medium supplemented with 2 % steroid-stripped FCS, PC346Flu1 and PC346Flu2 on medium supplemented with 2 % steroid-stripped FCS and 1 mM OH-flutamide. **A**, protein expression analyzed by western blotting. **B**, mRNA quantity determined by TaqMan real-time RT-PCR. AR and PSA quantities were normalized using the average of two internal controls: RNA polymerase II and GAPDH, and set at 1 for the parental PC346C. The relative values are presented as the mean of two different passages \pm SEM.

AR reporter transactivation studies

To determine whether the changes in cell proliferation in response to androgens and antiandrogens were concomitant with changes in AR pathway activity, transcriptional activity of the endogenous receptor was evaluated in a transactivation assay, using the androgen-responsive (ARE)₂-TATA minimum promoter linked to a luciferase reporter (Fig. 3). AR reporter activity in the parental PC346C was induced 12-fold by 1 nM R1881 but not by OH-flutamide. The PC346DCC subline showed background levels of AR reporter activity that remained unaffected by either hormone or antiandrogen. PC346Flu1, which expresses high levels of the AR protein, showed 50-fold induction with 1 nM R1881, a response that could not be effectively repressed by 1 μ M OH-flutamide. Flutamide, however, did not activate the AR reporter in this subline.

Animal studies

To extend the *in vivo* characterization in an *in vivo* setting, the parental PC346C and derivative sublines were injected orthotopically into male athymic nude mice and tumor growth was monitored weekly by transrectal ultrasonography (Fig. 4). Tumor take and tumor doubling time (TD) were compared in non-castrated versus castrated mice between the different cell lines (Table 1). In accordance to the *in vitro* studies, also in the *in vivo* assay, PC346C showed androgen-dependent characteristics. Although no tumor developed in castrated animals, tumor-growth in sham-operated males occurred in 17 out of the 18 animals tested, with doubling time (TD) of 6.7 days. The PC346DCC subline, which exhibited hormone-unresponsive proliferation *in vitro*, produced tumors in both castrated and sham-operated mice. However, tumor growth was slower and more variable in castrated mice than in sham-operated mice (TD 16.3 vs. 7.6 days, $P = 0.06$).

In contrast, PC346Flu1 tumors grew faster in castrated animals than in androgenically intact males (TD 6.7 vs. 13.0 days, $P < 0.0001$). These results are in agreement with the growth-inhibitory effect of androgens on this subline initially revealed by the *in vitro* assay. Like that of PC346C, *in vivo* tumor growth of PC346Flu2 was also greatly affected by castration of the animals, with only 3 out of 8 castrated mice developing tumors bigger than 100 mm³.

At the end of the experiments, serum samples were taken from each animal to quantify the PSA produced by the orthotopic xenografts. PSA levels were the highest in the mice bearing the androgen-sensitive PC346C and PC346Flu2 tumors, and very low in castrated mice and mice bearing the androgen-unresponsive PC346DCC (Table 1). It is noteworthy that, in androgenically intact mice, PC346Flu1 expresses considerably less PSA than the parental line, despite showing an augmented response to hormone in the *in vitro* transactivation assay.

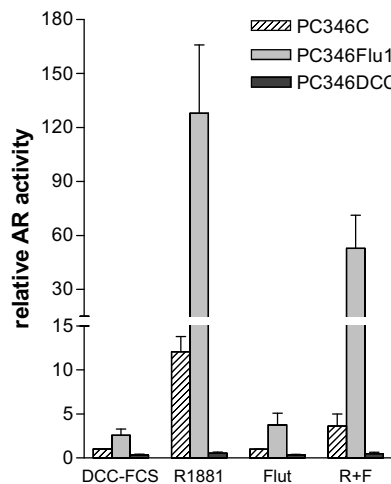


Figure 3 - Transactivation of the (ARE)₂-TATA-Luc reporter in PC346C, PC346Flu1 and PC346DCC. Cells were transiently transfected with the (ARE)₂-TATA-Luc reporter and pEF₄LacZ for normalization, and stimulated for 24h with either steroid-stripped medium alone (DCC-FCS) or supplemented with 1 nM R1881 (R1881), 1 μM OH-flutamide (Flut) or 1 nM R1881 + 1 μM OH-flutamide (R+F). AR activity is presented as the normalized luciferase activity relative to the basal activity of parental PC346C in steroid-stripped medium (DCC-FCS), which was set at 1.

Genome-wide Comparative Genomic Hybridization (CGH) Arrays

Array CGH was performed to assess the genomic stability of the cell lines and to determine whether major chromosomal alterations were associated with the development of androgen independence. PC346 and derivative sublines appeared to be stable presenting few chromosomal abnormalities. All cell lines showed amplifications of chromosomes 1, 7, 8q and 20, and deletion of 13q and of a small region in chromosome 10q around the PTEN locus (Fig. 5). Only three major chromosomal modifications were found in the androgen-independent sublines: PC346Flu2 showed amplification of chromosome 18 and deletion of Y, whereas PC346DCC presented a deletion in 8p.

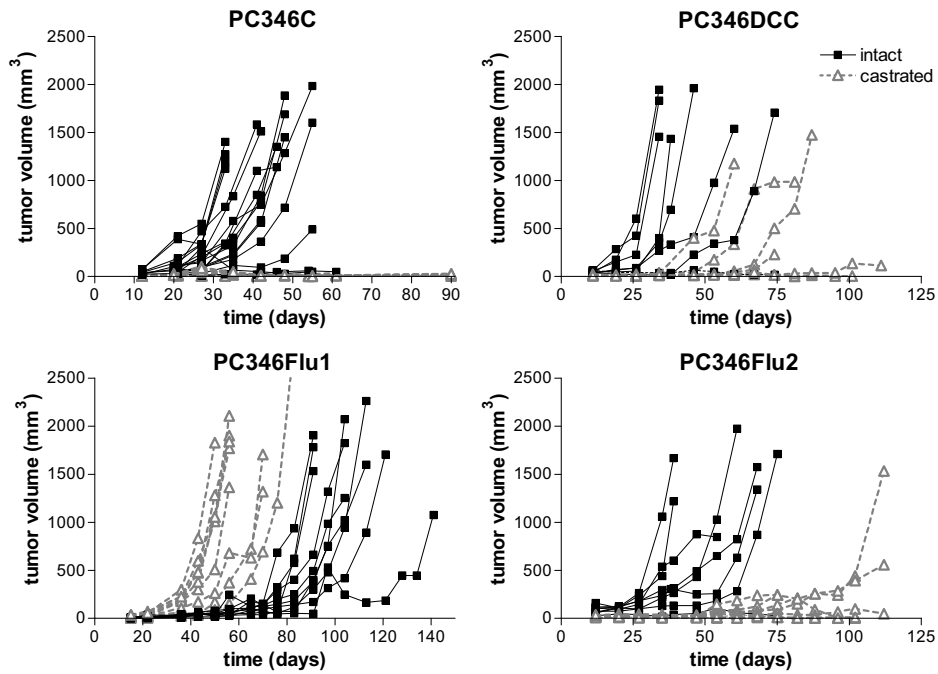


Figure 4 - In vivo growth of the parental and derivative cell lines in castrated versus androgenically intact male mice. 1 million cells were injected orthotopically in the dorsal-lateral lobe of the prostate of NMRI nu/nu mice and tumor growth was monitored weekly by transurethral ultrasonography. Graphical representation of tumor growth in sham-operated males —■— compared to growth in animals castrated 1 week prior to injection --△--. Each line represents one animal.

Table 1 - Tumor doubling time (TD) and PSA secretion in intact versus castrated mice

| | Intact males | | Castrated males | | P-value TD Intact vs. Castrated |
|------------------|----------------------|----------------------------|-----------------------|----------------------------|--|
| | TD (days) | PSA index (ng/ml per g) | TD (days) | PSA index (ng/ml per g) | |
| PC346C | 6.7 (5.6 - 8.3) | 459.8 ± 136.4 | — | — | <0.0001 |
| PC346DCC | 7.6 (5.8 - 11.3) | 58.8 ± 29.4 | 16.3 (10.0 - 44.9) | <i>b.d.</i> | 0.0600 |
| PC346Flu1 | 13.0 (9.3 - 21.3) | 169.6 ± 139.6 | 6.7 (5.4 - 8.8) | 70.5 ± 5.6 | 0.0096 |
| PC346Flu2 | 12.4 (8.4 - 23.7) | 342.3 ± 145.4 | 58.2 * | 65.6 ± 5.3 | <0.0001 |

Tumor doubling times (TD), 95% confidence intervals (in parentheses below TD) and p-values were calculated using the SAS procedure Proc Mixed [35]. Tumor PSA expression was determined in mouse serum from tumor-takers, and is presented as ng PSA / ml serum per g of tumor (PSA index). Since PC346C castrated mice did not develop tumors, TD and PSA index were not determined for this group. * Calculation of the TD was not statistically reliable since only 3 animals developed tumors. *b.d.*, below detection.

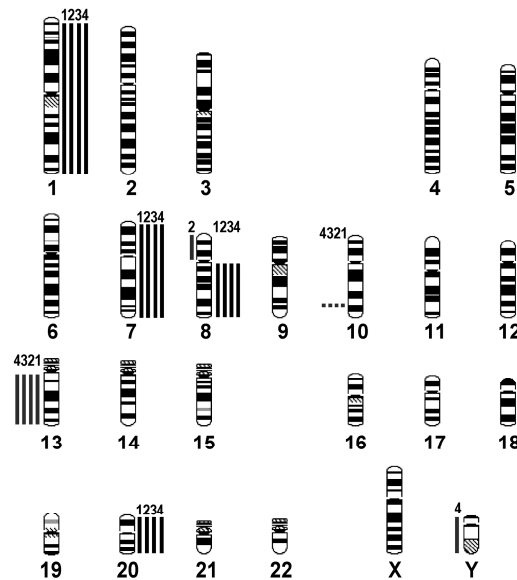


Figure 5 - Chromosomal alterations identified by genome-wide CGH Arrays. A black bar to the right of the chromosome indicates amplification, whereas a grey bar to the left indicates loss of a chromosomal region. The numbers above the lines represent the cell lines: PC324C (1), PC346DCC (2), PC346Flu1 (3) and PC346Flu2 (4).

DISCUSSION

Theoretically, androgen-dependent prostate cancer (Pca) cells have two possible strategies to evade androgen ablation and/or antiandrogen therapy: to adapt the AR pathway, or to invoke an alternative survival/growth pathway. In practice however, these strategies are not mutually exclusive and PCa cells probably use a balance of both to their advantage. We show here that long-term *in vitro* hormone depletion can reproduce the most common AR modifications observed in hormone-refractory prostate cancer patients: PC346Flu1 and PC346Flu2 have adapted their AR pathway, by AR overexpression or mutation, respectively, whereas PC346DCC seems to have bypassed the AR pathway (Fig. 6).

Human prostate carcinomas are among the most difficult cell types from which to establish permanent *in vitro* cultures, which has hampered the development of cell line models representative of the different stages of this disease. Until recently, the majority of the *in vitro* studies were based on a limited number of cell lines: LNCaP, PC3 and DU145. Although most prostate tumors are AR-positive, the “classical” PC3 [37] and Du145 [38] cells show little or no AR and PSA expression [39]. Also, the androgen-

responsive LNCaP cell line, often used as a model for early androgen-responsive disease, has altered hormone-responsive properties due to the expression of a mutated AR [40]. Over the past decade, a few novel PCa cell lines have become available, among which the ARCaP, VCaP, DuCaP, LAPC-4, MDA PCa 2a/b and CWR22Rv1 [41]. However, all of these cell lines but the CWR22Rv1 are derived from metastatic lesions and LAPC-4 is the only that presents truly androgen-dependent characteristics [41]. Our new PC346C cell line is unique in the combination of androgen-responsive growth, *wild-type* AR expression, PSA secretion and primary tumor origin, providing a valuable model system for the androgen-dependent stages of the disease. We used this cell line to replicate the clinical progression of PCa in patients under endocrine therapy, producing a panel of androgen-independent sublines: PC346DCC, PC346Flu1 and PC346Flu2.

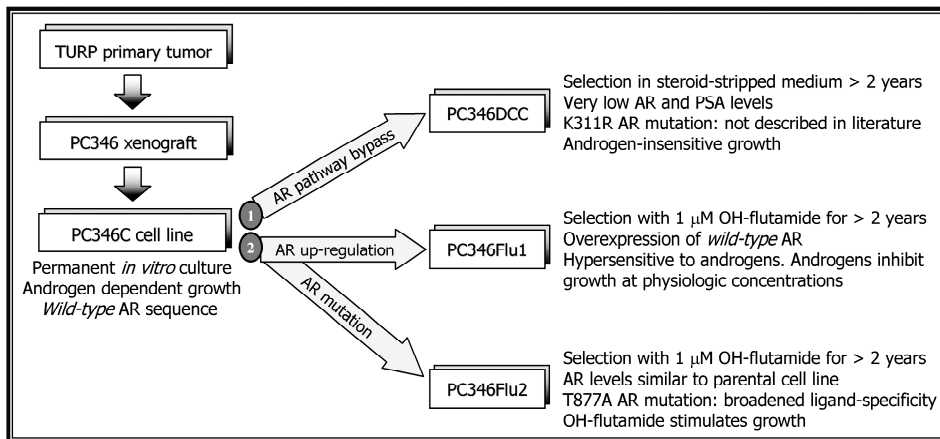


Figure 6 - Overview of the PC346 cell line panel. Prostate cancer cells have two possible strategies to grow in a low-androgen environment: (1) to activate alternative growth stimulatory pathways bypassing the demand for an active AR (PC346DCC), or (2) to sensitize the AR pathway to the low androgen concentrations, for example, by AR up-regulation (PC346Flu1) or AR mutations (PC346Flu2). These strategies are not mutually exclusive and PCa cells probably use a balance of both to survive and grow under androgen-ablation treatment.

PC346DCC exhibits *in vitro* a fast androgen-independent growth, which is unresponsive to both R1881 and OH-flutamide. AR and PSA were found to be very low expressed both at the mRNA and protein levels, but no deletion of the AR gene was detected by FISH analysis. We also found no evidence of AR promoter methylation by either bisulfite sequencing or methylation-specific PCR (data not shown). This is in contrast to the methylation of the AR promoter in DU145 and suggesting that the AR in PC346DCC was downregulated at the transcriptional level rather than epigenetically [42]. A novel mutation was detected in codon 311 of the AR, resulting in Lys to Arg substitution. The effect of this mutation on AR trans-activation is unknown and difficult to assess from the reporter assay due to the very low levels of endogenous receptor. Nevertheless, AR reporter activity was at background levels and was not induced by

R1881, excluding the K311R substitution as a potent activating AR mutation. These data suggest that PC346DCC has bypassed the AR pathway, and we are currently investigating the mechanisms regulating its proliferation. Interestingly, the orthotopic tumor growth assay appears to contradict the *in vitro* results. It seems that PC346DCC proliferation *in vivo* may be affected by castration. A possible explanation for this apparent contradiction could be that the effect of castration on PC346DCC cells is an indirect effect on the host prostate environment. Androgens stimulate prostate stromal cells to produce growth factors that regulate the proliferation of epithelial cells [43]. Recent studies suggest that androgens are also essential for the survival of vascular endothelial cells in androgen-dependent tissues [44,45] and stimulate regrowth of the prostatic vasculature in castrated rats [46]. Taken together, castration does not affect only the cancer epithelial cells, but the whole prostate environment by reducing the blood flow and disrupting stromal-epithelial interactions.

The PC346Flu1 subline expresses high androgen-receptor levels and in an AR reporter assay, it showed a 10-fold stronger response to androgens than the parental PC346C. FISH analysis revealed no AR genomic amplification and other mechanisms such as transcriptional control or protein stabilization may be involved in increasing AR protein levels in this cell line. Although Chen *et al*/previously suggested that increased AR levels conferred agonistic activity to AR antagonists [10], we did not observe AR stimulation by OH-flutamide in the PC346Flu1 line. Interestingly, PC346Flu1 proliferation is inhibited by androgens at concentrations that are normally stimulatory for PC346C. This paradoxical growth inhibitory effect by androgens has been previously reported for various LNCaP variants similarly subjected to long-term culture in the absence of androgens [47,48,49]. All three studies reported an overexpression of the AR protein and, for the two variants LNCaP-abl and LNCaP-104R, the hormone inhibitory effect was preceded at early passages by a hypersensitivity to low levels of androgens. Kokontis *et al* also observed that androgen inhibited LNCaP-104R proliferation by cell-cycle arrest and not by induction of apoptosis, and that this effect could be reverted by subsequent continuous passage in androgen-containing medium [50]. This androgenic repression phenomenon could be a possible mechanism underlying withdrawal responses observed in some patients upon discontinuation of the endocrine treatment. In this context, intermittent hormone therapy, in cycles blocking growth and restoring androgen-regulation, may be an interesting treatment option to retard tumor progression.

The PC346Flu2 subline expresses a mutated AR with altered ligand-binding properties, such that OH-flutamide, the antiandrogen upon which this subline was selected, is converted into an agonist [12]. This type of AR point mutations, that broaden the ligand-specificity of the receptor to antiandrogens, have also been proposed as a possible explanation for the antiandrogen withdrawal syndrome [51]. These data support that AR activating mutations may confer growth advantage upon androgen-ablation therapy to a subset of prostate tumors, particularly in patients treated with antiandrogens.

The karyotype of two variants of the parental PC346C has been previously reported [52]. The PC346C variant described in our study exhibited a near-tetraploid chromosome complement and few structural abnormalities, which were homogeneously present in almost every cell: 92~99 (4n), XXYY, +1, +5, +7, +7, del(8)(p11.1), +i(8)(q10),

-13, -13, +19, +20, -22. Our array CGH data confirmed most of the alterations reported in the previous karyotype, but did not detect a significant amplification of chromosomes 5 and 19 and deletion of 22. The sensitivity of the array CGH technology may not be high enough to detect single copy amplifications or deletions in a tetraploid background. Most of the chromosomal abnormalities detected by CGH were present in all the cell lines of the panel, showing that these originated in the parental PC346C prior to the development of the sublines. Amplification of 8q and deletion of 10q and 13q are among the most common genetic alterations in prostate cancer [53]. Several candidate genes have been previously identified in these locations: the c-MYC oncogene in 8q, the PTEN tumor-suppressor gene in 10q, RB1 and BRCA2 in 13q [54]. Gain of chromosomes 1, 7 and 20 are also frequently detected in prostate tumor specimens and cell lines [55]. Only three major chromosomal modifications were detected in the androgen-independent sublines, which were not present in the parental PC346C, confirming the relative genomic stability of the cell lines. The loss of chromosome Y in PC346Flu2 and 8p in PC356DCC are well-known aberrations that have been associated with prostate cancer progression [53]. This suggests that the long-term androgen ablation selected not only for AR mutations but also for chromosomal alterations that benefit tumor growth, and therefore that the sublines are derived from PC346C by clonal selection.

In conclusion, the PC346 cell line panel mimics many biological characteristics of different stages of *in vivo* prostate tumors. It comprises properties ranging from androgen-dependent growth to fast androgen-independent growth characteristic of advanced progressive disease, while reproducing the most common AR modifications observed in hormone-refractory disease. It therefore provides a valuable model system to investigate the mechanisms that dictate androgen-independent growth, with emphasis to the role of AR signaling in prostate cancer progression.

ACKNOWLEDGEMENTS

We thank Denie Zonruiter and Suzanne Reneman for technical assistance in the animal experiments and Mark Wildhagen for assistance with the statistical analysis.

This study was supported by the Netherlands Organization for Scientific Research (NWO) through ZonMW grant 903-46-187 and by the Dutch Cancer Society (KWF) through grant NKB97-1479.

REFERENCES

1. Gelmann EP (2002) Molecular biology of the androgen receptor. *J Clin Oncol* 20: 3001-3015.
2. Klotz L (2000) Hormone therapy for patients with prostate carcinoma. *Cancer* 88: 3009-3014.
3. Feldman BJ, Feldman D (2001) The development of androgen-independent prostate cancer. *Nat Rev Cancer* 1: 34-45.
4. Jenster G (1999) The role of the androgen receptor in the development and progression of prostate cancer. *Semin Oncol* 26: 407-421.
5. van der Kwast TH, Schalken J, Ruizeveld de Winter JA, van Vroonhoven CC, Mulder E, et al. (1991) Androgen receptors in endocrine-therapy-resistant human prostate cancer. *Int J Cancer* 48: 189-193.
6. Ruizeveld de Winter JA, Janssen PJ, Sleddens HM, Verleun-Mooijman MC, Trapman J, et al. (1994) Androgen receptor status in localized and locally progressive hormone refractory human prostate cancer. *Am J Pathol* 144: 735-746.
7. Linja MJ, Savinainen KJ, Saramaki OR, Tammela TL, Vessella RL, et al. (2001) Amplification and overexpression of androgen receptor gene in hormone-refractory prostate cancer. *Cancer Res* 61: 3550-3555.
8. Brown RS, Edwards J, Dogan A, Payne H, Harland SJ, et al. (2002) Amplification of the androgen receptor gene in bone metastases from hormone-refractory prostate cancer. *J Pathol* 198: 237-244.
9. Koivisto P, Kononen J, Palmberg C, Tammela T, Hyytinen E, et al. (1997) Androgen receptor gene amplification: a possible molecular mechanism for androgen deprivation therapy failure in prostate cancer. *Cancer Res* 57: 314-319.
10. Chen CD, Welsbie DS, Tran C, Baek SH, Chen R, et al. (2004) Molecular determinants of resistance to antiandrogen therapy. *Nat Med* 10: 33-39.
11. Huang ZQ, Li J, Wong J (2002) AR possesses an intrinsic hormone-independent transcriptional activity. *Mol Endocrinol* 16: 924-937.
12. Veldscholte J, Ris-Stalpers C, Kuiper GG, Jenster G, Berrevoets C, et al. (1990) A mutation in the ligand binding domain of the androgen receptor of human LNCaP cells affects steroid binding characteristics and response to anti-androgens. *Biochem Biophys Res Commun* 173: 534-540.
13. Gottlieb B, Beitel LK, Wu JH, Trifiro M (2004) The androgen receptor gene mutations database (ARDB): 2004 update. *Hum Mutat* 23: 527-533.
14. Jenster G (2000) Ligand-independent activation of the androgen receptor in prostate cancer by growth factors and cytokines. *J Pathol* 191: 227-228.
15. Gregory CW, He B, Johnson RT, Ford OH, Mohler JL, et al. (2001) A mechanism for androgen receptor-mediated prostate cancer recurrence after androgen deprivation therapy. *Cancer Res* 61: 4315-4319.
16. Li P, Yu X, Ge K, Melamed J, Roeder RG, et al. (2002) Heterogeneous expression and functions of androgen receptor co-factors in primary prostate cancer. *Am J Pathol* 161: 1467-1474.
17. Linja MJ, Porkka KP, Kang Z, Savinainen KJ, Janne OA, et al. (2004) Expression of androgen receptor coregulators in prostate cancer. *Clin Cancer Res* 10: 1032-1040.
18. Vlietstra RJ, van Alewijk DC, Hermans KG, van Steenbrugge GJ, Trapman J (1998) Frequent inactivation of PTEN in prostate cancer cell lines and xenografts. *Cancer Res* 58: 2720-2723.
19. Catz SD, Johnson JL (2003) BCL-2 in prostate cancer: a minireview. *Apoptosis* 8: 29-37.
20. McDonnell TJ, Troncoso P, Brisbay SM, Logothetis C, Chung LW, et al. (1992) Expression of the protooncogene bcl-2 in the prostate and its association with emergence of androgen-independent prostate cancer. *Cancer Res* 52: 6940-6944.
21. Gray IC, Stewart LM, Phillips SM, Hamilton JA, Gray NE, et al. (1998) Mutation and expression analysis of the putative prostate tumour-suppressor gene PTEN. *Br J Cancer* 78: 1296-1300.
22. Feilolter HE, Nagai MA, Boag AH, Eng C, Mulligan LM (1998) Analysis of PTEN and the 10q23 region in primary prostate carcinomas. *Oncogene* 16: 1743-1748.

23. Russell PJ, Bennett S, Stricker P (1998) Growth factor involvement in progression of prostate cancer. *Clin Chem* 44: 705-723.
24. van Weerden WM, de Ridder CM, Verdaasdonk CL, Romijn JC, van der Kwast TH, et al. (1996) Development of seven new human prostate tumor xenograft models and their histopathological characterization. *Am J Pathol* 149: 1055-1062.
25. van Weerden WM, Romijn JC (2000) Use of nude mouse xenograft models in prostate cancer research. *Prostate* 43: 263-271.
26. Romijn JC, Verkoelen CF, Schroeder FH (1988) Application of the MTT assay to human prostate cancer cell lines in vitro: establishment of test conditions and assessment of hormone-stimulated growth and drug-induced cytostatic and cytotoxic effects. *Prostate* 12: 99-110.
27. Bruggenwirth HT, Boehmer AL, Verleun-Mooijman MC, Hoogenboezem T, Kleijer WJ, et al. (1996) Molecular basis of androgen insensitivity. *J Steroid Biochem Mol Biol* 58: 569-575.
28. Jenster G, de Ruiter PE, van der Korput HA, Kuiper GG, Trapman J, et al. (1994) Changes in the abundance of androgen receptor isoforms: effects of ligand treatment, glutamine-stretch variation, and mutation of putative phosphorylation sites. *Biochemistry* 33: 14064-14072.
29. Zegers ND, Claassen E, Neelen C, Mulder E, van Laar JH, et al. (1991) Epitope prediction and confirmation for the human androgen receptor: generation of monoclonal antibodies for multi-assay performance following the synthetic peptide strategy. *Biochim Biophys Acta* 1073: 23-32.
30. Gallee MP, Visser-de Jong E, van der Korput JA, van der Kwast TH, ten Kate FJ, et al. (1990) Variation of prostate-specific antigen expression in different tumour growth patterns present in prostatectomy specimens. *Urol Res* 18: 181-187.
31. Sui X, Bramlett KS, Jorge MC, Swanson DA, von Eschenbach AC, et al. (1999) Specific androgen receptor activation by an artificial coactivator. *J Biol Chem* 274: 9449-9454.
32. Cleutjens KB, van Eekelen CC, van der Korput HA, Brinkmann AO, Trapman J (1996) Two androgen response regions cooperate in steroid hormone regulated activity of the prostate-specific antigen promoter. *J Biol Chem* 271: 6379-6388.
33. Rembrink K, Romijn JC, van der Kwast TH, Rubben H, Schroder FH (1997) Orthotopic implantation of human prostate cancer cell lines: a clinically relevant animal model for metastatic prostate cancer. *Prostate* 31: 168-174.
34. Kraaij R, van Weerden WM, de Ridder CM, Gussenhoven EJ, Honkoop J, et al. (2002) Validation of transrectal ultrasonographic volumetry for orthotopic prostate tumours in mice. *Lab Anim* 36: 165-172.
35. Schroder FH, Kranse R, Barbet N, Hop WC, Kandra A, et al. (2000) Prostate-specific antigen: A surrogate endpoint for screening new agents against prostate cancer? *Prostate* 42: 107-115.
36. Vissers LE, de Vries BB, Osoegawa K, Janssen IM, Feuth T, et al. (2003) Array-based comparative genomic hybridization for the genomewide detection of submicroscopic chromosomal abnormalities. *Am J Hum Genet* 73: 1261-1270.
37. Kaighn ME, Narayan KS, Ohnuki Y, Lechner JF, Jones LW (1979) Establishment and characterization of a human prostatic carcinoma cell line (PC-3). *Invest Urol* 17: 16-23.
38. Stone KR, Mickey DD, Wunderli H, Mickey GH, Paulson DF (1978) Isolation of a human prostate carcinoma cell line (DU 145). *Int J Cancer* 21: 274-281.
39. Chlenski A, Nakashiro K, Ketels KV, Korovaitseva GI, Oyasu R (2001) Androgen receptor expression in androgen-independent prostate cancer cell lines. *Prostate* 47: 66-75.
40. Veldscholte J, Berrevoets CA, Ris-Stalpers C, Kuiper GG, Jenster G, et al. (1992) The androgen receptor in LNCaP cells contains a mutation in the ligand binding domain which affects steroid binding characteristics and response to antiandrogens. *J Steroid Biochem Mol Biol* 41: 665-669.
41. Van Bokhoven A, Varella-Garcia M, Korch C, Johannes WU, Smith EE, et al. (2003) Molecular characterization of human prostate carcinoma cell lines. *Prostate* 57: 205-225.
42. Nakayama T, Watanabe M, Suzuki H, Toyota M, Sekita N, et al. (2000) Epigenetic regulation of androgen receptor gene expression in human prostate cancers. *Lab Invest* 80: 1789-1796.

43. Lee C (1996) Role of androgen in prostate growth and regression: stromal-epithelial interaction. *Prostate Suppl* 6: 52-56.
44. Shabisgh A, Tanji N, D'Agati V, Burchardt M, Rubin M, et al. (1999) Early effects of castration on the vascular system of the rat ventral prostate gland. *Endocrinology* 140: 1920-1926.
45. Shabsigh A, Chang DT, Heitjan DF, Kiss A, Olsson CA, et al. (1998) Rapid reduction in blood flow to the rat ventral prostate gland after castration: preliminary evidence that androgens influence prostate size by regulating blood flow to the prostate gland and prostatic endothelial cell survival. *Prostate* 36: 201-206.
46. Franck-Lissbrant I, Haggstrom S, Damber JE, Bergh A (1998) Testosterone stimulates angiogenesis and vascular regrowth in the ventral prostate in castrated adult rats. *Endocrinology* 139: 451-456.
47. Culig Z, Hoffmann J, Erdel M, Eder IE, Hobisch A, et al. (1999) Switch from antagonist to agonist of the androgen receptor bicalutamide is associated with prostate tumour progression in a new model system. *Br J Cancer* 81: 242-251.
48. Kokontis J, Takakura K, Hay N, Liao S (1994) Increased androgen receptor activity and altered c-myc expression in prostate cancer cells after long-term androgen deprivation. *Cancer Res* 54: 1566-1573.
49. Shi XB, Ma AH, Tepper CG, Xia L, Gregg JP, et al. (2004) Molecular alterations associated with LNCaP cell progression to androgen independence. *Prostate* 60: 257-271.
50. Kokontis JM, Hay N, Liao S (1998) Progression of LNCaP prostate tumor cells during androgen deprivation: hormone-independent growth, repression of proliferation by androgen, and role for p27Kip1 in androgen-induced cell cycle arrest. *Mol Endocrinol* 12: 941-953.
51. Taplin ME, Bubley GJ, Ko YJ, Small EJ, Upton M, et al. (1999) Selection for androgen receptor mutations in prostate cancers treated with androgen antagonist. *Cancer Res* 59: 2511-2515.
52. van Bokhoven A, Caires A, Maria MD, Schulte AP, Lucia MS, et al. (2003) Spectral karyotype (SKY) analysis of human prostate carcinoma cell lines. *Prostate* 57: 226-244.
53. Brothman AR (1997) Cytogenetic studies in prostate cancer: are we making progress? *Cancer Genet Cytogenet* 95: 116-121.
54. Nupponen NN, Visakorpi T (2000) Molecular cytogenetics of prostate cancer. *Microsc Res Tech* 51: 456-463.
55. Brothman AR, Maxwell TM, Cui J, Deubler DA, Zhu XL (1999) Chromosomal clues to the development of prostate tumors. *Prostate* 38: 303-312.

Chapter 4

Gene Expression Profile of the Androgen Receptor Pathway in Androgen-Responsive versus Hormone-Refractory PC346 Prostate Cancer Cells

Rute B. Marques¹, Natasja F. Dits¹, Sigrun Erkens-Schulze¹, Wilfred F.J. van IJcken², Wytske M. van Weerden¹, Guido Jenster¹

¹Department of Urology, Josephine Nefkens Institute and ²Erasmus Center for Biomics, Erasmus Medical Center, PO Box 2040, 3000 CA, Rotterdam, The Netherlands

submitted for publication

ABSTRACT

Background: Prostate cells are dependent on androgens for their survival and growth. This characteristic is maintained in (early) prostate cancer, where the androgen-regulated prostate-specific antigen (PSA) is used in the diagnosis and follow-up of the disease, and has been exploited in the management of metastatic disease using androgen ablation therapy.

Objective: To characterize the role of the androgen-receptor (AR) pathway in prostate cancer progression and identify potential diagnostic/prognostic disease markers.

Methods: Microarray analysis was used to establish the androgen-regulated gene expression profile of PC346 cell lines. The resulting AR-target gene signature was linked to multiple prostate cancer databases, from *in vitro* cell lines, xenografts and patient-derived samples, published previously. ENDOD1, MCCC2 and ACSL3 were selected as potential disease markers for RT-PCR quantification in a distinct set of human prostate specimens.

Results: A total of 107 transcripts were differentially-expressed upon stimulation of PC346 cells with the synthetic androgen R1881 or the antiandrogen flutamide. Among these were well-known AR-target genes such as TMPRSS2, KLK2, and FKBP5, but also novel genes, including MAFB, KLF9, NFIB and EHF. Gene ontology annotations clustering revealed enrichment towards genes involved in transcription regulation, signal transduction, regulation of cell cycle and apoptotic processes, and cellular differentiation. Additionally, R1881 induced the expression of genes related to the metabolism of proteins, carbohydrates and lipids that contribute to the production and secretion of prostatic fluid. These distinct functional clusters were differentially modulated during prostate cancer progression. A considerable fraction of AR pathway genes involved in differentiation and secretory function of the prostate were up-regulated in primary prostate cancer but repressed in metastasis. Conversely, genes implicated in cell survival, proliferation, cytoskeletal remodeling and adhesion, were overexpressed in metastasis. Ultimately, three candidate genes were selected as potential disease markers: MCCC2 was overexpressed in low-grade prostate cancer, whereas ENDOD1 and ACSL3 were down-regulated in high-grade tumors and metastatic samples.

Conclusions: The AR pathway is adapted in advanced and hormone-refractory prostate cancer, through selective modulation of differentiation, proliferation and invasion functions. These findings may have implications in the current therapy for metastatic prostate tumors and in the development of prostate cancer markers.

INTRODUCTION

Prostate cancer is the most frequently diagnosed non-cutaneous malignancy in men and the second leading cause of cancer deaths in the western countries [1]. Prostate cancer is a highly heterogeneous condition, exhibiting a wide range of biological and clinical manifestations. While some patients develop an asymptomatic disease course and rather die with the cancer than from the cancer, others present with a more aggressive and/or more advanced disease at the time of diagnosis [2]. When the tumor is confined to the prostate, it can be efficiently treated by radical surgery and/or radiation therapy, but once the tumor has disseminated, systemic therapy is required. Since prostate cells, normal or malignant, require androgens for their survival, the golden standard for the treatment of evasive prostate tumors is androgen ablation through chemical or surgical castration, which may be combined with the administration of androgen receptor (AR) antagonists [2]. Most patients will benefit from this therapy, the tumors may shrink and the symptoms ameliorate. Unfortunately, the cancer will eventually recur as a fatal hormone-refractory condition, for which at the moment no curative treatment exists [3,4]. A pertinent question is how prostate cancer cells that are initially dependent on androgens for survival can resume growth in an androgen-deprived environment. One possibility is that prostate cancer cells achieve this by adapting their AR pathway to the low androgen/high antiandrogen levels. On the other hand, cancer cells may activate alternative growth pathways, while shutting down tumor suppressors and apoptotic signals [5,6].

In the present study, we focused on the role of the AR pathway in prostate cancer progression. The expression pattern of androgen-regulated genes in androgen-responsive and castration-resistant cell lines was established, with the goal to: (i) determine whether the AR pathway is still functionally active in hormone-refractory disease; (ii) identify the mechanism(s) by which the AR pathway may be adjusted to the low androgen/high antiandrogen levels; (iii) identify androgen-regulated genes that could potentially be used in the diagnosis/prognosis of prostate cancer or as a therapeutic target. For this purpose, we used microarray technology to characterize the transcriptional program activated by the synthetic androgen R1881 and the antiandrogen hydroxyflutamide. As model system we used the PC346 cell lines (Table 1): the androgen-responsive PC346C parental cell line and its hormone-refractory derivative sublines PC346DCC, PC346Flu1 and PC346Flu2 [7]. These castration-resistant sublines reproduce common AR modifications observed in hormone-refractory disease: AR down-regulation (PC346DCC), AR mutation (PC346Flu2) and AR over-expression (PC346Flu1), making it a unique and valuable model for this study.

Table 1 - Characteristics of the PC346 cell line panel: AR status and hormone response

| | PC346C | PC346DCC | PC346Flu1 | PC346Flu2 |
|------------------------------------|--------|----------|-----------|-----------|
| AR status | wt AR | AR low | AR high | T877A AR |
| PSA expression | ++ | - | ++ | ++ |
| Growth on steroid-stripped medium | -/+ | ++ | ++ | + |
| Growth with 0.1 nM R1881 | ++ | ++ | + | ++ |
| Growth with 1 μ M OH-flutamide | -/+ | ++ | ++ | ++ |

MATERIALS AND METHODS

Reagents and cell lines

The basic culture medium used in the maintenance of PC346 cell lines consisted of DMEM-F12 medium (Cambrex BioWhitaker, Belgium) supplemented with 2% fetal calf serum (FCS; PAN Biotech GmbH, Aidenbach, Germany), 1% insulin-transferrin-selenium (Gibco BRL), 0.01% bovine serum albumin (Boehringer Mannheim, Germany), 10 ng/ml epidermal growth factor (Sigma-Aldrich), penicillin/streptomycin antibiotics (100 U/ml penicillin, 100 mg/ml streptomycin; BioWhitaker, Belgium); plus the following additions: 100 ng/ml fibronectin (Harbor Bio-Products, Tebu-bio, The Netherlands), 20 mg/ml fetuine (ICN Biomedicals, The Netherlands), 50 ng/ml cholera toxin, 0.1 mM phosphoethanolamine, 0.6 ng/ml triiodothyronine and 500 ng/ml dexametason (all from Sigma). PC346C cells were maintained in culture in the complete medium mentioned above, supplemented with 0.1 nM 17-methyltrienolone (R1881; NEN, Boston MA, USA). PC346DCC selection medium was supplemented as described above, but depleted from androgens by using dextran-coated charcoal (DCC) treated FCS. PC346Flu1 and PC346Flu2 culture medium was also androgen depleted by using 2% DCC-FCS, and supplemented with 1 μ M of hydroxyflutamide (OH-flutamide, Schering-Plough Research Institute, New Jersey, USA). For the hormone stimulations, a simplified version of the culture medium was used, containing 2% DCC- FCS without the above mentioned additions (minimal medium). Cells were grown in T25 Primaria™ tissue culture flasks (BD Biosciences Benelux N.V, The Netherlands) at 37°C under 5% CO₂ humidified atmosphere.

Hormone stimulations and expression microarray analysis

Cells were seeded in their respective selection medium to reach ~50% confluency and allowed to attach overnight. The next day, medium was replaced with 2% DCC-FCS in minimal medium and cells were starved for 48h, to bring AR activity to basal levels before the hormone stimulations. Subsequently, cells were stimulated with either vehicle, 1 nM R1881 or 1 μ M OH-flutamide for 4, 8 or 16h. After stimulations, cells were rinsed twice with PBS and stored at -20°C until RNA isolation. Total RNA was isolated with RNAzol B reagent (Campro Scientific, Veenendaal, The Netherlands) and further purified through RNeasy columns (Qiagen) with on-column DNA digestion, according to the manufacturer's protocol. RNA quality was checked on 1% agarose gel.

Cy3- or Cy5-labelled RNA probes were produced by incorporating amino-allyl UTP during RNA amplification, followed by coupling to N-hydroxysuccinimide modified dye. Briefly, 3 μ g RNA was used for a T7-based linear mRNA amplification protocol, described previously [8]. Amino-allyl UTP, plus equal amount of unmodified rUTP, was incorporated into aRNA with T7 Megascript Kit (all from Ambion), according to manufacturer's protocol. Amplified RNA was purified and concentrated using Microcon-YM 30 columns (Amicon®) to rinse three times with 300 μ l RNase-free water. Finally, 2 μ g aminoallyl-modified RNA, in a maximum of 3.33 μ l of RNase-free water, was incubated with 1.66 μ l sodium bicarbonate buffer (0.3 M, pH 9) and 5 μ l Cy3- or Cy5-dye (CyScribe Post-Labeling Kit, Amersham, NJ, USA), for 1h in the dark at room temperature. Reaction was stopped with 5 μ l 4 M hydroxylamine HCl (Sigma), contra-labelled probes were combined and purified/concentrated using Microcon-YM 30

columns. Probe was collected in 5-15 μ l final volume and resuspended in 80 μ l Ambion hybridization buffer number 1.

For the microarray we used double-dye oligoarrays representing about 15,000 human genes, on which labelled hormone-stimulated RNA was cohybridized with its contra-labelled time-matched vehicle (ethanol) control. Two microarrays were performed per condition: in one experiment the stimulated samples were labeled with Cy3 and the unstimulated reference with Cy5, in the other experiment in vice-versa (dye-swap); this was done to exclude dye-preferential binding to oligonucleotides on the microarray. In addition, two independent cell passages were used for each of these experiments, to account for the biological variability.

The oligoarrays used in this study were produced at the Erasmus Center for Biomics. Briefly, a human 18,584 oligonucleotides library (Compugen, Sigma-Genosys) was spotted on aminosilane slides using a Virtek Chipwriter Professional arrayer (Virtek Vision International, Waterloo, Canada). Control spots included landmarks, spotting buffer, alien oligonucleotides (SpotReport Alien Oligo Array, La Jolla, Stratagene), poly d[A]40-60, salmon sperm DNA, and human COT-1 DNA. Before the hybridization, microarray slides were prehybridized in 5x SSC, 0.05% SDS, 4% BSA solution for 30 min at 45°C, washed twice with RNase-free water for 2 min, rinsed with isopropanol and spin-dried for 3 min at 1500 g. Microarray hybridizations were performed overnight at 45°C, with continuous agitation, in a HS4800 Hybridization Station (Tecan Benelux BV). Finally, the arrays were washed automatically in the Hybridization Station using: 2x SSC/0.05% SDS (at 45°C), 1x SSC and 0.2x SSC (at room temperature), and dried under a stream of N₂, before scanning.

Data extraction and analysis

Arrays were scanned in a ScanArray Express HT scanner (Perkin Elmer, Nederland BV) and spot intensities were quantified using Imagene software (Bio Discovery Inc, El Segundo, CA, USA). To balance Cy3 and Cy5 spot intensities, Loewess normalization per subarray was performed using limma-package (<http://bioinf.wehi.edu.au/limma/>) from Bioconductor (<http://www.bioconductor.org>) [9,10]. To scale between arrays, the global median intensity per array was set at 1000. Dye intensities below 200 were then thresholded at 200, to minimize noise and make fold-change on the low-intensity range more robust against outliers. Spots with intensities below the threshold (200) for both Cy3 and Cy5 channels, in more than 50% (>3/6) of the arrays for each time-course, were excluded from the analysis. Sample to vehicle-control ratios were then calculated and 2log transformed. Spots that showed opposite effects for the dye-swap/biological replicates were excluded from further analysis; effects were called opposite if the mean 2log ratio for the three time-points tested were $\geq 0,5$ for one dye and below $\leq -0,5$ for the dye-swap. Following normalization and all the above-mentioned quality controls, the 2log intensity ratios from both replicates were averaged for each time point. This data was stored in SRS7 (Sequence Retrieval System version 7, Lion Bioscience AG, Heidenberg, Germany), which was also used for the comparisons with other previously published/publicly available databases [11].

Hierarchical clustering and data visualization was performed using Cluster and TreeView programs (Eisen Labs: <http://rama.lbl.gov>), respectively. Significance Analysis of Microarrays (SAM; <http://www-stat.stanford.edu/~tibs/SAM>) was used to determine

which genes were statistically different between stimulated samples and non-stimulated references. Gene ontology clustering was performed using Database for Annotation, Visualization and Integrated Discovery (DAVID: <http://david.abcc.ncifcrf.gov>) [12,13]. The pathway and functional analyses were generated through the use of Ingenuity Pathways Analysis (Ingenuity® Systems, www.ingenuity.com).

cDNA synthesis and RT-PCR analysis

Total RNA was isolated as described above and cDNA was synthesized using MMLV-reverse transcriptase kit and Oligo(dT)₁₂₋₁₈ primer (Invitrogen), according to manufacturer's protocol. cDNA samples were stored at -20°C. The PCR reaction mixtures for the semi-quantitative microarray validation PCRs contained 1.25 µL of 0.5 U/µL Taq polymerase, 2.5 µL 10x PCR buffer, 1.5 µL 25 mM MgCl₂ (Promega Benelux b.v., the Netherlands), 1 µL 10 mM dNTPs, 1.5 µL 100 ng/µL forward and reversed primers (Invitrogen, Breda, the Netherlands) and 5 µL cDNA (previously diluted 1:20), in a final volume of 25 µL. Primers were designed using the computer program Oligo Primer Analysis Software version 6.22 (Molecular Biology Insights Inc, USA). Gene specificity was checked by BLAST and, whenever possible, intron-spanning primers were chosen to avoid amplification of contaminating DNA. RT-PCRs were performed in a 3 step cycling program consisting: of an initial denaturation step at 94°C for 5 min, followed by N cycles of: 94°C - 45 sec, Annealing°C - 45 sec, 72°C - 45 sec; and a final 10 min extension step at 72°C. Primer sequences, annealing temperatures (Annealing) and number of cycles (N) for each PCR are summarized in Table 2. Experiments were repeated twice, using distinct cell passages. The household gene GAPDH was used for normalization.

For the quantitative PCR analysis, normal and tumor samples from patients were obtained from the frozen tissue bank of the Erasmus Medical Center (Rotterdam, the Netherlands). The specimens were collected between 1984 and 2001. The experimental protocols were approved by the Erasmus MC Medical Ethics Committee according to the Medical Research Involving Human Subjects Act. Additional information about these specimens was provided previously [14]. TaqMan real-time PCR analysis was performed in an ABI Prism 7700 Sequence Detection System (Applied Biosystems, Foster City, CA), using AmpliTaq Gold DNA polymerase (Applied Biosystems), according to manufacturer's specifications. Validated primers and probes from TaqMan Gene Expression Assays (Applied Biosystems) were used for quantification of ACSL3 (Hs01071247_m1), MCCC2 (Hs00223257_m1), ENDOD1 (Hs00826684_m1) and GAPDH (Hs99999905_m1), according to the PCR settings provided by Applied Biosystems. PBGD was quantified using 0.33 µM of primers forward: 5'-CAT GTC TGG TAA CGG CAA TG-3' and reverse: 5'-GTA CGA GGC TTT CAA TGT TG-3' primers, in Power SybrGreen PCR Master mix (Applied Biosystems), according to thermocycling protocol recommended by the manufacturer. Transcript quantities for each sample were normalized against the average of two endogenous references and relative to a calibrator. The two housekeeping genes used as endogenous references were PBGD and GAPDH; a mixture of cDNAs from prostate carcinoma xenografts was used as the calibrator. Graphs and statistics were performed with GraphPad Prism (version 3.0). P-values < 0.05 were considered significant.

Table 2 - Primer sequences, annealing temperature and number of cycles for RT-PCR

| Gene | Forward primer | Reverse primer | T _{annealing} (°C) | Cycles N |
|---------|-----------------------------------|-----------------------------------|--------------------------------|-------------|
| AR | CTA CCA GCT CAC CAA GCT CCT G | ACA AGG CAC TGC AGA GGA GTA G | 60 | 30 |
| PSA | TTG TTA CAT TGA CAG GAG ACA CAC T | CTC AGG TCT GAG AAG TTA AGG TCA G | 60 | 30 |
| KLK2 | AGA TGA AGA CTC CAG CCA T | GAT ACC TTG AAG CAC ACC A | 60 | 30 |
| PART1 | GAG CCA GCC AAT CAC TT | AGC AGC ACT CAG GCG T | 58 | 35 |
| TPD52 | TTT CAA TGT GTT GGA AAC TGT AA | TAG AAT ACC TTG GCC TCT ATG C | 58 | 30 |
| GPR88 | CCA AGG CGT CTC TTT AAG T | ATG GCA ACT CAT ACT GGT G | 60 | 30 |
| FKBP5 | GAA TAC ACC AAA GCT GTT GA | CTC TTC CTT GGC ATC CT | 58 | 30 |
| TMPRSS2 | CCT CTG GTC ACT TCG AAG AAC | GTA AAA CGA CGT CAA GGA CG | 60 | 35 |
| STEAP1 | AGA AGA TGC CTG GAT TGA | CTT CTT CCT CAA GCA TGG | 58 | 30 |
| ID3 | GGA GCT TTT GCC ACT GAC TC | GCT CCT GAG CAC CAG GTT TA | 60 | 30 |
| TRIB1 | ATG GGA CTT TGA GAA GAG G | GCC ATC TCA CTG TTC ACA T | 60 | 35 |
| GAPDH | ATG GCA TGG ACT GTG GTC | ACG GGA AGC TTG TCA TCA | 58 | 25 |

Cycling program used was 94°C: 5min; (94°C: 45 sec/ Tannealing°C: 45 sec/ 72°C: 45 sec) x N cycles; 72°C: 10 min

RESULTS

Gene expression pattern of PC346 cells treated with R1881 and hydroxyflutamide

To characterize the expression profile of androgen receptor target genes in prostate cancer cells, we used expression microarray analysis on the PC346 cell line panel incubated with the androgen analogue R1881 or the antiandrogen OH-flutamide. The PC346 model system is composed of four cell lines: the androgen-sensitive PC346C and three hormone-refractory sublines, derived from the parental PC346C by long-term androgen ablation (PC346DCC), supplemented with the antiandrogen OH-flutamide (PC346Flu1 and PC346Flu2). All these sublines exhibit different properties with respect to AR status and responsiveness (summarized in Table 1) [7].

For the expression analysis we stimulated the cells with 1 nM R1881 or 1 μ M OH-flutamide for 4, 8 or 16h and cohybridized the labeled RNA with its time-matched vehicle (ethanol) control. Two microarrays were performed per condition, using two independent cell passages in dye-swap, to account for the biological variability and potential dye-preferential effects. Early time-points were chosen in order to enrich for primary AR targets, and minimize indirect secondary targets.

The two replicates per time-point were averaged and a total of 107 differentially-expressed transcripts were selected to constitute the AR pathway signature: 74 up-regulated and 33 down-regulated by R1881 and/or OH-flutamide (Tables 3 to 6). Spots were considered to be differentially-expressed if the absolute 2log ratio ≥ 0.5 (ratio ≥ 1.42 or ≤ 0.71) for all three time-points, for at least one cell type. Significance Analysis of Microarrays (SAM) was used to determine which genes were statistically different between stimulated samples and non-stimulated references. In total, there were 253 SAM significant genes, with a false discovery rate (FDR) set at 0.05 (Supplementary Tables S1 to S4). From our 107 signature transcripts, considered differentially-expressed according to the above-mentioned selection criteria, 77 were statistically significant by SAM. Although being clearly regulated (absolute 2log ratio > 0.5 for all 3 time-points), the remaining 30 (28%) transcripts of our AR-target signature were not SAM significant, which was due to a large variation across the 3 time-points. Since temporal regulation was observed for such few transcripts, possibly because of the narrow time frame chosen, no analysis was performed on the dynamics of gene-expression variation across time. Therefore, the expression ratios presented in the tables and figure 4 are from the average of all three time-points per condition. Finally, the fact that a considerable number of SAM significant transcripts were not included in our AR-regulated signature was due to our choice to set the 2log ratio threshold at 0.5.

The androgen-sensitive PC346C subline responded to the R1881 stimulation with increased expression of 18 genes, while 2 were down-regulated. Among these are some well-known AR regulated genes, such as KLK2, STEAP1, TMPRSS2 and FKBP5. The hormone-refractory sublines showed distinct responses to R1881 and OH-flutamide. PC346Flu1, which expresses 4-fold higher AR levels than the parental cell line, showed a “super-activation” of the AR pathway by R1881, not only in the magnitude of the gene expression but also in the number of regulated genes (20 androgen-regulated genes in the parental PC346C versus 91 in PC346Flu1). Conversely, the PC346DCC subline, which expresses residual levels of AR protein, showed no detectable changes in gene expression after the hormone treatments. Neither PC346C,

PC346DCC nor PC346Flu1 showed significant alterations in the transcriptional profile in response to OH-flutamide. In contrast, PC346Flu2 cells, which express the T877A mutated AR, responded to both R1881 and this antiandrogen, although the response to the latter was weaker (14 genes up-regulated by R1881 versus 8 up-regulated by OH-flutamide; Tables 3 and 5, respectively).

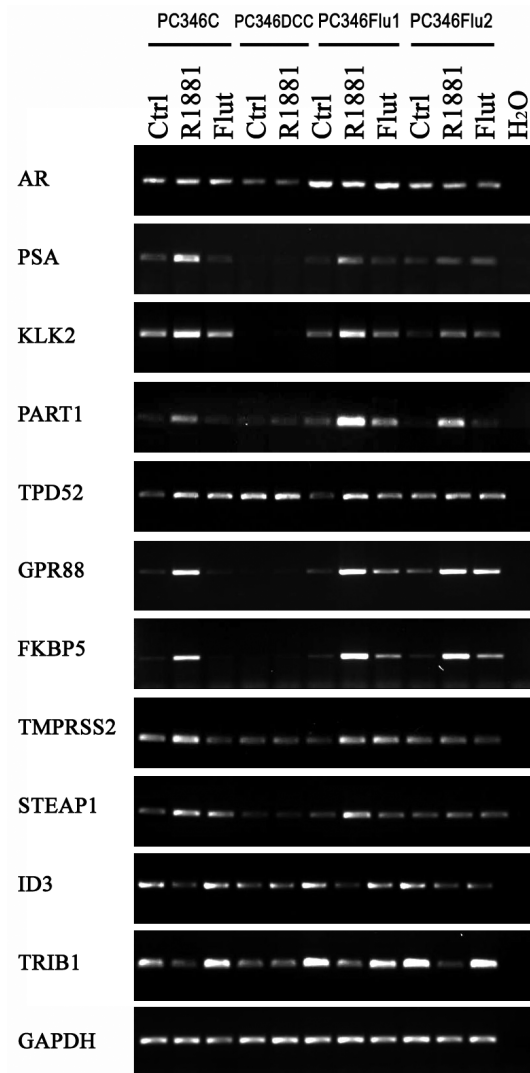


Figure 1 - Validation of the microarray results. Reverse-transcriptase PCR analysis of a set of 10 androgen-regulated genes in PC346 cell lines. Cells were stimulated with 1 nM R1881 (R1881), 1 μ M OH-flutamide (Flut) or vehicle control (Ctrl) for 16h. AR expression is also shown here, although the receptor was not androgen-regulated in the microarray analysis. ID3 and TRIB1 were shown to be androgen-repressed in the microarray assays, whereas the other genes were up-regulated by androgens. GAPDH was used as endogenous reference.

Table 3 - List of genes up-regulated by R1881

| GenBank ID | HUGO_Symbol | HUGO_Name | Cytoband | Cell line | 2log ratio | SAM q-value |
|------------|-------------|--|--------------|-----------|------------|-------------|
| NM_018674 | ACCN4 | amiloride-sensitive cation channel 4 pituitary | 2q35 | PC346C | 0.74 | 0.000 |
| NM_004457 | ACSL3 | acyl-CoA synthetase long-chain family member 3 | 2q34-q35 | PC346Flu1 | 2.04 | 0.000 |
| NM_014109 | ATAD2 | ATPase family AAA domain containing 2 | 8q24.13 | PC346Flu1 | 0.83 | 0.000 |
| AK027213 | BBS10 | Bardet-Biedl syndrome 10 | 12q21.2 | PC346Flu1 | 0.77 | 0.000 |
| NM_020235 | BBX | bobby sox homolog Drosophila | 3q13.1 | PC346Flu1 | 0.76 | 0.007 |
| AK024850 | C2orf31 | chromosome 2 open reading frame 31 | 2q34 | PC346Flu1 | 1.32 | 0.000 |
| NM_006079 | CITED2 | Cbp/p300-interacting transactivator with Glu/Asp-rich carboxy-terminal domain 2 | 6q23.3 | PC346Flu1 | 0.96 | 0.000 |
| AK026498 | CYP2U1 | cytochrome P450 family 2 subfamily U polypeptide 1 | 4q25 | PC346Flu1 | 1.50 | 0.000 |
| NM_012062 | DNM1L | dynamitin 1-like | 12p11.21 | PC346Flu1 | 1.36 | 0.000 |
| NM_018456 | EAF2 | ELL associated factor 2 | 3q13.33 | PC346Flu1 | 2.28 | 0.000 |
| AK026517 | EHF | ets homologous factor | 11p12 | PC346Flu1 | 0.62 | 0.000 |
| AK022827 | EIF2C3 | eukaryotic translation initiation factor 2C 3 | 1p34.3 | PC346C | 0.55 | 0.056 |
| AK022827 | EIF2C3 | eukaryotic translation initiation factor 2C 3 | 1p34.3 | PC346Flu1 | 1.03 | 0.000 |
| NM_012081 | ELL2 | elongation factor RNA polymerase II 2 | 5q15 | PC346Flu1 | 1.75 | 0.000 |
| NM_012081 | ELL2 | elongation factor RNA polymerase II 2 | 5q15 | PC346Flu2 | 1.04 | 1.093 |
| AF111849 | ELOVL5 | ELOVL family member 5 elongation of long chain fatty acids FEN1/Elo2 | 6p21.1-p12.1 | PC346Flu1 | 1.46 | 0.000 |
| AB020637 | ENDOD1 | endonuclease domain containing 1 | 11q21 | PC346Flu1 | 1.26 | 0.000 |
| AB020637 | ENDOD1 | endonuclease domain containing 1 | 11q21 | PC346Flu2 | 1.11 | 1.093 |
| NM_019018 | FAM105A | family with sequence similarity 105 member A | 5p15.2 | PC346Flu1 | 1.04 | 0.000 |
| AK024648 | FAM107B | family with sequence similarity 107 member B | 10p13 | PC346Flu1 | 0.76 | 0.007 |
| AL137343 | FAM84A | family with sequence similarity 84 member A | 2p24.3 | PC346Flu1 | 1.14 | 0.000 |
| NM_004117 | FKBP5 | FK506 binding protein 5 | 6p21.3-21.2 | PC346C | 1.88 | 0.000 |
| NM_004117 | FKBP5 | FK506 binding protein 5 | 6p21.3-21.2 | PC346Flu1 | 4.21 | 0.000 |
| NM_004117 | FKBP5 | FK506 binding protein 5 | 6p21.3-21.2 | PC346Flu2 | 1.66 | 1.093 |
| AK024715 | FLJ21062 * | Hypothetical protein FLJ21062 * | 7q21.13 | PC346Flu1 | 1.41 | 0.000 |
| NM_020474 | GALNT1 | UDP-N-acetyl-alpha-D-galactosamine:polypeptide | 18q12.1 | PC346Flu1 | 0.79 | 0.000 |
| NM_005271 | GLUD1 | glutamate dehydrogenase 1 | 10q23.3 | PC346Flu1 | 1.11 | 0.000 |
| NM_002069 | GNAI1 | guanine nucleotide binding protein G protein alpha inhibiting activity polypeptide 1 | 7q21 | PC346Flu1 | 0.94 | 0.000 |
| AB042410 | GPR88 | G protein-coupled receptor 88 | 1p21.3 | PC346C | 1.35 | 0.000 |
| AB042410 | GPR88 | G protein-coupled receptor 88 | 1p21.3 | PC346Flu1 | 3.04 | 0.000 |
| AB042410 | GPR88 | G protein-coupled receptor 88 | 1p21.3 | PC346Flu2 | 2.56 | 0.125 |

| | | | | | | |
|-----------|------------|--|---------------|-----------|------|-------|
| NM_001530 | HIF1A | hypoxia-inducible factor 1 alpha subunit basic helix-loop-helix transcription factor | 14q21-q24 | PC346Flu1 | 1.16 | 0.000 |
| NM_003543 | HIST1H4H | histone cluster 1 H4h | 6p21.3 | PC346Flu1 | 1.72 | 0.000 |
| M60721 | HLX | H2.0-like homeobox | 1q41-q42.1 | PC346Flu1 | 0.73 | 0.000 |
| M60721 | HLX | H2.0-like homeobox | 1q41-q42.1 | PC346Flu2 | 0.63 | 1.093 |
| NM_014642 | IQCB1 | IQ motif containing B1 | 3q13.33 | PC346Flu1 | 0.81 | 0.139 |
| NM_002241 | KCNJ10 | potassium inwardly-rectifying channel subfamily J member 10 | 1q22-q23 | PC346C | 0.67 | 0.056 |
| AL137384 | KIAA1109 | KIAA1109 | 4q27 | PC346C | 0.63 | 0.027 |
| NM_001206 | KLF9 | Kruppel-like factor 9 | 9q13 | PC346Flu1 | 0.83 | 0.000 |
| AF188747 | KLK2 | kallikrein-related peptidase 2 | 19q13.41 | PC346C | 0.79 | 0.000 |
| AF188747 | KLK2 | kallikrein-related peptidase 2 | 19q13.41 | PC346Flu1 | 1.12 | 0.000 |
| AF188747 | KLK2 | kallikrein-related peptidase 2 | 19q13.41 | PC346Flu2 | 1.03 | 1.093 |
| AK026375 | LOC93622 * | Hypothetical protein BC006130 * | 4p16.1 | PC346Flu1 | 1.02 | 0.000 |
| NM_005461 | MAFB | v-maf musculoaponeurotic fibrosarcoma oncogene homolog B avian | 20q11.2-q13.1 | PC346Flu1 | 1.06 | 0.000 |
| NM_003010 | MAP2K4 | mitogen-activated protein kinase kinase 4 | 17p11.2 | PC346Flu1 | 0.78 | 0.000 |
| AB050049 | MCCC2 | methylcrotonyl-Coenzyme A carboxylase 2 beta | 5q12-q13 | PC346Flu1 | 1.05 | 0.000 |
| AK021627 | MORC4 | MORC family CW-type zinc finger 4 | Xq22.3 | PC346Flu1 | 1.24 | 0.000 |
| AF142409 | MS4A6A | membrane-spanning 4-domains subfamily A member 6A | 11q12.1 | PC346Flu1 | 0.76 | 0.450 |
| NM_005956 | MTHFD1 | Methylenetetrahydrofolate dehydrogenase (NADP+ dependent) 1 | 14q24 | PC346C | 0.61 | 0.000 |
| NM_016498 | MTP18 * | Mitochondrial protein 18 kDa * | 22q | PC346C | 0.64 | 0.000 |
| NM_000662 | NAT1 | N-acetyltransferase 1 arylamine N-acetyltransferase | 8p23.1-p21.3 | PC346Flu1 | 1.68 | 0.000 |
| AF039944 | NDRG1 | N-myc downstream regulated gene 1 | 8q24.3 | PC346Flu1 | 1.63 | 0.000 |
| NM_006096 | NDRG1 | N-myc downstream regulated gene 1 | 8q24.3 | PC346Flu1 | 2.60 | 0.000 |
| NM_005596 | NFIB | nuclear factor I/B | 9p24.1 | PC346Flu1 | 0.77 | 0.077 |
| NM_020529 | NFKBIA | nuclear factor of kappa light polypeptide gene enhancer in B-cells inhibitor alpha | 14q13 | PC346C | 0.74 | 0.000 |
| NM_020529 | NFKBIA | nuclear factor of kappa light polypeptide gene enhancer in B-cells inhibitor alpha | 14q13 | PC346Flu1 | 2.39 | 0.000 |
| NM_020529 | NFKBIA | nuclear factor of kappa light polypeptide gene enhancer in B-cells inhibitor alpha | 14q13 | PC346Flu2 | 0.65 | 1.093 |
| NM_016590 | PART1 * | prostata androgen-regulated transcript 1 * | 5q12.1 | PC346Flu1 | 1.45 | 0.000 |
| NM_006810 | PDI A5 | protein disulfide isomerase family A member 5 | 3q21.1 | PC346C | 0.50 | 0.000 |
| NM_006810 | PDI A5 | protein disulfide isomerase family A member 5 | 3q21.1 | PC346Flu1 | 1.42 | 0.000 |
| NM_016166 | PIAS1 | protein inhibitor of activated STAT 1 | 15q | PC346Flu1 | 1.31 | 0.000 |
| AF070670 | PPM1A | protein phosphatase 1A formerly 2C magnesium-dependent alpha isoform | 14q23.1 | PC346Flu1 | 0.72 | 0.000 |
| NM_004156 | PPP2CB | Protein phosphatase 2 formerly 2A catalytic subunit beta isoform | 8p12-p11.2 | PC346Flu1 | 0.94 | 0.000 |
| NM_002923 | RGS2 | regulator of G-protein signaling 2 24kDa | 1q31 | PC346Flu2 | 0.73 | 0.000 |
| D16875 | RHOB | ras homolog gene family member B | 2p24 | PC346Flu1 | 1.61 | 0.000 |

| | | | | | | |
|-----------|---------|--|---------------|-----------|------|-------|
| AK001478 | RHOU | ras homolog gene family member U | 1q42.11-q42.3 | PC346C | 0.77 | 0.000 |
| AK001478 | RHOU | ras homolog gene family member U | 1q42.11-q42.3 | PC346Flu1 | 2.29 | 0.000 |
| AK001478 | RHOU | ras homolog gene family member U | 1q42.11-q42.3 | PC346Flu2 | 1.05 | 0.000 |
| AB051826 | RHOU | ras homolog gene family member U | 1q42.11-q42.3 | PC346Flu1 | 2.54 | 0.000 |
| NM_005627 | SGK1 | serum/glucocorticoid regulated kinase 1 | 6q23 | PC346Flu1 | 0.85 | 0.000 |
| AB040914 | SHROOM3 | shroom family member 3 | 4q21.1 | PC346Flu1 | 1.01 | 0.012 |
| NM_004595 | SMS | spermine synthase | Xp22.1 | PC346Flu1 | 1.14 | 0.000 |
| NM_003082 | SNAPC1 | small nuclear RNA activating complex polypeptide 1 43kDa | 14q22 | PC346Flu1 | 0.62 | 0.166 |
| NM_003104 | SORD * | sorbitol dehydrogenase * | 15q15.3 | PC346Flu1 | 1.20 | 0.000 |
| NM_012449 | STEAP1 | six transmembrane epithelial antigen of the prostate 1 | 7q21 | PC346C | 0.79 | 0.000 |
| NM_012449 | STEAP1 | six transmembrane epithelial antigen of the prostate 1 | 7q21 | PC346Flu1 | 1.69 | 0.000 |
| NM_012449 | STEAP1 | six transmembrane epithelial antigen of the prostate 1 | 7q21 | PC346Flu2 | 0.97 | 1.091 |
| AK026813 | STEAP2 | six transmembrane epithelial antigen of the prostate 2 | 7q21 | PC346Flu1 | 1.07 | 0.000 |
| AK026813 | STEAP2 | six transmembrane epithelial antigen of the prostate 2 | 7q21 | PC346Flu2 | 0.74 | 0.000 |
| NM_005656 | TMPRSS2 | Transmembrane protease serine 2 | 21q22.3 | PC346C | 0.59 | 0.117 |
| NM_005079 | TPD52 | tumor protein D52 | 8q21 | PC346Flu1 | 1.22 | 0.000 |
| NM_005079 | TPD52 | tumor protein D52 | 8q21 | PC346Flu2 | 0.69 | 0.208 |
| AF294628 | TWSG1 | twisted gastrulation homolog 1 Drosophila | 18p11.3 | PC346Flu1 | 0.99 | 0.000 |
| NM_003115 | UAP1 | UDP-N-acetylglucosamine pyrophosphorylase 1 | 1q23.3 | PC346Flu1 | 0.96 | 0.000 |
| NM_003359 | UGDH | UDP-glucose dehydrogenase | 4p15.1 | PC346C | 0.58 | 0.098 |
| NM_003359 | UGDH | UDP-glucose dehydrogenase | 4p15.1 | PC346Flu1 | 1.91 | 0.000 |
| AK001647 | USP40 | ubiquitin specific peptidase 40 | 2q37.1 | PC346C | 0.68 | 0.000 |
| AB020676 | WWC1 | WW and C2 domain containing 1 | 5q34 | PC346Flu1 | 0.74 | 0.000 |
| AK022814 | ZBTB10 | zinc finger and BTB domain containing 10 | 8q13-q21.1 | PC346Flu1 | 1.34 | 0.000 |
| AK022814 | ZBTB10 | zinc finger and BTB domain containing 10 | 8q13-q21.1 | PC346Flu2 | 0.54 | 1.093 |
| NM_006006 | ZBTB16 | zinc finger and BTB domain containing 16 | 11q23.1 | PC346C | 0.88 | 0.000 |
| NM_006006 | ZBTB16 | zinc finger and BTB domain containing 16 | 11q23.1 | PC346Flu1 | 1.55 | 0.000 |
| NM_006006 | ZBTB16 | zinc finger and BTB domain containing 16 | 11q23.1 | PC346Flu2 | 1.55 | 1.093 |
| AF025771 | ZNF189 | zinc finger protein 189 | 9q22-q31 | PC346Flu1 | 1.50 | 0.000 |
| AK026383 | NDRG1 | cDNA clone * | | PC346Flu1 | 2.05 | 0.000 |
| AL157445 | | cDNA clone * | | PC346Flu1 | 1.02 | 0.007 |
| D17210 | | cDNA clone * | | PC346Flu1 | 0.97 | 0.000 |

* no approved HUGO symbol / name exist for this entry. If present, gene symbol / name from the UNIGENE database are given in alternative.

Table 4 - List of genes down-regulated by R1881

| GenBank ID | HUGO Symbol | HUGO Name | Cytoband | Cell line | 2log ratio | SAM q-value |
|------------|-------------|---|----------------|-----------|------------|-------------|
| NM_005688 | ABCC5 | ATP-binding cassette sub-family C CFTR/MRP member 5 | 3q27 | PC346Flu1 | -0.68 | 0.282 |
| AK026288 | ATHL1 | ATH1 acid trehalase-like 1 yeast | 11p15.5 | PC346Flu1 | -0.96 | 0.008 |
| NM_012342 | BAMBI | BMP and activin membrane-bound inhibitor homolog Xenopus laevis | 10p12.3-p11.2 | PC346Flu1 | -0.98 | 0.000 |
| NM_001197 | BIK | BCL2-interacting killer apoptosis-inducing | 22q13.31 | PC346Flu1 | -0.82 | 0.112 |
| AF075110 | C14orf4 | chromosome 14 open reading frame 4 | 14q24.3 | PC346Flu1 | -1.29 | 0.000 |
| NM_017766 | CASZ1 | castor zinc finger 1 | 1p36.22 | PC346Flu1 | -0.98 | 0.112 |
| NM_001305 | CLDN4 | claudin 4 | 7q11.23 | PC346Flu1 | -0.63 | 0.282 |
| AK024378 | FAM131A | family with sequence similarity 131 member A | 3q27.1 | PC346Flu1 | -0.71 | 0.052 |
| NM_004480 | FUT8 | fucosyltransferase 8 alpha 1 6 fucosyltransferase | 14q24.3 | PC346Flu1 | -1.01 | 0.316 |
| NM_002165 | ID1 | inhibitor of DNA binding 1 dominant negative helix-loop-helix protein | 20q11 | PC346Flu1 | -0.81 | 0.018 |
| NM_002165 | ID1 | inhibitor of DNA binding 1 dominant negative helix-loop-helix protein | 20q11 | PC346Flu2 | -1.07 | 1.087 |
| X69111 | ID3 | inhibitor of DNA binding 3 dominant negative helix-loop-helix protein | 1p36.13-p36.12 | PC346Flu1 | -1.25 | 0.000 |
| NM_006769 | LMO4 | LIM domain only 4 | 1p22.3 | PC346Flu1 | -0.82 | 0.000 |
| NM_017572 | MKNK2 | MAP kinase interacting serine/threonine kinase 2 | 19p13.3 | PC346Flu1 | -0.68 | 0.088 |
| NM_005377 | MYCL2 | v-myc myelocytomatosis viral oncogene homolog 2 (avian) | Xq22-q23 | PC346C | -0.97 | 0.116 |
| NM_006312 | NICOR2 | nuclear receptor co-repressor 2 | 12q24 | PC346Flu1 | -0.57 | 0.052 |
| U90907 | PIK3R3 | phosphoinositide-3-kinase regulatory subunit 3 p55 gamma | 1p34.1 | PC346Flu1 | -1.01 | 0.008 |
| AF113132 | PSAT1 | phosphoserine aminotransferase 1 | 9q21.2 | PC346Flu1 | -0.78 | 0.000 |
| NM_004577 | PSPH | phosphoserine phosphatase | 7p15.2-p15.1 | PC346Flu1 | -0.85 | 0.041 |
| NM_015923 | SLC3A2 | solute carrier family 3, member 2 | 11q13 | PC346Flu1 | -0.61 | 0.263 |
| NM_003943 | STBD1 | starch binding domain 1 | 4q24-q25 | PC346Flu1 | -0.79 | 0.022 |
| NM_003714 | STC2 | stanniocalcin 2 | 5q35.1 | PC346Flu1 | -0.63 | 0.088 |
| AK000401 | TANC1 | tetratricopeptide repeat ankyrin repeat and coiled-coil containing 1 | 2q24.2 | PC346Flu2 | -0.72 | 1.087 |
| AL133074 | TP53INP1 | tumor protein p53 inducible nuclear protein 1 | 8q22 | PC346Flu1 | -1.25 | 0.000 |
| NM_003287 | TPD52L1 | tumor protein D52-like 1 | 6q22-q23 | PC346Flu1 | -0.71 | 0.402 |
| AF205437 | TRIB1 | tribbles homolog 1 Drosophila | 8q24.13 | PC346Flu1 | -1.63 | 0.000 |
| U55055 | | Oral cancer candidate gene mRNA clone | 8q24.13 | PC346Flu2 | -1.01 | 1.087 |
| NM_018588 | | hypothetical protein * | | PC346C | -0.64 | 0.194 |
| NM_018588 | | hypothetical protein * | | PC346Flu1 | -0.55 | 0.422 |
| AK022971 | | cDNA clone * | | PC346Flu1 | -0.66 | 0.450 |
| AK022971 | | cDNA clone * | | PC346Flu2 | -0.71 | 1.087 |

* no approved HUGO symbol / name exist for this entry. If present, gene symbol / name from the UNIGENE database are given in alternative.

Table 5 - List of genes up-regulated by hydroxyflutamide

| GenBank ID | HUGO_Symbol | HUGO_Name | Cytoband | Cell line | 2log ratio | SAM q-value |
|------------|-------------|--|-------------|-----------|------------|-------------|
| AB020637 | ENDOD1 | endonuclease domain containing 1 | 11q21 | PC346Flu2 | 0.51 | 0.158 |
| NM_004117 | FKBP5 | FK506 binding protein 5 | 6p21.3-21.2 | PC346Flu2 | 0.57 | 0.226 |
| AB042410 | GPR88 | G protein-coupled receptor 88 | 1p21.3 | PC346Flu2 | 1.57 | 0.000 |
| NM_002923 | RGS2 | regulator of G-protein signaling 2 24kDa | 1q31 | PC346Flu2 | 0.57 | 0.000 |
| AK026813 | STEAP2 | six transmembrane epithelial antigen of the prostate 2 | 7q21 | PC346Flu2 | 0.61 | 0.118 |
| AB020676 | WWC1 | WW and C2 domain containing 1 | 5q34 | PC346Flu2 | 0.52 | 0.158 |
| D17099 | | cDNA clone * | | PC346Flu2 | 0.90 | 0.926 |
| AL049966 | | cDNA clone * | | PC346Flu2 | 0.92 | 0.926 |

* no approved HUGO symbol / name exist for this entry. If present, gene symbol / name from the UNIGENE database are given in alternative.

Table 6 - List of genes down-regulated by hydroxyflutamide

| GenBank ID | HUGO_Symbol | HUGO_name | Cytoband | Cell line | 2log ratio | SAM q-value |
|------------|-------------|---|--------------|-----------|------------|-------------|
| NM_002165 | ID1 | inhibitor of DNA binding 1 | 20q11 | PC346Flu2 | -0.58 | 0.301 |
| NM_002241 | KCNJ10 | potassium inwardly-rectifying channel subfamily J member 10 | 1q22-q23 | PC346Flu2 | -0.84 | 0.301 |
| NM_006854 | KDELFR2 | KDEL Lys-Asp-Glu-Leu endoplasmic reticulum protein retention receptor 2 | 7p22.1 | PC346C | -0.78 | 1.118 |
| AB028451 | NCOR1 | nuclear receptor co-repressor 1 | 17p11.2 | PC346Flu2 | -1.00 | 0.301 |
| NM_001269 | RCC1 | regulator of chromosome condensation 1 | 1p36.1 | PC346Flu2 | -0.70 | 0.301 |
| NM_000370 | TTPA | tocopherol alpha transfer protein | 8q13.1-q13.3 | PC346Flu2 | -0.83 | 0.301 |

* no approved HUGO symbol / name exist for this entry. If present, gene symbol / name from the UNIGENE database are given in alternative.

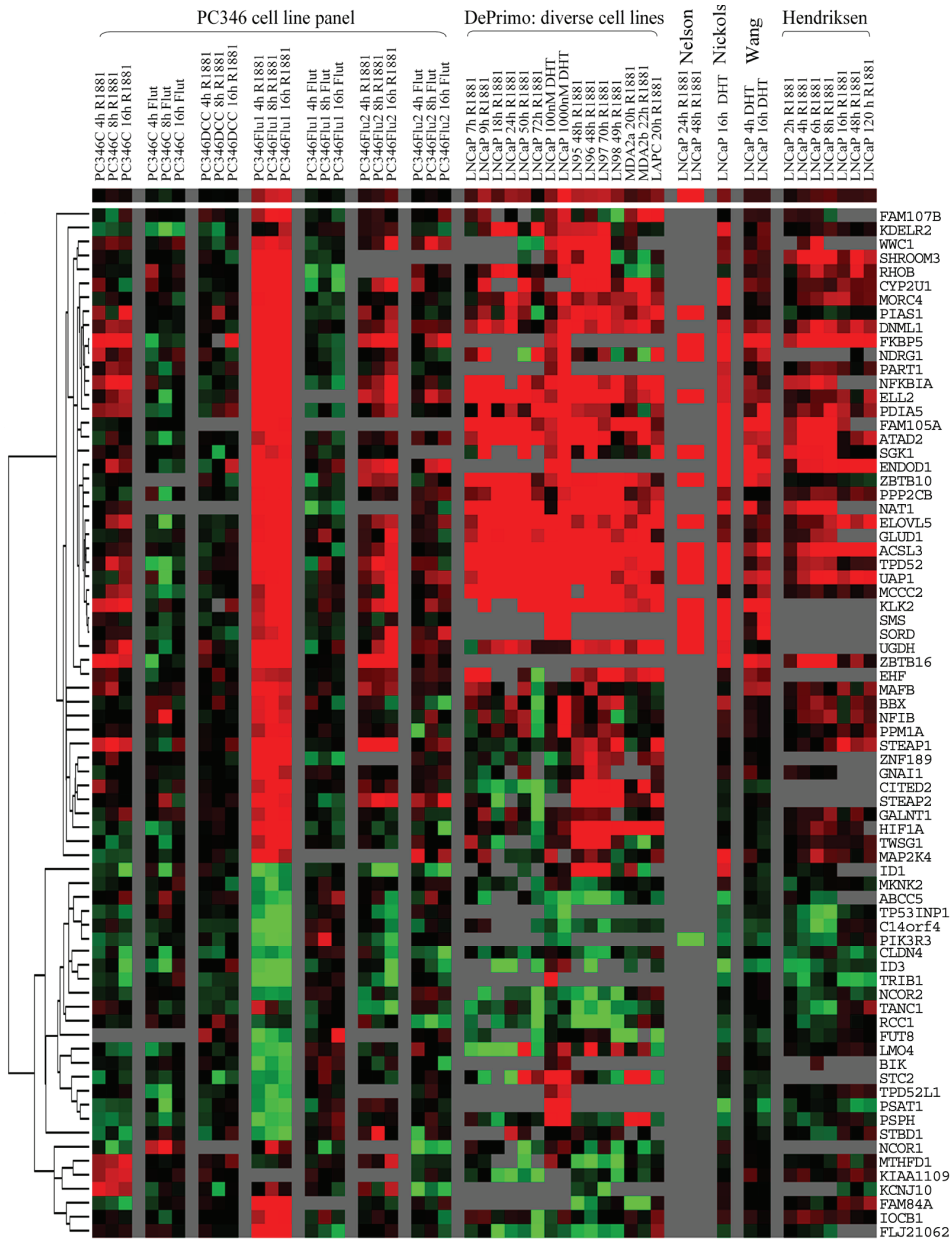


Figure 2 - Expression profile of androgen-responsive genes in PC346 cells linked to publicly available databases on AR transcriptional regulation. On the left side, PC346C, PC346Flu1 and PC346Flu2 were exposed to 1 nM R1881 or 1 μ M OH-flutamide for 4, 8 and 16h, whereas PC346DCC was stimulated with 1 nM R1881 only. On the right side, our gene signature was assessed in the databases from DePrimo et al., Nelson et al., Nickols et al., Wang et al. and Hendriksen et al. (see table 7 for database details). Heatmap is presented for the 2log expression ratio between hormone-treated samples and respective time-matched vehicle controls. Red and green colors represent induction and repression, respectively, whereas black indicates no regulation. Grey squares indicate missing data due to low expression, poor data quality or absence of probes for the respective transcript in the array platform used for the study.

Table 7 - Description of the androgen-regulation and prostate cancer databases linked via SRS

| First Author (date) | Reference | Query |
|------------------------|---|---|
| DePrimo (2002) [46] | LNCaP, LN95, LN96, LN97, LN98, LAPC, MDA2a, MDA2b cell lines | 1nM R1881, 10nM DHT, 100nM DHT and 1000nM DHT different time points from 7 to 72h |
| Hendriksen (2006) [28] | LNCaP | 1nM R1881 time-course from 2h to 120h |
| Nelson (2002) [47] | LNCaP | 24h and 48h 1nM R1881 |
| Nickols (2007) [48] | LNCaP | 16h 1nM DHT |
| Wang (2007) [49] | LNCaP | 4h and 16h 100nM DHT |
| Best (2005) [50] | 10 hormone-naive prostate cancers | 10 hormone-refractory primary prostate tumors |
| Chandran (2007) [51] | 64 primary prostate tumor samples | 24 hormone-refractory metastatic samples from 4 patients |
| Lapointe (2004) [52] | 41 benign prostate tissue adjacent to cancer | 62 primary prostate tumor samples 9 lymph node metastasis |
| Singh (2002) [53] | 50 benign prostate tissue adjacent to cancer | 52 primary prostate tumor samples, of which 8 recurred after radical prostatectomy and 13 remained relapse-free (>4 years) |
| Tamura (2007) [54] | 10 hormone-naive prostate cancers | 18 hormone-refractory primary and metastatic tumor samples |
| Varambally (2005) [55] | 4 benign prostate tissues | 5 clinically localized prostate cancers 5 metastatic samples |
| Yu (2007) [16] | 60 benign prostate tissue adjacent to cancer 23 disease free donor prostate tissue | 62 primary prostate tumors 24 metastatic samples from 4 patients |

Validation of the microarray data

The microarray data was validated by two approaches: an experimental approach using RT-PCR, and a bioinformatics approach linking our gene signature to a set of publicly available databases on androgen response. We selected 10 androgen-regulated genes to be further validated by RT-PCR: PSA, KLK2, PART1, TPD52, GPR88, FKBP5, TMPRSS2, STEAP1, ID3 and TRIB1. It is worth noting that our microarray analysis did not detect regulation of PSA expression in response to the hormonal treatments, but since this is a prominent AR target gene, it was included in the RT-PCR analysis. The AR and GAPDH genes were also included in the RT-PCR assay, to confirm the AR status of the cell lines and for normalization purposes, respectively. Consistent to previous knowledge on the PC346 cell panel, RT-PCR showed decreased expression of AR in PC346DCC and over-expression in PC346Flu1. The AR mRNA itself was not regulated by hormonal treatment. RT-PCR analysis further confirmed the differential expression of all selected genes in the same direction predicted by the microarray analysis (Fig. 1). Furthermore, the RT-PCR also showed a stronger effect of the hormone-treatment on the PC346Flu1 cell line, in contrast to the almost absent induction of PC346DCC cells, when compared to the parental PC346C, for most genes analysed. As observed in the microarray assay, PC346Flu2 showed equivalent responses to R1881 and OH-flutamide for many regulated genes (Fig. 1, Tables 3-6).

Recently, a series of studies have been published that analyzed gene expression in response to androgens stimulation in cell lines and xenografts (Table 7). Of the 107 transcripts in our signature, 73 were present in at least 3 of the 5 databases and were included for further analysis. More than 90% of the linked genes overlapped with previously reported androgen-regulated targets. Genes with the strongest inductions in our present work also showed consistently high inductions in multiple previous reports, suggesting that the products of these genes may play a basic role in the biological function of the prostate (Fig. 2). Using our unique cell line panel, we were able to identify novel androgen-responsive genes such as MAFB, KLF9, NFIB, STBD1, BIK or HLX.

Biologic processes coordinated by the AR pathway

The androgen-regulated signature genes were classified according to Gene Ontology (GO) Biological Processes using the Database for Annotation, Visualization and Integrated Discovery (DAVID: <http://david.abcc.ncifcrf.gov>) [12,13].

Consistent with the physiological roles of androgens, this approach revealed that the AR target genes selected in the present study operate in the regulation of transcription and intracellular signaling pathways, the metabolism of proteins, lipids and carbohydrates, and the regulation of cell proliferation and differentiation (Figure 3A). The largest category includes genes encoding for transcription factors and transcription regulators, such as NFIB, KLF9, HIF1A, MAFB, EHF, NCOR1, NCOR2, PIAS1 and several zinc finger proteins (ZNF189, ZBTB10, ZBTB16 and CASZ1). This was followed by genes involved in intracellular signal transduction, including the G protein-coupled receptors pathway (GPR88, RGS2, GNAI1), small GTPases of the Ras family (RHOB, RHOU), mitogen-activated protein kinase cascade (MAP2K4, MKNK2, TRIB1) and other protein kinases/phosphatases (PPM1A, PPP2CB, PIK3R3, SGK1). Other AR responsive genes have an effect on cellular proliferation through regulation of cell cycle and apoptotic processes (e.g. RCC1, BBX, BIK, TP53INP1). Concomitant with the role of

androgens on prostate development and maturation, another major cluster included genes involved in cellular differentiation, such as TPD52, TWSG1, NDRG1, ID1 and ID3. Finally, androgen induced the metabolism of proteins, carbohydrates and lipids that contribute to the production and secretion of prostatic fluid. R1881 target genes included MTHFD1, PSPH, PSAT1 and MCCC2, encoding enzymes in the metabolism of methionine, serine and leucine amino acids, respectively. Furthermore, up-regulation of the translation initiation factor EIF2C3 potentially promotes peptide synthesis. Moreover, genes participating in protein folding (PDIAS5, FKBP5), glycosylation (FUT8, GALNT1) and trafficking (DMN1L, KDELR2) were also regulated by R1881. Apart from proteins and amino acids, prostatic fluid is also rich in lipids, polyamines, sorbitol and several metal ions. Indeed, R1881 also stimulated expression of ACSL3 and ELOVL5, which participate in the elongation of fatty-acids, spermine synthase (SMS), part of the polyamine synthetic pathway, sorbitol dehydrogenase (SORD), secreted by the prostate into the seminal fluid, and the ion channels ACCN4 and KCNJ10.

Table 8 - Summary of significantly enriched Gene Ontology (GO) categories

| Annotation Cluster 1 | Enrichment Score: 2.43 | Count | P_Value | Gene List |
|--|------------------------|-------|---------|--|
| organic acid metabolic process | | 10 | 0.0025 | ACSL3, ELOVL5, PSPH, |
| amine metabolic process | | 9 | 0.0022 | SMS, UGDH, GLUD1, MTHFD1, |
| amino acid metabolic process | | 7 | 0.0046 | PPP2CB, MCCC2, PSAT1 |
| Annotation Cluster 2 | Enrichment Score: 2.34 | Count | P_Value | Gene List |
| apoptosis | | 12 | 0.0019 | DNM1L, PPP2CB, ELL2, BIK, |
| programmed cell death | | 12 | 0.0021 | RHOB, MTP18, TPD52L1, TP53INP1, |
| cell development | | 12 | 0.049 | SGK1, NFKBIA, ID3, ZBTB16 |
| Annotation Cluster 3 | Enrichment Score: 2.27 | Count | P_Value | Gene List |
| developmental process | | 27 | 0.0088 | FUT8, MAFB, MTP18, TPD52L1, CITED2, |
| cell differentiation | | 19 | 0.0042 | TTPA, SHROOM3, EHF, NDRG1, TP53INP1, SGK1, BIK, RHOB, ZBTB16, UGDH, IQCB1, ID1, ID3, ELL2, DNM1L, LMO4, HLX, KLF9, PPP2CB, TPD52, TWSG1, NFKBIA |
| Annotation Cluster 4 | Enrichment Score: 2.12 | Count | P_Value | Gene List |
| regulation of developmental process | | 7 | 0.002 | MAFB, PPP2CB, |
| regulation of cell differentiation | | 6 | 0.0013 | TWSG1, NFKBIA, ZBTB16, |
| hemopoiesis | | 5 | 0.016 | SHROOM3, IQCB1 |
| Annotation Cluster 5 | Enrichment Score: 1.69 | Count | P_Value | Gene List |
| negative regulation of metabolic process | | 7 | 0.023 | PPP2CB, ZNF189, NCOR1, |
| negative regulation of transcription | | 6 | 0.018 | NCOR2, ID1, ID3, ZBTB16 |
| Annotation Cluster 6 | Enrichment Score: 1.49 | Count | P_Value | Gene List |
| regulation of cellular process | | 33 | 0.014 | TP3INP1, SNAPC1, TPD52L1, ZBTB16, |
| regulation of gene expression | | 23 | 0.017 | NFKBIA, ZBTB10, LMO4, NFIB, PIAS1, |
| regulation of transcription | | 22 | 0.017 | MKNK2, EHF, NCOR1, NCOR2, MAFB, KLF9, BIK, RHOB, BBX, ID1, ID3, HLX, ZNF18, TWSG1, IQCB1, PPM1A, RGS2, CITED2, PPP2CB, HIF1A, CASZ1, RCC1 |

To automate the functional classification, quantify the degree of enrichment of each cluster and select statistically significant functional categories we used the DAVID Functional Annotation Clustering tool. This tool identified 6 statistically significant Annotation Clusters, which associated with the metabolism of organic acids (lipids and amino acids), apoptosis, cell differentiation, developmental processes, regulation of transcription and regulation of cellular processes (Table 8).

The involvement of androgen-regulated genes in pathological conditions was further investigated by using the Ingenuity database (Ingenuity® Systems, www.ingenuity.com). The strongest associations were found for cancer, reproductive system, dermatological and cardiovascular diseases (Fig. 3B).

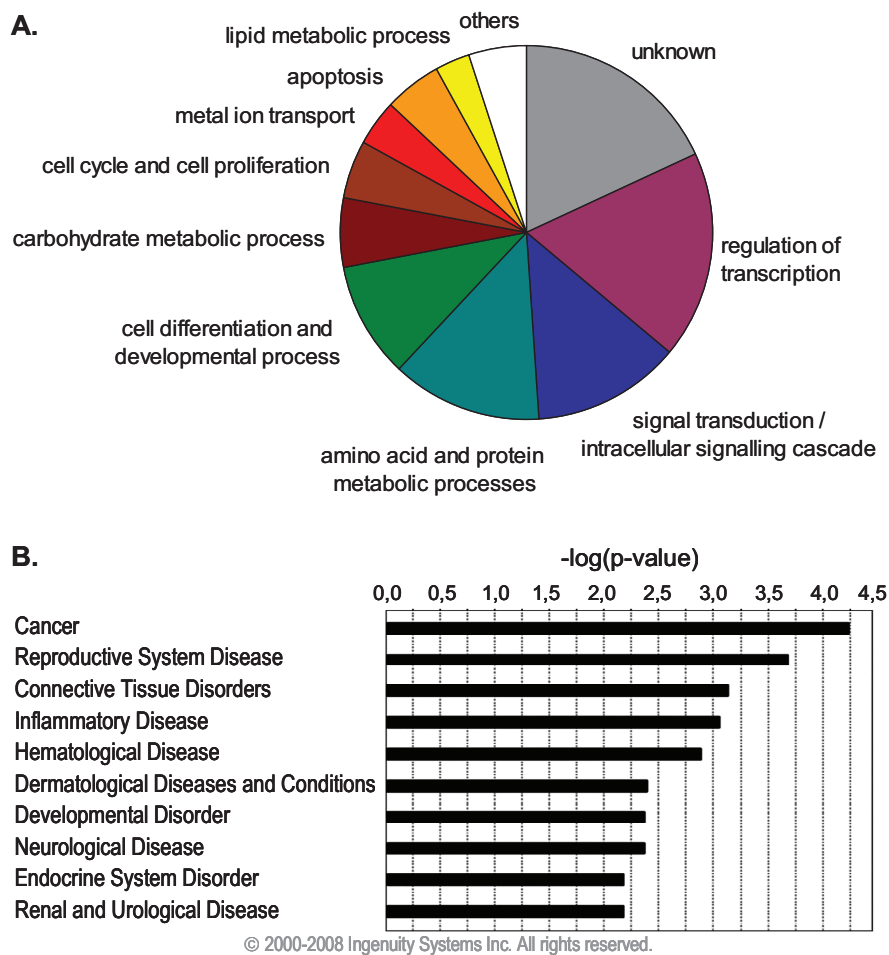


Figure 3 - Biological processes regulated by the selected androgen-target genes. **(A)** Pie-graph representing genes categorized according to most prominent biological function. Gene ontology annotations were extracted using DAVID [12,13]. **(B)** Involvement of the AR pathway genes in disease determined using Ingenuity Pathway Analysis (Ingenuity® Systems, www.ingenuity.com).

The AR pathway in prostate cancer development and progression

To investigate how the AR pathway is modulated during the development and progression of prostate cancer we linked our androgen-regulated gene signature to seven independent prostate cancer microarray databases. These studies included specimens of “normal prostate” and prostate tumors from diverse disease stages, whose main characteristics are summarized in Table 7. A total of 89 hormone-responsive genes were present in at least 4 of the 7 databases, and were selected for further analysis. In Figure 4, we show the hierarchical clustering of the R1881-responsive genes (first block of 4 columns), next to primary cancer versus normal prostate (second block), metastasis versus primary cancer (third block), and finally recurrent versus non-recurrent and hormone-refractory versus hormone-naïve disease (fourth block). The clustering analysis revealed four major gene groups: R1881-repressed and up-regulated during progression to metastatic disease (Cluster 1), R1881-repressed and down-regulated during progression (Cluster 2), R1881-induced and down-regulated during progression (Cluster 3), R1881-induced and up-regulated during progression (Cluster 4). About one third of the R1881-regulated genes was differentially-expressed between primary tumors and normal prostate in at least two databases. To this group contributed mainly R1881-induced genes that showed up-regulation in prostate cancer. These are genes that play a role in the production of prostatic fluid and in secretory function of the prostate, including SORD, ACSL3, ELOVL5, FKBP5, PDIA5, GLUD1 and UAP1. However, when comparing metastatic cancer to primary tumors, 23 of the R1881-induced genes were down-regulated (Fig. 4, Cluster 3), while 11 androgen-repressed genes were up-regulated (Fig. 4, Cluster 1). In total, these two clusters made up a considerable fraction (40%) of the androgen-responsive genes, and their expression pattern in metastasis suggests that the AR pathway is selectively down-regulated at this stage of the disease. In contrast, another group of R1881-stimulated genes showed increased expression in metastasis compared to primary tumors (Fig. 4, Cluster 4). This cluster is enriched for genes involved in survival/cellular proliferation (MAFB, ELL2, TPD52, EHF, HIF1A, HLX and SGK) and cell remodeling/adhesion (RHOU, SHROOM3, MORC4, TWSG1). Conversely, a group of R1881-repressed genes down-regulated in metastasis included genes involved in cellular differentiation and development (ID1, ID3, LMO4 and TPD52L1) (Fig. 4, Cluster 2). Finally, we assessed the activation state of the AR pathway in recurrent and in hormone-refractory disease. The collection of datasets in this category is limited to three non-concordant databases: Best *et al.* and Tamura *et al.* compared hormone-naïve with hormone-refractory samples, Singh *et al.* evaluated biochemical recurrence following radical prostatectomy. Therefore, the overlap between the three databases was modest. Nevertheless, the general trend is the same as for the progression of primary cancer to metastatic disease: genes down-regulated in metastasis tend to be down-regulated in recurrent versus non-recurrent and/or hormone-refractory versus hormone-naïve disease, and vice-versa. These results suggest that the common mechanisms may govern the progression to different states of prostate cancer disease.

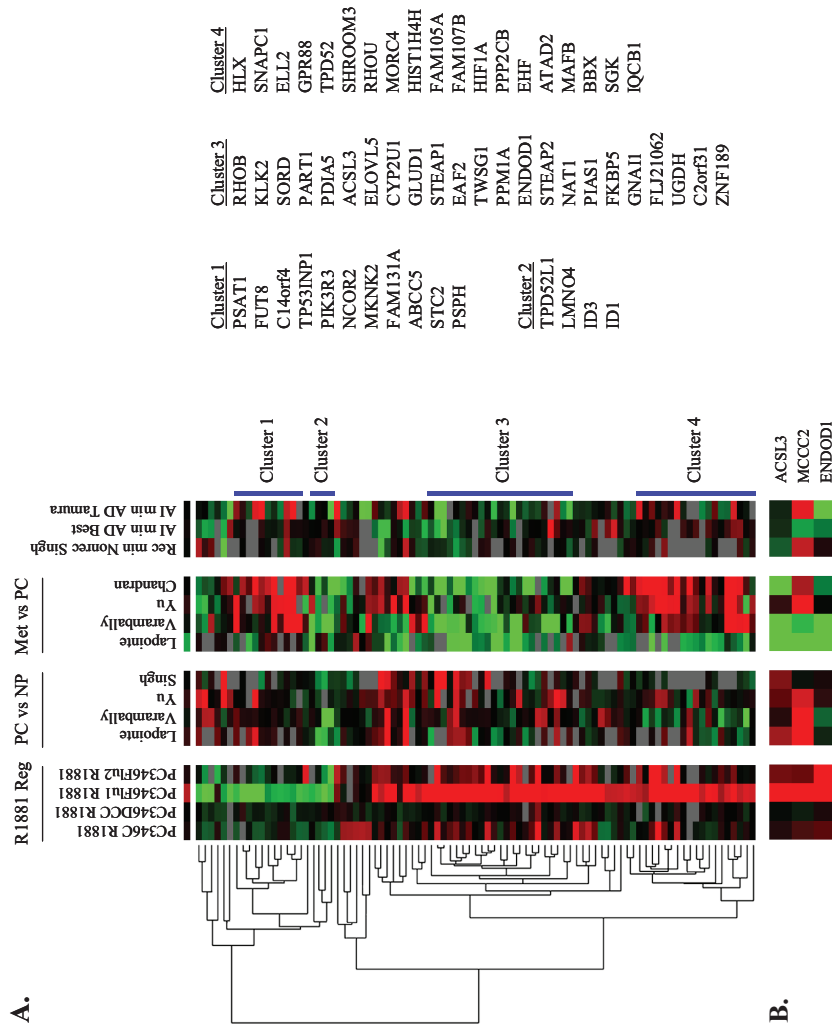


Figure 4 - Expression of androgen-responsive genes in prostate cancer samples from patients. **(A)** Heat-map representation of publicly available expression data from human prostate cancer using the 107-gene signature (see table 7 for database details). **(B)** Androgen-responsive genes selected for further quantitative PCR analysis. Color scheme as described for figure 2.

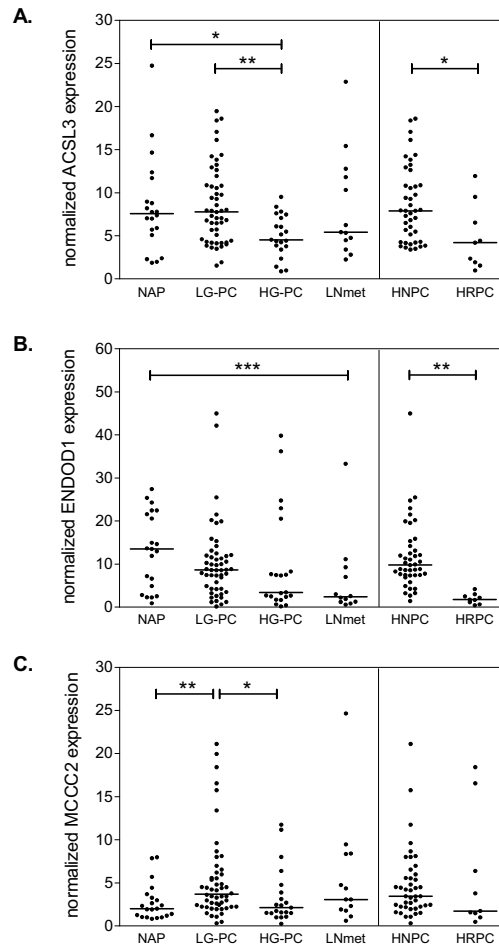


Figure 5 - Quantitative RT-PCR analysis of four androgen-responsive genes ACSL3, ENDOD1 and MCCC2 in a distinct set of prostate samples. NAP: normal adjacent prostate; LG-PC: low-grade prostate cancer, including Gleason score from 5-7; HG-PC: high-grade prostate cancer, including Gleason score from 8-10; LNmet: lymph-node metastasis; HNPC: hormone-naïve prostate cancer (primary location); HRPC: hormone-refractory prostate cancer (primary location); (*) p-value ≤ 0.05 and (**) p-value ≤ 0.005 using Mann-Whitney two-tailed test; (***) p-value ≤ 0.05 with Post linear-trend test.

AR target genes as markers for disease diagnosis and prognosis

The last objective of this study was to identify genes that could possibly be used as tools in the diagnosis of prostate cancer or in predicting the course of disease. We selected three R1881-regulated genes to be analyzed by quantitative PCR on normal prostate and prostate carcinoma specimens obtained at our institute: ACSL3, MCCC2 and ENDOD1. These candidates were selected based on their strong androgen-induction, potential pathological function but, most importantly, on the fact that their expression was confirmed to be altered across multiple prostate cancer databases analyzed (Fig.

4B). In this sense, ACSL3 seems to be slightly up-regulated in primary prostate tumors and strongly repressed in metastatic cancer. Furthermore, fusion of the ACSL3 gene to the ETS family member ETV1 has recently been reported, making it an interesting gene for follow-up [41]. MCCC2 was strongly up-regulated in primary cancer, although its expression in metastasis and hormone-refractory disease varies in the different databases (Fig. 4B). Finally, ENDOD1 was one of the strongest R1881-induced genes in our microarray profile, and showed decreased expression in metastasis and hormone-refractory tumors, suggesting a possible role in disease progression (Fig. 4B).

Quantitative PCR analysis included 21 samples of benign prostate tissue (adjacent to cancer), 73 primary prostate tumors and 13 lymph node metastasis. The primary tumors consist of 52 low-grade samples, 21 samples from late-stage poorly-differentiated tumors and 9 hormone-refractory specimens, obtained from patients operated by radical prostatectomy or transurethral resection of the prostate (TURP). ACSL3 expression was significantly decreased during progression from low-grade to high-grade tumors ($P=0.005$; Fig. 5A). ENDOD1 exhibited a stepwise down-regulation during disease progression ($P<0.05$ for Post linear-trend test), which is consistent with the results from the prostate cancer databases (Fig. 5B). Finally, MCCC2 was up-regulated in well-differentiated tumors ($P<0.005$), but its expression decreased during progression to high-grade cancer ($P<0.05$; Fig. 5C). This biphasic expression of MCCC2 during prostate cancer progression might explain the variation observed across the different databases mentioned above. Furthermore, expression of all three candidate genes was decreased during progression to hormone-refractory disease, although the trend for MCCC2 was not statistically significant.

DISCUSSION

In order to design better diagnostic and prognostic tools for prostate cancer and to develop more efficient therapies for late stage disease, it is essential to methodically understand the processes by which this disease develops and progresses. In this sense the AR pathway is of great interest for clinicians, researchers and pharmaceutical industry as it plays a crucial role in prostate malignancy. To investigate whether the AR pathway is functionally active in hormone-refractory prostate disease, we started by establishing the expression program of AR target genes in PC346 cell lines stimulated with R1881 or hydroxyflutamide.

R1881 stimulation of the androgen-sensitive PC346C subline resulted in differential expression of 20 genes, including the well-known AR target genes TMPRSS2, KLK2 and TPD52. Consistent with the expression of *wild-type* AR, OH-flutamide did not mediate transcription of AR-target genes in PC346C cells.

The castration-resistant PC346DCC subline, which expresses very low levels of the receptor, showed to be insensitive to R1881 stimulation. These results suggest that the AR pathway is not essential for the growth of PC346DCC cells. How these cells have bypassed the AR pathway, surviving and proliferating in the absence of androgens, is still not clear. Hypothetically, it could have been achieved through activation of oncogenes or alternative growth pathways, and/or repression of tumor suppressors.

Conversely, the cell line overexpressing the AR, PC346Flu1, showed a “super-activation” of the pathway, not only in the number of regulated genes but also in the strength of this regulation. This reveals two important aspects: (i) although these cells have been cultured in the absence of androgens for longer than two years, the AR is still functional and can be activated by the presence of its ligand; (ii) the AR seems to be hyper-sensitive, likely due to the high levels of the receptor, which may be sufficient to support cell growth under the hormone-depleted conditions. Interestingly, PC346Flu1 proliferation is inhibited by physiological concentrations of androgens, both *in vivo* and *in vitro*, suggesting that AR “super-activation” is unfavorable for cell growth, possibly by inducing cellular differentiation [7]. This is in line with a previous report, which showed that prostate epithelial cells tolerate a narrow-range of AR expression and activity, by undergoing apoptosis in the absence of AR expression and cell cycle arrest upon AR hyper-stimulation [15].

In PC346Flu2 subline, carrying a mutated receptor, transcription of AR-target genes was regulated by both R1881 and OH-flutamide, although the stimulatory effect of the latter was weaker. This is in agreement with the agonistic action of OH-flutamide on the T877A mutated AR in promoting rather than inhibiting the growth of PC34Flu2 cells.

In general, from these analyses we can conclude that, in the majority of hormone-refractory prostate cancer cells subjected to long-term androgen ablation, the AR pathway is modified and still able to respond to stimuli. Furthermore, it is worth noting how the AR transcription patterns of the three hormone-refractory sublines reflected their respective AR modifications and growth characteristics.

To investigate the biologic processes coordinated by the AR target genes we used DAVID and Ingenuity tools to extract and cluster Gene Ontology Annotations. Consistent with the physiological roles of androgens in prostate development and maturation, the selected gene-signature is enriched for functions in transcription regulation, intracellular signal transduction, differentiation and regulation of cell proliferation and cell death. Further functions are associated with the metabolism of proteins, lipids and carbohydrates, which can be related to the production and secretion of prostatic fluid. Pathway analysis using Ingenuity showed strong association of the androgen-regulated genes to pathological conditions as cancer, reproductive system, dermatological and cardiovascular diseases (Fig. 3 and Table 8).

Next we evaluated the role of the AR pathway in prostate cancer development and how it is modulated during cancer progression by linking our androgen-regulated gene signature to seven previously published microarray databases on clinical tumor samples. Together, these databases comprise 178 “normal prostate” samples and 331 malignant specimens, including metastasis, recurrent tumors and hormone-refractory samples (Table 7). It is worth noting that the definition of “normal prostate” is not the same across the different studies. While most authors used benign tissue adjacent to the tumor as the “normal” reference, Yu *et al.* used normal prostatic epithelia from individuals without evidence of prostatic disease [16]. They showed that the expression profile of prostate cells was not only altered within the tumor itself, but alterations were also detected in apparently benign tissue around the borders of the tumor. This so-called field-effect has been reported in various other studies, and it is believed to be more evident the closer the distance to the tumor [17,18,19]. Disparity in the sampling of

the “normal prostate” reference may certainly contribute to the variation seen between the diverse studies, together with differences in study design, microarray platforms, and most importantly, in the characteristics of the tumors included.

In summary, our AR-response profiling revealed that a considerable fraction of AR pathway genes were up-regulated in primary prostate cancer compared to normal prostate and down-regulated in metastasis. Further inspection of this gene cluster showed enrichment for genes involved in differentiation and secretory function of the prostate, functions which are redundant, if not detrimental, in progressive disease (Fig. 4, Cluster 3). On the other hand, the cluster of androgen-regulated genes over-expressed in metastasis is enriched for genes involved in cell survival, proliferation, cytoskeletal remodelling and adhesion, all crucial functions in tumor progression and invasion (Fig. 4, Cluster 4).

It is generally accepted that the AR pathway accounts for the tumor growth in most prostate cancer patients even under hormonal ablation therapy. This hypothesis is supported by numerous reports that the AR itself is expressed in the majority of prostate cancers and often amplified in metastasis and hormone-refractory tumors [20,21,22,23,24]. Chen *et al.* has shown recently that AR overexpression is the most common modification following androgen ablation treatment, and is sufficient to confer hormone-refractory growth [25]. Furthermore, clinical tumor relapse is determined by PSA recurrence, which may give the impression that the AR pathway has become again fully functional. However, the results of our present study showed a selective down-regulation of AR target genes, questioning the over-simplistic view of the AR pathway as the driving force for prostate cancer growth and proliferation. In fact, the raise in serum PSA levels during relapse rather reflects the expansion of the tumor burden than increased AR activity in the tumor tissue self [26]. Indeed, Sterbis *et al.* reported that increased risk of biochemical recurrence was associated with low expression of tissue PSA mRNA [27]. Furthermore, the authors observed that serum PSA levels did not correlate with tissue mRNA expression, which was decreased in malignant compared to benign prostate epithelial cells [27]. By using distinct cell lines to establish the androgen-response signature and expanding the patient-derived database sets, our results corroborate previous observations from Hendriksen *et al.*, which used the androgen-response expression profile from LNCaP cells to interrogate a set of prostate cancer xenografts and Lapointe’s patient-derived samples [28]. Shortly thereafter, with distinct bioinformatics approaches, two other studies confirmed an attenuated androgen signaling signature in high-grade and metastatic prostate cancer, indicating that down-regulation of the AR pathway, although controversial, is not likely to be an artifact [29,30].

The mechanisms for this selective modulation of the AR pathway during prostate cancer progression are yet undefined, but we speculate that it may be dictated by an imbalance in AR co-regulators and/or interactions with other signaling pathways. Indeed, alterations in several AR co-activators and co-repressors have been previously detected in prostate cancer and, in particular, in hormone-refractory disease [31,32]. Furthermore, crosstalk between the AR and other growth factor pathways has been shown to activate AR signaling and selectively regulate a fraction of the AR transcriptional program, in response to IGF and EGF [33,34].

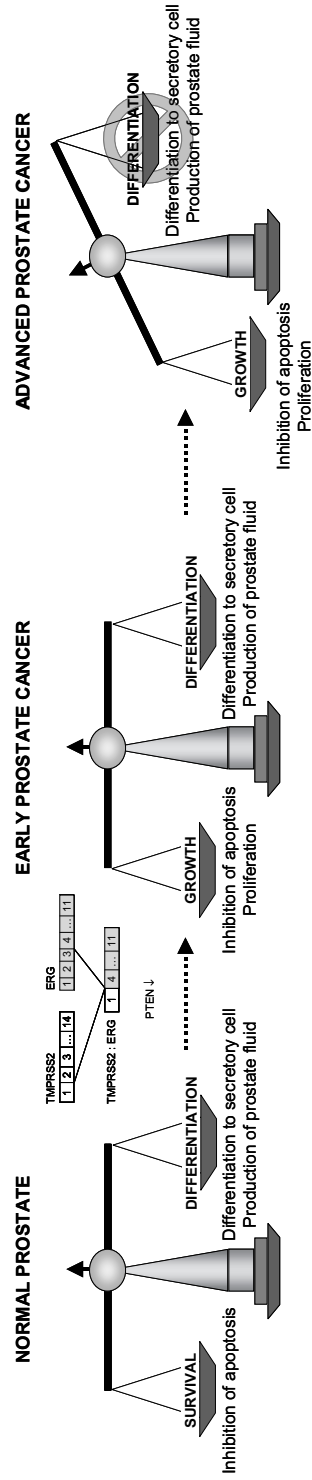


Figure 6 - Proposed model for prostate cancer progression. In normal prostate epithelial cells the AR maintains the balance between survival and differentiation. Cooperation between TMRSS2:ERG and PTEN loss, is a potential mechanism suggested to drive the transition from prostatic intraepithelial neoplasia (PIN) to prostate adenocarcinoma. These aberrations are early events in prostate cancer development and are present in a large fraction of tumors. Initiation of prostate cancer is marked by a switch from androgen-dependent survival to androgen-responsive proliferation. As cancer progresses, the balance is tilted towards tumor growth, while genes involved in prostate differentiation and secretory function are selectively repressed and genes promoting proliferation are up-regulated. In advanced disease, this mechanism eventually culminates in poorly-differentiated fast-growing tumors

To accommodate these novel insights into our current knowledge of prostate cancer disease, we propose the following model for the development and progression of prostate tumors (Fig. 6): in the normal prostate the AR maintains prostate homeostasis and secretory functions through a delicate balance between cell survival and differentiation. A yet unknown trigger leads to a switch from androgen-dependent survival to androgen-stimulated cellular proliferation. Recent findings implicate gene fusions between androgen-regulated genes and ETS transcription factor family members in this process. The TMPRSS2-ERG fusion is the most frequent rearrangement, being detected in up to 50% of prostate tumors [35]. The androgen-responsive promoter region of the TMPRSS2 gene drives robust expression of ERG, an oncogene that is also frequently involved in chromosomal translocations in Ewing sarcoma, myeloid leukemia and cervical carcinoma [36,37,38]. Up to date, multiple other ETS family members and 5' fusion partners have been identified in related rearrangements in prostate cancer [39,40,41,42]. However, the biological role of ETS fusions in prostate cancer development is still controversial, since ERG and ETV1 by themselves, do not seem to be tumorigenic [40,43]. Recent evidence suggests that ERG overexpression cooperates with PTEN loss in the progression from PIN to prostate adenocarcinoma [44,45]. It is worth noting that PC346 cells do not carry the TMPRSS2-ERG or TMPRSS2-ETV1 fusions, nor show increased expression of these oncogenes (unpublished data). Therefore, it remains unclear which mechanism may drive androgen-sensitive growth of PC346C cells. Nevertheless, it is still possible that other less common fusion partners that we did not test yet may be involved. We hypothesize that at early stages, when tumors are well differentiated, expression of prostate-specific genes and genes involved in the production/secretion of prostatic fluid is maintained or even increased due to the growth of the epithelial cell compartment. As tumors progress and become more aggressive, genes involved in prostate differentiation and secretory function are selectively repressed, while genes promoting proliferation are up-regulated. This mechanism will eventually culminate in a fast-growing, poorly-differentiated late-stage disease (Fig. 6).

In order to identify androgen-regulated genes that could possibly be used in the diagnosis/prognosis of prostate cancer, we selected from our 107-gene signature three androgen-regulated genes: MCCC2, ENDOD1 and ACSL3. Quantitative PCR analysis showed increased MCCC2 expression in early-stage, well-differentiated tumors, while ENDOD1 and ACSL3, were decreased in late-stage tumors and metastasis. To assess the prognostic value of these genes we compared primary prostate cancer that eventually developed distant metastasis after radical surgery with the non-recurrent tumors, but saw no significant differences (data not shown). Ultimately, the large inter-individual variation resulted in a poor separation between the diverse disease stages, even when the differences in expression were statistically significant. This limits the applicability of MCCC2, ENDOD1 or ACSL3 as independent diagnostic markers, by preventing the setting of an expression cutoff with both high specificity and sensitivity. However, the performance of these candidates may be improved in combination with other disease markers, such as PSA or ETS gene fusions, which has yet to be evaluated in the diagnosis and prognosis of prostate cancer. Finally, the down-regulation of all three candidate genes in hormone-refractory compared to hormone-

naïve disease is in agreement with an attenuation of the AR pathway, providing important clues on the mechanisms of prostate cancer progression.

CONCLUSIONS

The gene expression profile of the AR pathway in the three hormone-refractory sublines reflected their respective AR modifications: AR down-regulation correlated with deficient activation of AR-target genes; high-levels of AR resulted in more differentially-expressed genes and stronger regulation upon R1881 stimulation; finally, the T877A mutated AR responded to both R1881 and flutamide.

The AR pathway is very versatile, being involved in many biological processes including cellular proliferation, regulation of apoptosis and differentiation. The balance between these different functions dictates the homeostasis of the prostatic gland. The results of the present study suggest that the AR pathway is selectively modulated during prostate cancer progression, leading to repression of genes involved in cellular differentiation and up-regulation of anti-apoptotic and proliferation genes. Future studies are ongoing to elucidate the mechanisms of this selective adaptation of the AR signaling and how it may be targeted in prostate cancer therapy.

ACKNOWLEDGEMENTS

We thank Christel Kockx for the technical support with the microarray procedure, Antoine Veldhoven and Don de Lange for providing bioinformatics tools. Further, we would like to acknowledge the pathologists Arno van Leenders and Theo van de Kwast for the histopathological analysis of the patient samples.

This study was supported by the Netherlands Organization for Scientific Research (NWO) through ZonMW grant 903-46-187 and by the Dutch Cancer Society (KWF) through grant NKB97-1479.

REFERENCES

1. Ferlay J, Autier P, Boniol M, Heanue M, Colombet M, et al. (2007) Estimates of the cancer incidence and mortality in Europe in 2006. *Ann Oncol* 18: 581-592.
2. Frydenberg M, Stricker PD, Kaye KW (1997) Prostate cancer diagnosis and management. *Lancet* 349: 1681-1687.
3. Crawford ED, Eisenberger MA, McLeod DG, Spaulding JT, Benson R, et al. (1989) A controlled trial of leuprolide with and without flutamide in prostatic carcinoma. *N Engl J Med* 321: 419-424.
4. Eisenberger MA, Blumenstein BA, Crawford ED, Miller G, McLeod DG, et al. (1998) Bilateral orchiectomy with or without flutamide for metastatic prostate cancer. *N Engl J Med* 339: 1036-1042.
5. Jenster G (1999) The role of the androgen receptor in the development and progression of prostate cancer. *Semin Oncol* 26: 407-421.
6. Devlin HL, Mudryj M (2009) Progression of prostate cancer: multiple pathways to androgen independence. *Cancer Lett* 274: 177-186.
7. Marques RB, Erkens-Schulze S, de Ridder CM, Hermans KG, Waltering K, et al. (2005) Androgen receptor modifications in prostate cancer cells upon long-term androgen ablation and antiandrogen treatment. *Int J Cancer* 117: 221-229.
8. Baugh LR, Hill AA, Brown EL, Hunter CP (2001) Quantitative analysis of mRNA amplification by in vitro transcription. *Nucleic Acids Res* 29: E29.
9. Smyth GK (2005) Limma: linear models for microarray data; Gentleman R, Carey V, Dudoit S, Irizarry R, Huber W, editors. New York: Springer. 397-420 p.
10. Smyth GK, Speed T (2003) Normalization of cDNA microarray data. *Methods* 31: 265-273.
11. Veldhoven A, de Lange D, Smid M, de Jager V, Kors JA, et al. (2005) Storing, linking, and mining microarray databases using SRS. *BMC Bioinformatics* 6: 192.
12. Dennis G, Jr., Sherman BT, Hosack DA, Yang J, Gao W, et al. (2003) DAVID: Database for Annotation, Visualization, and Integrated Discovery. *Genome Biol* 4: P3.
13. Huang da W, Sherman BT, Lempicki RA (2009) Systematic and integrative analysis of large gene lists using DAVID bioinformatics resources. *Nat Protoc* 4: 44-57.
14. van der Heul-Nieuwenhuijsen L, Hendriksen PJ, van der Kwast TH, Jenster G (2006) Gene expression profiling of the human prostate zones. *BJU Int* 98: 886-897.
15. Tararova ND, Narizhneva N, Krivokrisenko V, Gudkov AV, Gurova KV (2007) Prostate cancer cells tolerate a narrow range of androgen receptor expression and activity. *Prostate* 67: 1801-1815.
16. Yu YP, Landsittel D, Jing L, Nelson J, Ren B, et al. (2004) Gene expression alterations in prostate cancer predicting tumor aggression and preceding development of malignancy. *J Clin Oncol* 22: 2790-2799.
17. Chandran UR, Dhir R, Ma C, Michalopoulos G, Becich M, et al. (2005) Differences in gene expression in prostate cancer, normal appearing prostate tissue adjacent to cancer and prostate tissue from cancer free organ donors. *BMC Cancer* 5: 45.
18. Dhanasekaran SM, Barrette TR, Ghosh D, Shah R, Varambally S, et al. (2001) Delineation of prognostic biomarkers in prostate cancer. *Nature* 412: 822-826.
19. Waghray A, Schober M, Feroze F, Yao F, Virgin J, et al. (2001) Identification of differentially expressed genes by serial analysis of gene expression in human prostate cancer. *Cancer Res* 61: 4283-4286.
20. van der Kwast TH, Schalken J, Ruizeveld de Winter JA, van Vroonhoven CC, Mulder E, et al. (1991) Androgen receptors in endocrine-therapy-resistant human prostate cancer. *Int J Cancer* 48: 189-193.
21. Ruizeveld de Winter JA, Janssen PJ, Sleddens HM, Verleun-Mooijman MC, Trapman J, et al. (1994) Androgen receptor status in localized and locally progressive hormone refractory human prostate cancer. *Am J Pathol* 144: 735-746.

22. Brown RS, Edwards J, Dogan A, Payne H, Harland SJ, et al. (2002) Amplification of the androgen receptor gene in bone metastases from hormone-refractory prostate cancer. *J Pathol* 198: 237-244.
23. Koivisto P, Kononen J, Palmberg C, Tammela T, Hyytinen E, et al. (1997) Androgen receptor gene amplification: a possible molecular mechanism for androgen deprivation therapy failure in prostate cancer. *Cancer Res* 57: 314-319.
24. Linja MJ, Savinainen KJ, Saramaki OR, Tammela TL, Vessella RL, et al. (2001) Amplification and overexpression of androgen receptor gene in hormone-refractory prostate cancer. *Cancer Res* 61: 3550-3555.
25. Chen CD, Welsbie DS, Tran C, Baek SH, Chen R, et al. (2004) Molecular determinants of resistance to antiandrogen therapy. *Nat Med* 10: 33-39.
26. Bostwick DG (1994) Prostate-specific antigen. Current role in diagnostic pathology of prostate cancer. *Am J Clin Pathol* 102: S31-37.
27. Sterbis JR, Gao C, Furusato B, Chen Y, Shaheduzzaman S, et al. (2008) Higher expression of the androgen-regulated gene PSA/HK3 mRNA in prostate cancer tissues predicts biochemical recurrence-free survival. *Clin Cancer Res* 14: 758-763.
28. Hendriksen PJ, Dits NF, Kokame K, Veldhoven A, van Weerden WM, et al. (2006) Evolution of the androgen receptor pathway during progression of prostate cancer. *Cancer Res* 66: 5012-5020.
29. Tomlins SA, Mehra R, Rhodes DR, Cao X, Wang L, et al. (2007) Integrative molecular concept modeling of prostate cancer progression. *Nat Genet* 39: 41-51.
30. Mendiratta P, Mostaghel E, Guinney J, Tewari AK, Porrello A, et al. (2009) Genomic Strategy for Targeting Therapy in Castration-Resistant Prostate Cancer. *J Clin Oncol*.
31. Brooke GN, Parker MG, Bevan CL (2008) Mechanisms of androgen receptor activation in advanced prostate cancer: differential co-activator recruitment and gene expression. *Oncogene* 27: 2941-2950.
32. Chmelar R, Buchanan G, Need EF, Tilley W, Greenberg NM (2007) Androgen receptor coregulators and their involvement in the development and progression of prostate cancer. *Int J Cancer* 120: 719-733.
33. Culig Z, Hobisch A, Cronauer MV, Hittmair A, Radmayr C, et al. (1995) Activation of the androgen receptor by polypeptide growth factors and cellular regulators. *World J Urol* 13: 285-289.
34. York TP, Plymate SR, Nelson PS, Eaves LJ, Webb HD, et al. (2005) cDNA microarray analysis identifies genes induced in common by peptide growth factors and androgen in human prostate epithelial cells. *Mol Carcinog* 44: 242-251.
35. Tomlins SA, Rhodes DR, Perner S, Dhanasekaran SM, Mehra R, et al. (2005) Recurrent fusion of TMPRSS2 and ETS transcription factor genes in prostate cancer. *Science* 310: 644-648.
36. Shimizu K, Ichikawa H, Tojo A, Kaneko Y, Maseki N, et al. (1993) An ets-related gene, ERG, is rearranged in human myeloid leukemia with t(16;21) chromosomal translocation. *Proc Natl Acad Sci U S A* 90: 10280-10284.
37. Ida K, Kobayashi S, Taki T, Hanada R, Bessho F, et al. (1995) EWS-FLI-1 and EWS-ERG chimeric mRNAs in Ewing's sarcoma and primitive neuroectodermal tumor. *Int J Cancer* 63: 500-504.
38. Simpson S, Woodworth CD, DiPaolo JA (1997) Altered expression of Erg and Ets-2 transcription factors is associated with genetic changes at 21q22.2-22.3 in immortal and cervical carcinoma cell lines. *Oncogene* 14: 2149-2157.
39. Han B, Mehra R, Dhanasekaran SM, Yu J, Menon A, et al. (2008) A fluorescence in situ hybridization screen for E26 transformation-specific aberrations: identification of DDX5-ETV4 fusion protein in prostate cancer. *Cancer Res* 68: 7629-7637.
40. Tomlins SA, Laxman B, Dhanasekaran SM, Helgeson BE, Cao X, et al. (2007) Distinct classes of chromosomal rearrangements create oncogenic ETS gene fusions in prostate cancer. *Nature* 448: 595-599.
41. Attard G, Clark J, Ambrosine L, Mills IG, Fisher G, et al. (2008) Heterogeneity and clinical significance of ETV1 translocations in human prostate cancer. *Br J Cancer* 99: 314-320.

42. Maher CA, Kumar-Sinha C, Cao X, Kalyana-Sundaram S, Han B, et al. (2009) Transcriptome sequencing to detect gene fusions in cancer. *Nature* 458: 97-101.
43. Tomlins SA, Laxman B, Varambally S, Cao X, Yu J, et al. (2008) Role of the TMPRSS2-ERG gene fusion in prostate cancer. *Neoplasia* 10: 177-188.
44. Carver BS, Tran J, Gopalan A, Chen Z, Shaikh S, et al. (2009) Aberrant ERG expression cooperates with loss of PTEN to promote cancer progression in the prostate. *Nat Genet* 41: 619-624.
45. King JC, Xu J, Wongvipat J, Hieronymus H, Carver BS, et al. (2009) Cooperativity of TMPRSS2-ERG with PI3-kinase pathway activation in prostate oncogenesis. *Nat Genet* 41: 524-526.
46. DePrimo SE, Diehn M, Nelson JB, Reiter RE, Matese J, et al. (2002) Transcriptional programs activated by exposure of human prostate cancer cells to androgen. *Genome Biol* 3: RESEARCH0032.
47. Nelson PS, Clegg N, Arnold H, Ferguson C, Bonham M, et al. (2002) The program of androgen-responsive genes in neoplastic prostate epithelium. *Proc Natl Acad Sci U S A* 99: 11890-11895.
48. Nickols NG, Dervan PB (2007) Suppression of androgen receptor-mediated gene expression by a sequence-specific DNA-binding polyamide. *Proc Natl Acad Sci U S A* 104: 10418-10423.
49. Wang Q, Li W, Liu XS, Carroll JS, Janne OA, et al. (2007) A hierarchical network of transcription factors governs androgen receptor-dependent prostate cancer growth. *Mol Cell* 27: 380-392.
50. Best CJ, Gillespie JW, Yi Y, Chandramouli GV, Perlmutter MA, et al. (2005) Molecular alterations in primary prostate cancer after androgen ablation therapy. *Clin Cancer Res* 11: 6823-6834.
51. Chandran UR, Ma C, Dhir R, Bisceglia M, Lyons-Weiler M, et al. (2007) Gene expression profiles of prostate cancer reveal involvement of multiple molecular pathways in the metastatic process. *BMC Cancer* 7: 64.
52. Lapointe J, Li C, Higgins JP, van de Rijn M, Bair E, et al. (2004) Gene expression profiling identifies clinically relevant subtypes of prostate cancer. *Proc Natl Acad Sci U S A* 101: 811-816.
53. Singh D, Febbo PG, Ross K, Jackson DG, Manola J, et al. (2002) Gene expression correlates of clinical prostate cancer behavior. *Cancer Cell* 1: 203-209.
54. Tamura K, Furihata M, Tsunoda T, Ashida S, Takata R, et al. (2007) Molecular features of hormone-refractory prostate cancer cells by genome-wide gene expression profiles. *Cancer Res* 67: 5117-5125.
55. Varambally S, Yu J, Laxman B, Rhodes DR, Mehra R, et al. (2005) Integrative genomic and proteomic analysis of prostate cancer reveals signatures of metastatic progression. *Cancer Cell* 8: 393-406.

SUPPLEMENTARY DATA

Table S1 – List of SAM significant genes (q-value < 0.05) for PC346C cell line

| GenBank ID | HUGO_Symbol | HUGO_Name | Stimuly | 2log ratio | SAM q-value |
|------------|-------------|--|---------|------------|-------------|
| NM_004117 | FKBP5 | FK506 binding protein 5 | R1881 | 1.88 | 0.000 |
| AB042410 | GPR88 | G protein-coupled receptor 88 | R1881 | 1.35 | 0.000 |
| AB035266 | NRXN2 | neurexin 2 | R1881 | 0.91 | 0.048 |
| NM_006006 | ZBTB16 | zinc finger and BTB domain containing 16 | R1881 | 0.88 | 0.000 |
| AF188747 | KLK2 | kallikrein-related peptidase 2 | R1881 | 0.79 | 0.000 |
| NM_012449 | STEAP1 | six transmembrane epithelial antigen of the prostate 1 | R1881 | 0.79 | 0.000 |
| AK001478 | RHOJ | ras homolog gene family member J | R1881 | 0.77 | 0.000 |
| NM_020529 | NFKBIA | nuclear factor of kappa light polypeptide gene enhancer in B-cells | R1881 | 0.74 | 0.000 |
| NM_018674 | ACCN4 | amiloride-sensitive cation channel 4, pituitary | R1881 | 0.74 | 0.000 |
| AL109698 | ZNF710 | zinc finger protein 710 | R1881 | 0.71 | 0.000 |
| AK001647 | USP40 | ubiquitin specific peptidase 40 | R1881 | 0.68 | 0.000 |
| AL360260 | METRN | metetrin glial cell differentiation regulator | R1881 | 0.68 | 0.000 |
| NM_004231 | ATP6V1F | ATPase H transporting lysosomal 14kDa V1 subunit F | R1881 | 0.66 | 0.027 |
| NM_017802 | HEATR2 | HEAT repeat containing 2 | R1881 | 0.64 | 0.000 |
| NM_016498 | MTP18 * | Mitochondrial protein 18 kDa * | R1881 | 0.64 | 0.000 |
| AL137384 | KIAA1109 | KIAA1109 | R1881 | 0.63 | 0.027 |
| NM_014606 | HERC3 | hect domain and RLD 3 | R1881 | 0.62 | 0.048 |
| Z21967 | POU6F1 | POU class 6 homeobox 1 | R1881 | 0.62 | 0.039 |
| NM_012099 | CD3EAP | CD3e molecule epsilon associated protein | R1881 | 0.61 | 0.000 |
| NM_005956 | MTHFD1 | Methylenetetrahydrofolate dehydrogenase (NADP+ dependent) 1 | R1881 | 0.61 | 0.000 |
| U36561 | FUS | fusion involved in t 12 16 in malignant liposarcoma | R1881 | 0.60 | 0.027 |
| AK024535 | STAT3 | signal transducer and activator of transcription 3 acute-phase | R1881 | 0.59 | 0.000 |
| NM_006624 | ZMYND11 | zinc finger MYND domain containing 11 | R1881 | 0.59 | 0.027 |
| Y12018 | PSEN1 | presenilin 1 Alzheimer disease 3 | R1881 | 0.59 | 0.027 |
| NM_005081 | ZNF142 | zinc finger protein 142 | R1881 | 0.58 | 0.048 |
| AK022564 | C14orf159 | chromosome 14 open reading frame 159 | R1881 | 0.57 | 0.000 |
| NM_014848 | SV2B | synaptic vesicle glycoprotein 2B | R1881 | 0.55 | 0.000 |
| NM_003738 | PTCH2 | patched homolog 2 Drosophila | R1881 | 0.55 | 0.039 |
| AJ002787 | PRKCB1 | protein kinase C beta 1 | R1881 | 0.54 | 0.000 |
| NM_012164 | FBXW2 | F-box and WD repeat domain containing 2 | R1881 | 0.54 | 0.039 |
| NM_006992 | LRRC23 | leucine rich repeat containing 23 | R1881 | 0.53 | 0.000 |
| NM_017772 | TBC1D22B | TBC1 domain family member 22B | R1881 | 0.51 | 0.048 |
| NM_006810 | PDIA5 | protein disulfide isomerase family A member 5 | R1881 | 0.50 | 0.000 |

| | | | | | |
|-----------|---------|---|-----------|-------|-------|
| NM_015865 | SLC14A1 | solute carrier family 14 urea transporter member 1 Kidd blood group | R1881 | 0.50 | 0.048 |
| NM_006869 | CENTA1 | centaurin alpha 1 | R1881 | 0.49 | 0.000 |
| NM_002493 | NDUFB6 | NADH dehydrogenase ubiquinone 1 beta subcomplex 6 17kDa | R1881 | 0.48 | 0.048 |
| AB033023 | YEATS2 | YEATS domain containing 2 | R1881 | 0.46 | 0.048 |
| AK021498 | | hypothetical protein FLJ36031 * | R1881 | 0.44 | 0.027 |
| AK001829 | | Hypothetical gene * | R1881 | 0.42 | 0.027 |
| NM_000844 | GRM7 | glutamate receptor metabotropic 7 | R1881 | 0.42 | 0.000 |
| NM_000855 | GUCY1A2 | guanylate cyclase 1 soluble alpha 2 | R1881 | 0.35 | 0.048 |
| NM_001741 | CALCA | calcitonin/calcitonin-related polypeptide alpha | R1881 | 0.26 | 0.027 |
| AF159093 | | Homo sapiens endogenous retrovirus RAN1 polymerase-like protein (pol) | R1881 | 0.21 | 0.048 |
| NM_016318 | P2RX2 | purinergic receptor P2X ligand-gated ion channel 2 | Flutamide | -0.39 | 0.000 |

* no approved HUGO symbol / name exist for this entry. If present, gene symbol / name from the UNIGENE database are given in alternative.

Table S2 - List of SAM significant genes (q-value < 0.05) for PC346DCC cell line

| GenBank ID | HUGO_Symbol | HUGO_Name | Stimuly | 2log ratio | SAM q-value |
|------------|-------------|---|---------|------------|-------------|
| NM_013284 | POLM | polymerase DNA directed multipolymerase DNA directed mu | R1881 | 0.56 | 0.000 |
| NM_006685 | SMR3B | submaxillary gland androgen regulated protein 3 homolog B mouse | R1881 | 0.44 | 0.000 |

* no approved HUGO symbol / name exist for this entry. If present, gene symbol / name from the UNIGENE database are given in alternative.

Table S3 - List of SAM significant genes (q-value < 0.05) for PC346Flu1 cell line

| GenBank ID | HUGO_Symbol | HUGO_Name | Stimuly | 2log ratio | SAM q-value |
|------------|-------------|--|---------|------------|-------------|
| NM_004117 | FKBP5 | FK506 binding protein 5 | R1881 | 4.21 | 0.000 |
| AB042410 | GPR88 | G protein-coupled receptor 88 | R1881 | 3.04 | 0.000 |
| NM_006096 | NDRG1 | N-myc downstream regulated gene 1 | R1881 | 2.60 | 0.000 |
| AB051826 | RHOU | ras homolog gene family member U | R1881 | 2.54 | 0.000 |
| NM_020529 | NFKBIA | Nuclear factor of kappa light polypeptide gene enhancer in B-cells | R1881 | 2.39 | 0.000 |
| AK001478 | RHOU | ras homolog gene family member U | R1881 | 2.29 | 0.000 |
| NM_018456 | EAF2 | ELL associated factor 2 | R1881 | 2.28 | 0.000 |
| AK026383 | | cdNA clone * | R1881 | 2.05 | 0.000 |
| NM_004457 | ACSL3 | acyl-CoA synthetase long-chain family member 3 | R1881 | 2.04 | 0.000 |
| NM_003359 | UGDH | UDP-glucose dehydrogenase | R1881 | 1.91 | 0.000 |

| | | | | | |
|-----------|-----------|---|-------|------|-------|
| NM_012081 | ELL2 | elongation factor RNA polymerase II 2 | R1881 | 1.75 | 0.000 |
| NM_003543 | HIST1H4H | histone cluster 1 H4h | R1881 | 1.72 | 0.000 |
| NM_012449 | STEAP1 | six transmembrane epithelial antigen of the prostate 1 | R1881 | 1.69 | 0.000 |
| NM_000662 | NAT1 | N-acetyltransferase 1 arylamine N-acetyltransferase | R1881 | 1.68 | 0.000 |
| AF039944 | NDRG1 | N-myc downstream regulated gene 1 | R1881 | 1.63 | 0.000 |
| D16875 | RHOB | ras homolog gene family member B | R1881 | 1.61 | 0.000 |
| NM_006006 | ZBTB16 | zinc finger and BTB domain containing 16 | R1881 | 1.55 | 0.000 |
| AK026498 | CYP2U1 | cytochrome P450 family 2 subfamily U polypeptide 1 | R1881 | 1.50 | 0.000 |
| AF025771 | ZNF189 | zinc finger protein 189 | R1881 | 1.50 | 0.000 |
| AF111849 | ELOVL5 | ELOVL family member 5 elongation of long chain fatty acids FEN1 Elo2 | R1881 | 1.46 | 0.000 |
| NM_016590 | PART1* | Prostate androgen-regulated transcript 1* | R1881 | 1.45 | 0.000 |
| NM_006810 | PDIA5 | protein disulfide isomerase family A member 5 | R1881 | 1.42 | 0.000 |
| AK024715 | FLJ21062* | Hypothetical protein FLJ21062* | R1881 | 1.41 | 0.000 |
| NM_012062 | DNM1L | dynammin 1-like | R1881 | 1.36 | 0.000 |
| AK022814 | ZBTB10 | zinc finger and BTB domain containing 10 | R1881 | 1.34 | 0.000 |
| AK024850 | C2orf31 | chromosome 2 open reading frame 31 | R1881 | 1.32 | 0.000 |
| NM_016166 | PIAS1 | protein inhibitor of activated STAT 1 | R1881 | 1.31 | 0.000 |
| AB020637 | ENDOD1 | endonuclease domain containing 1 | R1881 | 1.26 | 0.000 |
| AK021627 | MORC4 | MORC family CW-type zinc finger 4 | R1881 | 1.24 | 0.000 |
| NM_005079 | TPD52 | tumor protein D52 | R1881 | 1.22 | 0.000 |
| NM_003104 | SORD* | Sorbitol dehydrogenase* | R1881 | 1.20 | 0.000 |
| NM_001530 | HIF1A | hypoxia-inducible factor 1, alpha subunit (basic helix-loop-helix transcription factor) | R1881 | 1.16 | 0.000 |
| AL137343 | FAM84A | family with sequence similarity 84 member A | R1881 | 1.14 | 0.000 |
| NM_004595 | SMS | spermine synthase | R1881 | 1.14 | 0.000 |
| AF188747 | KLK2 | kallikrein-related peptidase 2 | R1881 | 1.12 | 0.000 |
| NM_005271 | GLUD1 | glutamate dehydrogenase 1 | R1881 | 1.11 | 0.000 |
| AK026813 | STEAP2 | six transmembrane epithelial antigen of the prostate 2 | R1881 | 1.07 | 0.000 |
| NM_005461 | MAFB | v-maf musculoaponeurotic fibrosarcoma oncogene homolog B avian | R1881 | 1.06 | 0.000 |
| NM_016050 | MRPL11 | mitochondrial ribosomal protein L11 | R1881 | 1.05 | 0.000 |
| AB050049 | MCCC2 | methylcrotonoyl-Coenzyme A carboxylase 2 beta | R1881 | 1.05 | 0.000 |
| NM_019018 | FAM105A | family with sequence similarity 105 member A | R1881 | 1.04 | 0.000 |
| AK022827 | EIF2C3 | eukaryotic translation initiation factor 2C 3 | R1881 | 1.03 | 0.000 |
| AK026375 | LOC93622* | Hypothetical protein BC006130* | R1881 | 1.02 | 0.000 |
| AL157445 | | cDNA clone* | R1881 | 1.02 | 0.007 |
| AB040914 | SHROOM3 | shroom family member 3 | R1881 | 1.01 | 0.012 |
| AK024941 | DNAJC3 | DnaJ Hsp40 homolog subfamily C member 3 | R1881 | 0.99 | 0.041 |
| AF294628 | TWSG1 | twisted gastrulation homolog 1 Drosophila | R1881 | 0.99 | 0.000 |
| D17210 | | cDNA clone* | R1881 | 0.97 | 0.000 |
| NM_006079 | CITED2 | Cbp p300-interacting transactivator with Glu Asp-rich carboxy-terminal domain 2 | R1881 | 0.96 | 0.000 |
| NM_003115 | UAP1 | UDP-N-acetylglucosamine pyrophosphorylase 1 | R1881 | 0.96 | 0.000 |
| NM_004156 | PPP2C8 | Protein phosphatase 2 formerly 2A catalytic subunit beta isoform | R1881 | 0.94 | 0.000 |

| | | | | | |
|-----------|----------|--|-------|------|-------|
| NM_002069 | GNAI1 | Guanine nucleotide binding protein G protein alpha inhibiting activity polipeptide 1 | R1881 | 0.94 | 0.000 |
| NM_004434 | EMIL1 | echinoderm microtubule associated protein like 1 | R1881 | 0.94 | 0.012 |
| NM_007107 | SSR3 | signal sequence receptor gamma translocon-associated protein gamma | R1881 | 0.92 | 0.005 |
| AK000691 | SLC22A23 | solute carrier family 22 member 23 | R1881 | 0.90 | 0.012 |
| NM_014269 | ADAM29 | ADAM metalloproteinase domain 29 | R1881 | 0.89 | 0.007 |
| NM_006788 | RALBP1 | ralA binding protein 1 | R1881 | 0.87 | 0.028 |
| NM_005627 | SGK1 | serum/glucocorticoid regulated kinase 1 | R1881 | 0.85 | 0.000 |
| NM_006697 | MTMR11 | myotubularin related protein 11 | R1881 | 0.85 | 0.005 |
| AK025240 | ZNRF2 | zinc and ring finger 2 | R1881 | 0.84 | 0.005 |
| NM_001206 | KLF9 | Kruppel-like factor 9 | R1881 | 0.83 | 0.000 |
| NM_014109 | ATAD2 | ATPase family AAA domain containing 2 | R1881 | 0.83 | 0.000 |
| NM_012152 | EDG7 | endothelial differentiation, lysophosphatidic acid G-protein-coupled receptor, 7 | R1881 | 0.83 | 0.000 |
| AK025119 | C3orf58 | chromosome 3 open reading frame 58 | R1881 | 0.82 | 0.000 |
| AL080209 | CREB3L2 | cAMP responsive element binding protein 3-like 2 | R1881 | 0.81 | 0.022 |
| AL049998 | PIK3C2A | phosphoinositide-3-kinase class 2 alpha polypeptide | R1881 | 0.81 | 0.000 |
| NM_014174 | THYN1 | thymocyte nuclear protein 1 | R1881 | 0.81 | 0.005 |
| NM_001655 | ARCN1 | archain 1 | R1881 | 0.80 | 0.005 |
| NM_020474 | GALNT1 | UDP-N-acetyl-alpha-D-galactosamine: N-acetylgalactosaminyltransferase 1 | R1881 | 0.79 | 0.000 |
| NM_006343 | MERTK | c-mer proto-oncogene tyrosine kinase | R1881 | 0.79 | 0.000 |
| NM_003010 | MAP2K4 | mitogen-activated protein kinase kinase 4 | R1881 | 0.78 | 0.000 |
| AK027213 | BBS10 | Bardet-Biedl syndrome 10 | R1881 | 0.77 | 0.000 |
| M14200 | DBI | diazepam binding inhibitor | R1881 | 0.77 | 0.000 |
| NM_020188 | C16orf61 | chromosome 16 open reading frame 61 | R1881 | 0.76 | 0.005 |
| AK024648 | FAM107B | family with sequence similarity 107 member B | R1881 | 0.76 | 0.007 |
| NM_020235 | BBX | bobby sox homolog Drosophila | R1881 | 0.76 | 0.007 |
| AB029018 | PDZRN3 | PDZ domain containing RING finger 3 | R1881 | 0.75 | 0.033 |
| AB020676 | WWC1 | WW and C2 domain containing 1 | R1881 | 0.74 | 0.000 |
| NM_018037 | RALGPS2 | Ral GEF with PH domain and SH3 binding motif 2 | R1881 | 0.74 | 0.007 |
| NM_006516 | SLC2A1 | solute carrier family 2 facilitated glucose transporter member 1 | R1881 | 0.74 | 0.005 |
| M60721 | HLX | H2.0-like homeobox | R1881 | 0.73 | 0.000 |
| NM_000849 | GSTM3 | glutathione S-transferase M3 brain | R1881 | 0.73 | 0.007 |
| AF070670 | PPM1A | protein phosphatase 1A formerly 2C magnesium-dependent alpha isoform | R1881 | 0.72 | 0.000 |
| M27544 | IGF1 | insulin-like growth factor 1 somatomedin C | R1881 | 0.70 | 0.012 |
| NM_005606 | LGMN | legumain | R1881 | 0.69 | 0.007 |
| AF052174 | BBX | bobby sox homolog Drosophila | R1881 | 0.69 | 0.018 |
| NM_018067 | MAP7D1 | MAP7 domain containing 1 | R1881 | 0.66 | 0.018 |
| NM_012132 | CLDN8 | claudin 8 | R1881 | 0.65 | 0.000 |
| NM_007212 | RNF2 | ring finger protein 2 | R1881 | 0.65 | 0.012 |
| NM_013257 | SGK3 | serum/glucocorticoid regulated kinase family member 3 | R1881 | 0.64 | 0.000 |
| AK026762 | CBLL1 | Cas-Bi-M murine ecotropic retroviral transforming sequence-like 1 | R1881 | 0.64 | 0.012 |
| AB020633 | FRYL | FRY-like | R1881 | 0.63 | 0.018 |

| | | | | | |
|-----------|----------|---|-------|------|-------|
| NM_006323 | SEC24B | SEC24 related gene family member B <i>S. cerevisiae</i> | R1881 | 0.63 | 0.000 |
| AL080078 | TMEM30B | transmembrane protein 30B | R1881 | 0.63 | 0.007 |
| AK000122 | IQCK | IQ motif containing K | R1881 | 0.63 | 0.005 |
| AK027250 | HOOK1 | hook homolog 1 <i>Drosophila</i> | R1881 | 0.63 | 0.012 |
| NM_014384 | ACAD8 | acyl-Coenzyme A dehydrogenase family member 8 | R1881 | 0.62 | 0.007 |
| NM_018116 | MSTO1 | misato homolog 1 <i>Drosophila</i> | R1881 | 0.62 | 0.033 |
| AB037765 | TXNDC16 | thioredoxin domain containing 16 | R1881 | 0.62 | 0.005 |
| AK026517 | EHF | eis homologous factor | R1881 | 0.62 | 0.000 |
| NM_019844 | SLCO1B3 | solute carrier organic anion transporter family member 1B3 | R1881 | 0.61 | 0.000 |
| NM_014822 | SEC24D | SEC24 related gene family member D <i>S. cerevisiae</i> | R1881 | 0.61 | 0.007 |
| AL117666 | LRIG1 | leucine-rich repeats and immunoglobulin-like domains 1 | R1881 | 0.61 | 0.000 |
| AB032991 | NDVIP2 | Nedd4 family interacting protein 2 | R1881 | 0.61 | 0.028 |
| AB018314 | PPP1R13B | protein phosphatase 1 regulatory inhibitor subunit 13B | R1881 | 0.60 | 0.012 |
| NM_006885 | ZFH3 | zinc finger homeobox 3 | R1881 | 0.60 | 0.018 |
| NM_003389 | CORO2A | coronin actin binding protein 2A | R1881 | 0.60 | 0.028 |
| AB033040 | RNF150 | ring finger protein 150 | R1881 | 0.59 | 0.041 |
| NM_004039 | ANXA2 | annexin A2 | R1881 | 0.59 | 0.028 |
| NM_006380 | APBP2 | amyloid beta precursor protein cytoplasmic tail binding protein 2 | R1881 | 0.59 | 0.012 |
| NM_000860 | HPGD | hydroxyprostaglandin dehydrogenase 15- NAD | R1881 | 0.59 | 0.012 |
| NM_003243 | TGFBR3 | transforming growth factor beta receptor III | R1881 | 0.59 | 0.012 |
| NM_002539 | ODC1 | ornithine decarboxylase 1 | R1881 | 0.59 | 0.041 |
| NM_005746 | PBEF1 | pre-B-cell colony enhancing factor 1 | R1881 | 0.58 | 0.018 |
| AK001822 | ARRDC1 | arrestin domain containing 1 | R1881 | 0.58 | 0.005 |
| AL049969 | PDLIM5 | PDZ and LIM domain 5 | R1881 | 0.56 | 0.012 |
| NM_003489 | NRIP1 | nuclear receptor interacting protein 1 | R1881 | 0.56 | 0.007 |
| L27479 | C9orf61 | chromosome 9 open reading frame 61 | R1881 | 0.54 | 0.000 |
| NM_020233 | C17orf48 | chromosome 17 open reading frame 48 | R1881 | 0.54 | 0.005 |
| AK000028 | BCAP29 | Hypothetical LOC90024 * | R1881 | 0.54 | 0.007 |
| NM_018844 | SSR1 | B-cell receptor-associated protein 29 | R1881 | 0.52 | 0.012 |
| NM_003144 | PPAP2A | signal sequence receptor alpha translocon-associated protein alpha | R1881 | 0.52 | 0.041 |
| NM_003711 | Y09836 | phosphatidic acid phosphatase type 2A | R1881 | 0.52 | 0.041 |
| AK022884 | SGEF * | 3 UTR of hypothetical protein ORF1 * | R1881 | 0.52 | 0.028 |
| NM_019891 | ERO1LB | Src homology 3 domain-containing guanine nucleotide exchange factor * | R1881 | 0.52 | 0.012 |
| NM_002245 | KCNK1 | ERO1-like beta <i>S. cerevisiae</i> | R1881 | 0.51 | 0.005 |
| NM_013255 | MKLN1 | potassium channel subfamily K member 1 | R1881 | 0.51 | 0.033 |
| NM_007229 | PACSIN2 | muskelin 1 intracellular mediator containing kelch motifs | R1881 | 0.51 | 0.012 |
| AF147388 | ADAM10 | protein kinase C and casein kinase substrate in neurons 2 | R1881 | 0.51 | 0.007 |
| NM_004315 | ASAH1 | ADAM metallopeptidase domain 10 | R1881 | 0.51 | 0.041 |
| AF052107 | MBOAT2 | N-acylsphingosine amidohydrolase acid ceramidase 1 | R1881 | 0.50 | 0.028 |
| AK000776 | ROR1 | membrane bound O-acyltransferase domain containing 2 receptor tyrosine kinase-like orphan receptor 1 | R1881 | 0.49 | 0.033 |
| | | | R1881 | 0.49 | 0.012 |

| | | | | | |
|-----------|------------|--|-------|------|-------|
| AF303889 | ROPN1 | ropporin rhophilin associated protein 1 | R1881 | 0.48 | 0.012 |
| NM_006117 | PECI | peroxisomal D3 D2-enoyl-CoA isomerase | R1881 | 0.48 | 0.018 |
| NM_017530 | ZNF821 | zinc finger protein 821 | R1881 | 0.48 | 0.041 |
| NM_001695 | ATP6V1C1 | ATPase H transporting lysosomal 42kDa V1 subunit C1 | R1881 | 0.48 | 0.041 |
| NM_002210 | ITGAV | integrin alpha V vitronectin receptor alpha polypeptide antigen CD51 | R1881 | 0.48 | 0.000 |
| NM_018455 | CENPN | centromere protein N | R1881 | 0.47 | 0.022 |
| NM_004040 | RHOB | ras homolog gene family member B | R1881 | 0.46 | 0.000 |
| S71611 | | cDNA clone * | R1881 | 0.46 | 0.012 |
| NM_006705 | GADD45G | growth arrest and DNA-damage-inducible gamma | R1881 | 0.45 | 0.012 |
| NM_005853 | IRX5 | irouquis homeobox 5 | R1881 | 0.45 | 0.022 |
| AK023844 | GRHL2 | grainyhead-like 2 Drosophila | R1881 | 0.45 | 0.007 |
| AB040936 | KIAA1503 * | Similar to KIAA1503 protein * | R1881 | 0.45 | 0.033 |
| NM_002553 | ORC5L | origin recognition complex subunit 5-like yeast | R1881 | 0.44 | 0.005 |
| AK023249 | PLEKHF2 | Pleckstrin homology domain containing family F with FYVE domain member | R1881 | 0.43 | 0.012 |
| NM_004578 | HRES1 | HTLV-1 related endogenous sequence | R1881 | 0.43 | 0.012 |
| NM_004226 | STK17B | serine/threonine kinase 17b | R1881 | 0.42 | 0.005 |
| NM_004267 | CHST2 | carbohydrate N-acetylglucosamine-6-O sulfotransferase 2 | R1881 | 0.42 | 0.005 |
| NM_017992 | EDEM3 | ER degradation enhancer, mannosidase alpha-like 3 | R1881 | 0.41 | 0.033 |
| AF294278 | PRDM16 | PR domain containing 16 | R1881 | 0.40 | 0.007 |
| NM_002736 | PRKAR2B | protein kinase cAMP-dependent regulatory type II beta | R1881 | 0.40 | 0.033 |
| AF038174 | C9orf91 | chromosome 9 open reading frame 91 | R1881 | 0.40 | 0.012 |
| AL049471 | ARID5B | AT rich interactive domain 5B MRF1-like | R1881 | 0.39 | 0.033 |
| AF124819 | TM9SF3 | transmembrane 9 superfamily member 3 | R1881 | 0.39 | 0.022 |
| NM_014584 | ERO1L | ERO1-like S. cerevisiae | R1881 | 0.37 | 0.033 |
| NM_005648 | TCEB1 | transcription elongation factor B SIII polypeptide 1 15kDa elongin C | R1881 | 0.37 | 0.033 |
| NM_001609 | ACADSB | acyl-Coenzyme A dehydrogenase short/branched chain | R1881 | 0.37 | 0.033 |
| NM_017694 | FLJ20160 * | FLJ20160 protein * | R1881 | 0.35 | 0.022 |
| NM_000514 | GDNF | glial cell derived neurotrophic factor | R1881 | 0.35 | 0.012 |
| AJ250475 | EPDR1 | ependymin related protein 1 zebrafish | R1881 | 0.35 | 0.012 |
| NM_020182 | TMEPAI | transmembrane prostate androgen induced RNA | R1881 | 0.34 | 0.012 |
| AK025772 | RABL3 | RAB member of RAS oncogene family-like 3 | R1881 | 0.34 | 0.028 |
| NM_014666 | CLINT1 | clathrin interactor 1 | R1881 | 0.33 | 0.022 |
| NM_005300 | GPR34 | G protein-coupled receptor 34 | R1881 | 0.33 | 0.018 |
| AK026239 | FAM118A | family with sequence similarity 118 member A | R1881 | 0.32 | 0.012 |
| NM_001284 | AP3S1 | adaptor-related protein complex 3 sigma 1 subunit | R1881 | 0.32 | 0.041 |
| NM_018366 | CNO | cappuccino homolog mouse | R1881 | 0.32 | 0.041 |
| NM_013332 | HIG2 * | Hypoxia-inducible protein 2 * | R1881 | 0.31 | 0.033 |
| NM_002806 | PSMC6 | proteasome prosome macropain 26S subunit ATPase 6 | R1881 | 0.31 | 0.033 |
| AF075098 | LTBP1 | latent transforming growth factor beta binding protein 1 | R1881 | 0.31 | 0.022 |
| AK024586 | TNC | tenascin C hexabrachion | R1881 | 0.29 | 0.033 |
| NM_014664 | N4BP1 * | Nedd4 binding protein 1 * | R1881 | 0.29 | 0.028 |

| | | | | | |
|-----------|---------|---|-------|-------|-------|
| AK022331 | FAM152A | family with sequence similarity 152 member A | R1881 | 0.28 | 0.012 |
| NM_000446 | PON1 | paraoxonase 1 | R1881 | 0.27 | 0.012 |
| U79249 | CCDC52 | coiled-coil domain containing 52 | R1881 | 0.27 | 0.012 |
| NM_000815 | GABRD | gamma-aminobutyric acid GABA A receptor delta | R1881 | 0.26 | 0.028 |
| NM_016262 | TUBE1 | tubulin epsilon 1 | R1881 | 0.26 | 0.018 |
| NM_000068 | CACNA1A | calcium channel voltage-dependent P/Q type alpha 1A subunit | R1881 | 0.25 | 0.007 |
| NM_012318 | LETM1 | leucine zipper-EF-hand containing transmembrane protein 1 | R1881 | 0.25 | 0.022 |
| AK027235 | CRTAP | cartilage associated protein | R1881 | 0.25 | 0.012 |
| NM_004147 | DRG1 | developmentally regulated GTP binding protein 1 | R1881 | 0.24 | 0.033 |
| AF116709 | FUS | Homo sapiens PRO2605 mRNA, complete cds * | R1881 | 0.24 | 0.033 |
| S75763 | NOTCH1 | fusion involved in t 12 16 in malignant liposarcoma | R1881 | 0.24 | 0.012 |
| NM_017617 | | Notch homolog 1 translocation-associated Drosophila | R1881 | 0.22 | 0.028 |
| AK027219 | | cDNA FLJ23566 fis clone LNG10880 * | R1881 | 0.22 | 0.000 |
| AF070620 | | cDNA clone * | R1881 | 0.21 | 0.012 |
| AF085985 | CRYGD | Full length insert cDNA clone YU03C05 * | R1881 | 0.20 | 0.033 |
| NM_006891 | MTMR4 | crystallin gamma D | R1881 | 0.18 | 0.033 |
| AF264717 | | myotubularin related protein 4 | R1881 | 0.18 | 0.041 |
| AF147337 | | cDNA clone * | R1881 | -0.41 | 0.022 |
| AF075080 | FLVCR2 | Full length insert cDNA YQ8D07 * | R1881 | -0.43 | 0.022 |
| NM_017791 | PCDH17 | feline leukemia virus subgroup C cellular receptor family member 2 | R1881 | -0.46 | 0.041 |
| NM_014459 | EPB41L5 | protocadherin 17 | R1881 | -0.47 | 0.000 |
| AB046768 | LRRRC8D | erythrocyte membrane protein band 4.1 like 5 | R1881 | -0.51 | 0.008 |
| NM_018103 | MIR16 * | leucine rich repeat containing 8 family member D | R1881 | -0.53 | 0.000 |
| NM_015556 | SIPA1L1 | Membrane interacting protein of RGS16 * | R1881 | -0.54 | 0.018 |
| NM_006113 | VAV3 | signal-induced proliferation-associated 1 like 1 | R1881 | -0.54 | 0.033 |
| NM_001913 | CUX1 | vav 3 guanine nucleotide exchange factor | R1881 | -0.55 | 0.041 |
| NM_004760 | STK17A | cut-like homeobox 1 | R1881 | -0.55 | 0.041 |
| NM_000675 | ADORA2A | serine/threonine kinase 17a | R1881 | -0.56 | 0.018 |
| NM_003897 | IER3 | adenosine A2a receptor | R1881 | -0.65 | 0.033 |
| NM_003311 | PHLDA2 | immediate early response 3 | R1881 | -0.67 | 0.013 |
| AF113132 | PSAT1 | pleckstrin homology-like domain family A member 2 | R1881 | -0.77 | 0.041 |
| NM_003943 | STBD1 | phosphoserine aminotransferase 1 | R1881 | -0.78 | 0.000 |
| NM_002165 | ID1 | starch binding domain 1 | R1881 | -0.79 | 0.022 |
| NM_006769 | LMO4 | inhibitor of DNA binding 1 dominant negative helix-loop-helix protein | R1881 | -0.81 | 0.018 |
| NM_012446 | SSBP2 | LIM domain only 4 | R1881 | -0.82 | 0.000 |
| NM_004577 | PSPH | single-stranded DNA binding protein 2 | R1881 | -0.84 | 0.018 |
| D28449 | ID3 | phosphoserine phosphatase | R1881 | -0.85 | 0.041 |
| AK026945 | TRIB3 | inhibitor of DNA binding 3 dominant negative helix-loop-helix protein | R1881 | -0.88 | 0.000 |
| AK026288 | ATHL1 | tribbles homolog 3 Drosophila | R1881 | -0.92 | 0.028 |
| NM_012342 | BAMBI | ATH1 acid trehalase-like 1 yeast | R1881 | -0.96 | 0.008 |
| | | BMP and activin membrane-bound inhibitor homolog Xenopus laevis | R1881 | -0.98 | 0.000 |

| | | | | | |
|-----------|----------|---|-------|-------|-------|
| U90907 | PIK3R3 | phosphoinositide-3-kinase regulatory subunit 3 p55 gamma | R1881 | -1.01 | 0.008 |
| NM_004864 | GDF15 | growth differentiation factor 15 | R1881 | -1.10 | 0.033 |
| AL133074 | TP53INP1 | tumor protein p53 inducible nuclear protein 1 | R1881 | -1.25 | 0.000 |
| X69111 | ID3 | inhibitor of DNA binding 3 dominant negative helix-loop-helix protein | R1881 | -1.25 | 0.000 |
| AF075110 | C14orf4 | chromosome 14 open reading frame 4 | R1881 | -1.29 | 0.000 |
| NM_004316 | ASCL1 | achaete-scute complex homolog 1 Drosophila | R1881 | -1.42 | 0.018 |
| AF205437 | TRIB1 | tribbles homolog 1 Drosophila | R1881 | -1.63 | 0.000 |

* no approved HUGO symbol / name exist for this entry. If present, gene symbol / name from the UNIGENE database are given in alternative.

Table S4 - List of SAM significant genes (q-value < 0.05) for PC346Flu2 cell line

| GenBank ID | HUGO_Symbol | HUGO_Name | Stimuly | 2log ratio | SAM q-value |
|------------|-------------|---|-----------|------------|-------------|
| AB042410 | GPR88 | G protein-coupled receptor 88 | Flutamide | 1.57 | 0.000 |
| AK001478 | RHOJ | ras homolog gene family member U | R1881 | 1.05 | 0.000 |
| AK026813 | STEAP2 | six transmembrane epithelial antigen of the prostate 2 | R1881 | 0.74 | 0.000 |
| NM_002923 | RGS2 | regulator of G-protein signaling 2 24kDa | R1881 | 0.73 | 0.000 |
| NM_002923 | RGS2 | regulator of G-protein signaling 2 24kDa | Flutamide | 0.57 | 0.000 |
| NM_003676 | DEGS | degenerative spermatocyte homolog 1 lipid desaturase Drosophila | Flutamide | 0.67 | 0.000 |
| NM_019844 | SLCO1B3 | solute carrier organic anion transporter family member 1B3 | Flutamide | 0.63 | 0.000 |
| NM_001206 | KLF9 | Kruppel-like factor 9 | Flutamide | 0.47 | 0.000 |
| AK002088 | UBE2E3 | ubiquitin-conjugating enzyme E2E 3 UBC4/5 homolog yeast | Flutamide | 0.40 | 0.000 |

* no approved HUGO symbol / name exist for this entry. If present, gene symbol / name from the UNIGENE database are given in alternative.

Chapter 5

Bypass Mechanisms of the Androgen Receptor Pathway in PC346 Hormone-Refractory Prostate Cancer Cells

Rute B. Marques, Natasja F. Dits, Sigrun Erkens-Schulze, Wytke M. van
Weerden, Guido Jenster

Department of Urology, Josephine Nefkens Institute, Erasmus Medical
Center, PO Box 2040, 3000 CA, Rotterdam, The Netherlands

submitted for publication

ABSTRACT

Background: Prostate cancer is at its onset dependent on androgens for survival and growth, making androgen ablation/blockade the cornerstone treatment for invasive tumors. However, despite initial remission, the cancer will inevitably recur as hormone-refractory disease.

Objective: The aim of this study is to investigate how androgen-dependent prostate cancer cells eventually survive and resume growth under androgen-deprived and antiandrogen supplemented conditions, with focus on genes particularly involved in the bypass of the androgen-receptor (AR) pathway.

Methods: For this purpose, microarray technology was used to analyze the differential expression pattern between androgen-responsive and hormone-refractory prostate cancer cell lines. As model system we used the androgen-responsive PC346C cells and its derivative castration-resistant sublines: PC346DCC (very low AR levels), PC346Flu1 (AR overexpressed) and PC346Flu2 (T877A mutated AR). VAV3, TWIST1 and DKK3 were selected for further quantification by specific real-time PCR, in an independent set of prostate cancer samples.

Results: Microarray analysis revealed 487 transcripts differentially expressed between the androgen-responsive and the castration-resistant cell lines. Most of these genes were common to all three hormone-refractory sublines and only a minority (~5%) was AR-regulated target genes. Pathway analysis revealed enrichment in functions involving cellular movement, cellular growth/proliferation and cell death, as well as association with cancer and reproductive system disease. PC346DCC presented the highest number (276) of differentially expressed genes and a significant down-regulation of AR target genes (p-value 10^{-7}), supporting the hypothesis that this subline bypassed the AR pathway. Among these, VAV3 and TWIST1 oncogenes were overexpressed, whereas the expression of the tumor-suppressor DKK3 was repressed. Subsequent validation in human prostate tumor samples confirmed deregulation of these genes during prostate cancer progression.

Conclusions: The large overlap of differentially-expressed genes between all castration-resistant sublines suggests an ultimate convergence to similar growth enhancing adaptations, despite the different AR modifications. PC346Flu1 and PC346Flu2 acquired this hormone-refractory growth by adaptation of the AR pathway, whereas PC346DCC activated alternative survival/growth pathways through down-regulation of the apoptosis-promoting DKK3 gene and overexpression of TWIST1 and VAV3 proto-oncogenes. Furthermore, these genes were deregulated in clinical samples of prostate tumors and lymph-node metastasis, making them potential disease markers and interesting targets for novel therapeutical approaches.

INTRODUCTION

Prostate cancer is the second leading cause of male cancer deaths in the Western countries and an increasing problem in those adopting Western lifestyle and diet [1]. Advances in screening and diagnosis have allowed the detection of tumors at earlier stages, when curative therapy is still feasible [2]. For late stage disseminated disease however, current therapies are merely palliative and no curative treatment exists. Since the growth of prostate tumors is originally androgen-dependent, metastatic cancers are generally treated with androgen ablation therapy, with or without antiandrogen supplementation [2]. The vast majority of these patients show a significant (12-18 months) clinical regression, but the cancer eventually escapes androgen suppression and recurs as incurable hormone-refractory condition [3,4]. To survive and resume growth in an androgen-deprived environment prostate cancer cells must either adapt the AR pathway to the androgen-depleted conditions or invoke alternative survival and growth pathways [5]. Much experimental evidence exists to support both mechanisms, which are not necessarily mutually exclusive. AR expression was shown to be maintained in the majority of patients that underwent hormonal therapy and showed recurrence of disease, suggesting a role of the AR also in late stage disease [6,7]. Moreover, the AR gene is amplified and/or overexpressed in about 30% of the hormone-refractory tumors, and it has been proposed this could sensitize the receptor for the residual androgen concentrations present under hormonal therapies [8,9,10]. Furthermore, several AR mutations, resulting in increased activity or broadened ligand-specificity to alternative steroids and antiandrogens, have been associated with disease progression [11,12]. Other modifications of the AR pathway that may induce hormone-refractory growth include intratumoral steroidogenesis, ligand-independent activation by cross-talk with other signaling pathways, alterations in the balance of AR co-regulators or expression of constitutively active truncated AR isoforms [5,13,14]. Interestingly, recent work from others and us has revealed that the AR pathway may be selectively attenuated in advanced/metastatic disease [15,16,17]. Since the AR pathway is also involved in the processes of cellular differentiation and prostate maturation, it is tempting to suggest that prostate cancer cells may eventually gain growth advantage by inhibiting the AR induced differentiation. Prompted by these results, we focused the present study on alternative survival and growth pathways, which are independent of androgen-receptor activation. To effectively bypass the AR pathway, cancer epithelial cells must be able to survive the apoptotic signals triggered by hormonal therapies and invoke alternative growth pathways. Autocrine production of growth factors or its receptors, activation of oncogenes and inhibition of tumor-suppressor genes are all possible mechanisms for bypassing the AR pathway. Consistent with this hypothesis, paracrine growth factors that are normally secreted by prostate stroma cells, such as EGF, IGF1, HGF, KGF or IL6, are found to be overexpression in hormone-refractory cancer in association with a switch to autocrine production by cancer epithelial cells [18]. In addition to being potential mitogens, mounting evidence indicates that these growth hormones are also able to cross-talk with the AR signaling pathway, leading to expression of AR target genes in the absence of androgens [19]. Therefore, it still has to be established whether the autocrine production of these growth factors represents an

adaptation or a true bypass of the AR signaling pathway. Alterations in the anti-apoptotic BCL2 oncogene and in the pro-apoptotic P53 and PTEN tumor-suppressor genes have also been found in prostate cancer [20,21]. However, these events mostly occur earlier in prostate progression, making them less likely candidates for the switch to hormone-refractory growth in late stage disease. Nevertheless, by inhibiting prostate cancer cell death and shifting the balance towards cellular proliferation, genes involved in the regulation of apoptosis may also play a role in hormone-refractory growth.

To explore the mechanism(s) by which androgen-dependent prostate cancer cells become resistant to hormonal therapy, we used microarray technology to interrogate the differences in gene expression between androgen-responsive and castration-resistant cell lines. As model system we used the androgen-responsive PC346C cell line and its hormone-refractory sublines PC346DCC, PC346Flu1 and PC346Flu2. These sublines were derived from the parental PC346C by long-term androgen ablation (PC346DCC), supplemented with the antiandrogen hydroxyflutamide (PC346Flu1 and PC346Flu2). Previous studies revealed distinct AR modifications in all three castration-resistant sublines, which corresponded to diverse mechanism of hormone-refractory growth. Whereas PC346DCC, expressing very low levels of AR and PSA, showed evidence of bypassing of the AR pathway, PC346Flu1 exhibited 4-fold AR up-regulation and PC346Flu2 was shown to carry the T877A AR mutation. Both PC346Flu1 and PC346Flu2 sublines replicate the progression to hormone-refractory disease through adaptations of the AR pathway. Therefore, we focused on the PC346DCC subline to select for genes particularly involved in the bypass of the AR pathway. In addition to providing novel insights into the mechanisms of prostate cancer progression, the genes identified here may prove useful as prognostic markers and potential targets for novel therapeutical approaches.

MATERIALS AND METHODS

Reagents and cell lines

The basic culture medium used in the maintenance of PC346 cell lines consisted of DMEM-F12 medium (Cambrex BioWhitaker, Belgium) supplemented with 2% fetal calf serum (FCS; PAN Biotech GmbH, Aidenbach, Germany), 1% insulin-transferrin-selenium (Gibco BRL), 0.01% bovine serum albumin (Boehringer Mannheim, Germany), 10 ng/ml epidermal growth factor (Sigma-Aldrich), penicillin/streptomycin antibiotics (100 U/ml penicillin, 100 mg/ml streptomycin; BioWhitaker, Belgium); plus the following additions: 100 ng/ml fibronectin (Harbor Bio-Products, Tebu-bio, The Netherlands), 20 mg/ml fetuine (ICN Biomedicals, The Netherlands), 50 ng/ml cholera toxin, 0.1 mM phosphoethanolamine, 0.6 ng/ml triiodothyronine and 500 ng/ml dexametason (all from Sigma). PC346C cells were maintained in culture in the complete medium described above, supplemented with 0.1 nM 17-methyltrienolone (R1881; NEN, Boston MA, USA). PC346DCC selection medium was supplemented as described above, but depleted from androgens by using dextran-coated charcoal (DCC) treated FCS. PC346Flu1 and PC346Flu2 culture medium was also androgen depleted by using 2% DCC-FCS, and supplemented with 1 μ M of hydroxyflutamide (OH-flutamide, Schering-Plough Research Institute, New Jersey, USA).

Cells were grown in T25 Primaria™ tissue culture flasks (BD Biosciences Benelux N.V, The Netherlands) at 37°C under 5% CO₂ humidified atmosphere.

Expression microarray analysis

Cells were seeded in their respective selection medium to reach ~50% confluency and allowed to grow for 2 days. Then, cells were rinsed twice with PBS and stored at -20°C until RNA isolation. Total RNA was isolated with RNAzol B reagent (Campro Scientific, Veenendaal, The Netherlands) and further purified through RNeasy columns (Qiagen) with on-column DNA digestion, according to the manufacturer's protocol. RNA quality was checked on 1% agarose gel.

Cy3- or Cy5-labelled RNA probes were produced by incorporating amino-allyl UTP during RNA amplification, followed by coupling to N-hydroxysuccinimide modified dye. Briefly, 3 µg RNA was used for a T7-based linear mRNA amplification protocol, described previously [22]. Amino-allyl UTP, plus equal amount of unmodified rUTP, was incorporated into aRNA with T7 Megascript Kit (all from Ambion), according to manufacturer's protocol. Amplified RNA was purified and concentrated using Microcon-YM 30 columns (Amicon®) to rinse three times with 300 µl RNase-free water. Finally, 2 µg aminoallyl-modified RNA, in a maximum of 3.33 µl of RNase-free water, was incubated with 1.66 µl sodium bicarbonate buffer (0.3 M, pH 9) and 5 µl Cy3- or Cy5-dye (CyScribe Post-Labeling Kit, Amersham, NJ, USA), for 1h in the dark at room temperature. Reaction was stopped with 5 µl 4 M hydroxylamine HCl (Sigma), contra-labelled probes were combined and purified/concentrated using Microcon-YM 30. Probe was collected in 5-15 µl final volume and resuspended in 80 µl Ambion hybridization buffer number 1.

For the microarray we used double-dye oligoarrays representing about 15,000 human genes, on which labelled RNA from the each hormone-refractory subline was cohybridized with contra-labelled PC346C. Four microarrays were performed per condition, using two distinct cell passages in dye-swap. This was done to account for the biological variability and to exclude dye-preferential binding to oligonucleotides on the microarray. The oligoarrays used in this study were produced at the Erasmus Center for Biomics. Briefly, a human 18,584 oligonucleotides library (Compugen, Sigma-Genosys) was spotted on aminosilane slides using a Virtek Chipwriter Professional arrayer (Virtek Vision International, Waterloo, Canada). Control spots included landmarks, spotting buffer, alien oligonucleotides (SpotReport Alien Oligo Array, La Jolla, Stratagene), poly d[A]40-60, salmon sperm DNA, and human COT-1 DNA. Before the hybridization, microarray slides were prehybridized in 5x SSC, 0.05% SDS, 4% BSA solution for 30 min at 45°C, washed twice with RNase-free water for 2 min, rinsed with isopropanol and spin-dried for 3 min at 1500g. Microarray hybridizations were performed overnight at 45°C, with continuous agitation, in a HS4800 Hybridization Station (Tecan Benelux BV). Finally, the arrays were washed automatically in the Hybridization Station using: 2x SSC/0.05% SDS (at 45°C), 1x SSC and 0.2x SSC (at room temperature), and dried under a stream of N₂, before scanning.

Data extraction and analysis

Arrays were scanned in a ScanArray Express HT scanner (Perkin Elmer, Nederland BV) and spot intensities were quantified using Imagen software (Bio Discovery Inc, El

Sequndo, CA, USA). To balance Cy3 and Cy5 spot intensities, Loewess normalization per subarray was performed using limma-package (<http://bioinf.wehi.edu.au/limma/>) from Bioconductor (<http://www.bioconductor.org>) [23,24]. To scale between arrays, the global median intensity per array was set at 1000. Dye intensities below 200 were then thresholded at 200, to minimize noise and make fold-change on the low-intensity range more robust against outliers. Spots with intensities below the threshold (200) for both Cy3 and Cy5 channels in more than 2 of the 4 arrays performed per subline were excluded from the analysis. Sample to reference ratios were then calculated and 2log transformed. Spots that showed opposite effects for the dye-swap/biological replicates were excluded from further analysis; effects were called opposite if the mean 2log ratio for the per subline were $\geq 0,5$ for one dye and below $\leq -0,5$ for the dye-swap. Following normalization and all the above-mentioned quality controls, the 2log intensity ratios were averaged for the replicates of each subline. This data was stored in SRS7 (Sequence Retrieval System version 7, Lion Bioscience AG, Heidenberg, Germany), which was also used for the comparisons with other previously published/publicly available databases [25]. Hierarchical clustering and data visualization was performed using Cluster and TreeView programs (Eisen Labs: <http://rama.lbl.gov>). Significance Analysis of Microarrays (SAM; <http://www-stat.stanford.edu/~tibs/SAM>) was used to determine which genes were statistically different between stimulated samples and non-stimulated references. Gene ontology clustering was performed using Database for Annotation, Visualization and Integrated Discovery (DAVID: <http://david.abcc.ncifcrf.gov>) [26,27]. The pathway and functional analyses were generated through the use of Ingenuity Pathways Analysis (Ingenuity® Systems, www.ingenuity.com).

cDNA synthesis and RT- PCR analysis

Normal and tumor specimens from patients used for quantitative real-time RT-PCR analysis were obtained from the frozen tissue bank of the Erasmus Medical Center (Rotterdam, the Netherlands). The specimens were collected between 1984 and 2001. The experimental protocols were approved by the Erasmus MC Medical Ethics Committee according to the Medical Research Involving Human Subjects Act. Additional information about these specimens was provided previously [28]. Total RNA was isolated as described above and cDNA was synthesized using MMLV-reverse transcriptase kit and Oligo(dT)₁₂₋₁₈ primer (Invitrogen), according to manufacturer's protocol. cDNA samples were stored at -20°C. TaqMan real-time PCR analysis was performed in an ABI Prism 7700 Sequence Detection System (Applied Biosystems, Foster City, CA), using AmpliTaq Gold DNA polymerase (Applied Biosystems), according to manufacturer's specifications. Validated primers and probes from TaqMan Gene Expression Assays (Applied Biosystems) were used for quantification of VAV3 (Hs00916821_m1), TWIST1 (Hs00361186_m1), DKK3 (Hs00951307_m1) and GAPDH (Hs99999905_m1), according to the PCR settings provided by Applied Biosystems. PBGD was quantified using 0.33 μ M of primers forward: CATGTCTGGTAACGGCAATG and reverse: GTACGAGGCTTTCAATGTTG primers, in Power SybrGreen PCR Master Mix (Applied Biosystems), according to thermocycling protocol recommended by the manufacturer. Transcript quantities for each sample were normalized against the average of two endogenous references and relative to a calibrator. The two housekeeping genes used as endogenous references were PBGD and GAPDH; a

mixture of cDNAs from prostate carcinoma xenografts was used as the calibrator. Graphs and statistics were performed with GraphPad Prism (version 3.0). P-values < 0.05 were considered significant.

RESULTS

Microarray profile of differentially expressed genes between the androgen-responsive PC346C and its hormone-refractory sublines PC346DCC, PC346Flu1 and PC346Flu2

Expression array analysis was performed to explore whether the AR pathway is still active in the hormone-refractory cells under androgen-deprived conditions and identify putative alternative growth/survival pathways. Each of the hormone-refractory sublines were cultured in their respective selection medium (steroid-stripped medium for PC346DCC, supplemented with 1 μ M OH-Flutamide for PC346Flu1 and Flu2) and hybridized on the microarrays, together with the parental androgen-responsive PC346C (cultured in complete medium supplemented with 0.1 nM R1881). To account for the biological variability and dye-preferential binding to oligonucleotides on the microarray, four arrays were performed per condition, using two independent cell passages in dye-swap. Variation in expression pattern was analysed per hormone-refractory subline, and spots were considered to be differentially expressed if the absolute $2\log$ ratio ≥ 0.5 (ratio ≥ 1.42 or ≤ 0.71) for at least three of the 4 arrays and for the average of all 4 arrays. According to these criteria, there were a total of 487 differentially regulated transcripts in the castration-resistant sublines compared to androgen-sensitive PC346C, most of which were overlapping all three refractory sublines (Fig. 1). With 276 differentially regulated transcripts, PC346DCC showed the strongest divergence from the parental line, whereas PC346Flu2 revealed the least alterations (127 transcripts). Significance Analysis of Microarrays (SAM) was used to determine statistical significance of the selected genes and, at a 5% false discovery rate, 392 of the 487 (80%) selected reached statistical significance. A list of the top 100 differentially expressed genes, respective expression ratios and statistical analysis is presented in Table 1. Interestingly, a considerable proportion (64/487) of the differentially regulated genes clustered at distinct genomic locations on chromosomes 4, 5, 6, 8, 11 and 18 (Table 2). A comprehensive list of all the regulated genes per cell line is provided in Supplementary Tables S1 to S3.

AR pathway is down-regulated in PC346DCC

To investigate the activation state of the AR pathway in the PC346DCC, PC346Flu1 and PC346Flu2, the SRS database was used to link and compare our present data with a previously established androgen-response gene signature (Fig. 2A). The androgen-response signature of the PC346 cell lines consisted of 114 AR target genes, which are listed in Supplementary Table S4. Of the 487 differentially-regulated transcripts in the castration-resistant sublines, only 27 were AR target genes (<6%), indicating that other genes and pathways are also involved in hormone-refractory proliferation of these sublines. Furthermore, AR target genes were down-regulated in PC346DCC (p-value = 10^{-7}), whereas their expression in PC346Flu1 and PC346Flu2 was not significantly affected (Fig. 2B). However, although not statistically significant for the AR pathway as a

whole, PC346Flu1 and PC346Flu2 did show lower induction of some androgen-responsive genes such as KLK2, STEAP1, STEAP2 and EHF.

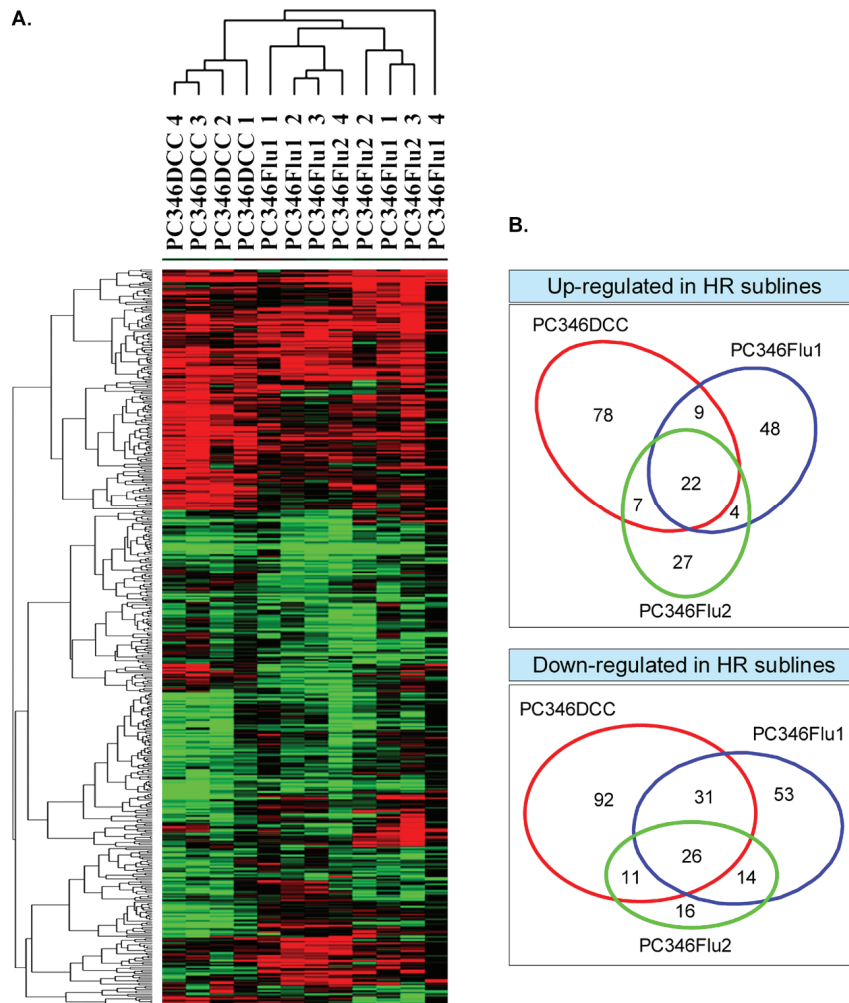


Figure 1 - Differentially-expressed genes in PC346DCC, PC346Flu1 and PC346Flu2 sublines compared to the androgen-responsive PC346C. PC346C was cultured in complete medium with 0.1 nM R1881, whereas the hormone-refractory sublines were culture in dextran-coated charcoal stripped medium (PC346DCC), supplemented with 1 μ M of the antiandrogen hydroxyflutamide (PC346Flu1 and PC346Flu2). A) Heat-map representation: red and green colors represent up-regulation and down-regulation, respectively, whereas black indicates no difference between sublines and parental PC234C cells. Grey squares indicate missing data, either due to low expression levels, poor data quality or absence of probes for the respective transcript in the array platform used for the study. B) Venn-diagram of the number of regulated genes in the different sublines.

Table 1 - Top 100 differentially expressed genes, expression ratios and SAM q-values

| GenBank_Acc | Cytoband | HUGO_symbol | HUGO_Gene Name | PC346DCC | | PC346Flu1 | | PC346Flu2 | |
|-------------|-------------|-------------|--|------------|--------|------------|--------|------------|--------|
| | | | | 2log ratio | qvalue | 2log ratio | qvalue | 2log ratio | qvalue |
| NM_004982 | 12p11.23 | KCNJ8 | potassium inwardly-rectifying channel subfamily J member 8 | 2.7 | 0.000 | 1.2 | 0.000 | 1.9 | 0.000 |
| NM_000790 | 7p11 | DDC | dopa decarboxylase aromatic L-amino acid decarboxylase | 1.9 | 0.005 | 0.1 | 0.253 | 2.4 | 0.218 |
| NM_013452 | Xp22 | VCX | variable charge X-linked | 2.3 | 0.000 | 1.6 | 0.015 | 1.7 | 0.049 |
| NM_014269 | 4q34 | ADAM29 | ADAM metalloproteinase domain 29 | 1.5 | 0.000 | 1.4 | 0.011 | 2.2 | 0.000 |
| NM_004750 | 19p12 | CRLF1 | cytokine receptor-like factor 1 | 2.1 | 0.000 | | | | |
| NM_006113 | 1p13.3 | VAV3 | vav 3 guanine nucleotide exchange factor | 2.0 | 0.000 | 0.2 | 0.031 | 0.4 | 0.218 |
| NM_003226 | 21q22.3 | TFF3 | trefoil factor 3 intestinal | 1.9 | 0.000 | -0.5 | 0.211 | 1.5 | 0.049 |
| NM_012463 | 12q24.31 | ATP6V0A2 | ATPase H transporting lysosomal V0 subunit a2 | 0.8 | 0.028 | 1.2 | 0.051 | 1.7 | 0.000 |
| AB037810 | 1q42.2 | SIPA1L2 | signal-induced proliferation-associated 1 like 2 | 0.9 | 0.046 | 1.5 | 0.000 | 1.7 | 0.049 |
| NM_001823 | 14q32 | CKB | creatine kinase brain | 1.7 | 0.000 | 1.5 | 0.015 | 1.6 | 0.000 |
| NM_006332 | 19p13.1 | IFI30 | interferon gamma-inducible protein 30 | 1.7 | 0.000 | 1.1 | 0.025 | 0.7 | 0.218 |
| NM_001072 | 2q37 | UGT1A1 | UDP glucuronosyltransferase 1 family polypeptide A1 | 0.2 | 0.380 | 1.7 | 0.015 | -0.1 | 0.714 |
| NM_016084 | 17p11.2 | RASD1 | RAS dexamethasone-induced 1 | 1.6 | 0.000 | 1.2 | 0.000 | 0.5 | 0.218 |
| NM_005794 | 14q11.2 | DHRS2 | dehydrogenase/reductase SDR family member 2 | 1.4 | 0.003 | 1.5 | 0.071 | 1.2 | 0.051 |
| U58096 | Yp11.2 | TSPY1 | testis specific protein Y-linked 1 | 1.0 | 0.037 | 1.4 | 0.000 | | |
| NM_013253 | 11p15.2 | DKK3 | dickkopf homolog 3 Xenopus laevis | -0.6 | 0.005 | 1.4 | 0.000 | 0.7 | 0.218 |
| NM_005804 | 19p13.12 | DDX39 | DEAD Asp-Glu-Ala-Asp box polypeptide 39 | 1.4 | 0.000 | 0.3 | 0.253 | 0.8 | 0.194 |
| NM_006721 | 10q22 | ADK | adenosine kinase | 1.4 | 0.000 | 0.1 | 0.422 | 0.7 | 0.194 |
| AK026892 | 22q13.31 | CERK | ceramide kinase | 1.4 | 0.000 | 0.0 | 0.321 | 0.5 | 0.218 |
| AL049949 | 10q22.3 | C10orf56 | chromosome 10 open reading frame 56 | 1.3 | 0.000 | 0.5 | 0.048 | 0.4 | 0.218 |
| NM_016639 | 16p13.3 | TNFRSF12A | tumor necrosis factor receptor superfamily member 12A | 0.6 | 0.028 | 1.3 | 0.000 | 0.5 | 0.218 |
| NM_001902 | 1p31.1 | CTH | cystathionase cystathionine gamma-lyase | 1.3 | 0.020 | 0.5 | 0.044 | 0.7 | 0.194 |
| S67154 | 3q28 | E1F4A2 | eukaryotic translation initiation factor 4A isoform 2 | 0.1 | 0.589 | 1.3 | 0.021 | -0.5 | 0.101 |
| NM_003516 | 1q21.2 | HIST2H2AA3 | histone cluster 2 H2aa3 | -0.1 | 0.645 | 1.2 | 0.000 | 0.8 | 0.194 |
| NM_003712 | 19p13 | PPAP2C | phosphatidic acid phosphatase type 2C | 1.2 | 0.000 | 0.9 | 0.044 | 1.2 | 0.000 |
| Y09836 | ORF* | ORF* | 3 UTR of hypothetical protein ORF1* | 0.7 | 0.046 | 1.0 | 0.011 | 1.2 | 0.101 |
| L07383 | 3p21.3 | RPSA | ribosomal protein SA | 0.1 | 0.513 | 1.2 | 0.071 | | |
| NM_005311 | 7p12-p11.2 | GRB10 | growth factor receptor-bound protein 10 | 1.1 | 0.028 | 0.7 | 0.008 | 0.5 | 0.218 |
| Y11158 | 16p13.3 | SNORA10 | small nucleolar RNA H/ACA box 10 | -0.1 | 0.513 | 1.1 | 0.000 | 0.5 | 0.218 |
| AF086251 | 11q21 | SESN3 | sestrin 3 | 0.1 | 0.534 | 1.1 | 0.048 | 1.1 | 0.049 |
| NM_014214 | 18p11.2 | IMPA2 | inositol myo-1 or 4-monophosphatase 2 | 0.3 | 0.242 | 0.0 | 0.515 | 1.1 | 0.000 |
| NM_003234 | 3q29 | TFR3 | transferrin receptor p90 CD71 | 1.1 | 0.000 | 0.8 | 0.025 | 0.4 | 0.218 |
| U90878 | 10q22-q26.3 | PDLIM1 | PDZ and LIM domain 1 elfin | 1.0 | 0.000 | 0.4 | 0.135 | 0.4 | 0.287 |
| NM_003243 | 1p33-p32 | TGFBR3 | transforming growth factor beta receptor III | 1.0 | 0.000 | 0.1 | 0.287 | 0.5 | 0.236 |
| NM_014061 | Xp11.22 | MAGEH1 | melanoma antigen family H 1 | 1.0 | 0.020 | -0.5 | 0.090 | 0.0 | 0.725 |

| | | | | | | | | | |
|-----------|--------------|-----------|--|------|-------|------|-------|------|-------|
| NM_002795 | 17q12 | PSMB3 | proteasome prosome macropain subunit beta type 3 | 0.5 | 0.113 | 0.6 | 0.063 | 1.0 | 0.000 |
| NM_001814 | 11q14.2 | CTSC | cathepsin C | 1.0 | 0.000 | | | | |
| NM_016192 | 2q32.3 | TMEFF2 | transmembrane protein with EGF-like and two follistatin-like domains 2 | 0.0 | 0.645 | 0.3 | 0.115 | 1.0 | 0.049 |
| AF190900 | 1q32.1 | KLHL12 | kelch-like 12 Drosophila | 0.2 | 0.466 | 0.7 | 0.000 | 1.0 | 0.194 |
| NM_001327 | Xq28 | CTAG1A | cancer/testis antigen 1A | 0.6 | 0.046 | 0.9 | 0.000 | 0.6 | 0.194 |
| NM_004282 | 6p12.3-p11.2 | BAG2 | BCL2-associated athanogene 2 | 0.9 | 0.020 | 0.4 | 0.044 | 0.7 | 0.194 |
| NM_003524 | 6p21.3 | HIST1H2BH | histone cluster 1 H2bh | 0.2 | 0.380 | 0.9 | 0.000 | 0.2 | 0.384 |
| NM_018303 | 6p25.3 | EXOC2 | exocyst complex component 2 | 0.9 | 0.000 | 0.2 | 0.253 | 0.2 | 0.636 |
| AK021498 | 7q22.3 | FLJ36031* | Hypothetical protein FLJ36031* | 0.9 | 0.028 | -0.1 | 0.321 | 0.1 | 0.755 |
| AF200348 | 2p25 | PXDN | peroxidasin homolog Drosophila | -1.2 | 0.003 | -1.3 | 0.000 | 0.9 | 0.064 |
| AL157449 | 17q21.33 | PPP1R9B | protein phosphatase 1 regulatory inhibitor subunit 9B | 0.9 | 0.007 | 0.9 | 0.000 | 0.6 | 0.218 |
| NM_001262 | 1p32 | CDKN2C | cyclin-dependent kinase inhibitor 2C p18 inhibits CDK4 | 0.5 | 0.211 | 0.1 | 0.459 | 0.9 | 0.194 |
| NM_001831 | 8p21-p12 | GLU | clusterin | 0.1 | 0.534 | 0.9 | 0.000 | 0.7 | 0.049 |
| NM_003311 | 11p15.5 | PHLDA2 | pleckstrin homology-like domain family A member 2 | 0.0 | 0.624 | 0.9 | 0.011 | 0.8 | 0.194 |
| NM_000213 | 17q25 | ITGB4 | integrin beta 4 | 0.9 | 0.086 | -1.3 | 0.000 | 0.1 | 0.777 |
| NM_002165 | 20q11 | ID1 | inhibitor of DNA binding 1 dominant negative helix-loop-helix protein | -1.2 | 0.018 | | | | |
| AK024495 | 11p15.5 | LRRC56 | leucine rich repeat containing 56 | -1.2 | 0.000 | 0.2 | 0.321 | 0.5 | 0.218 |
| NM_017860 | 1q21.2 | C1orf56 | chromosome 1 open reading frame 56 | -0.5 | 0.037 | -1.2 | 0.000 | -0.6 | 0.053 |
| NM_004457 | 2q34-q35 | ACSL3 | acyl-CoA synthetase long-chain family member 3 | -1.2 | 0.009 | -0.7 | 0.025 | -0.3 | 0.101 |
| NM_005544 | 2q36 | IRS1 | insulin receptor substrate 1 | -1.2 | 0.020 | -0.1 | 0.394 | 0.0 | 0.714 |
| D80010 | 2p25.1 | LPIN1 | lipin 1 | -1.2 | 0.000 | -1.1 | 0.015 | -0.9 | 0.053 |
| NM_005045 | 7q22 | RELN | reelin | -1.2 | 0.003 | -0.6 | 0.101 | -0.2 | 0.714 |
| NM_007173 | 11q14.1 | PRSS23 | protease serine 23 | -1.2 | 0.018 | -0.9 | 0.021 | -0.9 | 0.101 |
| NM_003255 | 17q25 | TIMP2 | TIMP metalloproteinase inhibitor 2 | 0.6 | 0.028 | -1.3 | 0.031 | -0.2 | 0.678 |
| AF200348 | 2p25 | PXDN | peroxidasin homolog Drosophila | -1.2 | 0.003 | -1.3 | 0.000 | 0.9 | 0.064 |
| NM_007011 | 15q26.1 | ABHD2 | abhydrolase domain containing 2 | -1.5 | 0.000 | -1.1 | 0.032 | 0.1 | 0.573 |
| AF271070 | 12q13.11 | SLC38A1 | solute carrier family 38 member 1 | -1.3 | 0.000 | -0.7 | 0.044 | -0.2 | 0.678 |
| L29496 | Xq11.2-q12 | AR | androgen receptor | -1.3 | 0.018 | 0.9 | 0.000 | -0.3 | 0.194 |
| NM_019005 | 7p22-p21 | FLJ20323* | Hypothetical protein FLJ20323* | -0.9 | 0.000 | -1.3 | 0.000 | -0.6 | 0.134 |
| AK026517 | 11p12 | EHF | ets homologous factor | -0.7 | 0.028 | -1.3 | 0.000 | -0.6 | 0.309 |
| NM_000213 | 17q25 | ITGB4 | integrin beta 4 | 0.9 | 0.086 | -1.3 | 0.000 | 0.1 | 0.777 |
| NM_001311 | 14q32.33 | CRIP1 | cysteine-rich protein 1 intestinal | -1.4 | 0.018 | 0.4 | 0.101 | -0.9 | 0.115 |
| AL050367 | 10p13 | C10orf38 | chromosome 10 open reading frame 38 | 0.1 | 0.380 | -1.4 | 0.000 | -0.6 | 0.084 |
| AL122055 | 6q21 | CDC2L6 | cell division cycle 2-like 6 CDK8-like | -1.4 | 0.000 | -1.3 | 0.000 | -1.2 | 0.000 |
| NM_005864 | 14q11.2-q12 | EFS | embryonal Fyn-associated substrate | -1.4 | 0.009 | 0.4 | 0.135 | -0.6 | 0.064 |
| NM_002151 | 19q11-q13.2 | HPN | hepsin transmembrane protease serine 1 | -1.0 | 0.000 | -0.9 | 0.000 | -1.4 | 0.053 |
| NM_016598 | 3p21.31 | ZDHHC3 | zinc finger DHH-type containing 3 | -1.4 | 0.003 | -1.1 | 0.000 | -0.9 | 0.053 |
| NM_005510 | 6p21.3 | DOM3Z | dom-3 homolog Z C. elegans | 0.5 | 0.211 | 0.1 | 0.422 | -1.4 | 0.053 |
| NM_000944 | 4q21-q24 | PPP3CA | protein phosphatase 3 formerly 2B catalytic subunit alpha isoform | -1.4 | 0.028 | -1.2 | 0.000 | -1.0 | 0.084 |

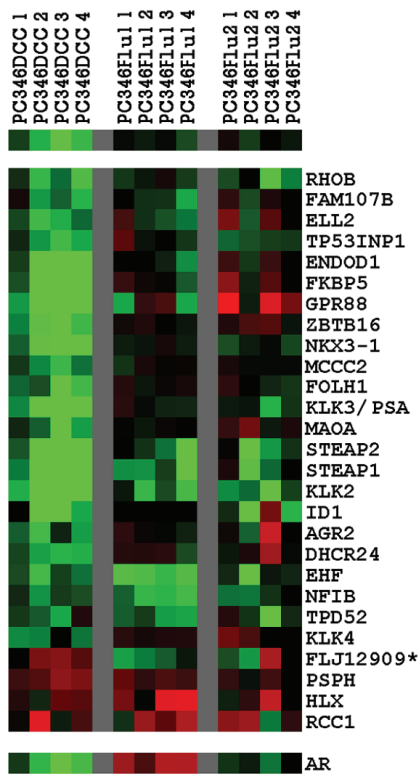
Table 2 - Chromosomal clustering of the differentially expressed transcripts

| Cell line | #genes regulated | up/down regulated | Cytoband | #genes cytoband* | Bonferroni p-value |
|-----------|------------------|-------------------|----------|------------------|--------------------|
| PC346DCC | 7 | down | 4q21-24 | 56 | 0.003 |
| PC346DCC | 9 | down | 5q11-23 | 130 | 0.028 |
| PC346DCC | 6 | down | 6q14-23 | 65 | 0.026 |
| PC346DCC | 8 | down | 8p11-22 | 74 | 0.003 |
| PC346DCC | 10 | down | 8q11-24 | 131 | 0.006 |
| PC346Flu1 | 6 | down | 11p11-15 | 92 | 0.068 |
| PC346Flu2 | 14 | up | 18 | 109 | <0.0001 |

p-values determined by Fisher's exact test with Bonferroni correction for multiple testing

* number of genes located in the cytoband that are expressed by the indicated cell line

A.



B.

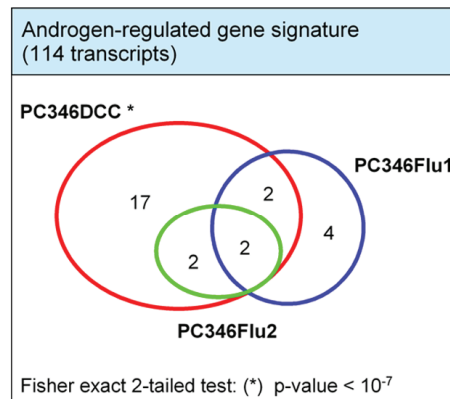


Figure 2 - Activation state of the AR pathway in the PC346DCC, PC346Flu1 and PC346Flu2. Differentially-expressed genes in PC346 hormone-refractory sublines versus parental PC346C were linked to a previously established androgen-response gene signature (see Materials and Methods section). **(A)** Heat-map representation of androgen-responsive genes deregulated in any of the PC346 hormone-refractory sublines. Color scheme as described in Fig. 1. **(B)** Venn-diagram and respective statistics.

Gene ontology and pathway analysis identifies cancer signature

The selected 487-gene signature was classified according to Gene Ontology (GO) Biological Processes using the Database for Annotation, Visualization and Integrated Discovery (DAVID) [26,27]. Annotation clustering analysis showed enrichment in categories involved in organ development, reproductive system differentiation, cellular growth, differentiation and apoptosis (Table 3). Ingenuity Pathway Analysis was used to identify enrichment in “diseases and disorders”, “molecular and cellular functions”, and to search for intrinsic pathways/networks within the selected gene sets (www.ingenuity.com). Cancer and reproductive system disease were ranked in the top 3 of “diseases and disorders”, which logically confirmed the enrichment of genes associated with prostate cancer, such as hepsin, clusterin, vitamin D receptor, trefoil factor 3, tumor protein D52, the androgen-receptor self and several of its target genes (Fig. 3A and 3B, respectively). Furthermore, we used Network analysis to screen the 276-gene signature of PC346DCC for potential alternative growth pathways that could be involved in bypassing the AR signaling. Interestingly, signaling via growth-hormone receptor (GHR), insulin receptor (INSR) and epidermal growth factor receptor was among the top 10 Networks (score = 20) showing deregulation in PC346DCC (Fig. 3C).

Integrative analysis reveals genes deregulated in prostate cancer progression

To identify genes modulated in prostate cancer that could explain hormone-refractory growth through bypass of the AR pathway, we linked the 276-gene signature from PC346DCC with data from seven prostate cancer microarray studies published previously [16,29,30,31,32,33,34] (Table 4). Only genes present in at least 5/7 databases (209 genes) and deregulated in at least 3/7 (111 genes) were included for further analysis. Hierarchical clustering performed on the signature genes (first column), next to primary cancer vs. normal prostate (second column), metastatic cancer vs. primary cancer (third column), and finally hormone-refractory vs. hormone-naïve disease (fourth column), is shown in Fig. 4. Approximately 30% of the genes differentially expressed in PC346DCC were found to be consistently deregulated in metastatic prostate cancer compared to organ-confined disease.

TWIST1, DKK3 and VAV3 as markers for disease diagnosis and prognosis

Based on their recognized pathological functions and consistent deregulation in multiple prostate cancer databases, TWIST1, VAV3 and DKK3 were selected for their potential role in the bypass of the AR pathway. In this manner, TWIST1 and VAV3 are putative oncogenes involved in growth hormone signaling, as revealed by Ingenuity Pathway Analysis (Fig. 3C). On the other hand, DKK3 is a tumor suppressor, showing strong down-regulation in the datasets from Chandran *et al.*, Lapointe *et al.* and Varambally *et al.* (Fig. 4C). Whereas TWIST1 showed consistent up-regulation in primary and metastatic prostate cancer datasets from Varambally *et al.*, Yu *et al.*, Lapointe *et al.* and Chandran *et al.*, VAV3 was down-regulated in primary tumors followed by up-regulation in metastasis (Fig. 4C).

Table 3 - Summary of the Gene Ontology (GO) biological processes significantly enriched in the hormone-refractory gene signature

| | | count | P value |
|------------------------------|--|-------|---------|
| Annotation Cluster 1 | Enrichment Score: 4.42 | | |
| | multicellular organismal development | 86 | 1.8E-05 |
| | anatomical structure development | 78 | 7.7E-05 |
| | system development | 68 | 3.9E-05 |
| Annotation Cluster 2 | Enrichment Score: 4.24 | | |
| | cell differentiation | 69 | 7.7E-05 |
| | cell development | 53 | 3.1E-05 |
| Annotation Cluster 3 | Enrichment Score: 4.09 | | |
| | apoptosis | 38 | 4.1E-05 |
| | programmed cell death | 38 | 5.0E-05 |
| Annotation Cluster 4 | Enrichment Score: 2.68 | | |
| | regulation of phosphorylation | 8 | 1.7E-03 |
| | regulation of phosphate metabolic process | 8 | 2.3E-03 |
| Annotation Cluster 5 | Enrichment Score: 2.67 | | |
| | amino acid and derivative metabolic process | 21 | 5.8E-04 |
| | amine metabolic process | 21 | 6.0E-03 |
| | nitrogen compound metabolic process | 22 | 6.7E-03 |
| Annotation Cluster 6 | Enrichment Score: 2.15 | | |
| | regulation of biological process | 134 | 3.0E-03 |
| | regulation of cellular process | 124 | 1.4E-02 |
| | regulation of gene expression | 63 | 6.7E-02 |
| Annotation Cluster 7 | Enrichment Score: 2.15 | | |
| | neurogenesis | 16 | 7.0E-03 |
| | neuron differentiation | 14 | 6.2E-03 |
| Annotation Cluster 8 | Enrichment Score: 2.03 | | |
| | cellular lipid metabolic process | 29 | 3.8E-03 |
| | lipid metabolic process | 28 | 1.6E-03 |
| Annotation Cluster 9 | Enrichment Score: 1.82 | | |
| | DNA packaging | 16 | 8.9E-03 |
| | establishment and/or maintenance of chromatin architecture | 15 | 1.7E-02 |
| | chromosome organization and biogenesis | 17 | 2.3E-02 |
| | chromatin assembly or disassembly | 9 | 2.1E-02 |
| | nucleosome assembly | 7 | 1.8E-02 |
| Annotation Cluster 10 | Enrichment Score: 1.70 | | |
| | development of primary sexual characteristics | 7 | 2.0E-02 |
| | sex differentiation | 6 | 1.8E-02 |
| | reproductive developmental process | 6 | 2.2E-02 |
| | gonad development | 5 | 4.9E-02 |
| Annotation Cluster 11 | Enrichment Score: 1.42 | | |
| | growth | 12 | 8.3E-02 |
| | regulation of cell size | 11 | 1.8E-02 |
| | cell growth | 10 | 3.7E-02 |

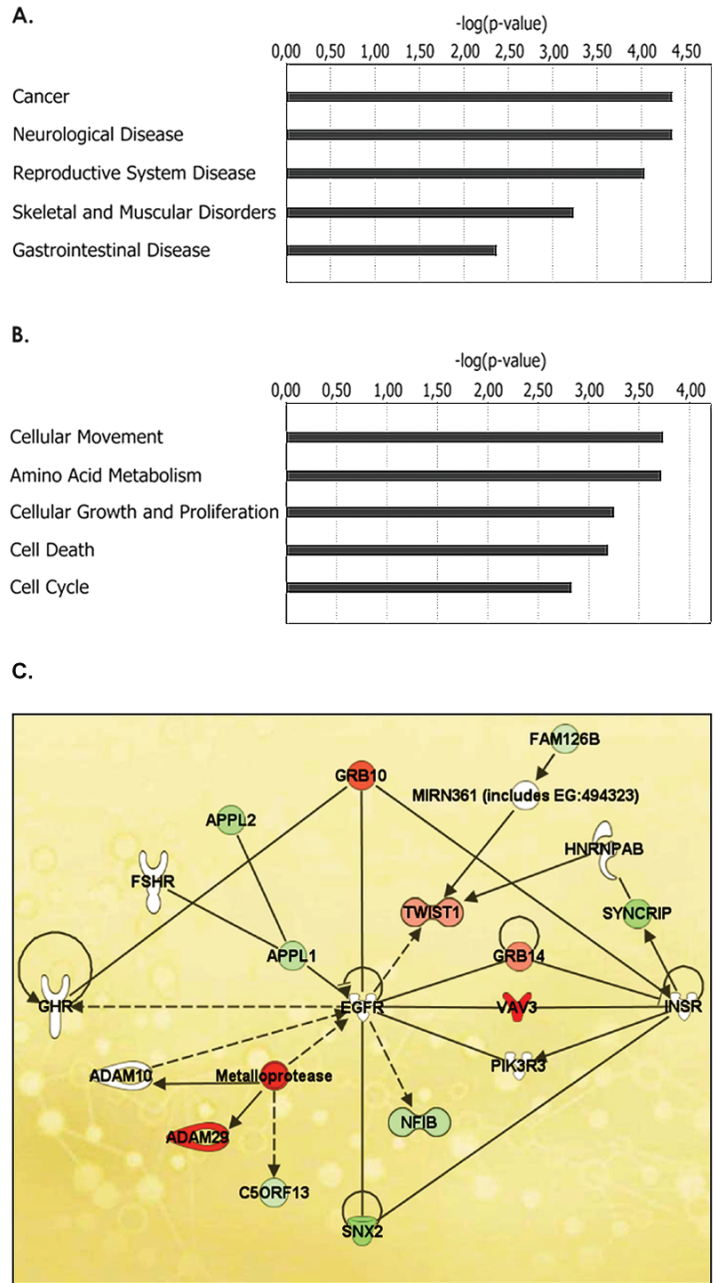


Figure 3 - Biological processes deregulated in the hormone-refractory sublines. Top 5 biological functions enriched in the castration-resistant sublines: **(A)** diseases and disorders, **(B)** molecular and cellular functions. **(C)** Example of Network analysis for PC346DCC showing deregulation of hormone and growth-factor receptor signaling: up-regulated genes are represented in red and repressed genes in green. Analysis was performed using Ingenuity Pathway Analysis software (www.ingenuity.com).

Table 4 - Description of prostate cancer databases linked via SRS

| First Author | Reference | Samples |
|------------------------|---|---|
| Best (2005) [29] | 10 hormone-naive prostate cancers | 10 hormone-refractory primary prostate tumors |
| Chandran (2007) [30] | 64 primary prostate tumor samples | 24 hormone-refractory metastatic samples from 4 patients |
| Lapointe (2004) [31] | 41 benign prostate tissue adjacent to cancer | 62 primary prostate tumor samples 9 lymph node metastasis |
| Tamura (2007) [32] | 10 hormone-naive prostate cancers | 18 hormone-refractory primary and metastatic tumor samples |
| Tomlins (2007) [16] | 15 benign epithelial tissue adjacent to cancer | 30 primary prostate tumor samples 3 hormone-naive and 17 hormone-refractory metastasis |
| Varambally (2005) [33] | 5 benign prostate tissues | 5 clinically localized prostate cancers 5 hormone-refractory metastatic samples |
| Yu (2004) [34] | 60 benign prostate tissue adjacent to cancer 23 disease free donor prostate tissue | 62 primary prostate tumors 24 hormone-refractory metastasis |

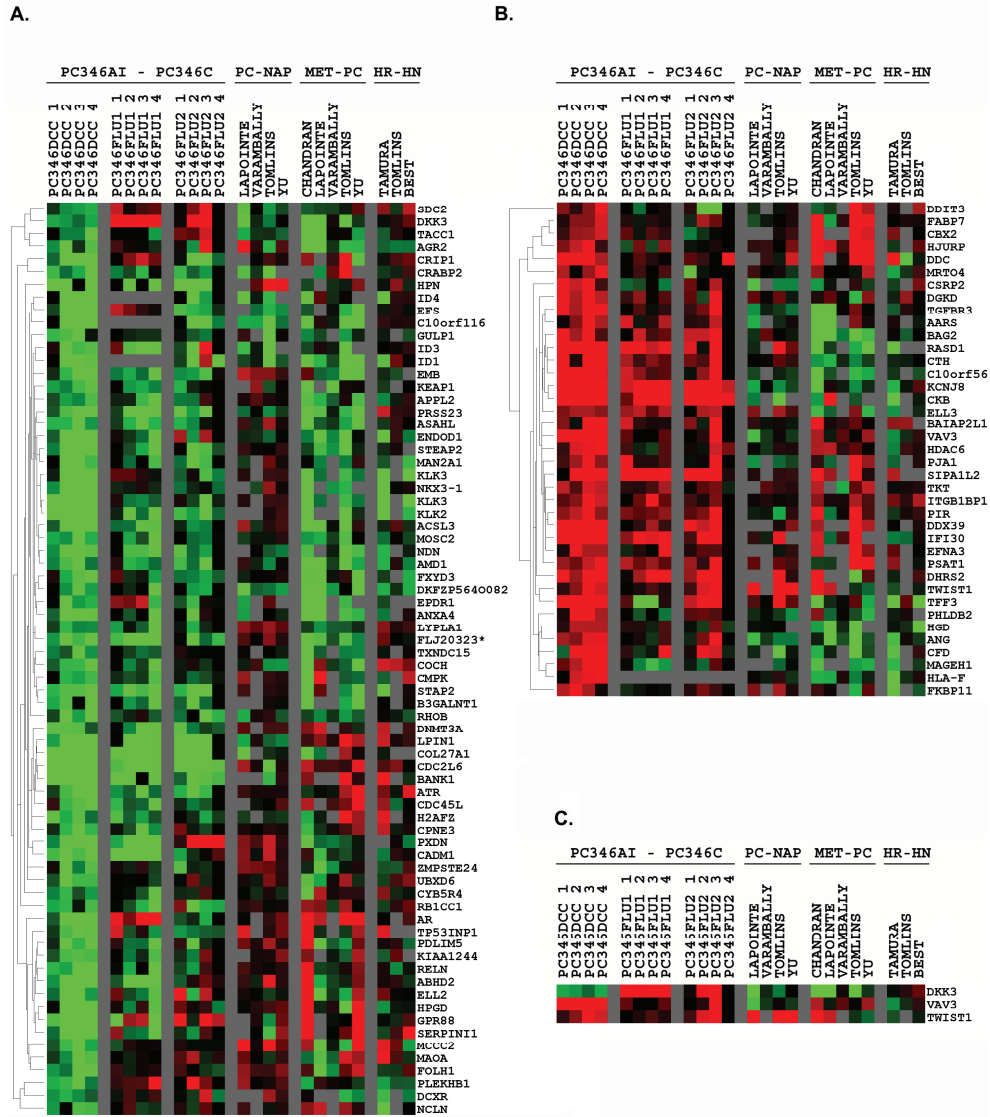


Figure 4 - Expression of the androgen-independent PC346DCC signature genes in prostate cancer samples from patient tumors. The 276-gene signature from PC346DCC was linked to data from 7 prostate cancer microarray databases of primary (Lapointe, Varambally, Tomlins, Yu), metastatic (Chandran, Lapointe, Varambally, Tomlins, Yu) and hormone-refractory tumors (Tamura, Tomlins and Best). Only genes present in at least 5/7 databases (209 genes) and deregulated in at least 3/7 (111 genes) were included in the analysis. Heat-map representation of (A) 72 overexpressed and (B) 39 repressed genes in PC346DCC. (C) Deregulated genes selected for further qPCR analysis. Color scheme as described in Fig.1. Grey squares indicate missing data, either due to low expression levels, poor data quality or absence of probes for the respective transcript in the array platform used for the study. PC-NAP: prostate cancer minus normal adjacent prostate; MET-PC: metastasis minus primary prostate tumors; HR-HN: hormone-refractory minus hormone-naïve tumors.

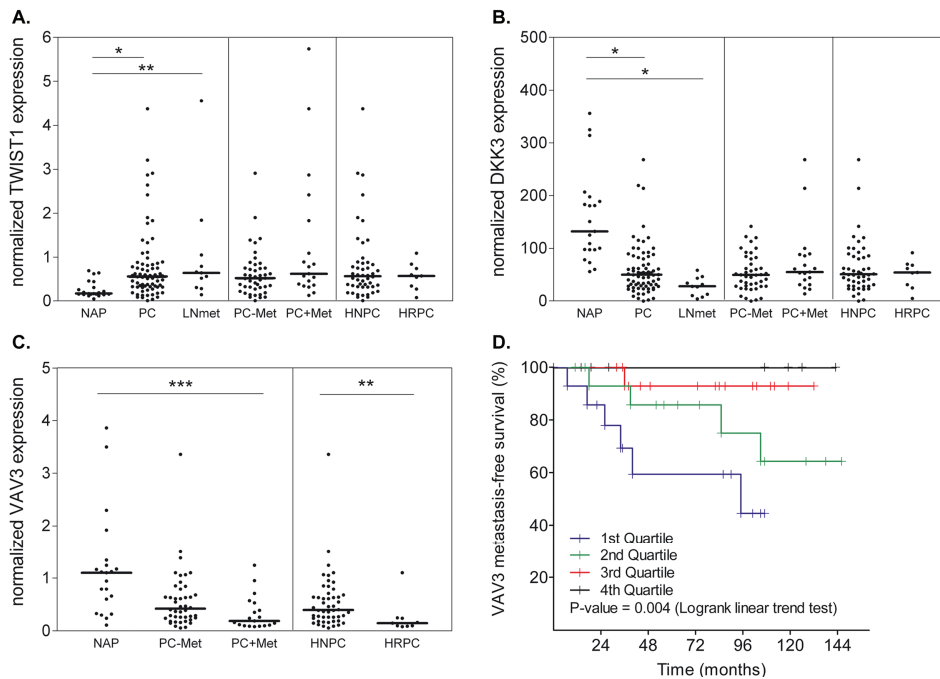


Figure 5 - Quantitative RT-PCR analysis of TWIST1, DKK3 and VAV3 in an independent set of prostate samples. Prostate tumor samples were obtained by radical prostatectomy or transurethral resection of the prostate of patients being operated at Erasmus MC clinic. This panel contains 21 benign prostate tissue samples and 74 adenocarcinomas at different disease stages. **(A)** TWIST1; **(B)** DKK3; **(C)** VAV3 expression in prostate samples; **(D)** VAV3 metastasis-free survival analysis. NAP: normal adjacent prostate; PC: primary prostate cancer; LNmet: lymph-node metastasis; PC-Met: non-progressive organ-confined prostate cancer; PC+Met: primary tumor from progressive prostate cancer that either had or developed metastasis during subsequent follow-up; HN: hormone-naïve; HR: hormone-refractory; (*) p-value ≤ 0.0001 and (**) p-value ≤ 0.005 using Mann-Whitney two-tailed test. (***) p-value ≤ 0.0001 with Post linear-trend test.

Quantitative PCR analysis was performed on an independent set of prostate samples, obtained by radical prostatectomy or transurethral resection of the prostate of patients being operated at Erasmus MC clinic. This panel contained 21 benign prostate tissue samples and 74 adenocarcinomas at different disease stages. Quantitative PCR analysis showed up-regulation of TWIST1 in primary prostate cancer samples and lymph-node metastasis (P-value = 0.0001 and 0.002, respectively). No difference was observed between hormone-refractory (HRPC) and hormone-naïve tumors (HNPC) (Fig. 5A). DKK3 expression was significantly decreased in prostate cancer and lymph-node metastasis (P-value ≤ 0.0001), although no difference was observed during progression from organ-confined to metastatic or hormone-refractory disease (Fig. 5B). VAV3 expression decreased gradually during prostate cancer progression, with the lowest levels observed in metastatic prostate tumors (P-value = 0.0001 for Post linear-trend test) and hormone-refractory samples (P-value = 0.005 for HNPC vs. HRPC; Fig. 5C).

Lymph-node samples were removed from the VAV3 analysis in Fig. 5C, because VAV3 expression was highly increased in normal lymph-node compared to normal prostate tissues (data not shown). In these settings, the presence of remnants of normal lymph-node tissue can lead to over-estimation of the real VAV3 quantity in lymph-node metastasis. Kaplan-Meier analysis showed a direct correlation between VAV3 expression and metastasis-free survival (P -value = 0.004 for Logrank trend test; Fig. 5D).

DISCUSSION

In the present study we used microarray analysis to identify differences in the gene expression pattern of the androgen-responsive PC346C cell line and its castration-resistant sublines: PC346DCC, PC346Flu1 and PC346Flu2. This analysis detected 487 transcripts differentially regulated in the hormone-refractory cells versus the parental PC346C. Many of these were common to all three hormone-refractory sublines, despite the different AR pathway modifications, suggesting similar growth enhancing adaptations (Fig. 1). These shared genes could be divided in four main categories: regulation of cell cycle progression and proliferation (ex. HPN, NDN, ATR, ABL2, DHRS2), development and cellular differentiation (CLEC3B, KCNJ8, ADAM29, DNMT3A), fatty acid and steroid metabolism (LPIN1, DECR1, ACSL3) and intracellular signaling transduction (PPAP2C, PPP3CA, PRSS23, GRB10, SIPA1L2). Interestingly, 40 of the genes down-regulated in PC346DCC clustered in just four genomic locations: 4q21-24 (7 genes), 5q11-23 (9 genes), 6q14-23 (6 genes) and chr8 (18 genes). This is more than would be expected by chance. Also 6 genes down-regulated in PC346Flu1 and 14 up-regulated genes in PC346Flu2 clustered at 11q11-15 and chr18, respectively (Table 2). Duplication of chromosome 18 and loss of 8p has been previously reported in PC346Flu2 and PC346DCC, respectively, and may explain the clustering observed at these loci [35]. However, no evidence of chromosomal amplifications or deletions was detected at the other loci mentioned. A possible explanation is that epigenetic mechanisms, such as promotor methylation or histone modifications, may be involved in the transcriptional regulation of these large chromosomal regions [36]. Indeed, expression of DNA methyltransferase DNMT3A and histone deacetylase HDAC6 was altered in PC346DCC, supporting this hypothesis. Nevertheless, losses at 4q, 5q, 6q, 8p and 11p have been frequently reported in prostate cancer specimens and these loci are suspected of harbouring potential tumor suppressor genes [37,38].

Previously, we have shown that PC346DCC, PC346Flu1 and PC346Flu2 display different AR modifications that resulted in distinct mechanisms of hormone-refractory growth [35]. PC346DCC revealed very low levels of the AR and its target gene prostate specific antigen (PSA), and was insensitive to androgen stimulation in growth assays, promotor transactivation assays and expression microarray profiling (submitted data)[35]. These results suggest that the AR pathway has been bypassed and is not essential for the growth of PC346DCC cells. The present study further substantiates this hypothesis by showing a strong down-regulation of AR target genes compared to the parental PC346C (Fig. 2). PC346Flu1, on the other hand, expresses

high levels of the AR and previously showed a “super-activation” of this receptor in response to androgens, both in transactivation assays as in expression microarray analysis. Interestingly, the proliferation of this subline is inhibited by physiological concentration of androgens, and is optimal in the absence of this ligand. A possible explanation for this growth suppressive effect is that the “super-activation” of the AR by androgens in PC346Flu1 may be tilting the balance towards cellular differentiation [39,40]. It is worth noting how few AR target genes are deregulated in PC346Flu1 versus the parental PC346C (Fig. 2). This suggests that the AR pathway remained active in the PC346Flu1 cells cultured in androgen-depleted medium supplemented with AR antagonist hydroxyflutamide. The few AR target genes that were differentially expressed in PC346Flu1 include EHF, NFIB and HLX, which are involved in development and differentiation processes. In this context, the EHF transcription factor (also known as ESE-3) is particularly interesting, as its expression is specific for epithelial cells and it is involved in glandular differentiation [41,42]. It has recently been shown that EHF is frequently down-regulated in prostate tumor specimens and silenced in PC3 and DU145 prostate cancer cell lines by promotor methylation at evolutionary conserved CpG sites [43]. Re-expression of EHF in these cells inhibited clonogenic survival and induced apoptosis [43]. EHF is one of the strongest repressed genes in PC346Flu1 being up-regulated upon androgen stimulation, which makes it a good candidate for the growth suppressive effect of androgens on this cell line. The third hormone-refractory subline studied here, PC346Flu2, carries the T877A AR mutation, well known for causing broadened receptor activation by non-androgenic ligands, including flutamide [44,45]. Consistent with the presence of this “promiscuous” AR, the growth of PC346Flu2, as well as expression of AR target genes, are stimulated by both the synthetic androgen R1881 and the antiandrogen hydroxyflutamide (submitted data) [35]. In PC346Flu2, the presence of the T877A AR mutation allows for the maintenance of AR activity in the selection medium supplemented with 1 μ M hydroxyflutamide. This is further substantiated in the present study by the observation that PC346Flu2 is the least divergent of the hormone-refractory sublines, with no more than 127 differentially regulated transcripts compared to the parental PC346C (Fig. 1).

Both PC346Flu1 and PC346Flu2 sublines have an active AR and acquired hormone-refractory proliferation through adaptations of the AR pathway. Therefore, to study alternative survival and growth pathways independent of the AR we further focused on the expression profile of PC346DCC cells. The Ingenuity Pathway Analysis program was used to screen the 276-gene signature of PC346DCC for potential gene Networks that could be involved in bypassing the AR signaling. Among the top 10 Networks, emerged the signaling pathway via growth-hormone receptor (GHR), insulin receptor (INSR) and epidermal growth factor receptor (EGFR) as a potential candidate (Fig. 3C). These receptors are not themselves deregulated in PC346DCC but several partners of this signaling pathway were, including VAV3 and TWIST1. VAV3 and TWIST1 are potential oncogenes, and while VAV3 can interact with and cross-activate signaling via hormone and growth receptors, expression of TWIST1 is in turn stimulated by EGF and IGF1 [46,47,48,49]. Both VAV3 and TWIST1 are overexpressed in PC346DCC cells, and survey of 7 previous microarray studies revealed a consistent up-regulation in metastatic patient material (Fig. 4C). Another interesting candidate gene for

the bypass of the AR pathway was the DKK3 tumor suppressor, which was down-regulated in PC346DCC and multiple databases of primary and metastatic tumors (Fig. 4C). While compelling evidence links these genes to prostate cancer pathogenesis, it is not known whether TWIST1, VAV3 or the tumor suppressor DKK3 may have a functional role in developing resistance to hormonal therapy.

TWIST1 is a helix-loop-helix transcription factor, regulator of embryonic morphogenesis, and highly expressed in many types of human cancer [50]. The role of TWIST1 as a potential oncogene was first suggested through a functional screen for cDNAs that could counteract the pro-apoptotic effects of the MYC oncogene. In that study, TWIST1 expression bypassed P53-induced growth arrest and promoted colony formation, consistent with a potential role as oncoprotein [51]. Yang *et al.* showed that suppression of TWIST1 expression in highly metastatic mammary carcinoma cells specifically inhibited their ability to metastasise to the lung, while ectopic expression resulted in activation of mesenchymal markers and induction of cell motility [52]. Previous studies also implicated TWIST1 in the development and progression of prostate cancer, showing that its expression was up-regulated in prostate adenocarcinomas and correlated with Gleason grading and increased metastatic potential [53,54,55]. Furthermore, inactivation of TWIST1, through small interfering RNA, induced growth arrest and suppressed migration and invasion abilities in androgen-independent prostate cancer cell lines DU145 and PC3 [54,56]. We quantified TWIST1 expression in a panel of patient derived material, comprising 21 normal prostate samples (adjacent to cancer), 74 primary prostate tumors, of which 9 hormone-refractory samples, and 13 lymph-node metastasis. Among the primary tumors are 59 samples of early organ-confined disease, 9 samples of invasive tumors that eventually developed metastasis during follow-up and 6 tumors with lymph-node and/or distant metastasis at the time of operation. Quantitative PCR confirmed overexpression of TWIST1 in primary prostate cancer samples and lymph-node metastasis (Fig. 5A). In this patient cohort, TWIST1 expression could not predict progression, as it did not differ between non-progressive organ-confined tumors and primary cancers that eventually developed metastasis. Furthermore, TWIST1 expression was not increased in hormone-refractory tumors when compared to hormone-naïve samples, suggesting that TWIST1 overexpression alone may not be enough to confer hormone-refractory growth. However, since TWIST1 is strongly up-regulated in prostate cancer samples it may still be useful as a cancer marker or therapeutic target.

VAV3 is a member of the VAV family of oncoproteins, GTPase guanine nucleotide exchange factors that regulate receptor protein tyrosine kinases. It can be activated upon engagement of growth factor receptors, such as EGFR, PDGFR, INSR or IGF1R, and in turn activate downstream PLC and PI3K signaling pathways [48,49,57]. Previous studies have implicated VAV3 in the pathogenesis of the prostate: (i) VAV3 expression has been detected in the prostate, at increased levels in cancer cells [58]; (ii) it has been shown to interact with the AR pathway, stimulating ligand-independent cell growth in LNCAP-hormone-refractory cells [58,59,60]; and (iii) targeting of constitutively active VAV3 expression to the prostate induced prostate cancer in mice [61]. Surprisingly, in our patient derived samples, VAV3 expression decreased gradually

during prostate cancer progression, with the lowest levels in metastatic and hormone-refractory samples (Fig. 5C). Furthermore, Kaplan-Meier analysis showed a direct correlation between VAV3 expression levels and metastasis-free survival (Fig. 5D). These results encourage the use of VAV3 as a potential prognosis marker in prostate cancer, and provide a possible mechanism for the bypass of AR pathway in hormone-refractory tumors. However, the decrease of VAV3 expression in prostate cancer progression was unexpected, considering the function of VAV3 as a potential oncogene. In fact, VAV3 has three transcript variants, the full length VAV3, the VAV3 beta isoform and the truncated VAV3.1 variant, which has no guanine nucleotide exchange activity (GEF) due to lack of N-terminal domains [48,57,62]. The truncated transcript is expressed in many tissues and is the major variant in the prostate [48,62]. Because the effect of VAV3 on cell division and AR activation is dependent on GEF activity, this variant is not oncogenic and has most likely a different function than the full-length protein. It was proposed that this VAV3.1 variant may function as a dominant negative of other VAV family members [48,62]. In this context, a decrease in the VAV3.1 variant could actually result in increased activity of oncogenic VAV proteins. Clearly, it is essential to characterize the different VAV3 variants in the prostate and evaluate how the balance of these is affected during prostate cancer progression, before one can consider its use in the clinic. These results exemplify the limitation of large-scale expression profiling assays that rely on a single probe per gene. Ultimately, to investigate gene expression in the context of human disease, it may not be enough to quantify the major known transcript but one may need to consider the different isoforms and how these variants interact with each other [63,64]. In the near future we expect to be able to answer how different splice variants from the same gene (including VAV3) can relate to prostate cancer, using exon microarray analysis of the patient tumor material.

DKK3 is part of an evolutionary conserved gene family encoding secreted proteins, which play an important role in vertebrate embryonic development as antagonists of Wnt/beta-catenin signaling. DKKs are further implicated in bone formation and bone disease, Alzheimer's and cancer [65]. DKK3 was proposed to function as a tumor suppressor since it was found to be down-regulated in a number of malignancies including kidney, bladder, lung, pancreas and prostate cancer [66]. Reduced DKK3 expression may, at least in part, be explained by promotor methylation, which has been detected in various cancers, including over 65% of prostate tumors [67]. Additional reports showed consistent reduction of DKK3 expression in prostate adenocarcinomas, particularly those with a high Gleason grade [68,69,70]. Moreover, small interfering RNA-mediated down-regulation of DKK3 enhanced cell cycle progression and disrupted three-dimensional acinar morphogenesis in RWPE-1 prostate epithelial cells [68]. Conversely, ectopic expression of DKK3 resulted in decreased proliferation, inhibited colony formation and induced apoptosis of LNCaP, PC3 and DU145 cell lines [67,68,69]. In our patient samples, DKK3 expression decreased in prostate cancer and lymph-node metastasis, but no difference was observed in hormone-refractory samples (Fig. 5B). As for TWIST1, DKK3 might be useful as a cancer marker, but could not predict tumor progression, nor explain recurrence after hormonal therapy. Interestingly, injection of an adenovirus vector carrying DKK3 showed a dramatic anti-tumor effect in a

xenograft human prostate cancer model, inhibiting tumor growth and lymph node metastasis and prolonging mice survival [69,71]. Such results encourage the development of therapies targeting DKK3 in advanced metastatic disease.

CONCLUSIONS

The present study showed that alterations in the AR pathway are common events in prostate cancer progression to hormone-refractory disease. While AR overexpression in PC346Flu1 and mutation in PC346Flu2 allowed the maintenance of AR activity under androgen ablation and antiandrogen treatment, PC346DCC acquired complete independence from AR signaling by activating alternative survival pathways. In PC346DCC, activation of VAV3 and TWIST1 oncogenes and down-regulation of DKK3 tumor suppressor may constitute a possible mechanism for bypassing the AR pathway. The fact that TWIST1 and DKK3 expression was deregulated in both hormone-refractory and hormone-naïve patient samples, suggests that these alterations occur earlier in prostate cancer progression and do not act alone in inducing hormone-refractory growth. Indeed, both VAV3 and TWIST1 are known to interact with growth factor signaling, which could be the effector mechanism in stimulating cellular proliferation, whereas DKK3 down-regulation may promote survival through inhibition of apoptosis. These results grant further investigations on the use of VAV3, TWIST1 and DKK3 as prostate cancer markers and in the development of targeted therapies for advanced disease.

ACKNOWLEDGEMENTS

We thank Wilfred van IJcken and Christel Kockx for technical support and for providing the microarrays, equipment and software from the Erasmus Center for Biomics. We also thank Antoine Veldhoven and Don de Lange for the bioinformatics tools. Further, we would like to acknowledge the pathologists Arno van Leenders and Theo van de Kwast for the histopathological analysis of the patient samples. This study was supported by the Netherlands Organization for Scientific Research (NWO) through ZonMW grant 903-46-187 and by the Dutch Cancer Society (KWF) through grant NKB97-1479.

REFERENCES

1. Ferlay J, Autier P, Boniol M, Heanue M, Colombet M, et al. (2007) Estimates of the cancer incidence and mortality in Europe in 2006. *Ann Oncol* 18: 581-592.
2. Frydenberg M, Stricker PD, Kaye KW (1997) Prostate cancer diagnosis and management. *Lancet* 349: 1681-1687.
3. Crawford ED, Eisenberger MA, McLeod DG, Spaulding JT, Benson R, et al. (1989) A controlled trial of leuprolide with and without flutamide in prostatic carcinoma. *N Engl J Med* 321: 419-424.
4. Eisenberger MA, Blumenstein BA, Crawford ED, Miller G, McLeod DG, et al. (1998) Bilateral orchiectomy with or without flutamide for metastatic prostate cancer. *N Engl J Med* 339: 1036-1042.
5. Jenster G (1999) The role of the androgen receptor in the development and progression of prostate cancer. *Semin Oncol* 26: 407-421.
6. van der Kwast TH, Schalken J, Ruizeveld de Winter JA, van Vroonhoven CC, Mulder E, et al. (1991) Androgen receptors in endocrine-therapy-resistant human prostate cancer. *Int J Cancer* 48: 189-193.
7. Ruizeveld de Winter JA, Janssen PJ, Sleddens HM, Verleun-Mooijman MC, Trapman J, et al. (1994) Androgen receptor status in localized and locally progressive hormone refractory human prostate cancer. *Am J Pathol* 144: 735-746.
8. Brown RS, Edwards J, Dogan A, Payne H, Harland SJ, et al. (2002) Amplification of the androgen receptor gene in bone metastases from hormone-refractory prostate cancer. *J Pathol* 198: 237-244.
9. Koivisto P, Kononen J, Palmberg C, Tammela T, Hyytinen E, et al. (1997) Androgen receptor gene amplification: a possible molecular mechanism for androgen deprivation therapy failure in prostate cancer. *Cancer Res* 57: 314-319.
10. Linja MJ, Savinainen KJ, Saramaki OR, Tammela TL, Vessella RL, et al. (2001) Amplification and overexpression of androgen receptor gene in hormone-refractory prostate cancer. *Cancer Res* 61: 3550-3555.
11. Cullig Z, Hobisch A, Hittmair A, Cronauer MV, Radmayr C, et al. (1997) Androgen receptor gene mutations in prostate cancer. Implications for disease progression and therapy. *Drugs Aging* 10: 50-58.
12. Taplin ME, Rajeshkumar B, Halabi S, Werner CP, Woda BA, et al. (2003) Androgen receptor mutations in androgen-independent prostate cancer: Cancer and Leukemia Group B Study 9663. *J Clin Oncol* 21: 2673-2678.
13. Grossmann ME, Huang H, Tindall DJ (2001) Androgen receptor signaling in androgen-refractory prostate cancer. *J Natl Cancer Inst* 93: 1687-1697.
14. Devlin HL, Mudryj M (2009) Progression of prostate cancer: multiple pathways to androgen independence. *Cancer Lett* 274: 177-186.
15. Hendriksen PJ, Dits NF, Kokame K, Veldhoven A, van Weerden WM, et al. (2006) Evolution of the androgen receptor pathway during progression of prostate cancer. *Cancer Res* 66: 5012-5020.
16. Tomlins SA, Mehra R, Rhodes DR, Cao X, Wang L, et al. (2007) Integrative molecular concept modeling of prostate cancer progression. *Nat Genet* 39: 41-51.
17. Mendiratta P, Mostaghel E, Guinney J, Tewari AK, Porrello A, et al. (2009) Genomic Strategy for Targeting Therapy in Castration-Resistant Prostate Cancer. *J Clin Oncol*.
18. Berry PA, Maitland NJ, Collins AT (2008) Androgen receptor signalling in prostate: effects of stromal factors on normal and cancer stem cells. *Mol Cell Endocrinol* 288: 30-37.
19. Zhu ML, Kyprianou N (2008) Androgen receptor and growth factor signaling cross-talk in prostate cancer cells. *Endocr Relat Cancer* 15: 841-849.
20. Lee EC, Tenniswood M (2004) Programmed cell death and survival pathways in prostate cancer cells. *Arch Androl* 50: 27-32.
21. Gurumurthy S, Vasudevan KM, Rangnekar VM (2001) Regulation of apoptosis in prostate cancer. *Cancer Metastasis Rev* 20: 225-243.

22. Baugh LR, Hill AA, Brown EL, Hunter CP (2001) Quantitative analysis of mRNA amplification by in vitro transcription. *Nucleic Acids Res* 29: E29.
23. Smyth GK (2005) *Limma: linear models for microarray data*; Gentleman R, Carey V, Dudoit S, Irizarry R, Huber W, editors. New York: Springer. 397-420 p.
24. Smyth GK, Speed T (2003) Normalization of cDNA microarray data. *Methods* 31: 265-273.
25. Veldhoven A, de Lange D, Smid M, de Jager V, Kors JA, et al. (2005) Storing, linking, and mining microarray databases using SRS. *BMC Bioinformatics* 6: 192.
26. Dennis G, Jr., Sherman BT, Hosack DA, Yang J, Gao W, et al. (2003) DAVID: Database for Annotation, Visualization, and Integrated Discovery. *Genome Biol* 4: P3.
27. Huang da W, Sherman BT, Lempicki RA (2009) Systematic and integrative analysis of large gene lists using DAVID bioinformatics resources. *Nat Protoc* 4: 44-57.
28. van der Heul-Nieuwenhuijsen L, Hendriksen PJ, van der Kwast TH, Jenster G (2006) Gene expression profiling of the human prostate zones. *BJU Int* 98: 886-897.
29. Best CJ, Gillespie JW, Yi Y, Chandramouli GV, Perlmutter MA, et al. (2005) Molecular alterations in primary prostate cancer after androgen ablation therapy. *Clin Cancer Res* 11: 6823-6834.
30. Chandran UR, Ma C, Dhir R, Bisceglia M, Lyons-Weiler M, et al. (2007) Gene expression profiles of prostate cancer reveal involvement of multiple molecular pathways in the metastatic process. *BMC Cancer* 7: 64.
31. Lapointe J, Li C, Higgins JP, van de Rijn M, Bair E, et al. (2004) Gene expression profiling identifies clinically relevant subtypes of prostate cancer. *Proc Natl Acad Sci U S A* 101: 811-816.
32. Tamura K, Furihata M, Tsunoda T, Ashida S, Takata R, et al. (2007) Molecular features of hormone-refractory prostate cancer cells by genome-wide gene expression profiles. *Cancer Res* 67: 5117-5125.
33. Varambally S, Yu J, Laxman B, Rhodes DR, Mehra R, et al. (2005) Integrative genomic and proteomic analysis of prostate cancer reveals signatures of metastatic progression. *Cancer Cell* 8: 393-406.
34. Yu YP, Landsittel D, Jing L, Nelson J, Ren B, et al. (2004) Gene expression alterations in prostate cancer predicting tumor aggression and preceding development of malignancy. *J Clin Oncol* 22: 2790-2799.
35. Marques RB, Erkens-Schulze S, de Ridder CM, Hermans KG, Waltering K, et al. (2005) Androgen receptor modifications in prostate cancer cells upon long-term androgen ablation and antiandrogen treatment. *Int J Cancer* 117: 221-229.
36. Esteller M (2008) Epigenetics in cancer. *N Engl J Med* 358: 1148-1159.
37. Dong JT (2001) Chromosomal deletions and tumor suppressor genes in prostate cancer. *Cancer Metastasis Rev* 20: 173-193.
38. Verma RS, Manikal M, Conte RA, Godoc CJ (1999) Chromosomal basis of adenocarcinoma of the prostate. *Cancer Invest* 17: 441-447.
39. Cinar B, Koeneman KS, Edlund M, Prins GS, Zhou HE, et al. (2001) Androgen receptor mediates the reduced tumor growth, enhanced androgen responsiveness, and selected target gene transactivation in a human prostate cancer cell line. *Cancer Res* 61: 7310-7317.
40. Tararova ND, Narizhneva N, Krivokrisenko V, Gudkov AV, Gurova KV (2007) Prostate cancer cells tolerate a narrow range of androgen receptor expression and activity. *Prostate* 67: 1801-1815.
41. Kas K, Finger E, Grall F, Gu X, Akbarali Y, et al. (2000) ESE-3, a novel member of an epithelium-specific ets transcription factor subfamily, demonstrates different target gene specificity from ESE-1. *J Biol Chem* 275: 2986-2998.
42. Kleinbaum LA, Duggan C, Ferreira E, Coffey GP, Buttice G, et al. (1999) Human chromosomal localization, tissue/tumor expression, and regulatory function of the ets family gene EHF. *Biochem Biophys Res Commun* 264: 119-126.
43. Cangemi R, Mensah A, Albertini V, Jain A, Mello-Grand M, et al. (2008) Reduced expression and tumor suppressor function of the ETS transcription factor ESE-3 in prostate cancer. *Oncogene* 27: 2877-2885.

44. Veldscholte J, Ris-Stalpers C, Kuiper GG, Jenster G, Berrevoets C, et al. (1990) A mutation in the ligand binding domain of the androgen receptor of human LNCaP cells affects steroid binding characteristics and response to anti-androgens. *Biochem Biophys Res Commun* 173: 534-540.
45. Veldscholte J, Berrevoets CA, Ris-Stalpers C, Kuiper GG, Jenster G, et al. (1992) The androgen receptor in LNCaP cells contains a mutation in the ligand binding domain which affects steroid binding characteristics and response to antiandrogens. *J Steroid Biochem Mol Biol* 41: 665-669.
46. Lo HW, Hsu SC, Xia W, Cao X, Shih JY, et al. (2007) Epidermal growth factor receptor cooperates with signal transducer and activator of transcription 3 to induce epithelial-mesenchymal transition in cancer cells via up-regulation of TWIST gene expression. *Cancer Res* 67: 9066-9076.
47. Dupont J, Fernandez AM, Glackin CA, Helman L, LeRoith D (2001) Insulin-like growth factor 1 (IGF-1)-induced twist expression is involved in the anti-apoptotic effects of the IGF-1 receptor. *J Biol Chem* 276: 26699-26707.
48. Zeng L, Sachdev P, Yan L, Chan JL, Trenkle T, et al. (2000) Vav3 mediates receptor protein tyrosine kinase signaling, regulates GTPase activity, modulates cell morphology, and induces cell transformation. *Mol Cell Biol* 20: 9212-9224.
49. Moores SL, Selfors LM, Fredericks J, Breit T, Fujikawa K, et al. (2000) Vav family proteins couple to diverse cell surface receptors. *Mol Cell Biol* 20: 6364-6373.
50. Puisieux A, Valsesia-Wittmann S, Ansieau S (2006) A twist for survival and cancer progression. *Br J Cancer* 94: 13-17.
51. Maestro R, Dei Tos AP, Hamamori Y, Krasnokutsky S, Sartorelli V, et al. (1999) Twist is a potential oncogene that inhibits apoptosis. *Genes Dev* 13: 2207-2217.
52. Yang J, Mani SA, Donaher JL, Ramaswamy S, Itzykson RA, et al. (2004) Twist, a master regulator of morphogenesis, plays an essential role in tumor metastasis. *Cell* 117: 927-939.
53. Yuen HF, Chua CW, Chan YP, Wong YC, Wang X, et al. (2007) Significance of TWIST and E-cadherin expression in the metastatic progression of prostatic cancer. *Histopathology* 50: 648-658.
54. Kwok WK, Ling MT, Lee TW, Lau TC, Zhou C, et al. (2005) Up-regulation of TWIST in prostate cancer and its implication as a therapeutic target. *Cancer Res* 65: 5153-5162.
55. Wallerand H, Robert G, Pasticier G, Ravaud A, Ballanger P, et al. (2009) The epithelial-mesenchymal transition-inducing factor TWIST is an attractive target in advanced and/or metastatic bladder and prostate cancers(). *Urol Oncol*.
56. Kwok WK, Ling MT, Yuen HF, Wong YC, Wang X (2007) Role of p14ARF in TWIST-mediated senescence in prostate epithelial cells. *Carcinogenesis* 28: 2467-2475.
57. Movilla N, Bustelo XR (1999) Biological and regulatory properties of Vav-3, a new member of the Vav family of oncoproteins. *Mol Cell Biol* 19: 7870-7885.
58. Dong Z, Liu Y, Lu S, Wang A, Lee K, et al. (2006) Vav3 oncogene is overexpressed and regulates cell growth and androgen receptor activity in human prostate cancer. *Mol Endocrinol* 20: 2315-2325.
59. Lyons LS, Rao S, Balkan W, Faysal J, Maiorino CA, et al. (2008) Ligand-independent activation of androgen receptors by Rho GTPase signaling in prostate cancer. *Mol Endocrinol* 22: 597-608.
60. Lyons LS, Burnstein KL (2006) Vav3, a Rho GTPase guanine nucleotide exchange factor, increases during progression to androgen independence in prostate cancer cells and potentiates androgen receptor transcriptional activity. *Mol Endocrinol* 20: 1061-1072.
61. Liu Y, Mo JQ, Hu Q, Boivin G, Levin L, et al. (2008) Targeted overexpression of vav3 oncogene in prostatic epithelium induces nonbacterial prostatitis and prostate cancer. *Cancer Res* 68: 6396-6406.
62. Trenkle T, McClelland M, Adlkofer K, Welsh J (2000) Major transcript variants of VAV3, a new member of the VAV family of guanine nucleotide exchange factors. *Gene* 245: 139-149.
63. Pan Q, Shai O, Lee LJ, Frey BJ, Blencowe BJ (2008) Deep surveying of alternative splicing complexity in the human transcriptome by high-throughput sequencing. *Nat Genet* 40: 1413-1415.

64. Castle JC, Zhang C, Shah JK, Kulkarni AV, Kalsotra A, et al. (2008) Expression of 24,426 human alternative splicing events and predicted cis regulation in 48 tissues and cell lines. *Nat Genet* 40: 1416-1425.
65. Niehrs C (2006) Function and biological roles of the Dickkopf family of Wnt modulators. *Oncogene* 25: 7469-7481.
66. Hsieh SY, Hsieh PS, Chiu CT, Chen WY (2004) Dickkopf-3/REIC functions as a suppressor gene of tumor growth. *Oncogene* 23: 9183-9189.
67. Lodygin D, Epanchintsev A, Menssen A, Diebold J, Hermeking H (2005) Functional epigenomics identifies genes frequently silenced in prostate cancer. *Cancer Res* 65: 4218-4227.
68. Kawano Y, Kitaoka M, Hamada Y, Walker MM, Waxman J, et al. (2006) Regulation of prostate cell growth and morphogenesis by Dickkopf-3. *Oncogene* 25: 6528-6537.
69. Abarzua F, Sakaguchi M, Takaishi M, Nasu Y, Kurose K, et al. (2005) Adenovirus-mediated overexpression of REIC/Dkk-3 selectively induces apoptosis in human prostate cancer cells through activation of c-Jun-NH2-kinase. *Cancer Res* 65: 9617-9622.
70. Zenzmaier C, Untergasser G, Hermann M, Dirnhofer S, Sampson N, et al. (2008) Dysregulation of Dkk-3 expression in benign and malignant prostatic tissue. *Prostate* 68: 540-547.
71. Edamura K, Nasu Y, Takaishi M, Kobayashi T, Abarzua F, et al. (2007) Adenovirus-mediated REIC/Dkk-3 gene transfer inhibits tumor growth and metastasis in an orthotopic prostate cancer model. *Cancer Gene Ther* 14: 765-772.

SUPPLEMENTARY DATA

Table S1 - Genes differentially expressed in PC346DCC vs PC346C expression ratios and SAM q-values

| GenBank ID | Cytoband | Symbol | HUGO Gene Name | PC346DCC 2log ratio | PC346DCC qvalue | PC346Flu1 2log ratio | PC346Flu1 qvalue | PC346Flu2 2log ratio | PC346Flu2 qvalue |
|------------|-------------|-----------|--|---------------------------|--------------------|----------------------------|---------------------|----------------------------|---------------------|
| NM_017935 | 4q24 | BANK1 | B-cell scaffold protein with ankyrin repeats 1 | -2.9 | 0.000 | -1.8 | 0.000 | -0.8 | 0.053 |
| AB042410 | 1p21.3 | GPR88 | G protein-coupled receptor 88 | -2.4 | 0.000 | -0.3 | 0.394 | 0.8 | 0.194 |
| S75755 | 19q13.41 | KLK3 | kallikrein-related peptidase 3 | -2.3 | 0.000 | -0.3 | 0.160 | -0.4 | 0.531 |
| AF188747 | 19q13.41 | KLK2 | kallikrein-related peptidase 2 | -2.3 | 0.000 | -0.7 | 0.063 | -0.8 | 0.053 |
| NM_012449 | 7q21 | STEAP1 | six transmembrane epithelial antigen of the prostate 1 | -2.3 | 0.000 | -0.9 | 0.036 | -0.5 | 0.236 |
| AK026813 | 7q21 | STEAP2 | six transmembrane epithelial antigen of the prostate 2 | -2.3 | 0.000 | -0.8 | 0.135 | -0.8 | 0.176 |
| NM_003307 | 21q22.3 | TRPM2 | transient receptor potential cation channel, subfamily M, member 2 | -2.1 | 0.000 | 0.0 | 0.536 | -0.1 | 0.725 |
| AF216077 | 9q32 | COL27A1 | collagen type XXVII alpha 1 | -2.1 | 0.000 | -2.8 | 0.000 | -1.7 | 0.053 |
| NM_004117 | 6p21.3-21.2 | FKBP5 | FK506 binding protein 5 | -2.0 | 0.000 | 0.1 | 0.459 | 0.4 | 0.218 |
| NM_001359 | 8q21.3 | DECR1 | 2 4-dienoyl CoA reductase 1 mitochondrial | -1.9 | 0.000 | -1.1 | 0.000 | -1.6 | 0.053 |
| M26663 | 19q13.41 | KLK3 | kallikrein-related peptidase 3 | -1.8 | 0.018 | 0.2 | 0.253 | -0.4 | 0.252 |
| AB020637 | 11q21 | ENDOD1 | endonuclease domain containing 1 | -1.7 | 0.000 | -0.4 | 0.160 | 0.2 | 0.678 |
| AK026331 | 2q35 | CHPF* | Chondroitin polymerizing factor* | -1.7 | 0.000 | -0.8 | 0.048 | -0.2 | 0.678 |
| AK000554 | 15q26.1 | ABHD2 | abhydrolase domain containing 2 | -1.7 | 0.000 | -1.5 | 0.000 | -0.2 | 0.657 |
| NM_012116 | 19q13.2 | CBLC | Cas-Br-M murine ecotropic retroviral transforming sequence c | -1.6 | 0.000 | -1.2 | 0.000 | -0.4 | 0.218 |
| NM_006167 | 8p21 | NKX3-1 | NK3 homeobox 1 | -1.6 | 0.003 | -0.1 | 0.459 | -0.3 | 0.413 |
| NM_006006 | 11q23.1 | ZBTB16 | zinc finger and BTB domain containing 16 | -1.6 | 0.003 | 0.1 | 0.444 | 0.3 | 0.328 |
| AB020968 | 6q22.2 | MARCKS | myristoylated alanine-rich protein kinase C substrate | -1.6 | 0.000 | -2.0 | 0.000 | -1.3 | 0.053 |
| X15667 | 14q24.1 | GPRP* | Glutathione peroxidase-related protein GPRP* | -1.6 | 0.022 | 0.2 | 0.185 | -0.8 | 0.053 |
| AL049963 | 4q22-q24 | SLC39A8 | solute carrier family 39 zinc transporter member 8 | -1.5 | 0.000 | -1.4 | 0.000 | -0.9 | 0.053 |
| AK000028 | 4q24 | LOC90024* | Hypothetical LOC90024* | -1.5 | 0.000 | -0.7 | 0.000 | -0.5 | 0.120 |
| AK000216 | 3p21.31 | FLJ20209* | Hypothetical protein FLJ20209* | -1.5 | 0.000 | -0.7 | 0.115 | -0.7 | 0.084 |
| AL109729 | 15q26.1 | ABHD2 | abhydrolase domain containing 2 | -1.5 | 0.000 | -1.0 | 0.044 | 0.2 | 0.531 |
| NM_003278 | 3p22-21.3 | CLEC3B | C-type lectin domain family 3 member B | -1.5 | 0.005 | -1.3 | 0.000 | -1.3 | 0.084 |
| AF252283 | 13q21 | KLHL1 | kelch-like 1 Drosophila | -1.5 | 0.000 | 0.5 | 0.115 | 0.1 | 0.738 |
| NM_000944 | 4q21-q24 | PPP3CA | protein phosphatase 3 formerly 2B catalytic subunit alpha isoform | -1.4 | 0.028 | -1.2 | 0.000 | -1.0 | 0.084 |
| AL122055 | 6q21 | GDC2L6 | cell division cycle 2-like 6 CDK8-like | -1.4 | 0.000 | -1.3 | 0.000 | -1.2 | 0.000 |
| NM_016598 | 3p21.31 | ZDHHC3 | zinc finger DHHC-type containing 3 | -1.4 | 0.003 | -1.1 | 0.000 | -0.9 | 0.053 |
| NM_005864 | 14q11.2-q12 | EFS | embryonal Fyn-associated substrate | -1.4 | 0.009 | 0.4 | 0.135 | -0.6 | 0.064 |
| NM_001311 | 14q32.33 | CRIP1 | cysteine-rich protein 1 intestinal | -1.4 | 0.018 | 0.4 | 0.101 | -0.9 | 0.115 |
| L29496 | Xq11.2-q12 | AR | androgen receptor dihydrotestosterone receptor | -1.3 | 0.018 | 0.9 | 0.000 | -0.3 | 0.194 |

| | | | | | | | | | |
|-----------|---------------|------------|---|------|-------|------|-------|------|-------|
| AF271070 | 12q13.11 | SLC38A1 | solute carrier family 38 member 1 | -1.3 | 0.000 | -0.7 | 0.044 | -0.2 | 0.678 |
| NM_007011 | 15q26.1 | ABHD2 | abhydrolase domain containing 2 | -1.3 | 0.000 | -0.8 | 0.051 | 0.3 | 0.531 |
| NM_007173 | 11q14.1 | PRSS23 | protease serine 23 | -1.2 | 0.018 | -0.9 | 0.021 | -0.9 | 0.101 |
| AF200348 | 2p25 | PXDN | peroxidasin homolog Drosophila | -1.2 | 0.003 | -1.3 | 0.000 | 0.9 | 0.064 |
| NM_005045 | 7q22 | RELN | reelin | -1.2 | 0.003 | -0.6 | 0.101 | -0.2 | 0.714 |
| D80010 | 2p25.1 | LPIN1 | lipin 1 | -1.2 | 0.000 | -1.1 | 0.015 | -0.9 | 0.053 |
| NM_004457 | 2q34-q35 | ACSL3 | acyl-CoA synthetase long-chain family member 3 | -1.2 | 0.009 | -0.7 | 0.025 | -0.3 | 0.101 |
| NM_005544 | 2q36 | IRS1 | insulin receptor substrate 1 | -1.2 | 0.020 | -0.1 | 0.394 | 0.0 | 0.714 |
| AK024495 | 11p15.5 | LRRCS6 | leucine rich repeat containing 56 | -1.2 | 0.000 | 0.2 | 0.321 | 0.5 | 0.218 |
| NM_002165 | 20q11 | ID1 | inhibitor of DNA binding 1 dominant negative helix-loop-helix protein | -1.2 | 0.018 | | | -0.6 | 0.500 |
| NM_001546 | 6p22-p21 | ID4 | inhibitor of DNA binding 4 dominant negative helix-loop-helix protein | -1.1 | 0.014 | | | -0.7 | 0.272 |
| NM_006829 | 10q23.2 | C10orf116 | chromosome 10 open reading frame 116 | -1.1 | 0.009 | | | -0.9 | 0.084 |
| NM_004315 | 8p22-p21.3 | ASAH1 | N-acylsphingosine amidohydrolase acid ceramidase 1 | -1.1 | 0.000 | -0.6 | 0.135 | | |
| M83822 | 4q31.23-31.3 | LRBA | LPS-responsive vesicle trafficking beach and anchor containing | -1.1 | 0.003 | -0.6 | 0.044 | -0.6 | 0.101 |
| NM_019844 | 12p12 | SLCO1B3 | solute carrier organic anion transporter family member 1B3 | -1.1 | 0.028 | -0.2 | 0.394 | 0.6 | 0.194 |
| AL137506 | 5q12.1 | ELOVL7 | ELOVL family member 7 elongation of long chain fatty acids yeast | -1.1 | 0.022 | -0.3 | 0.229 | 0.1 | 0.786 |
| NM_001153 | 2p13 | ANXA4 | annexin A4 | -1.1 | 0.003 | -0.6 | 0.160 | -0.2 | 0.556 |
| NM_003711 | 5q11 | PPAP2A | phosphatidic acid phosphatase type 2A | -1.1 | 0.018 | -0.8 | 0.015 | 0.0 | 0.789 |
| NM_000860 | 4q34-q35 | HPGD | hydroxyprostaglandin dehydrogenase 15- NAD | -1.1 | 0.022 | -0.3 | 0.253 | 0.1 | 0.785 |
| NM_002487 | 15q11.2-q12 | NDN | neclin homolog mouse | -1.1 | 0.000 | -0.8 | 0.063 | -0.5 | 0.101 |
| NM_014932 | 3q26.31 | NILGN1 | neurologin 1 | -1.0 | 0.022 | -0.7 | 0.051 | -0.6 | 0.089 |
| NM_001758 | 11q13 | CCND1 | cyclin D1 | -1.0 | 0.000 | -0.9 | 0.048 | -1.4 | 0.000 |
| NM_002151 | 19q11-q13.2 | HPN | hepsin transmembrane protease serine 1 | -1.0 | 0.000 | -0.9 | 0.000 | -1.4 | 0.053 |
| NM_005025 | 3q26.1 | SERPIN1 | serpin peptidase inhibitor clade 1 neuroserpin member 1 | -1.0 | 0.000 | -0.4 | 0.229 | -0.1 | 0.714 |
| NM_014333 | 11q23.2 | CADM1 | cell adhesion molecule 1 | -1.0 | 0.000 | -1.9 | 0.000 | -0.1 | 0.725 |
| NM_015415 | 1q24 | BRP44 | brain protein 44 | -1.0 | 0.009 | -0.5 | 0.090 | -0.7 | 0.089 |
| NM_007043 | 12q21.1 | KRR1 | KRR1 small subunit SSU processome component homolog yeast | -1.0 | 0.022 | -0.2 | 0.515 | -0.7 | 0.134 |
| AK026295 | | FLJ22642 * | CDNA FLJ22642 fis clone HSI06970* | -1.0 | 0.018 | -0.6 | 0.080 | -0.2 | 0.714 |
| NM_017720 | 19p13.3 | STAP2 | signal transducing adaptor family member 2 | -1.0 | 0.000 | -1.1 | 0.000 | -0.8 | 0.053 |
| AK024215 | 3q25.32 | MFS1 | major facilitator superfamily domain containing 1 | -1.0 | 0.009 | -0.2 | 0.287 | 0.0 | 0.725 |
| NM_004476 | 11p11.2 | FOLH1 | folate hydrolase prostate-specific membrane antigen 1 | -1.0 | 0.014 | 0.1 | 0.394 | -0.1 | 0.725 |
| NM_001634 | 6q21-q22 | AMD1 | adenosylmethionine decarboxylase 1 | -1.0 | 0.028 | -0.4 | 0.135 | -0.6 | 0.084 |
| NM_001184 | 3q22-q24 | ATR | ataxia telangiectasia and Rad3 related | -1.0 | 0.020 | -0.6 | 0.048 | -0.7 | 0.064 |
| NM_000240 | Xp11.4-11.3 | MAOA | monoamine oxidase A | -1.0 | 0.043 | 0.0 | 0.535 | 0.3 | 0.413 |
| NM_018050 | 12p13.2 | MANSC1 | MANSC domain containing 1 | -0.9 | 0.000 | -1.1 | 0.011 | | |
| X69111 | 1p36.13-36.12 | ID3 | inhibitor of DNA binding 3 dominant negative helix-loop-helix protein | -0.9 | 0.055 | -1.0 | 0.101 | -0.3 | 0.714 |
| D86976 | 19p13.3 | HIMH1 | histocompatibility minor HA-1 | -0.9 | 0.009 | -0.4 | 0.090 | 0.1 | 0.636 |
| AY007729 | 8p21.2 | C8orf58 | chromosome 8 open reading frame 58 | -0.9 | 0.022 | -0.3 | 0.229 | 0.3 | 0.309 |

| | | | | | | | | | |
|-----------|---------------|-----------|---|------|-------|------|-------|------|-------|
| AK024677 | 4q21.1 | ASAH1 | N-acylsphingosine amidohydrolase acid ceramidase -like | -0.9 | 0.009 | -0.8 | 0.044 | -0.3 | 0.531 |
| NM_005095 | 1p32-p34 | ZMYM4 | zinc finger MYM-type 4 | -0.9 | 0.000 | -0.2 | 0.459 | -0.6 | 0.115 |
| NM_019005 | 7p22-p21 | FLJ20323* | Hypothetical protein FLJ20323* | -0.9 | 0.000 | -1.3 | 0.000 | -0.6 | 0.134 |
| AF095844 | 2p24.3-q24.3 | FLIH1 | interferon induced with helicase C domain 1 | -0.9 | 0.028 | -0.5 | 0.185 | -0.5 | 0.194 |
| U52054 | 5q11.1 | EMB | embligin homolog mouse | -0.9 | 0.022 | -0.7 | 0.042 | -0.5 | 0.150 |
| AF261758 | 1p33-p31.1 | DHCR24 | 24-dehydrocholesterol reductase | -0.9 | 0.003 | 0.1 | 0.459 | 0.3 | 0.500 |
| D16875 | 2p24 | RHOB | ras homolog gene family member B | -0.9 | 0.020 | -0.2 | 0.253 | -0.7 | 0.064 |
| AL049969 | 4q22 | PDLIM5 | PDZ and LIM domain 5 | -0.8 | 0.022 | -0.5 | 0.160 | -0.3 | 0.691 |
| U89715 | 11q13.5-q14.1 | PLEKHB1 | pleckstrin homology domain containing family B evelctins member 1 | -0.8 | 0.014 | 0.5 | 0.115 | 0.4 | 0.218 |
| AL133074 | 8q22 | TP53INP1 | tumor protein p53 inducible nuclear protein 1 | -0.8 | 0.018 | 0.0 | 0.515 | -0.4 | 0.064 |
| D42039 | 15q13 | MESDC2 | mesoderm development candidate 2 | -0.8 | 0.022 | -0.5 | 0.071 | -0.2 | 0.691 |
| AB032962 | 10p12.1 | GPR158 | G protein-coupled receptor 158 | -0.8 | 0.018 | | | 0.0 | 0.789 |
| NM_002372 | 5q21-q22 | MAN2A1 | mannosidase alpha class 2A member 1 | -0.8 | 0.022 | -0.3 | 0.185 | -0.6 | 0.064 |
| NM_012081 | 5q15 | ELL2 | elongation factor RNA polymerase II 2 | -0.8 | 0.009 | -0.3 | 0.229 | 0.3 | 0.236 |
| NM_001878 | 1q21.3 | CRABP2 | cellular retinoic acid binding protein 2 | -0.8 | 0.014 | -0.4 | 0.115 | -0.4 | 0.084 |
| NM_018844 | 7q22-q31 | BCAP29 | B-cell receptor-associated protein 29 | -0.8 | 0.046 | -0.4 | 0.185 | -0.1 | 0.714 |
| AF067972 | 2p23 | DNMT3A | DNA cytosine-5- methyltransferase 3 alpha | -0.8 | 0.005 | -0.7 | 0.063 | -0.5 | 0.101 |
| NM_004086 | 14q12-q13 | COCH | coagulation factor C homolog cochlin Limulus polyphemus | -0.8 | 0.014 | -0.5 | 0.135 | -0.1 | 0.725 |
| NM_005671 | 8p12-p11.2 | UBXD6 | UBX domain containing 6 | -0.8 | 0.009 | -0.1 | 0.527 | 0.1 | 0.748 |
| U90904 | 15q11.2 | NIPA2 | non imprinted in Prader-Willi/Angelman syndrome 2 | -0.8 | 0.022 | 0.0 | 0.527 | -0.1 | 0.714 |
| AK000745 | 8q22.1 | MTDH | metadherin | -0.8 | 0.020 | -0.4 | 0.160 | -0.1 | 0.725 |
| NM_017898 | 1q41 | MOSC2 | MOCO sulphurase C-terminal domain containing 2 | -0.8 | 0.003 | -0.5 | 0.115 | -0.2 | 0.218 |
| D28450 | 4q24 | H2AFZ | H2A histone family member Z | -0.8 | 0.003 | -0.6 | 0.044 | -0.3 | 0.531 |
| NM_003100 | 5q23 | SNX2 | sorting nexin 2 | -0.8 | 0.022 | -0.3 | 0.101 | -0.4 | 0.134 |
| AL050082 | 8q21 | VWFP1 | VW domain containing E3 ubiquitin protein ligase 1 | -0.8 | 0.009 | -0.4 | 0.160 | -0.3 | 0.150 |
| NM_002103 | 19q13.3 | GYS1 | glycogen synthase 1 muscle | -0.8 | 0.003 | 0.2 | 0.287 | -0.1 | 0.714 |
| AB050049 | 5q12-q13 | MCCC2 | methylcrotonyl-Coenzyme A carboxylase 2 beta | -0.7 | 0.018 | 0.0 | 0.532 | 0.0 | 0.789 |
| NM_004540 | 21q21.1 | NCAM2 | neural cell adhesion molecule 2 | -0.7 | 0.009 | 0.0 | 0.321 | 0.0 | 0.781 |
| AB033070 | 6q23.3 | KIAA1244 | KIAA1244 | -0.7 | 0.009 | -0.4 | 0.051 | -0.1 | 0.725 |
| NM_012445 | 4p16.3 | SPON2 | spondin 2 extracellular matrix protein | -0.7 | 0.028 | 0.5 | 0.211 | 0.4 | 0.218 |
| NM_003909 | 8q21.3 | CPNE3 | copine III | -0.7 | 0.028 | -0.5 | 0.101 | 0.0 | 0.725 |
| NM_012289 | 19p13.2 | KEAP1 | keich-like ECH-associated protein 1 | -0.7 | 0.003 | -0.5 | 0.101 | -0.2 | 0.714 |
| NM_001777 | 3q13.1-q13.2 | CD47* | CD47 antigen RII-related antigen integrin-associated signal transducer* | -0.7 | 0.022 | 0.1 | 0.459 | 0.0 | 0.725 |
| NM_017423 | 4q31.1 | GALNT7 | UDP-N-acetyl-alpha-D-galactosamine: N-acetylgalactosaminyltransferase 7 | -0.7 | 0.028 | -0.5 | 0.115 | -0.1 | 0.691 |
| NM_006408 | 7p21.3 | AGR2 | anterior gradient homolog 2 Xenopus laevis | -0.7 | 0.028 | 0.0 | 0.485 | 0.2 | 0.236 |
| NM_004549 | 11q14.1 | NDUFC2 | NADH dehydrogenase ubiquinone 1 subcomplex unknown 2 14.5kDa | -0.7 | 0.022 | 0.2 | 0.287 | -0.7 | 0.000 |

| | | | | | | | | | |
|-----------|----------------|------------|--|------|-------|------|-------|------|-------|
| U84526 | 22q11.21 | CDC45L | CDC45 cell division cycle 45-like <i>S. cerevisiae</i> | -0.7 | 0.070 | -0.6 | 0.044 | -0.2 | 0.272 |
| AF147408 | 1p36.13 | PLEKHM2 | pleckstrin homology domain containing family M with RUN domain member 2 | -0.7 | 0.046 | -0.5 | 0.160 | -0.2 | 0.356 |
| AF161429 | 4q12 | FIP1L1 | FIP1 like 1 <i>S. cerevisiae</i> | -0.7 | 0.022 | -0.2 | 0.135 | 0.1 | 0.636 |
| NM_016315 | 2q32.3-q33 | GULP1 | GULP engulfment adaptor PTB domain containing 1 | -0.7 | 0.028 | -0.1 | 0.211 | -0.2 | 0.218 |
| NM_002715 | 5q23-q31 | PPP2CA | protein phosphatase 2 formerly 2A catalytic subunit alpha isoform | -0.7 | 0.037 | -0.3 | 0.160 | -0.4 | 0.089 |
| NM_015916 | 10p | FAM26B | family with sequence similarity 26 member B | -0.7 | 0.000 | -0.4 | 0.051 | -0.4 | 0.150 |
| NM_000465 | 2q34-q35 | BARD1 | BRCA1 associated RING domain 1 | -0.7 | 0.046 | -0.1 | 0.444 | 0.1 | 0.783 |
| NM_014074 | | | PRO0529 protein | -0.7 | 0.037 | -0.4 | 0.115 | -0.3 | 0.531 |
| AK025766 | 12q24.31 | BRI3BP | BRI3 binding protein | -0.7 | 0.014 | -0.6 | 0.025 | -0.1 | 0.714 |
| NM_006372 | 6q14-q15 | SYNCRIP | synaptotagmin binding cytoplasmic RNA interacting protein | -0.7 | 0.046 | 0.1 | 0.444 | -0.5 | 0.053 |
| AJ250475 | 7p14.1 | EPDR1 | ependymin related protein 1 zebrafish | -0.7 | 0.055 | 0.3 | 0.358 | -0.3 | 0.588 |
| NM_003781 | 3q25 | B3GALNT1 | beta-1 3-N-acetylgalactosaminyltransferase 1 globoside blood group | -0.7 | 0.000 | -0.6 | 0.090 | -0.5 | 0.084 |
| NM_005857 | 1p34 | ZMPSTE24 | zinc metalloproteinase STE24 homolog <i>S. cerevisiae</i> | -0.7 | 0.070 | 0.0 | 0.524 | -0.3 | 0.636 |
| AK023519 | | | cDNA FLJ13457 | -0.7 | 0.018 | -0.4 | 0.115 | -0.2 | 0.691 |
| AK023844 | 8q22.3 | GRHL2 | grainyhead-like 2 <i>Drosophila</i> | -0.6 | 0.022 | -0.3 | 0.253 | -0.3 | 0.084 |
| M73547 | 5q22-q23 | REEP5 | receptor accessory protein 5 | -0.6 | 0.037 | 0.0 | 0.515 | -0.1 | 0.714 |
| AK023339 | 8q22.1 | C8orf38 | chromosome 8 open reading frame 38 | -0.6 | 0.000 | 0.0 | 0.527 | -0.1 | 0.714 |
| NM_005971 | 19q13.11-13.12 | FXYD3 | FXYD domain containing ion transport regulator 3 | -0.6 | 0.055 | -0.1 | 0.422 | -0.5 | 0.053 |
| NM_015584 | 17q11.2 | POLDIP2 | polymerase DNA-directed delta interacting protein 2 | -0.6 | 0.037 | 0.2 | 0.253 | -0.1 | 0.725 |
| NM_002620 | 4q12-q21 | PF4V1 | platelet factor 4 variant 1 | -0.6 | 0.340 | 0.4 | 0.287 | -0.3 | 0.714 |
| NM_018279 | 12q21.1 | TMEM19 | transmembrane protein 19 | -0.6 | 0.055 | -0.2 | 0.321 | 0.4 | 0.471 |
| AK023269 | 2p23.1 | LCLAT1 | lysocardiolipin acyltransferase 1 | -0.6 | 0.043 | -0.5 | 0.135 | -0.3 | 0.714 |
| AF070569 | 17p13.3 | C17orf91 | chromosome 17 open reading frame 91 | -0.6 | 0.037 | 0.0 | 0.527 | -0.2 | 0.252 |
| NM_001505 | 7p22 | GPBR | G protein-coupled estrogen receptor 1 | -0.6 | 0.070 | 0.2 | 0.358 | -0.1 | 0.714 |
| AK024648 | 10p13 | FAM107B | family with sequence similarity 107 member B | -0.6 | 0.070 | -0.5 | 0.185 | 0.0 | 0.725 |
| AK026278 | 5q31.1 | TXNDC15 | thioredoxin domain containing 15 | -0.6 | 0.022 | -0.3 | 0.135 | 0.0 | 0.731 |
| AK025245 | 12q22 | KITLG | KIT ligand | -0.6 | 0.037 | -0.6 | 0.135 | -0.3 | 0.309 |
| AL133063 | 20q13.33 | C20orf158* | Chromosome 20 open reading frame 158* | -0.6 | 0.003 | -0.1 | 0.485 | -0.3 | 0.101 |
| AK000445 | 12q13.3 | HOXC9 | homeobox C9 | -0.6 | 0.020 | -0.2 | 0.394 | -0.4 | 0.252 |
| NM_018171 | 12q24.1 | APPL2 | adaptor protein phosphotyrosine interaction PH domain and leucine zipper 2 | -0.6 | 0.022 | -0.5 | 0.101 | -0.2 | 0.714 |
| AL365369 | 19p13.3 | NCLN | nicalin homolog zebrafish | -0.6 | 0.000 | 0.0 | 0.532 | 0.1 | 0.774 |
| NM_014781 | 8p22-q21.13 | RB1CC1 | RB1-inducible coiled-coil 1 | -0.6 | 0.037 | -0.6 | 0.115 | -0.6 | 0.328 |
| AL049964 | 2 | PS1TP4* | HBV preS1-transactivated protein 4* | -0.6 | 0.020 | -0.8 | 0.044 | -0.4 | 0.356 |
| NM_013253 | 11p15.2 | DKK3 | Dickkopf homolog 3 <i>Xenopus laevis</i> | -0.6 | 0.005 | 1.4 | 0.000 | 0.7 | 0.218 |
| D63477 | 8q24.22 | EFR3A | EFR3 homolog A <i>S. cerevisiae</i> | -0.6 | 0.037 | -0.2 | 0.321 | -0.1 | 0.725 |
| AF216292 | 9q33-q34.1 | HSPA5 | heat shock 70kDa protein 5 glucose-regulated protein 78kDa | -0.6 | 0.009 | 0.0 | 0.515 | -0.1 | 0.714 |

| | | | | | | | | | |
|-----------|---------------|---------------|---|------|-------|------|-------|------|-------|
| NM_004917 | 19q13.41 | KLK4 | kalikrein-related peptidase 4 | -0.6 | 0.000 | 0.2 | 0.160 | 0.3 | 0.309 |
| NM_016230 | 6p | CYB5R4 | cytochrome b5 reductase 4 | -0.6 | 0.020 | -0.3 | 0.253 | 0.0 | 0.725 |
| NM_016308 | 1p32 | CMPK1 | cytidine monophosphate (UMP-CMP) kinase 1, cytosolic | -0.6 | 0.046 | -0.4 | 0.115 | -0.2 | 0.531 |
| NM_016286 | 17q25.3 | DCXR | dicarboxyl-L-xylulose reductase | -0.6 | 0.009 | 0.1 | 0.358 | 0.0 | 0.789 |
| NM_002600 | 1p31 | PDE4B | phosphodiesterase 4B cAMP-specific phosphodiesterase E4 duncce homolog | -0.6 | 0.009 | -0.6 | 0.090 | -0.2 | 0.617 |
| AK025205 | 4q13.3-q21.3 | DKFZP564O0823 | DKFZP564O0823 protein* | -0.5 | 0.037 | -0.3 | 0.101 | -0.3 | 0.272 |
| AF250226 | 12q12-q13 | ADCY6 | adenylate cyclase 6 | -0.5 | 0.005 | -0.2 | 0.321 | -0.1 | 0.691 |
| NM_017947 | 18q12 | MOCOS | molybdenum cofactor sulfurase | -0.5 | 0.055 | -0.6 | 0.071 | 0.7 | 0.194 |
| NM_020390 | 3q26.2 | EIF5A2 | eukaryotic translation initiation factor 5A2 | -0.5 | 0.136 | 0.0 | 0.287 | 0.0 | 0.714 |
| NM_006283 | 8p11 | TACC1 | transforming acidic coiled-coil containing protein 1 | -0.5 | 0.022 | -0.2 | 0.422 | 0.4 | 0.218 |
| NM_005662 | 8p11.2 | VDAC3 | voltage-dependent anion channel 3 | -0.5 | 0.028 | 0.1 | 0.444 | -0.1 | 0.714 |
| NM_001431 | 6q23 | EPB41L2 | erythrocyte membrane protein band 4.1-like 2 | -0.5 | 0.018 | 0.1 | 0.253 | 0.1 | 0.738 |
| NM_014158 | Xq24 | C1GALT1C1 | C1GALT1-specific chaperone 1 | -0.5 | 0.046 | 0.0 | 0.530 | -0.1 | 0.657 |
| NM_007114 | 3p21-p12 | TMF1 | TATA element modulatory factor 1 | -0.5 | 0.157 | -0.1 | 0.422 | -0.3 | 0.500 |
| NM_006330 | 8q11.23 | LYPLA1 | lysophospholipase 1 | -0.5 | 0.028 | 0.4 | 0.135 | 0.4 | 0.218 |
| J04621 | 8q22-q23 | SDC2 | syndecan 2 | -0.5 | 0.028 | -0.2 | 0.160 | -0.1 | 0.714 |
| NM_020239 | 1q21.2 | CDC42SE1 | CDC42 small effector 1 | -0.5 | 0.022 | -0.2 | 0.253 | -0.2 | 0.272 |
| AK027200 | 15q25.2 | WDR73 | WD repeat domain 73 | -0.5 | 0.211 | -0.2 | 0.160 | -0.2 | 0.531 |
| AL079292 | 5q11.2 | DHX29 | DEAH Asp-Glu-Ala-His box polypeptide 29 | -0.5 | 0.211 | -0.1 | 0.444 | 0.3 | 0.218 |
| AK024732 | 6q13 | OGFRL1 | opioid growth factor receptor-like 1 | 0.5 | 0.211 | -0.1 | 0.444 | 0.3 | 0.218 |
| AK022971 | FLJ12909* | FLJ12909* | CDNA FLJ12909 fis clone NT2RP2004400* | 0.5 | 0.113 | -0.6 | 0.051 | -0.1 | 0.725 |
| NM_002795 | 17q12 | PSMB3 | proteasome proteasome macropain subunit beta type 3 | 0.5 | 0.086 | 0.1 | 0.394 | 0.2 | 0.500 |
| NM_001446 | 6q22-q23 | FABP7 | fatty acid binding protein 7 brain | 0.5 | 0.086 | 0.1 | 0.394 | 0.2 | 0.500 |
| NM_013240 | 21q21.3 | N6AMT1 | N-6 adenine-specific DNA methyltransferase 1 putative | 0.5 | 0.018 | 0.3 | 0.101 | | |
| NM_004083 | 12q13.1-q13.2 | DDIT3 | DNA-damage-inducible transcript 3 | 0.5 | 0.055 | -0.1 | 0.287 | -0.6 | 0.150 |
| X07695 | 12q12-q13 | KRT4 | keratin 4 | 0.6 | 0.157 | 0.1 | 0.358 | 0.2 | 0.471 |
| NM_017446 | 21q21.3 | MRPL39 | mitochondrial ribosomal protein L39 | 0.6 | 0.113 | 0.2 | 0.358 | -0.5 | 0.588 |
| NM_014505 | 12q | KCNMB4 | potassium large conductance calcium-activated channel subfamily M beta member 4 | 0.6 | 0.007 | 0.1 | 0.422 | | |
| NM_001605 | 16q22 | AARS | alanyl-tRNA synthetase | 0.6 | 0.100 | 0.4 | 0.185 | 0.3 | 0.356 |
| NM_017707 | 1p36.12 | DDEF1L | development and differentiation enhancing factor-like 1 | 0.6 | 0.007 | 0.2 | 0.358 | 0.0 | 0.731 |
| NM_000187 | 3q21-q23 | HGD | homogentisate 1,2-dioxygenase homogentisate oxidase | 0.6 | 0.037 | 0.1 | 0.321 | 0.0 | 0.731 |
| AL157459 | 17q25.3 | CBX2 | chromobox homolog 2 Pc class homolog Drosophila | 0.6 | 0.028 | 0.2 | 0.253 | -0.2 | 0.714 |
| NM_005737 | 2q37.1 | ARL4C | ADP-ribosylation factor-like 4C | 0.6 | 0.020 | 0.1 | 0.473 | 0.4 | 0.287 |
| NM_016183 | 1p36.13 | MRTO4 | mRNA turnover 4 homolog S. cerevisiae | 0.6 | 0.113 | 0.1 | 0.253 | -0.3 | 0.134 |
| NM_006620 | 6q23-q24 | HBS1L | HBS1-like S. cerevisiae | 0.6 | 0.293 | 0.0 | 0.485 | 0.1 | 0.789 |
| AK026290 | 15q15.3 | ELL3 | elongation factor RNA polymerase II-like 3 | 0.6 | 0.000 | 0.6 | 0.011 | 0.4 | 0.218 |
| NM_004952 | 1q21-q22 | EFNA3 | ephrin-A3 | 0.6 | 0.055 | 0.3 | 0.321 | 0.2 | 0.236 |

| | | | | | | | | | |
|-----------|--------------|-----------|--|-----|-------|------|-------|------|-------|
| M61872 | 7q11.21 | ZNF92 | zinc finger protein 92 | 0.6 | 0.007 | -0.1 | 0.422 | 0.2 | 0.218 |
| NM_016594 | 12q13.12 | FKBP11 | FK506 binding protein 11 19 kDa | 0.6 | 0.070 | -0.1 | 0.394 | 0.2 | 0.218 |
| NM_000903 | 16q22.1 | NQO1 | NAD P H dehydrogenase quinone 1 | 0.6 | 0.242 | 0.5 | 0.185 | 0.2 | 0.236 |
| AF181999 | 10p12.2 | PTF1A | pancreas specific transcription factor, 1a | 0.6 | 0.293 | -1.4 | 0.000 | 0.0 | 0.748 |
| AF263547 | 1p32-p31 | DAB1 | disabled homolog 1 (Drosophila) | 0.6 | 0.046 | 0.5 | 0.090 | 0.4 | 0.218 |
| NM_004577 | 7p15.2-p15.1 | PSPH | phosphoserine phosphatase | 0.6 | 0.014 | 0.4 | 0.038 | 0.2 | 0.617 |
| NM_013370 | 16q23.3 | OSGIN1 | oxidative stress induced growth inhibitor 1 | 0.6 | 0.000 | 0.5 | 0.101 | -0.1 | 0.725 |
| AF045229 | 10q25 | RGS10 | regulator of G-protein signaling 10 | 0.6 | 0.003 | -0.2 | 0.185 | 0.2 | 0.617 |
| NM_017966 | 11q12.2 | VPS37C | vacuolar protein sorting 37 homolog C (S. cerevisiae) | 0.6 | 0.007 | -0.1 | 0.473 | 0.0 | 0.783 |
| NM_018410 | 2q37.1 | HJURP | Holliday junction recognition protein | 0.6 | 0.037 | 0.1 | 0.444 | 0.0 | 0.789 |
| NM_014811 | 9q34.3 | KIAA0649 | KIAA0649 | 0.6 | 0.000 | 0.1 | 0.394 | 0.1 | 0.771 |
| AK021892 | Xq13.1 | PJA1 | praja 1 | 0.6 | 0.028 | 0.4 | 0.160 | 0.3 | 0.384 |
| NM_017661 | 15q21.3 | ZNF280D | zinc finger protein 280D | 0.6 | 0.014 | 0.1 | 0.444 | 0.7 | 0.218 |
| AK022847 | 20q11.23 | ACTR5 | ARP5 actin-related protein 5 homolog yeast | 0.6 | 0.043 | 0.3 | 0.229 | 0.1 | 0.500 |
| NM_016835 | 17q21.1 | MAPT | microtubule-associated protein tau | 0.6 | 0.293 | -0.2 | 0.358 | -0.5 | 0.194 |
| AK023807 | 2q12.1 | ANAPC1 | anaphase promoting complex subunit 1 | 0.7 | 0.136 | 0.2 | 0.253 | 0.1 | 0.725 |
| Y11177 | 7p21.2 | TWIST1 | twist homolog 1 acrocephalosyndactyl 3 Saethre-Chotzen syndrome Drosophila | 0.7 | 0.043 | 0.1 | 0.185 | 0.5 | 0.194 |
| NM_001468 | Xp11.23 | GAGE1 | G antigen 1 | 0.7 | 0.003 | 0.4 | 0.211 | 0.6 | 0.000 |
| NM_017705 | 15q23 | PAQR5 | progesterin and adipoQ receptor family member V | 0.7 | 0.000 | 0.4 | 0.025 | 0.4 | 0.176 |
| Y09836 | 5q13 | MAP1B | microtubule-associated protein 1B | 0.7 | 0.046 | 1.0 | 0.011 | 1.2 | 0.101 |
| AB028949 | 1p36.21 | KIAA1026* | KIAA1026 protein* | 0.7 | 0.020 | -0.2 | 0.090 | 0.3 | 0.556 |
| NM_016115 | 2p16-p14 | ASB3 | ankyrin repeat and SOCS box-containing 3 | 0.7 | 0.018 | 0.1 | 0.473 | 0.2 | 0.678 |
| NM_013275 | 16q24.3 | ANKRD11 | ankyrin repeat domain 11 | 0.7 | 0.179 | 0.3 | 0.115 | 0.2 | 0.413 |
| D17222 | 3p14.3 | TKT | transketolase Wernicke-Korsakoff syndrome | 0.7 | 0.007 | 0.3 | 0.135 | 0.2 | 0.556 |
| AK025974 | 11q12.2 | CCDC86 | coiled-coil domain containing 86 | 0.7 | 0.014 | 0.2 | 0.229 | 0.1 | 0.774 |
| NM_015369 | 16p13 | TP53TG3* | TP53TG3 protein* | 0.7 | 0.007 | | | | |
| AF034102 | 11q13 | SLC29A2 | solute carrier family 29 nucleoside transporters member 2 | 0.7 | 0.007 | 0.7 | 0.038 | 0.7 | 0.089 |
| NM_007158 | 1p22 | CSDE1 | cold shock domain containing E1 RNA-binding | 0.7 | 0.157 | 0.7 | 0.031 | 0.9 | 0.194 |
| AB040967 | 11p15.4 | OSBPL5 | oxysterol binding protein-like 5 | 0.7 | 0.086 | | | | 0.1 |
| NM_000476 | 9q34.1 | AK1 | adenylate kinase 1 | 0.7 | 0.022 | 0.4 | 0.115 | 0.2 | 0.272 |
| Z69892 | | | MRNA clone ICRFp50711077* | 0.7 | 0.005 | 0.3 | 0.185 | 0.0 | 0.789 |
| NM_003213 | 12p13.2-13.3 | TEAD4 | TEA domain family member 4 | 0.7 | 0.014 | 0.2 | 0.287 | 0.2 | 0.218 |
| NM_004763 | 2p25.2 | ITGB1BP1 | integrin beta 1 binding protein 1 | 0.7 | 0.022 | 0.5 | 0.160 | 0.2 | 0.356 |
| D16935 | 9q21.2 | PSAT1 | phosphoserine aminotransferase 1 | 0.7 | 0.007 | 0.5 | 0.031 | 0.5 | 0.218 |
| NM_018842 | 7q21.3-22.1 | BAIAP2L1 | BAI1-associated protein 2-like 1 | 0.7 | 0.113 | 0.3 | 0.229 | 0.4 | 0.218 |
| NM_001145 | 14q11.1 | ANG | angiogenin ribonuclease RNase A family 5 | 0.8 | 0.000 | 0.1 | 0.358 | 0.4 | 0.218 |
| NM_005631 | 7q32.3 | SMO | smoothened homolog Drosophila | 0.8 | 0.018 | 0.3 | 0.160 | 0.7 | 0.089 |
| NM_001928 | 19p13.3 | CFD | complement factor D adipsin | 0.8 | 0.157 | 0.3 | 0.321 | 0.4 | 0.272 |

| | | | | | | | | | |
|-----------|---------------|-----------|--|-----|-------|------|-------|------|-------|
| NM_012463 | 12q24.31 | ATP6V0A2 | ATPase H transporting lysosomal V0 subunit a2 | 0.8 | 0.028 | 1.2 | 0.051 | 1.7 | 0.000 |
| NM_018950 | 6p21.3 | HLA-F | major histocompatibility complex class I F | 0.8 | 0.014 | | | | |
| U35875 | 14q32.1-32.2 | BDKRB2 | bradykinin receptor B2 | 0.8 | 0.007 | 0.2 | 0.321 | 0.3 | 0.218 |
| AK023343 | 14q11.2 | RNASE7 | ribonuclease RNase A family 7 | 0.8 | 0.037 | 0.4 | 0.160 | 0.4 | 0.218 |
| NM_012168 | 1p36.22 | FBXO2 | F-box protein 2 | 0.8 | 0.000 | 0.0 | 0.459 | 0.1 | 0.731 |
| NM_006044 | Xp11.23 | HDAC6 | histone deacetylase 6 | 0.8 | 0.020 | 0.1 | 0.444 | 0.3 | 0.328 |
| NM_003662 | Xp22.2 | PIR | pirin iron-binding nuclear protein | 0.8 | 0.007 | 0.5 | 0.021 | 0.5 | 0.194 |
| NM_004490 | 2q22-q24 | GRB14 | growth factor receptor-bound protein 14 | 0.8 | 0.100 | 0.3 | 0.253 | 0.5 | 0.218 |
| AK022845 | 9q34.13-34.3 | C9orf58 | chromosome 9 open reading frame 58 | 0.8 | 0.014 | 0.2 | 0.287 | 0.2 | 0.657 |
| AL137663 | 3q13.2 | PHLDB2 | pleckstrin homology-like domain family B member 2 | 0.8 | 0.043 | -0.2 | 0.135 | 0.3 | 0.176 |
| AF086471 | 11p15.1 | SPTY2D1 | SPT2 Suppressor of Ty domain containing 1 <i>S. cerevisiae</i> | 0.8 | 0.100 | -0.1 | 0.515 | 0.0 | 0.731 |
| AK026812 | 1q32.3 | LOC91548* | Hypothetical protein LOC91548* | 0.8 | 0.020 | -0.1 | 0.473 | 0.1 | 0.748 |
| NM_003680 | 1p35.1 | YARS | tyrosyl-tRNA synthetase | 0.8 | 0.014 | 0.1 | 0.358 | 0.4 | 0.236 |
| NM_001321 | 12q21.1 | CSRP2 | cysteine and glycine-rich protein 2 | 0.8 | 0.014 | -0.3 | 0.135 | 0.3 | 0.328 |
| D17169 | | | | 0.8 | 0.070 | -0.1 | 0.506 | 0.2 | 0.755 |
| NM_000309 | 1q22 | PPOX | protoporphyrinogen oxidase | 0.8 | 0.020 | 0.2 | 0.321 | 0.0 | 0.725 |
| NM_014683 | 17p11.2 | ULK2 | unc-51-like kinase 2 <i>C. elegans</i> | 0.8 | 0.000 | 0.3 | 0.090 | -0.7 | 0.053 |
| NM_000376 | 12q12-14 | VDR | vitamin D 1,25-dihydroxyvitamin D3 receptor | 0.9 | 0.037 | 0.2 | 0.321 | 0.0 | 0.781 |
| NM_013401 | 11q12-q13.1 | RAB3L1 | RAB3A interacting protein rabin3-like 1 | 0.9 | 0.000 | -0.2 | 0.253 | -0.1 | 0.714 |
| AL157449 | 17q21.33 | PPP1R9B | protein phosphatase 1 regulatory inhibitor subunit 9B | 0.9 | 0.007 | 0.9 | 0.000 | 0.6 | 0.218 |
| AF086393 | 10q26.11 | NANOS1 | nanos homolog 1 <i>Drosophila</i> | 0.9 | 0.037 | 0.2 | 0.321 | 0.0 | 0.471 |
| AK025627 | 18q11.2 | CABLES1 | Cdk5 and Abl enzyme substrate 1 | 0.9 | 0.018 | 0.2 | 0.229 | 0.5 | 0.218 |
| AF088076 | | cDNA * | Full length insert cDNA clone ZE01A04* | 0.9 | 0.003 | -0.2 | 0.253 | 0.0 | 0.789 |
| NM_003648 | 2q37.1 | DGKD | diacylglycerol kinase delta 130kDa | 0.9 | 0.000 | 0.3 | 0.185 | 0.3 | 0.617 |
| AK023159 | 5q33.3 | LSM11 | LSM11 U7 small nuclear RNA associated | 0.9 | 0.003 | 0.1 | 0.422 | 0.5 | 0.218 |
| AF086924 | 4p16.1 | PPP2R2C | protein phosphatase 2 formerly 2A regulatory subunit B gamma isoform | 0.9 | 0.000 | | | 0.0 | 0.725 |
| AK023178 | 5p15.33 | EXOC3 | exocyst complex component 3 | 0.9 | 0.003 | 0.2 | 0.185 | 0.2 | 0.617 |
| NM_014883 | 4q22.1 | FAM13A1 | family with sequence similarity 13 member A1 | 0.9 | 0.003 | 0.1 | 0.287 | 0.0 | 0.678 |
| AB037810 | 1q42.2 | SIPA1L2 | signal-induced proliferation-associated 1 like 2 | 0.9 | 0.046 | 1.5 | 0.000 | 1.7 | 0.049 |
| NM_018303 | 6p25.3 | EXOC2 | exocyst complex component 2 | 0.9 | 0.000 | 0.2 | 0.253 | 0.2 | 0.636 |
| NM_004282 | 6p12.3-p11.2 | BAG2 | BCL2-associated athanogene 2 | 0.9 | 0.020 | 0.4 | 0.044 | 0.7 | 0.194 |
| Y11161 | 17p13.1 | EIF4A1 | eukaryotic translation initiation factor 4A, isoform 1 | 0.9 | 0.003 | 0.9 | 0.038 | 0.4 | 0.218 |
| AK021498 | 7q22.3 | FLJ36031* | Hypothetical protein FLJ36031* | 0.9 | 0.028 | -0.1 | 0.321 | 0.1 | 0.755 |
| U17632 | | | | 1.0 | 0.003 | 1.4 | 0.008 | 1.1 | 0.194 |
| NM_001814 | 11q14.1-q14.3 | CTSC | cathepsin C | 1.0 | 0.000 | | | | |
| NM_014061 | Xp11.22 | MAGEH1 | melanoma antigen family H 1 | 1.0 | 0.020 | -0.5 | 0.090 | 0.0 | 0.725 |
| NM_003243 | 1p33-p32 | TGFBR3 | transforming growth factor beta receptor III | 1.0 | 0.000 | 0.1 | 0.287 | 0.5 | 0.236 |
| U90878 | 10q22-q26.3 | PDLIM1 | PDZ and LIM domain 1 ellfin | 1.0 | 0.000 | 0.4 | 0.135 | 0.4 | 0.287 |

| | | | | | | | | | |
|-----------|------------|----------|--|-----|-------|------|-------|------|-------|
| U58096 | Yp11.2 | TSPY1 | testis specific protein Y-linked 1 | 1.0 | 0.037 | 1.4 | 0.000 | | |
| NM_003234 | 3q29 | TFRC | transferrin receptor p90 CD71 | 1.1 | 0.000 | 0.8 | 0.025 | 0.4 | 0.218 |
| AB049629 | | | | 1.1 | 0.000 | 0.0 | 0.515 | 0.3 | 0.588 |
| NM_005311 | 7p12-p11.2 | GRB10 | growth factor receptor-bound protein 10 | 1.1 | 0.028 | 0.7 | 0.008 | 0.5 | 0.218 |
| NM_003712 | 19p13 | PPAP2C | phosphatidic acid phosphatase type 2C | 1.2 | 0.000 | 0.9 | 0.044 | 1.2 | 0.000 |
| L36587 | | | | 1.3 | 0.000 | 0.2 | 0.358 | -0.2 | 0.714 |
| NM_001902 | 1p31.1 | CTH | cystathionase cystathionine gamma-lyase | 1.3 | 0.020 | 0.5 | 0.044 | 0.7 | 0.194 |
| AL049949 | 10q22.3 | C10orf56 | chromosome 10 open reading frame 56 | 1.3 | 0.000 | 0.5 | 0.048 | 0.4 | 0.218 |
| AK026892 | 22q13.31 | CERK | ceramide kinase | 1.4 | 0.000 | 0.0 | 0.321 | 0.5 | 0.218 |
| NM_006721 | 10q22 | ADK | adenosine kinase | 1.4 | 0.000 | 0.1 | 0.422 | 0.7 | 0.194 |
| NM_005804 | 19p13.12 | DDX39 | DEAD Asp-Glu-Ala-Asp box polypeptide 39 | 1.4 | 0.000 | 0.3 | 0.253 | 0.8 | 0.194 |
| NM_005794 | 14q11.2 | DHRS2 | dehydrogenase/reductase SDR family member 2 | 1.4 | 0.003 | 1.5 | 0.071 | 1.2 | 0.051 |
| NM_014269 | 4q34 | ADAM29 | ADAM metalloproteinase domain 29 | 1.5 | 0.000 | 1.4 | 0.011 | 2.2 | 0.000 |
| NM_016084 | 17p11.2 | RASD1 | RAS dexamethasone-induced 1 | 1.6 | 0.000 | 1.2 | 0.000 | 0.5 | 0.218 |
| NM_006332 | 19p13.1 | IFI30 | interferon gamma-inducible protein 30 | 1.7 | 0.000 | 1.1 | 0.025 | 0.7 | 0.218 |
| NM_001823 | 14q32 | CKB | creatine kinase brain | 1.7 | 0.000 | 1.5 | 0.015 | 1.6 | 0.000 |
| NM_000790 | 7p11 | DDC | dopa decarboxylase aromatic L-amino acid decarboxylase | 1.9 | 0.005 | 0.1 | 0.253 | 2.4 | 0.218 |
| NM_003226 | 21q22.3 | TFF3 | trefoil factor 3 intestinal | 1.9 | 0.000 | -0.5 | 0.211 | 1.5 | 0.049 |
| NM_006113 | 1p13.3 | VAV3 | vav 3 guanine nucleotide exchange factor | 2.0 | 0.000 | 0.2 | 0.031 | 0.4 | 0.218 |
| NM_004750 | 19p12 | CRLF1 | cytokine receptor-like factor 1 | 2.1 | 0.000 | | | | |
| NM_013452 | Xp22 | VCX | variable charge X-linked | 2.3 | 0.000 | | | | |
| NM_004982 | 12p11.23 | KCNJ8 | potassium inwardly-rectifying channel subfamily J member 8 | 2.7 | 0.000 | 1.2 | 0.000 | 1.9 | 0.000 |

* no approved HUGO symbol / name exist for this entry. If present, gene symbol / name from the UNIGENE database are given in alternative. 2log_ratio>0 indicates over-expression in the androgen-independent subline, compared to parental PC346C. 2log_ratio<0 indicates down-regulation in the androgen-independent subline.

Table S2 - Genes differentially expressed in PC346Flu1 vs PC346C expression ratios and SAM q-values

| GenBank ID | Cytoband | Symbol | HUGO Gene Name | PC346DCC 2log ratio | qvalue | PC346Flu1 2log ratio | qvalue | PC346Flu2 2log ratio | qvalue |
|------------|----------|---------|--|---------------------------|--------|----------------------------|--------|----------------------------|--------|
| AF216077 | 9q32 | COL27A1 | collagen type XXVII alpha 1 | -2.1 | 0.000 | -2.8 | 0.000 | -1.7 | 0.053 |
| NM_014380 | Xq22.2 | NGFRAP1 | nerve growth factor receptor TNFRSF16 associated protein 1 | -0.2 | 0.513 | -2.5 | 0.000 | -2.7 | 0.000 |
| AB020968 | 6q22.2 | MARCKS | myristoylated alanine-rich protein kinase C substrate | -1.6 | 0.000 | -2.0 | 0.000 | -1.3 | 0.053 |
| NM_014333 | 11q23.2 | CADM1 | cell adhesion molecule 1 | -1.0 | 0.000 | -1.9 | 0.000 | -0.1 | 0.725 |
| NM_017935 | 4q24 | BANK1 | B-cell scaffold protein with ankyrin repeats 1 | -2.9 | 0.000 | -1.8 | 0.000 | -0.8 | 0.053 |

| | | | | | | | | | |
|-----------|----------------|-----------|---|------|-------|------|-------|------|-------|
| X75684 | 3q21-q25 | TM4SF1 | transmembrane 4 L six family member 1 | 0.6 | 0.211 | -1.5 | 0.000 | 0.5 | 0.194 |
| AK024917 | 1p22 | DDAH1 | dimethylarginine dimethylaminohydrolase 1 | -0.3 | 0.380 | -1.5 | 0.000 | 0.1 | 0.760 |
| AK000554 | 15q26.1 | ABHD2 | abhydrolase domain containing 2 | -1.7 | 0.000 | -1.5 | 0.000 | -0.2 | 0.657 |
| AL050367 | 10p13 | C10orf38 | chromosome 10 open reading frame 38 | 0.1 | 0.380 | -1.4 | 0.000 | -0.6 | 0.084 |
| AL049963 | 4q22-q24 | SLC39A8 | solute carrier family 39 zinc transporter member 8 | -1.5 | 0.000 | -1.4 | 0.000 | -0.9 | 0.053 |
| AF181999 | 10p12.2 | PTF1A | pancreas specific transcription factor, 1a | 0.6 | 0.293 | -1.4 | 0.000 | 0.0 | 0.748 |
| NM_000213 | 17q25 | ITGB4 | integrin beta 4 | 0.9 | 0.086 | -1.3 | 0.000 | 0.1 | 0.777 |
| AK026517 | 11p12 | EHF | ets homologous factor | -0.7 | 0.028 | -1.3 | 0.000 | -0.6 | 0.309 |
| NM_019005 | 7p22-p21 | FLJ20323* | Hypothetical protein FLJ20323* | -0.9 | 0.000 | -1.3 | 0.000 | -0.6 | 0.134 |
| NM_003278 | 3p22-p21.3 | CLEC3B | C-type lectin domain family 3 member B | -1.5 | 0.005 | -1.3 | 0.000 | -1.3 | 0.084 |
| AF200348 | 2p25 | PXDN | peroxidasin homolog Drosophila | -1.2 | 0.003 | -1.3 | 0.000 | 0.9 | 0.064 |
| AL122055 | 6q21 | CDC2L6 | cell division cycle 2-like 6 CDK8-like | -1.4 | 0.000 | -1.3 | 0.000 | -1.2 | 0.000 |
| NM_003255 | 17q25 | TIMP2 | TIMP metalloproteinase inhibitor 2 | 0.6 | 0.028 | -1.3 | 0.031 | -0.2 | 0.678 |
| NM_012116 | 19q13.2 | CBLC | Cas-Br-M murine ecotropic retroviral transforming sequence c | -1.6 | 0.000 | -1.2 | 0.000 | -0.4 | 0.218 |
| NM_017860 | 1q21.2 | C1orf56 | chromosome 1 open reading frame 56 | -0.5 | 0.037 | -1.2 | 0.000 | -0.6 | 0.053 |
| NM_000944 | 4q21-q24 | PPP3CA | protein phosphatase 3 formerly 2B catalytic subunit alpha isoform | -1.4 | 0.028 | -1.2 | 0.000 | -1.0 | 0.084 |
| D80010 | 2p25.1 | LPIN1 | lipin 1 | -1.2 | 0.000 | -1.1 | 0.015 | -0.9 | 0.053 |
| NM_016598 | 3p21.31 | ZDHC3 | zinc finger DHC-type containing 3 | -1.4 | 0.003 | -1.1 | 0.000 | -0.9 | 0.053 |
| NM_018050 | 12p13.2 | MANSC1 | MANSC domain containing 1 | -0.9 | 0.000 | -1.1 | 0.011 | | |
| NM_005709 | 11p15.1-p14 | USH1C | Usher syndrome 1C autosomal recessive severe | -0.5 | 0.136 | -1.1 | 0.000 | -0.9 | 0.053 |
| D28449 | 1p36.13-p36.12 | ID3 | inhibitor of DNA binding 3 dominant negative helix-loop-helix protein | -0.8 | 0.070 | -1.1 | 0.042 | -0.3 | 0.714 |
| NM_001359 | 8q21.3 | DEC1 | 2 4-dienoyl CoA reductase 1 mitochondrial | -1.9 | 0.000 | -1.1 | 0.000 | -1.6 | 0.053 |
| NM_003688 | Xp11.4 | CASK | calcium/calmodulin-dependent serine protein kinase MAGUK family | 0.0 | 0.617 | -1.1 | 0.042 | 0.5 | 0.218 |
| NM_017720 | 19p13.3 | STAP2 | signal transducing adaptor family member 2 | -1.0 | 0.000 | -1.1 | 0.000 | -0.8 | 0.053 |
| AK026654 | 2q31.1 | CYBRD1 | cytochrome b reductase 1 | -0.1 | 0.638 | -1.0 | 0.000 | -0.1 | 0.714 |
| AK023221 | 6q12-q13 | SMAP1 | stromal membrane-associated GTPase-activating protein 1 | 0.1 | 0.466 | -1.0 | 0.000 | 0.1 | 0.617 |
| NM_018843 | 7q21.12 | SLC25A40 | solute carrier family 25 member 40 | 0.1 | 0.438 | -1.0 | 0.008 | -0.2 | 0.636 |
| NM_005596 | 9p24.1 | NF1B | nuclear factor 1B | -0.5 | 0.046 | -1.0 | 0.000 | -0.4 | 0.120 |
| AL109729 | 15q26.1 | ABHD2 | abhydrolase domain containing 2 | -1.5 | 0.000 | -1.0 | 0.044 | 0.2 | 0.531 |
| X69111 | 1p36.13-p36.12 | ID3 | inhibitor of DNA binding 3 dominant negative helix-loop-helix protein | -0.9 | 0.055 | -1.0 | 0.101 | -0.3 | 0.714 |
| NM_002414 | Xp22.32 | CD99 | CD99 molecule | 0.0 | 0.624 | -1.0 | 0.042 | -0.6 | 0.000 |
| NM_012449 | 7q21 | STEAP1 | six transmembrane epithelial antigen of the prostate 1 | -2.3 | 0.000 | -0.9 | 0.036 | -0.5 | 0.236 |
| AB023182 | 12p11.23 | STK38L | serine/threonine kinase 38 like | -0.2 | 0.534 | -0.9 | 0.044 | -0.4 | 0.272 |
| NM_004772 | 5q22.1 | C5orf13 | chromosome 5 open reading frame 13 | -0.4 | 0.380 | -0.9 | 0.015 | -0.5 | 0.120 |
| AF085880 | 5q31.1 | C5orf24 | chromosome 5 open reading frame 24 | -0.5 | 0.028 | -0.9 | 0.048 | -0.6 | 0.089 |
| NM_007173 | 11q14.1 | PRSS23 | protease serine 23 | -1.2 | 0.018 | -0.9 | 0.021 | -0.9 | 0.101 |
| NM_001758 | | | | -1.0 | 0.000 | -0.9 | 0.048 | -1.4 | 0.000 |
| NM_017992 | 1q24-q25 | EDEM3 | ER degradation enhancer, mannosidase alpha-like 3 | -0.5 | 0.028 | -0.9 | 0.042 | -0.2 | 0.588 |

| | | | | | | | | | |
|-----------|--------------|-----------|---|------|-------|------|-------|------|-------|
| AJ277587 | 18p11.21 | SPIRE1 | spire homolog 1 Drosophila | -0.2 | 0.493 | -0.9 | 0.036 | 0.4 | 0.218 |
| NM_002607 | 7p22 | PDGFA* | Platelet-derived growth factor alpha polypeptide* | -0.4 | 0.018 | -0.9 | 0.071 | -0.2 | 0.120 |
| NM_016613 | 4q32.1 | C4orf18 | chromosome 4 open reading frame 18 | -0.7 | 0.037 | -0.9 | 0.063 | -0.4 | 0.101 |
| AL133555 | 20q13.31 | C20orf108 | chromosome 20 open reading frame 108 | -0.7 | 0.046 | -0.9 | 0.031 | -0.7 | 0.084 |
| NM_003711 | 5q11 | PPAP2A | phosphatidic acid phosphatase type 2A | -1.1 | 0.018 | -0.8 | 0.015 | 0.0 | 0.789 |
| NM_002487 | 15q11.2-q12 | NDN | neclin homolog mouse | -1.1 | 0.000 | -0.8 | 0.063 | -0.5 | 0.101 |
| NM_002412 | 10q26 | MGMT | O-6-methylguanine-DNA methyltransferase | 0.0 | 0.624 | -0.8 | 0.008 | 0.0 | 0.731 |
| AK002197 | 12p11.22 | KLHDC5 | kelch domain containing 5 | -0.2 | 0.513 | -0.8 | 0.015 | -0.2 | 0.714 |
| NM_007011 | 15q26.1 | ABHD2 | abhydrolase domain containing 2 | -1.3 | 0.000 | -0.8 | 0.051 | 0.3 | 0.531 |
| AK026062 | 10p12.31 | DNAJC1 | DnaJ Hsp40 homolog subfamily C member 1 | -0.3 | 0.100 | -0.8 | 0.000 | -0.5 | 0.089 |
| NM_012096 | 3p21.1-p14.3 | APPL1 | adaptor protein phosphotyrosine interaction PH domain and leucine zipper containing 1 | -0.5 | 0.100 | -0.8 | 0.115 | -0.3 | 0.218 |
| AK026331 | 2q35 | CHPF* | Chondroitin polymerizing factor* | -1.7 | 0.000 | -0.8 | 0.048 | -0.2 | 0.678 |
| NM_002391 | 11p11.2 | MDK* | Midkine neurite growth-promoting factor 2* | 0.0 | 0.645 | -0.8 | 0.051 | 0.7 | 0.218 |
| AK024175 | 5p15.33 | PDCD6 | programmed cell death 6 | -0.2 | 0.513 | -0.8 | 0.044 | -0.1 | 0.725 |
| AK025697 | 3q29 | FBXO45 | F-box protein 45 | -0.3 | 0.380 | -0.8 | 0.000 | -0.5 | 0.252 |
| AL049964 | | PS1TP4 | HBV preS1-transactivated protein 4* | -0.6 | 0.020 | -0.8 | 0.044 | -0.4 | 0.356 |
| AL117661 | 10p15.1 | TAF3 | TAF3 RNA polymerase II TATA box binding protein TBP-associated factor 140kDa | -0.1 | 0.534 | -0.8 | 0.000 | -0.4 | 0.089 |
| NM_015973 | 11q13.2 | GAL | galanin prepropeptide | 0.6 | 0.179 | -0.8 | 0.000 | 0.1 | 0.738 |
| AF295378 | 3q13 | MAGEF1 | melanoma antigen family F 1 | -0.7 | 0.100 | -0.8 | 0.000 | -0.4 | 0.089 |
| AK024677 | 4q21.1 | ASAH1 | N-acylsphingosine amidohydrolase acid ceramidase-like | -0.9 | 0.009 | -0.8 | 0.044 | -0.3 | 0.531 |
| AJ011910 | | | MRNA sequence IMAGE clone 193253* | 0.3 | 0.340 | -0.8 | 0.025 | -0.1 | 0.725 |
| AF131846 | 2p13 | GFPT1 | glutamine-fructose-6-phosphate transaminase 1 | 0.3 | 0.242 | -0.7 | 0.000 | -0.1 | 0.714 |
| NM_018132 | 6p12.3 | CENPQ | centromere protein Q | -0.3 | 0.211 | -0.7 | 0.044 | -0.5 | 0.176 |
| NM_012211 | 15q23 | ITGA11 | integrin alpha 11 | -0.2 | 0.493 | -0.7 | 0.011 | -0.4 | 0.471 |
| NM_002156 | 2q33.1 | HSPD1 | heat shock 60kDa protein 1 chaperonin | 0.0 | 0.617 | -0.7 | 0.011 | -0.1 | 0.714 |
| NM_001873 | 4q32.3 | CPE | carboxypeptidase E | -0.4 | 0.022 | -0.7 | 0.044 | -0.5 | 0.053 |
| AB033034 | 12q23.3 | GNPTAB | N-acetylglucosamine-1-phosphate transferase alpha and beta subunits | -0.5 | 0.037 | -0.7 | 0.005 | -0.7 | 0.064 |
| AL049365 | 9q34.11 | FAM102A | family with sequence similarity 102, member A | -0.2 | 0.513 | -0.7 | 0.051 | -0.5 | 0.084 |
| AJ227869 | Xp11.21 | ZXDB | zinc finger X-linked duplicated B | -0.4 | 0.340 | -0.7 | 0.048 | -0.7 | 0.384 |
| AY007149 | 1p36.13-q41 | CEP350 | centrosomal protein 350kDa | -0.1 | 0.589 | -0.7 | 0.051 | -0.5 | 0.309 |
| AL049265 | 5q11 | IL6ST | interleukin 6 signal transducer gp130 oncostatin M receptor | -0.6 | 0.070 | -0.7 | 0.080 | -0.9 | 0.053 |
| AK000028 | 4q24 | FLJ20021* | Hypothetical LOC90024* | -1.5 | 0.000 | -0.7 | 0.000 | -0.5 | 0.120 |
| AF067972 | 2p23 | DNMT3A | DNA cytosine-5-methyltransferase 3 alpha | -0.8 | 0.005 | -0.7 | 0.063 | -0.5 | 0.101 |
| NM_005079 | 8q21 | TPD52 | tumor protein D52 | -0.4 | 0.293 | -0.7 | 0.025 | -0.6 | 0.442 |
| AF271070 | 12q13.11 | SLC38A1 | solute carrier family 38 member 1 | -1.3 | 0.000 | -0.7 | 0.044 | -0.2 | 0.678 |
| NM_002822 | 12q12 | TWF1 | twinfilin actin-binding protein homolog 1 Drosophila | -0.2 | 0.534 | -0.7 | 0.044 | -0.2 | 0.678 |

| | | | | | | | | | |
|-----------|---------------|----------|---|------|-------|------|-------|------|-------|
| NM_017606 | 8p21.1 | ZNF395 | zinc finger protein 395 | -0.3 | 0.380 | -0.7 | 0.000 | -0.4 | 0.588 |
| AB019565 | 1p35 | IFI6 | interferon, alpha-inducible protein 6 | -0.1 | 0.631 | -0.7 | 0.063 | 0.0 | 0.731 |
| AL355720 | 21q22.3 | AGPAT3 | 1-acylglycerol-3-phosphate O-acyltransferase 3 | -0.1 | 0.513 | -0.7 | 0.000 | -0.2 | 0.500 |
| NM_020317 | 1p36.13-p35.1 | C1orf63 | chromosome 1 open reading frame 63 | -0.3 | 0.513 | -0.7 | 0.051 | 0.0 | 0.725 |
| NM_014141 | 7q35-q36 | CNTNAP2 | contactin associated protein-like 2 | -0.3 | 0.293 | -0.7 | 0.025 | -0.2 | 0.556 |
| U95646 | 15q21-q22 | PPIB | peptidylprolyl isomerase B (cyclophilin B) | -0.1 | 0.573 | -0.7 | 0.036 | -0.5 | 0.115 |
| AK021818 | 11q21-q22.1 | DYNC2H1 | dynein cytoplasmic 2 heavy chain 1 | -0.4 | 0.070 | -0.7 | 0.042 | -0.5 | 0.101 |
| NM_005496 | 3q26.1 | SMC4 | structural maintenance of chromosomes 4 | -0.4 | 0.136 | -0.7 | 0.048 | -0.6 | 0.120 |
| NM_001733 | 12p13 | C1R | complement component 1 r subcomponent | 0.0 | 0.589 | -0.7 | 0.042 | -0.3 | 0.328 |
| AB033007 | 5q35.1 | ERGIC1 | endoplasmic reticulum-golgi intermediate compartment ERGIC 1 | -0.3 | 0.157 | -0.7 | 0.042 | -0.1 | 0.725 |
| NM_001089 | 16p13.3 | ABCA3 | ATP-binding cassette sub-family A ABC1 member 3 | -0.5 | 0.070 | -0.7 | 0.071 | -0.4 | 0.194 |
| AK023395 | 4q12 | FIP1L1 | FIP1 like 1 S. cerevisiae | 0.1 | 0.573 | -0.6 | 0.015 | -0.3 | 0.500 |
| AL137300 | Xp22.33 | DHRSX* | Dehydrogenase reductase SDR family X-linked* | -0.2 | 0.412 | -0.6 | 0.015 | -0.4 | 0.101 |
| NM_018465 | 9p24.1 | C9orf46 | chromosome 9 open reading frame 46 | 0.0 | 0.645 | -0.6 | 0.048 | 0.0 | 0.725 |
| AK025133 | 1q32.1 | NUCKS1 | nuclear casein kinase and cyclin-dependent kinase substrate 1 | 0.0 | 0.605 | -0.6 | 0.054 | -0.1 | 0.725 |
| AF301222 | 11p14.1 | CCDC34 | coiled-coil domain containing 34 | -0.3 | 0.380 | -0.6 | 0.044 | 0.3 | 0.500 |
| NM_004183 | 11q13 | BEST1 | bestrophin 1 | -0.1 | 0.629 | -0.6 | 0.042 | -0.2 | 0.678 |
| AK023397 | 3p21.31 | FYCO1 | FYVE and coiled-coil domain containing 1 | -0.2 | 0.558 | -0.6 | 0.042 | -0.5 | 0.089 |
| NM_007212 | 1q25.3 | RNF2 | ring finger protein 2 | 0.1 | 0.558 | -0.6 | 0.021 | -0.2 | 0.657 |
| NM_003851 | 1q24 | CREG1 | cellular repressor of E1A-stimulated genes 1 | 0.2 | 0.340 | -0.6 | 0.011 | -0.2 | 0.714 |
| AL049229 | 3q29 | SENP5 | SUMO1/sentrin specific peptidase 5 | -0.2 | 0.466 | -0.6 | 0.048 | -0.1 | 0.714 |
| AK025766 | 12q24.31 | BR13BP | BR13 binding protein | -0.7 | 0.014 | -0.6 | 0.025 | -0.1 | 0.714 |
| NM_002561 | 17p13.3 | P2RX5 | purinergic receptor P2X ligand-gated ion channel 5 | -0.4 | 0.380 | -0.6 | 0.054 | 0.0 | 0.789 |
| M83822 | 4q31.23-q31.3 | LRBA | LPS-responsive vesicle trafficking beach and anchor containing family with sequence similarity 126 member B | -1.1 | 0.003 | -0.6 | 0.044 | -0.6 | 0.101 |
| AK001843 | 2q33.1 | FAM126B | family with sequence similarity 126 member B | -0.1 | 0.573 | -0.6 | 0.101 | -0.7 | 0.064 |
| AK022971 | | | CDNA FLJ12909 fis clone NT2RP2004400* | 0.5 | 0.113 | -0.6 | 0.051 | -0.1 | 0.725 |
| AK021958 | 15q22.2 | NARG2 | NMDA receptor regulated 2 | 0.1 | 0.558 | -0.6 | 0.015 | -0.3 | 0.588 |
| NM_001498 | 6p12 | GCLC | glutamate-cysteine ligase catalytic subunit | -0.2 | 0.534 | -0.6 | 0.044 | -0.2 | 0.691 |
| NM_018155 | 3q23 | SLC25A36 | solute carrier family 25 member 36 | 0.3 | 0.380 | -0.6 | 0.021 | -0.2 | 0.309 |
| AF007128 | 12p13.33 | FBXL14 | F-box and leucine-rich repeat protein 14 | -0.2 | 0.438 | -0.6 | 0.115 | -0.3 | 0.531 |
| U03886 | Xp22.3 | PNPLA4 | patatin-like phospholipase domain containing 4 | 0.3 | 0.293 | -0.6 | 0.025 | 0.4 | 0.218 |
| AK001036 | 5q31 | SMAD5 | SMAD family member 5 | -0.3 | 0.211 | -0.6 | 0.071 | -0.4 | 0.101 |
| NM_002600 | 1p31 | PDE4B | phosphodiesterase 4B cAMP-specific phosphodiesterase E4 duncce homolog Drosophila | -0.6 | 0.009 | -0.6 | 0.090 | -0.2 | 0.617 |
| NM_006287 | 2q31-q32.1 | TFPI | tissue factor pathway inhibitor lipoprotein-associated coagulation inhibitor | -0.1 | 0.629 | -0.6 | 0.011 | -0.2 | 0.714 |
| AL117612 | 8q23 | MAL2 | mal T-cell differentiation protein 2 | -0.3 | 0.136 | -0.6 | 0.063 | -0.3 | 0.218 |
| AK023269 | 2p23.1 | LCLAT1 | lysocardiolipin acyltransferase 1 | -0.6 | 0.043 | -0.5 | 0.135 | -0.3 | 0.714 |
| AF272357 | 9q34.3 | NPDC1 | neural proliferation differentiation and control 1 | -0.5 | 0.070 | -0.5 | 0.090 | -0.4 | 0.176 |

| | | | | | | | | | |
|-----------|---------------|------------|---|------|-------|------|-------|------|-------|
| D70836 | 19p12 | ZNF714 | zinc finger protein 714 | 0.3 | 0.242 | -0.5 | 0.115 | -0.4 | 0.272 |
| D14678 | 6p21.3 | KIFC1 | kinesin family member C1 | 0.0 | 0.589 | -0.5 | 0.031 | -0.4 | 0.064 |
| NM_002948 | 3p24.2 | RPL15 | ribosomal protein L15 | -0.4 | 0.380 | -0.5 | 0.015 | -0.4 | 0.084 |
| AF131814 | 1p36.12-p35.1 | NPAL3 | NIPA-like domain containing 3 | -0.4 | 0.113 | -0.5 | 0.135 | -0.5 | 0.101 |
| NM_003676 | 1q42.12 | DEGS1 | degenerative spermatocyte homolog 1 lipid desaturase Drosophila | 0.8 | 0.020 | -0.5 | 0.160 | -0.1 | 0.725 |
| NM_018660 | 8p21.1 | ZNF395 | zinc finger protein 395 | -0.5 | 0.022 | -0.5 | 0.005 | -0.2 | 0.691 |
| NM_004864 | 19p13.1-13.2 | GDF15 | growth differentiation factor 15 | -0.4 | 0.513 | -0.5 | 0.160 | 0.7 | 0.194 |
| AL049998 | 11p15.5-p14 | PIK3C2A | phosphoinositide-3-kinase class 2 alpha polypeptide | -0.4 | 0.157 | -0.5 | 0.160 | -0.6 | 0.328 |
| AL133057 | 7q22.1 | LRWD1 | leucine-rich repeats and WD repeat domain containing 1 | 0.1 | 0.412 | 0.5 | 0.054 | 0.5 | 0.194 |
| NM_001998 | 3p25.1 | FBLN2 | fibulin 2 | | | 0.5 | 0.287 | | |
| NM_001513 | 14q24.3 | GSTZ1 | glutathione transferase zeta 1 maleylacetate isomerase | 0.1 | 0.493 | 0.5 | 0.080 | 0.2 | 0.413 |
| NM_017745 | Xp11.4 | BCOR | BCL6 co-repressor | 0.1 | 0.573 | 0.5 | 0.051 | 0.2 | 0.471 |
| M27544 | 12q22-q23 | IGF1 | insulin-like growth factor 1 somatomedin C | -0.4 | 0.028 | 0.5 | 0.080 | 0.0 | 0.789 |
| NM_000269 | 17q21.3 | NME1 | non-metastatic cells 1 protein NM23A expressed in | -0.2 | 0.493 | 0.5 | 0.090 | 0.1 | 0.471 |
| AK024100 | 9q34.11 | PTGES2 | prostaglandin E synthase 2 | 0.0 | 0.605 | 0.5 | 0.044 | 0.2 | 0.531 |
| AK023459 | 10p13 | C10orf97 | chromosome 10 open reading frame 97 | -0.3 | 0.513 | 0.5 | 0.031 | 0.0 | 0.725 |
| NM_001269 | 1p36.1 | RCC1 | regulator of chromosome condensation 1 | 0.4 | 0.293 | 0.6 | 0.160 | 0.3 | 0.531 |
| NM_014846 | 8p22 | KIAA0196 | KIAA0196 | 0.6 | 0.022 | 0.6 | 0.044 | 0.5 | 0.194 |
| S81522 | 2q33-q34 | EEF1B1 | eukaryotic translation elongation factor 1 beta 1 | 0.1 | 0.589 | 0.6 | 0.071 | 0.5 | 0.328 |
| NM_005246 | 5q21 | FER | fer fps/fes related tyrosine kinase phosphoprotein NCP94 | 0.6 | 0.037 | 0.6 | 0.000 | 0.1 | 0.748 |
| NM_017870 | 11q12.2 | TMEM132A | transmembrane protein 132A | 0.3 | 0.211 | 0.6 | 0.071 | 0.3 | 0.442 |
| NM_015940 | 14q24.3 | COQ6 | coenzyme Q6 homolog, monooxygenase (S. cerevisiae) | | | | | | |
| NM_000908 | 5p14-p13 | NPR3 | atriatriuretic peptide receptor C guanylate cyclase C | | | | | | |
| D50914 | 8q24.3 | BOP1 | block of proliferation 1 | -0.4 | 0.000 | 0.6 | 0.015 | 0.2 | 0.218 |
| NM_006432 | 14q24.3 | NPC2 | Niemann-Pick disease type C2 | -0.1 | 0.534 | 0.6 | 0.031 | -0.1 | 0.714 |
| NM_014501 | 19q13.43 | UBE2S | ubiquitin-conjugating enzyme E2S | 0.5 | 0.086 | 0.6 | 0.090 | 0.6 | 0.064 |
| NM_007314 | 1q24-q25 | ABL2 | v-abl Abelson murine leukemia viral oncogene homolog 2 arg Abelson-related gene | 0.7 | 0.037 | 0.6 | 0.054 | 0.5 | 0.218 |
| NM_006516 | 1p35-p31.3 | SLC2A1 | solute carrier family 2 facilitated glucose transporter member 1 | 0.1 | 0.558 | 0.6 | 0.063 | 0.1 | 0.774 |
| NM_003900 | 5q35 | SQSTM1 | sequestosome 1 | 0.1 | 0.380 | 0.6 | 0.063 | 0.2 | 0.218 |
| AK026290 | 15q15.3 | ELL3 | elongation factor RNA polymerase II-like 3 | 0.6 | 0.000 | 0.6 | 0.011 | 0.4 | 0.218 |
| NM_014731 | 20p13 | ProSAPIP1* | ProSAPIP1 protein* | -0.5 | 0.157 | 0.6 | 0.115 | -0.4 | 0.120 |
| NM_001757 | 21q22.13 | CBR1 | carbonyl reductase 1 | 0.4 | 0.242 | 0.6 | 0.135 | 0.3 | 0.531 |
| NM_002795 | 17q12 | PSMB3 | proteasome prosome macropain subunit beta type 3 | 0.5 | 0.113 | 0.6 | 0.063 | 1.0 | 0.000 |
| NM_000190 | 11q23.3 | HMB5 | hydroxymethylbilane synthase | 0.1 | 0.513 | 0.6 | 0.071 | 0.3 | 0.194 |
| M96843 | 3p21.1 | ID2B | inhibitor of DNA binding 2B dominant negative helix-loop-helix protein | 0.0 | 0.624 | 0.6 | 0.031 | 0.0 | 0.789 |
| NM_004804 | 2q11.2 | CIAO1 | cytosolic iron-sulfur protein assembly 1 homolog S. cerevisiae | 0.5 | 0.242 | 0.6 | 0.038 | 0.2 | 0.309 |
| Y11162 | 19p13 | SNORA68 | small nucleolar RNA H/ACA box 68 | 0.4 | 0.211 | 0.7 | 0.031 | 0.1 | 0.218 |
| AK023856 | 2p16.1 | LOC339803* | Hypothetical protein LOC339803* | 0.2 | 0.293 | 0.7 | 0.021 | 0.5 | 0.194 |

| | | | | | | | | | |
|-----------|----------------|-----------|---|------|-------|-----|-------|------|-------|
| AF034102 | 11q13 | SLC29A2 | solute carrier family 29 nucleoside transporters member 2 | 0.7 | 0.007 | 0.7 | 0.038 | 0.7 | 0.089 |
| Y11159 | 9q34 | RPL12 | ribosomal protein L12 | | | 0.7 | 0.031 | | |
| U87169 | | STYX | serine/threonine/tyrosine interacting protein | 0.2 | 0.340 | 0.7 | 0.054 | 0.4 | 0.218 |
| D83782 | 3p21.31 | SCAP | SREBF chaperone | 0.2 | 0.412 | 0.7 | 0.054 | 0.2 | 0.617 |
| NM_004184 | 14q32.31 | WARS | tryptophanyl-tRNA synthetase | 0.1 | 0.412 | 0.7 | 0.063 | 0.1 | 0.471 |
| AK024665 | 11q13 | MUS81 | MUS81 endonuclease homolog S. cerevisiae | 0.5 | 0.070 | 0.7 | 0.011 | 0.6 | 0.218 |
| NM_005311 | 7p12-p11.2 | GRB10 | growth factor receptor-bound protein 10 | 1.1 | 0.028 | 0.7 | 0.008 | 0.5 | 0.218 |
| NM_016539 | 19p13.3 | SIRT6 | sirtuin silent mating type information regulation 2 homolog 6 S. cerevisiae | 0.2 | 0.293 | 0.7 | 0.025 | 0.3 | 0.413 |
| NM_002455 | 1q21 | MTX1 | metaxin 1 | 0.5 | 0.046 | 0.7 | 0.036 | 0.3 | 0.328 |
| AF190900 | 1q32.1 | KLHL12 | kelch-like 12 Drosophila | 0.2 | 0.466 | 0.7 | 0.000 | 1.0 | 0.194 |
| NM_000713 | 19q13.1-q13.2 | BLVRB | bilirubin reductase B flavin reductase NADPH | -0.1 | 0.589 | 0.7 | 0.008 | 0.1 | 0.789 |
| NM_004039 | 15q21-q22 | ANXA2 | annexin A2 | -0.3 | 0.136 | 0.7 | 0.080 | 0.1 | 0.785 |
| NM_007158 | 1p22 | CSDE1 | cold shock domain containing E1 RNA-binding | 0.7 | 0.157 | 0.7 | 0.031 | 0.9 | 0.194 |
| AK026298 | 15q21.1 | C15orf48 | chromosome 15 open reading frame 48 | | | 0.7 | 0.015 | | |
| NM_007111 | 13q34 | TFDP1 | transcription factor Dp-1 | 0.7 | 0.018 | 0.8 | 0.048 | 0.5 | 0.218 |
| AL050024 | 7p21.1 | SOSTDC1 | sclerostin domain containing 1 | -0.1 | 0.493 | 0.8 | 0.038 | 0.1 | 0.755 |
| NM_001916 | 8q24.3 | CYC1 | cytochrome c-1 | 0.0 | 0.573 | 0.8 | 0.063 | 0.1 | 0.356 |
| NM_020411 | Xp11.22-p11.21 | XAGE1 | X antigen family member 1 | 0.3 | 0.003 | 0.8 | 0.038 | | |
| NM_003234 | 3q29 | TFRC | transferrin receptor p90 CD71 | 1.1 | 0.000 | 0.8 | 0.025 | 0.4 | 0.218 |
| M60721 | 1q41-q42.1 | HLX | H2.0-like homeobox | 0.3 | 0.293 | 0.8 | 0.063 | 0.3 | 0.218 |
| L29496 | Xq11.2-q12 | AR | androgen receptor dihydrotestosterone receptor | -1.3 | 0.018 | 0.9 | 0.000 | -0.3 | 0.194 |
| NM_003523 | 6p21.3 | HIST1H2BE | histone cluster 1 H2be | 0.5 | 0.113 | 0.9 | 0.021 | 0.4 | 0.218 |
| AL133572 | 12q24.31 | FBXL10 | F-box and leucine-rich repeat protein 10 | 0.5 | 0.086 | 0.9 | 0.005 | 1.1 | 0.049 |
| AJ223352 | 6p21.33 | HIST1H2BK | histone cluster 1 H2bk | 0.2 | 0.340 | 0.9 | 0.025 | 0.3 | 0.356 |
| NM_000849 | 1p13.3 | GSTM3 | glutathione S-transferase M3 brain | 0.6 | 0.086 | 0.9 | 0.000 | 0.9 | 0.176 |
| Y11161 | 17p13.1 | EIF4A1 | eukaryotic translation initiation factor 4A, isoform 1 | 0.9 | 0.003 | 0.9 | 0.038 | 0.4 | 0.218 |
| NM_001831 | 8p21-p12 | CLU | clusterin | 0.1 | 0.534 | 0.9 | 0.000 | 0.7 | 0.049 |
| NM_003311 | 11p15.5 | PHLDA2 | pleckstrin homology-like domain family A member 2 | 0.0 | 0.624 | 0.9 | 0.011 | 0.8 | 0.194 |
| AL157449 | 17q21.33 | PPP1R9B | protein phosphatase 1 regulatory inhibitor subunit 9B | 0.9 | 0.007 | 0.9 | 0.000 | 0.6 | 0.218 |
| NM_003712 | 19p13 | PPAP2C | phosphatidic acid phosphatase type 2C | 1.2 | 0.000 | 0.9 | 0.044 | 1.2 | 0.000 |
| NM_001327 | Xq28 | CTAG1A | cancer/testis antigen 1A | 0.6 | 0.046 | 0.9 | 0.000 | 0.6 | 0.194 |
| NM_003524 | 6p21.3 | HIST1H2BH | histone cluster 1 H2bh | 0.2 | 0.380 | 0.9 | 0.000 | 0.2 | 0.384 |
| NM_003525 | 6p21.3 | HIST1H2BI | histone cluster 1, H2bi | 0.3 | 0.293 | 1.0 | 0.008 | 0.1 | 0.789 |
| Y08836 | 5q13 | MAP1B | microtubule-associated protein 1B | 0.7 | 0.046 | 1.0 | 0.011 | 1.2 | 0.101 |
| AF086251 | 11q21 | SESN3 | sestrin 3 | 0.1 | 0.534 | 1.1 | 0.048 | 1.1 | 0.049 |
| NM_006332 | 19p13.1 | IFI30 | interferon gamma-inducible protein 30 | 1.7 | 0.000 | 1.1 | 0.025 | 0.7 | 0.218 |
| Y11158 | 16p13.3 | SNORA10 | small nucleolar RNA H/ACA box 10 | -0.1 | 0.513 | 1.1 | 0.000 | 0.5 | 0.218 |
| L07383 | 3p21.3 | RPSA | ribosomal protein SA | 0.1 | 0.513 | 1.2 | 0.071 | | |

| | | | | | | | | | |
|-----------|----------|------------|--|------|-------|-----|-------|------|-------|
| NM_016084 | 17p11.2 | RASD1 | RAS dexamethasone-induced 1 | 1.6 | 0.000 | 1.2 | 0.000 | 0.5 | 0.218 |
| NM_012463 | 12q24.31 | ATP6V0A2 | ATPase H transporting lysosomal V0 subunit a2 | 0.8 | 0.028 | 1.2 | 0.051 | 1.7 | 0.000 |
| NM_004982 | 12p11.23 | KCNJ8 | potassium inwardly-rectifying channel subfamily J member 8 | 2.7 | 0.000 | 1.2 | 0.000 | 1.9 | 0.000 |
| NM_003516 | 1q21.2 | HIST2H2AA3 | histone cluster 2 H2aa3 | -0.1 | 0.645 | 1.2 | 0.000 | 0.8 | 0.194 |
| NM_016639 | 16p13.3 | TNFRSF12A | tumor necrosis factor receptor superfamily member 12A | 0.6 | 0.028 | 1.3 | 0.000 | 0.5 | 0.218 |
| S67154 | 3q28 | EIF4A2 | eukaryotic translation initiation factor 4A isoform 2 | 0.1 | 0.589 | 1.3 | 0.021 | -0.5 | 0.101 |
| NM_014269 | 4q34 | ADAM29 | ADAM metallopeptidase domain 29 | 1.5 | 0.000 | 1.4 | 0.011 | 2.2 | 0.000 |
| U17632 | | | | 1.0 | 0.003 | 1.4 | 0.008 | 1.1 | 0.194 |
| U58096 | Yp11.2 | TSPY1 | testis specific protein Y-linked 1 | 1.0 | 0.037 | 1.4 | 0.000 | | |
| NM_013253 | 11p15.2 | DKK3 | dickkopf homolog 3 Xenopus laevis | -0.6 | 0.005 | 1.4 | 0.000 | 0.7 | 0.218 |
| NM_001823 | 14q32 | CKB | creatine kinase brain | 1.7 | 0.000 | 1.5 | 0.015 | 1.6 | 0.000 |
| NM_005794 | 14q11.2 | DHRS2 | dehydrogenase/reductase SDR family member 2 | 1.4 | 0.003 | 1.5 | 0.071 | 1.2 | 0.051 |
| AB037810 | 1q42.2 | SIPA1L2 | signal-induced proliferation-associated 1 like 2 | 0.9 | 0.046 | 1.5 | 0.000 | 1.7 | 0.049 |
| NM_013452 | Xp22 | VCX | variable charge X-linked | 2.3 | 0.000 | 1.6 | 0.015 | 1.7 | 0.049 |
| NM_001072 | 2q37 | UGT1A1 | UDP glucuronosyltransferase 1 family polypeptide A1 | 0.2 | 0.380 | 1.7 | 0.015 | -0.1 | 0.714 |

* no approved HUGO symbol / name exist for this entry. If present, gene symbol / name from the UNIGENE database are given in alternative.

2log_ratio>0 indicates over-expression in the androgen-independent subline, compared to parental PC346C. 2log_ratio<0 indicates down-regulation in the androgen-independent subline.

Table S3 - Genes differentially expressed in PC346Flu2 vs PC346C expression ratios and SAM q-values

| GenBank ID | Cytoband | Symbol | HUGO Gene Name | PC346DCC | | PC346Flu1 | | PC346Flu2 | |
|------------|-------------|---------|--|------------|--------|------------|--------|------------|--------|
| | | | | 2log ratio | qvalue | 2log ratio | qvalue | 2log ratio | qvalue |
| NM_014380 | Xq22.2 | NGFRAP1 | nerve growth factor receptor TNFRSF16 associated protein 1 | -0.2 | 0.513 | -2.5 | 0.000 | -2.7 | 0.000 |
| AF216077 | 9q32 | COL27A1 | collagen type XXVII alpha 1 | -2.1 | 0.000 | -2.8 | 0.000 | -1.7 | 0.053 |
| NM_001359 | 8q21.3 | DEC1 | 2,4-dienoyl CoA reductase 1 mitochondrial | -1.9 | 0.000 | -1.1 | 0.000 | -1.6 | 0.053 |
| NM_001758 | | | | -1.0 | 0.000 | -0.9 | 0.048 | -1.4 | 0.000 |
| NM_005510 | 6p21.3 | DOM3Z | dom-3 homolog Z C. elegans | 0.5 | 0.211 | 0.1 | 0.422 | -1.4 | 0.053 |
| NM_002151 | 19q11-q13.2 | HPN | hepsin transmembrane protease serine 1 | -1.0 | 0.000 | -0.9 | 0.000 | -1.4 | 0.053 |
| X04236 | 6p12.1 | RN7SK | RNA, 7SK small nuclear | -0.2 | 0.513 | -0.6 | 0.054 | -1.4 | 0.115 |
| AB020968 | 6q22.2 | MARCKS | myristoylated alanine-rich protein kinase C substrate | -1.6 | 0.000 | -2.0 | 0.000 | -1.3 | 0.053 |
| NM_003278 | 3p22-p21.3 | CLEC3B | C-type lectin domain family 3 member B | -1.5 | 0.005 | -1.3 | 0.000 | -1.3 | 0.084 |
| AL122055 | 6q21 | GDC2L6 | cell division cycle 2-like 6 CDK8-like | -1.4 | 0.000 | -1.3 | 0.000 | -1.2 | 0.000 |
| NM_016306 | 3q27.3 | DNAJB11 | DnaJ Hsp40 homolog subfamily B member 11 | -0.4 | 0.046 | -0.2 | 0.287 | -1.1 | 0.089 |
| AK000933 | 1q42-q44 | KMO | kynurenine 3-monooxygenase kynurenine 3-hydroxylase | -0.4 | 0.179 | 0.0 | 0.527 | -1.0 | 0.064 |
| NM_015544 | 17q11.2 | TMEM98 | transmembrane protein 98 | -0.1 | 0.534 | -0.3 | 0.211 | -1.0 | 0.053 |

| | | | | | | | | | |
|-----------|--------------|-----------|--|------|-------|------|-------|------|-------|
| NM_007173 | 11q14.1 | PRSS23 | protease serine 23 | -1.2 | 0.018 | -0.9 | 0.021 | -0.9 | 0.101 |
| D70833 | 19p12 | ZNF208 | zinc finger protein 208 | 0.0 | 0.645 | -0.7 | 0.044 | -0.9 | 0.089 |
| D80010 | 2p25.1 | LPIN1 | lipin 1 | -1.2 | 0.000 | -1.1 | 0.015 | -0.9 | 0.053 |
| NM_006829 | 10q23.2 | C10orf116 | chromosome 10 open reading frame 116 | -0.5 | 0.136 | -1.1 | 0.000 | -0.9 | 0.053 |
| NM_005709 | 11p15.1-p14 | USH1C | Usher syndrome 1C autosomal recessive severe | -1.4 | 0.003 | -1.1 | 0.000 | -0.9 | 0.053 |
| NM_016598 | 3p21.31 | ZDHC3 | zinc finger DHHC-type containing 3 | -1.5 | 0.000 | -1.4 | 0.000 | -0.9 | 0.053 |
| AL049963 | 4q22-q24 | SLC39A8 | solute carrier family 39 zinc transporter member 8 | -0.9 | 0.070 | -0.7 | 0.080 | -0.9 | 0.053 |
| AL049265 | 5q11 | IL6ST | interleukin 6 signal transducer gp130 oncostatins M receptor | -2.9 | 0.000 | -1.8 | 0.000 | -0.8 | 0.053 |
| NM_017935 | 4q24 | BANK1 | B-cell scaffold protein with ankyrin repeats 1 | -0.2 | 0.534 | -0.5 | 0.101 | -0.8 | 0.053 |
| NM_002245 | 1q42-q43 | KCNK1 | potassium channel subfamily K member 1 | -2.3 | 0.000 | -0.7 | 0.063 | -0.8 | 0.053 |
| AF188747 | 19q13.41 | KLK2 | kallikrein-related peptidase 2 | 0.2 | 0.438 | -0.6 | 0.080 | -0.8 | 0.053 |
| NM_002252 | 2p24 | KCNS3 | potassium voltage-gated channel delayed-rectifier subfamily S member 3 | -0.2 | 0.513 | -0.6 | 0.063 | -0.8 | 0.053 |
| NM_003489 | 21q11.2 | NRIP1 | nuclear receptor interacting protein 1 | -1.0 | 0.000 | -1.1 | 0.000 | -0.8 | 0.053 |
| NM_017720 | 19p13.3 | STAP2 | signal transducing adaptor family member 2 | 0.0 | 0.638 | -0.5 | 0.025 | -0.8 | 0.000 |
| AF076617 | Xp22.32 | SLC25A6 | solute carrier family 25 mitochondrial carrier adenine nucleotide translocator 6 | -1.6 | 0.022 | 0.2 | 0.185 | -0.8 | 0.053 |
| X15667 | | | | -0.6 | 0.022 | 0.1 | 0.444 | -0.8 | 0.053 |
| NM_013309 | 15q11.2-21.3 | SLC30A4 | solute carrier family 30 zinc transporter member 4 | 0.0 | 0.645 | -0.1 | 0.473 | -0.8 | 0.064 |
| NM_001417 | 12q13.13 | EIF4B | eukaryotic translation initiation factor 4B | -1.0 | 0.020 | -0.6 | 0.048 | -0.7 | 0.064 |
| NM_001184 | 3q22-q24 | ATR | ataxia telangiectasia and Rad3 related | 0.8 | 0.000 | 0.3 | 0.090 | -0.7 | 0.053 |
| NM_014883 | 17p11.2 | ULK2 | unc-51-like kinase 2 C. elegans | 0.3 | 0.380 | -0.3 | 0.160 | -0.7 | 0.000 |
| AK024018 | 19q13.32 | GEMIN7 | gem nuclear organelle associated protein 7 | -0.7 | 0.022 | 0.2 | 0.287 | -0.7 | 0.000 |
| NM_004549 | 11q14.1 | NDUFC2 | NADH dehydrogenase ubiquinone 1 subcomplex unknown 2 14.5kDa | -0.1 | 0.573 | -0.6 | 0.101 | -0.7 | 0.064 |
| AK001843 | 2q33.1 | FAM126B | family with sequence similarity 126 member B | 0.2 | 0.340 | 0.0 | 0.517 | -0.7 | 0.053 |
| NM_012384 | 20q13.33 | GMEB2 | glucocorticoid modulatory element binding protein 2 | -0.3 | 0.113 | -0.2 | 0.287 | -0.7 | 0.084 |
| AY008271 | 4q22-q23 | SMARCAD1 | SWI/SNF-related matrix-associated actin-dependent regulator of chromatin subfamily a containing DEAD/H box 1 | -1.0 | 0.009 | -0.5 | 0.090 | -0.7 | 0.089 |
| NM_015415 | 1q24 | BRP44 | brain protein 44 | -0.5 | 0.037 | -0.7 | 0.005 | -0.7 | 0.064 |
| AB033034 | 12q23.3 | GNPTAB | N-acetylglucosamine-1-phosphate transferase alpha and beta subunits | 0.1 | 0.493 | -0.7 | 0.080 | -0.7 | 0.194 |
| D70835 | 19p12 | ZNF675 | zinc finger protein 675 | -0.4 | 0.242 | -0.3 | 0.211 | -0.6 | 0.053 |
| L38937 | 17q21.2 | FAM134C | family with sequence similarity 134 member C | -0.2 | 0.513 | -0.5 | 0.101 | -0.6 | 0.053 |
| NM_001173 | 14q12 | ARHGAP5 | Rho GTPase activating protein 5 | -0.4 | 0.242 | -0.3 | 0.160 | -0.6 | 0.089 |
| AF100640 | | | | -1.1 | 0.003 | -0.6 | 0.044 | -0.6 | 0.101 |
| M83822 | 4q31.23-31.3 | LRBA | LPS-responsive vesicle trafficking beach and anchor containing | -0.5 | 0.293 | 0.0 | 0.533 | -0.6 | 0.101 |
| NM_003541 | 6p22-p21.3 | HIST1H4K | histone cluster 1 H4K | -0.7 | 0.046 | -0.4 | 0.160 | -0.6 | 0.053 |
| NM_014936 | 6p21.1 | ENPP4 | ectonucleotide pyrophosphatase/phosphodiesterase 4 putative function | -1.4 | 0.009 | 0.4 | 0.135 | -0.6 | 0.064 |
| NM_005884 | 14q11.2-q12 | EFS | embryonal Fyn-associated substrate | -0.2 | 0.534 | -0.3 | 0.115 | -0.6 | 0.115 |
| M32219 | 5q14.2 | RPS23 | ribosomal protein S23 | -0.4 | 0.157 | -0.5 | 0.160 | -0.6 | 0.328 |
| AL049998 | 11p15.5-p14 | PIK3C2A | phosphoinositide-3-kinase class 2 alpha polypeptide | | | | | | |

| | | | | | | | | | |
|-----------|--------------|----------|---|------|-------|------|-------|------|-------|
| NM_016171 | 2q35-q36 | PTMA | prothymosin, alpha | 0.1 | 0.573 | 0.1 | 0.444 | -0.6 | 0.150 |
| AK024800 | 20q13.2-13.3 | NFATC2 | nuclear factor of activated T-cells cytoplasmic calcineurin-dependent 2 | -0.1 | 0.558 | -0.4 | 0.101 | -0.6 | 0.176 |
| AF024698 | 19q13.43 | ZNF583 | zinc finger protein 583 | -0.1 | 0.573 | -0.4 | 0.090 | -0.6 | 0.150 |
| AJ276095 | 6p21.33-21.1 | DEF6 | differentially expressed in FDCP 6 homolog mouse | -0.6 | 0.014 | -0.2 | 0.287 | -0.6 | 0.053 |
| AF085838 | | | | -0.1 | 0.589 | 0.1 | 0.444 | -0.6 | 0.084 |
| NM_002414 | Xp22.32 | CD99 | CD99 molecule | 0.0 | 0.624 | -1.0 | 0.042 | -0.6 | 0.000 |
| NM_002165 | 20q11 | ID1 | inhibitor of DNA binding 1 | -1.2 | 0.018 | | | -0.6 | 0.500 |
| NM_014781 | 8p22-q21.13 | RB1CC1 | RB1-inducible coiled-coil 1 | -0.6 | 0.037 | -0.6 | 0.115 | -0.6 | 0.328 |
| NM_001190 | 19q13 | BCAT2 | branched chain aminotransferase 2 mitochondrial | 0.1 | 0.558 | 0.0 | 0.524 | -0.5 | 0.053 |
| NM_001873 | 4q32.3 | CPE | carboxypeptidase E | -0.4 | 0.022 | -0.7 | 0.044 | -0.5 | 0.053 |
| NM_017948 | 9q22.31 | NOL8 | nucleolar protein 8 | -0.2 | 0.558 | -0.3 | 0.160 | -0.5 | 0.053 |
| NM_006294 | 8q22 | UQCRCB | ubiquinol-cytochrome c reductase binding protein | -0.4 | 0.242 | -0.1 | 0.517 | -0.5 | 0.120 |
| AF086462 | 10q22.3 | C10orf58 | chromosome 10 open reading frame 58 | 0.1 | 0.605 | -0.3 | 0.287 | -0.5 | 0.101 |
| NM_005646 | 1q42.3 | TARBP1 | TAR HIV-1 RNA binding protein 1 | -0.2 | 0.466 | -0.1 | 0.473 | -0.5 | 0.120 |
| NM_001958 | 20q13.3 | EEF1A2 | eukaryotic translation elongation factor 1 alpha 2 | -0.1 | 0.558 | 0.3 | 0.211 | -0.5 | 0.134 |
| NM_018123 | 1q31 | ASPM | asp (abnormal spindle) homolog, microcephaly associated (Drosophila) | -0.4 | 0.100 | 0.1 | 0.422 | -0.5 | 0.101 |
| U52054 | 5q11.1 | EMB | embigin homolog mouse | -0.9 | 0.022 | -0.7 | 0.042 | -0.5 | 0.150 |
| NM_001197 | 22q13.31 | BIK | BCL2-interacting killer apoptosis-inducing | -0.1 | 0.573 | -0.5 | 0.115 | -0.5 | 0.053 |
| NM_004510 | 2q37.1 | SP110 | SP110 nuclear body protein | 0.2 | 0.340 | -0.2 | 0.185 | -0.5 | 0.471 |
| AF086535 | 1p34.3 | C1orf102 | chromosome 1 open reading frame 102 | -0.2 | 0.009 | 0.0 | 0.422 | 0.5 | 0.218 |
| NM_018255 | 18q12.2 | ELP2 | elongation protein 2 homolog S. cerevisiae | 0.1 | 0.645 | 0.0 | 0.358 | 0.5 | 0.194 |
| AF086001 | | | | 0.5 | 0.070 | 0.0 | 0.524 | 0.5 | 0.089 |
| NM_001494 | 10p15 | GDJ2 | GDP dissociation inhibitor 2 | 0.1 | 0.412 | -0.1 | 0.473 | 0.5 | 0.037 |
| AK001829 | 18q23 | | | 0.0 | 0.605 | -0.2 | 0.185 | 0.6 | 0.176 |
| NM_004046 | 18q12-q21 | ATP5A1 | ATP synthase H transporting mitochondrial F1 complex alpha subunit 1 | 0.3 | 0.380 | 0.0 | 0.515 | 0.6 | 0.194 |
| NM_004287 | 17q21 | GOSR2 | golgi SNAP receptor complex member 2 | 0.2 | 0.380 | 0.5 | 0.031 | 0.6 | 0.194 |
| NM_015681 | 17p11.2 | B9D1 | B9 protein domain 1 | 0.2 | 0.293 | 0.3 | 0.160 | 0.6 | 0.194 |
| NM_001660 | 3p21.2-p21.1 | ARF4 | ADP-ribosylation factor 4 | 0.1 | 0.573 | -0.3 | 0.287 | 0.6 | 0.218 |
| NM_011468 | 7q11.23 | STYXL1 | serine/threonine/tyrosine interacting-like 1 | 0.6 | 0.100 | 0.2 | 0.071 | 0.6 | 0.194 |
| NM_001984 | Xp11.23 | GAGE1 | G antigen 1 | 0.7 | 0.003 | 0.4 | 0.211 | 0.6 | 0.000 |
| NM_019844 | 12p12 | SLCO1B3 | solute carrier organic anion transporter family member 1B3 | -1.1 | 0.028 | -0.2 | 0.394 | 0.6 | 0.194 |
| AK026854 | 9p13.2 | WDR32 | WD repeat domain 32 | 0.3 | 0.086 | 0.1 | 0.211 | 0.6 | 0.194 |
| NM_016215 | 9q34.3 | EGFL7 | EGF-like-domain multiple 7 | 0.6 | 0.242 | -0.1 | 0.135 | 0.6 | 0.194 |
| NM_014913 | 18q23 | ADNP2 | ADNP homeobox 2 | 0.1 | 0.293 | 0.1 | 0.287 | 0.6 | 0.218 |
| AF151810 | 11q13 | STAR10 | STAR-related lipid transfer START domain containing 10 | 0.6 | 0.070 | 0.2 | 0.358 | 0.6 | 0.194 |
| NM_002391 | 11p11.2 | MDK* | | 0.0 | 0.645 | -0.8 | 0.051 | 0.7 | 0.218 |
| NM_016097 | 18q12 | IER3IP1 | immediate early response 3 interacting protein 1 | 0.1 | 0.513 | -0.3 | 0.211 | 0.7 | 0.218 |
| NM_004786 | 18q21.2 | TXNL1 | thioredoxin-like 1 | 0.1 | 0.493 | -0.1 | 0.321 | 0.7 | 0.049 |

| | | | | | | | | | |
|-----------|---------------|------------|--|------|-------|------|-------|-----|-------|
| NM_017947 | 18q12 | MOCOS | molybdenum cofactor sulfurase | -0.5 | 0.055 | -0.6 | 0.071 | 0.7 | 0.194 |
| NM_005151 | 18p11.32 | USP14 | ubiquitin specific peptidase 14 RNA-guanine transglycosylase | -0.2 | 0.493 | -0.1 | 0.321 | 0.7 | 0.089 |
| NM_014302 | 7p11.2 | SEC61G | Sec61 gamma subunit | 0.2 | 0.438 | 0.2 | 0.287 | 0.7 | 0.176 |
| NM_018570 | | | | 0.4 | 0.211 | 0.5 | 0.063 | 0.7 | 0.150 |
| AK000543 | 18q12.2 | C18orf10 | chromosome 18 open reading frame 10 | 0.1 | 0.466 | 0.0 | 0.515 | 0.7 | 0.194 |
| NM_000104 | 2p21 | CYP1B1 | cytochrome P450 family 1 subfamily B polypeptide 1 | -0.6 | 0.293 | 0.0 | 0.515 | 0.7 | 0.218 |
| NM_004282 | 6p12.3-p11.2 | BAG2 | BCL2-associated athanogene 2 | 0.9 | 0.020 | 0.4 | 0.044 | 0.7 | 0.194 |
| NM_006893 | 10q24.31 | NPM3 | nucleophosmin/nucleoplasm 3 | 0.6 | 0.157 | 0.1 | 0.485 | 0.7 | 0.150 |
| NM_005631 | 7q32.3 | SMO | smoothed homolog Drosophila | 0.8 | 0.018 | 0.3 | 0.160 | 0.7 | 0.089 |
| NM_001831 | 8p21-p12 | CLU | clusterin | 0.1 | 0.534 | 0.9 | 0.000 | 0.7 | 0.049 |
| NM_001075 | 4q13.2 | UGT2B10 | UDP glucuronosyltransferase 2 family polypeptide B10 | 0.0 | 0.589 | 0.2 | 0.211 | 0.7 | 0.194 |
| AK001079 | 18q11.1 | OSBPL1A | oxysterol binding protein-like 1A | 0.5 | 0.022 | 0.0 | 0.394 | 0.7 | 0.194 |
| NM_004864 | 19p13.1-13.2 | GDF15 | growth differentiation factor 15 | -0.4 | 0.513 | -0.5 | 0.160 | 0.7 | 0.194 |
| M22538 | 18p11.31-11.2 | NDUFV2 | NADH dehydrogenase ubiquinone flavoprotein 2 24kDa | -0.1 | 0.573 | -0.1 | 0.444 | 0.7 | 0.047 |
| NM_002867 | 1p32-p31 | RAB3B | RAB3B member RAS oncogene family | -0.3 | 0.000 | 0.1 | 0.090 | 0.8 | 0.194 |
| AB037735 | 18p11.23 | ARHGAP28 | Rho GTPase activating protein 28 | | | | | 0.8 | 0.218 |
| AK002107 | 1p32-p31 | RAB3B | RAB3B member RAS oncogene family | -0.4 | 0.018 | 0.2 | 0.287 | 0.8 | 0.194 |
| NM_005178 | 19q13.1-q13.2 | BCL3 | B-cell CLL/lymphoma 3 | -0.4 | 0.046 | -0.3 | 0.229 | 0.8 | 0.194 |
| NM_005804 | 19p13.12 | DDX39 | DEAD Asp-Glu-Ala-Asp box polypeptide 39 | 1.4 | 0.000 | 0.3 | 0.253 | 0.8 | 0.194 |
| AB042410 | 1p21.3 | GPR88 | G protein-coupled receptor 88 | -2.4 | 0.000 | -0.3 | 0.394 | 0.8 | 0.194 |
| NM_003516 | 1q21.2 | HIST2H2AA3 | histone cluster 2 H2aa3 | -0.1 | 0.645 | 1.2 | 0.000 | 0.8 | 0.194 |
| NM_000985 | 18q21 | RPL17 | ribosomal protein L17 | 0.4 | 0.043 | 0.2 | 0.185 | 0.8 | 0.000 |
| NM_000849 | 1p13.3 | GSTM3 | glutathione S-transferase M3 brain | 0.6 | 0.086 | 0.9 | 0.000 | 0.9 | 0.176 |
| NM_005909 | 5q13 | MAP1B | microtubule-associated protein 1B | 0.3 | 0.380 | 0.1 | 0.394 | 0.9 | 0.194 |
| NM_001262 | 1p32 | CDKN2C | cyclin-dependent kinase inhibitor 2C p18 inhibits CDK4 | 0.5 | 0.211 | 0.1 | 0.459 | 0.9 | 0.194 |
| AF200348 | 2p25 | PXDN | peroxidasin homolog Drosophila | -1.2 | 0.003 | -1.3 | 0.000 | 0.9 | 0.064 |
| AF190900 | 1q32.1 | KLHL12 | kelch-like 12 Drosophila | 0.2 | 0.466 | 0.7 | 0.000 | 1.0 | 0.194 |
| NM_016192 | 2q32.3 | TMEFF2 | transmembrane protein with EGF-like and two follistatin-like domains 2 | 0.0 | 0.645 | 0.3 | 0.115 | 1.0 | 0.049 |
| NM_002795 | 17q12 | PSMB3 | proteasome protein with EGF-like and two follistatin-like domains 2 | 0.5 | 0.113 | 0.6 | 0.063 | 1.0 | 0.000 |
| AL133572 | 12q24.31 | FBXL10 | F-box and leucine-rich repeat protein 10 | 0.5 | 0.086 | 0.9 | 0.005 | 1.1 | 0.049 |
| NM_014214 | 18p11.2 | IMPA2 | inositol myo -1 or 4 -monophosphatase 2 | 0.3 | 0.242 | 0.0 | 0.515 | 1.1 | 0.000 |
| AF086251 | 11q21 | SESN3 | sestrin 3 | 0.1 | 0.534 | 1.1 | 0.048 | 1.1 | 0.049 |
| NM_005794 | 14q11.2 | DHRS2 | dehydrogenase/reductase SDR family member 2 | 1.4 | 0.003 | 1.5 | 0.071 | 1.2 | 0.051 |
| Y09836 | 5q13 | MAP1B | microtubule-associated protein 1B | 0.7 | 0.046 | 1.0 | 0.011 | 1.2 | 0.101 |
| NM_003712 | 19p13 | PPAP2C | phosphatidic acid phosphatase type 2C | 1.2 | 0.000 | 0.9 | 0.044 | 1.2 | 0.000 |
| NM_003226 | 21q22.3 | TFF3 | trefoil factor 3 intestinal | 1.9 | 0.000 | -0.5 | 0.211 | 1.5 | 0.049 |
| NM_001823 | 14q32 | CKB | creatine kinase brain | 1.7 | 0.000 | 1.5 | 0.015 | 1.6 | 0.000 |
| AB037810 | 1q42.2 | SIPA1L2 | signal-induced proliferation-associated 1 like 2 | 0.9 | 0.046 | 1.5 | 0.000 | 1.7 | 0.049 |

| | | | | | | | | | |
|-----------|----------|----------|--|-----|-------|-----|-------|-----|-------|
| NM_013452 | Xp22 | VCX | variable charge X-linked | 2.3 | 0.000 | 1.6 | 0.015 | 1.7 | 0.049 |
| NM_012463 | 12q24.31 | ATP6V0A2 | ATPase H transporting lysosomal V0 subunit a2 | 0.8 | 0.028 | 1.2 | 0.051 | 1.7 | 0.000 |
| NM_004982 | 12p11.23 | KCNJ8 | potassium inwardly-rectifying channel subfamily J member 8 | 2.7 | 0.000 | 1.2 | 0.000 | 1.9 | 0.000 |
| NM_014269 | 4q34 | ADAM29 | ADAM metalloproteinase domain 29 | 1.5 | 0.000 | 1.4 | 0.011 | 2.2 | 0.000 |

* no approved HUGO symbol / name exist for this entry. if present, gene symbol / name from the UNIGENE database are given in alternative. 2log₂ratio>0 indicates over-expression in the androgen-independent subline, compared to parental PC346C. 2log₂ratio<0 indicates down-regulation in the androgen-independent subline.

Table S4 - List of androgen-receptor target genes

| GenBank ID | Symbol | HUGO Name | R1881 up-regulated genes |
|------------|---------|-----------|---|
| NM_018674 | ACCN4 | | amiloride-sensitive cation channel 4 pituitary |
| NM_004457 | ACSL3 | | acyl-CoA synthetase long-chain family member 3 |
| NM_006408 | AGR2 | | anterior gradient homolog 2 (Xenopus laevis) |
| NM_014109 | ATAD2 | | ATPase family AAA domain containing 2 |
| AK027213 | BBS10 | | Bardet-Biedl syndrome 10 |
| NM_020235 | BBX | | bobby sox homolog Drosophila |
| AK024850 | C2orf31 | | chromosome 2 open reading frame 31 |
| NM_006079 | CITED2 | | Cbp/p300-interacting transactivator with Glu/Asp-rich carboxy-terminal domain 2 |
| AK026498 | CYP2U1 | | cytochrome P450 family 2 subfamily U polypeptide 1 |
| NM_014762 | DHCR24 | | 24-dehydrocholesterol reductase |
| NM_012062 | DNM1L | | dynammin 1-like |
| NM_018456 | EAF2 | | ELL associated factor 2 |
| AK026517 | EHF | | ets homologous factor |
| AK022827 | EIF2C3 | | eukaryotic translation initiation factor 2C 3 |
| NM_012081 | ELL2 | | elongation factor RNA polymerase II 2 |
| AF111849 | ELOVL5 | | ELOVL family member 5 elongation of long chain fatty acids FEN1/Elo2 |
| AB020637 | ENDOD1 | | endonuclease domain containing 1 |
| NM_019018 | FAM105A | | family with sequence similarity 105 member A |

| | | |
|-----------|------------|--|
| AK024648 | FAM107B | family with sequence similarity 107 member B |
| AL137343 | FAM84A | family with sequence similarity 84 member A |
| NM_004117 | FKBP5 | FK506 binding protein 5 |
| AK024715 | FLJ21062 * | Hypothetical protein FLJ21062 * |
| NM_004476 | FOLH1 | folate hydrolase (prostate-specific membrane antigen) 1 |
| NM_020474 | GALNT1 | UDP-N-acetyl-alpha-D-galactosamine:polypeptide glutamate dehydrogenase 1 |
| NM_005271 | GLUD1 | glutamate dehydrogenase 1 |
| NM_002069 | GNAI1 | guanine nucleotide binding protein G protein alpha inhibiting activity polypeptide 1 |
| AB042410 | GPR88 | G protein-coupled receptor 88 |
| NM_001530 | HIF1A | hypoxia-inducible factor 1 alpha subunit basic helix-loop-helix transcription factor |
| NM_003543 | HIST1H4H | histone cluster 1 H4h |
| M60721 | HLX | H2.0-like homeobox |
| NM_014642 | IQCB1 | IQ motif containing B1 |
| NM_002241 | KCNJ10 | potassium inwardly-rectifying channel subfamily J member 10 |
| AL137384 | KIAA1109 | KIAA1109 |
| NM_001206 | KLF9 | Kruppel-like factor 9 |
| AF188747 | KLK2 | kallikrein-related peptidase 2 |
| NM_001648 | KLK3 | kallikrein-related peptidase 3 |
| NM_004917 | KLK4 | kallikrein-related peptidase 4 |
| AK026375 | LOC93622 * | Hypothetical protein BC006130 * |
| NM_005461 | MAFB | v-maf musculoaponeurotic fibrosarcoma oncogene homolog B avian |
| NM_000240 | MAOA | monoamine oxidase A |
| NM_003010 | MAP2K4 | mitogen-activated protein kinase kinase 4 |
| AB050049 | MCCC2 | methylcrotonoyl-Coenzyme A carboxylase 2 beta |
| AK021627 | MORC4 | MORC family CW-type zinc finger 4 |
| AF142409 | MS4A6A | membrane-spanning 4-domains subfamily A member 6A |
| NM_005956 | MTHFD1 | Methylenetetrahydrofolate dehydrogenase (NADP+ dependent) 1 |
| NM_016498 | MTP18 * | Mitochondrial protein 18 kDa * |
| NM_000662 | NAT1 | N-acetyltransferase 1 arylamine N-acetyltransferase |

| | | |
|-----------|---------|--|
| NM_006167 | NKX3-1 | NK3 homeobox 1 |
| AF039944 | NDRG1 | N-myc downstream regulated gene 1 |
| NM_006096 | NDRG1 | N-myc downstream regulated gene 1 |
| NM_005596 | NFIB | nuclear factor I/B |
| NM_020529 | NFKBIA | nuclear factor of kappa light polypeptide gene enhancer in B-cells inhibitor alpha |
| NM_016590 | PART1 * | prostate androgen-regulated transcript 1 * |
| NM_006810 | PDIA5 | protein disulfide isomerase family A member 5 |
| NM_016166 | PIAS1 | protein inhibitor of activated STAT 1 |
| AF070670 | PPM1A | protein phosphatase 1A formerly 2C magnesium-dependent alpha isoform |
| NM_004156 | PPP2CB | Protein phosphatase 2 formerly 2A catalytic subunit beta isoform |
| NM_002923 | RGS2 | regulator of G-protein signaling 2 24kDa |
| D16875 | RHOB | ras homolog gene family member B |
| AK001478 | RHOU | ras homolog gene family member U |
| AB051826 | RHOU | ras homolog gene family member U |
| NM_005627 | SGK1 | serum/glucocorticoid regulated kinase 1 |
| AB040914 | SHROOM3 | shroom family member 3 |
| NM_004595 | SMS | spermine synthase |
| NM_003082 | SNAPC1 | small nuclear RNA activating complex polypeptide 1 43kDa |
| NM_003104 | SORD * | sorbitol dehydrogenase * |
| NM_012449 | STEAP1 | six transmembrane epithelial antigen of the prostate 1 |
| AK026813 | STEAP2 | six transmembrane epithelial antigen of the prostate 2 |
| NM_005656 | TMPRSS2 | Transmembrane protease serine 2 |
| NM_005079 | TPD52 | tumor protein D52 |
| AF294628 | TWSG1 | twisted gastrulation homolog 1 Drosophila |
| NM_003115 | UAP1 | UDP-N-acetylglucosamine pyrophosphorylase 1 |
| NM_003359 | UGDH | UDP-glucose dehydrogenase |
| AK001647 | USP40 | ubiquitin specific peptidase 40 |
| AB020676 | WWC1 | WW and C2 domain containing 1 |
| AK022814 | ZBTB10 | zinc finger and BTB domain containing 10 |

| R1881 down-regulated genes | | |
|----------------------------|----------|---|
| NM_006006 | ZBTB16 | zinc finger and BTB domain containing 16 |
| AF025771 | ZNF189 | zinc finger protein 189 |
| AK026383 | NDRG1 | N-myc downstream regulated 1 |
| AL157445 | | cDNA clone * |
| D17210 | | cDNA clone * |
| NM_005688 | ABCC5 | ATP-binding cassette sub-family C CFTR/MRP member 5 |
| AK026288 | ATHL1 | ATH1 acid trehalase-like 1 yeast |
| NM_012342 | BAMBI | BMP and activin membrane-bound inhibitor homolog Xenopus laevis |
| NM_001197 | BIK | BCL2-interacting killer apoptosis-inducing |
| AF075110 | C14orf4 | chromosome 14 open reading frame 4 |
| NM_017766 | CASZ1 | castor zinc finger 1 |
| NM_001305 | CLDN4 | claudin 4 |
| AK024378 | FAM131A | family with sequence similarity 131 member A |
| NM_004480 | FUT8 | fucosyltransferase 8 alpha 1 6 fucosyltransferase |
| NM_002165 | ID1 | inhibitor of DNA binding 1 dominant negative helix-loop-helix protein |
| X69111 | ID3 | inhibitor of DNA binding 3 dominant negative helix-loop-helix protein |
| NM_006769 | LMO4 | LIM domain only 4 |
| NM_017572 | MKNK2 | MAP kinase interacting serine/threonine kinase 2 |
| NM_005377 | MYCL2 | v-myc myelocytomatosis viral oncogene homolog 2 (avian) |
| NM_006312 | NCOR2 | nuclear receptor co-repressor 2 |
| U90907 | PIK3R3 | phosphoinositide-3-kinase regulatory subunit 3 p55 gamma |
| AF113132 | PSAT1 | phosphoserine aminotransferase 1 |
| NM_004577 | PSPH | phosphoserine phosphatase |
| NM_015923 | SLC3A2 | solute carrier family 3, member 2 |
| NM_003943 | STBD1 | starch binding domain 1 |
| NM_003714 | STC2 | stanniocalcin 2 |
| AK000401 | TANC1 | tetratricopeptide repeat ankyrin repeat and coiled-coil containing 1 |
| AL133074 | TP53INP1 | tumor protein p53 inducible nuclear protein 1 |

| | | |
|---------------------------------------|---------|---|
| NM_003287 | TPD52L1 | tumor protein D52-like 1 |
| AF205437 | TRIB1 | tribbles homolog 1 Drosophila |
| U55055 | | Oral cancer candidate gene mRNA clone |
| NM_018588 | | hypothetical protein * |
| AK022971 | | cDNA clone * |
| Flutamide up-regulated genes | | |
| AB020637 | ENDOD1 | endonuclease domain containing 1 |
| NM_004117 | FKBP5 | FK506 binding protein 5 |
| AB042410 | GPR88 | G protein-coupled receptor 88 |
| NM_002923 | RGS2 | regulator of G-protein signaling 2 24kDa |
| AK026813 | STEAP2 | six transmembrane epithelial antigen of the prostate 2 |
| AB020676 | WWC1 | WW and C2 domain containing 1 |
| D17099 | | cDNA clone * |
| AL049966 | | cDNA clone * |
| Flutamide down-regulated genes | | |
| NM_002165 | ID1 | inhibitor of DNA binding 1 dominant negative helix-loop-helix protein |
| NM_002241 | KCNJ10 | potassium inwardly-rectifying channel subfamily J member 10 |
| NM_006854 | KDELR2 | KDEL Lys-Asp-Glu-Leu endoplasmic reticulum protein retention receptor 2 |
| AB028451 | NCOR1 | nuclear receptor co-repressor 1 |
| NM_001269 | RCC1 | regulator of chromosome condensation 1 |
| NM_000370 | TTPA | tocopherol alpha transfer protein |

* no approved HUGO symbol / name exist for this entry. This gene list includes the 107 transcripts of the PC346 cell lines AR-regulated signature, previously characterized in Chapter 4, plus 7 well-validated AR targets that failed to be detected by the referred microarray analysis: AGR2, DHCR24, FOLH1, KLK3 (PSA), KLK4, MAOA and NKX3-1.

Chapter 6

General Discussion

Introduction

Currently, prostate cancer detected at an early stage can be successfully eradicated by radical prostatectomy or radiotherapy, but no curative treatment exists for metastatic disease. Since the discovery that androgens promote the growth of prostate tumors, androgen ablation therapy, often combined with androgen receptor (AR) antagonists, is used to treat disseminated disease [1,2]. Unfortunately, this treatment is merely palliative as the cancer will eventually become resistant to hormonal therapy and recur [3,4]. Therefore, the development of prognostic markers and targeted therapies for advanced disease are urgent topics in prostate cancer research. To achieve this, a thorough understanding of the intrinsic mechanisms governing prostate cancer survival, proliferation and progression to hormone-refractory stage is crucial. Since the androgen receptor pathway is essential for prostate development, homeostasis and malignant outgrowth, a main goal of this study was to address the role of this pathway in the proliferation of hormone-resistant cells. Simultaneously, we were interested in identifying genes and pathways that besides the AR could also promote survival and growth of androgen-independent cells. In this process, the last aim was to identify genes and pathways involved in prostate cancer progression and potential disease markers.

AR pathway modifications during progression to hormone-refractory disease

To investigate the mechanisms of prostate cancer progression and identify potential disease markers the choice of a suitable model system is critical. During the course of this research, we used the PC346 cell line panel, a progression model especially established to study the mechanisms of hormone-refractory outgrowth that inevitably follows endocrine therapy of prostate cancer patients. The parental PC346C cell line was unique in the combination of primary tumor origin, *wild-type* AR expression, PSA secretion and androgen-responsive growth, replicating the hormone-naïve stage of prostate cancer. To mimic the mono and combined hormonal therapies offered to prostate cancer patients, the PC346C cells were cultured, for a minimum period of 2 years, in steroid-stripped medium either alone or supplemented with the AR antagonist flutamide. In this manner, three hormone-resistant sublines PC346DCC (monotherapy), PC346Flu1 and PC346Flu2 (combined-therapy) were established. The AR pathway status of all these cell lines was fully characterized using *in vitro* and *in vivo* hormone-stimulated growth assays, AR sequencing, AR and PSA quantification and AR reporter assays. Afterwards, microarray analysis on the PC346 cell line panel stimulated with the androgen analogue R1881 or the anti-androgen OH-Flutamide was performed to characterize the expression profile of AR target genes in prostate cancer cells.

While PC346C expresses a *wild-type* AR, requires androgens for optimal proliferation and is inhibited by the antiandrogen flutamide, the three hormone-resistant sublines acquired a variety of AR modifications: overexpression, mutation and down-regulation. Two main conclusions can already be drawn from the development of these cell lines and the xenograft model system described in Chapter 2: (i) AR modifications are frequent events following long-term hormonal manipulations and (ii) the AR pathway seems to play an important role in prostate cancer progression, since AR adaptations associated with hormone-refractory growth. In addition, by reproducing common AR modifications observed in hormone-refractory disease, the *in vitro* PC346 cell lines provide a valuable model system for the study of prostate cancer progression.

AR gene amplification is probably the most common AR modification in prostate cancer, being detected in up to 30% of hormone-refractory [5,6,7]. It is still not known how AR overexpression can activate the receptor under androgen-depleted conditions. Hypothetically, two mechanisms are possible: increased sensitivity to residual androgen levels or constitutive ligand-independent activation. AR overexpression is represented in our panel by the PC346Flu1 cell line. Although FISH analysis did not show genomic AR amplification in PC346Flu1, elevated AR mRNA levels were measured by RT-PCR, indicating increased transcriptional activity or RNA stability as probable modes of AR up-regulation. PC346Flu1 expressed a *wild-type* AR sequence but expression levels of the receptor were 4-fold higher than in the parental PC346C. This AR overexpression coincided with a 10-fold higher AR reporter activity and a “super-activation” of AR target genes in the microarray analysis, in response to the synthetic androgen R1881. Some authors have proposed that increased AR levels not only sensitised the receptor to residual androgen concentrations but also conferred agonistic activity to AR antagonists [8,9]. However, PC346Flu1 proliferation was optimal in the absence of androgens and was unaffected by flutamide supplementation. The lack of agonistic activity of flutamide on PC346Flu1 cells was further confirmed in the AR reporter assays and expression microarray analysis. Likewise, Konkontis *et al.* also failed to replicate the antagonist to agonist conversion in hormone-refractory LNCaP-104R cells, which express 15-fold more AR protein than respective androgen-sensitive parental LNCaP-104S cells. Furthermore, whereas proliferation of LNCaP-104S cells was inhibited by the AR antagonist casodex the growth of LNCaP-104R cells was not [10,11]. These results suggest that the proliferation of PC346Flu1 cells, as well as LNCaP-104R, is not dependent on residual androgens, but is maintained by constitutive AR activation resistant to AR antagonists. This view is supported by findings from Dehm *et al.*, which, by introducing disabling mutations in the ligand-binding domain, showed that ligand binding was not necessary for constitutive AR activation in C4-2 cells [12]. The authors also observed increased transactivation activity of the AR N-terminal domain in these cells, compared to parental LNCaP. Similar processes could be playing a role in constitutive AR activation in PC346Flu1 cells. All together, AR overexpression may lead to different mechanisms of activation, depending on the background of the cells, the type or the duration of the androgen-depletion treatment.

Curiously, growth of PC346Flu1 was inhibited by physiologic concentrations of androgens both *in vitro* and *in vivo*. This paradoxical growth inhibitory effect of androgens was previously reported in various hormone-resistant LNCaP sublines with similar AR overexpression, being preceded at earlier passages by hypersensitivity to low levels of androgens [9,10,11,13]. A possible explanation for this phenomenon resides on the Janus-faced functions of the AR, on one hand promoting survival and proliferation, on the other hand inducing cellular differentiation and maturation [14]. In this context, super-activation of the AR may tilt the balance towards terminal differentiation, thus hampering cell growth [15].

The EHF transcription factor is an AR up-regulated gene that was strongly repressed in PC346Flu1 in flutamide supplemented selection medium, when compared to the R1881 supplemented parental PC346C. EHF is a good candidate for the growth suppressive effect of androgens on PC346Flu1 subline as: (i) it is epithelial cell specific, (ii) involved in glandular differentiation, (iii) frequently down-regulated in prostate tumor

specimens and (iv) ectopic expression in prostate cancer cells inhibited clonogenic survival and induced apoptosis [16,17,18,19]. Whether EHF indeed suppresses PC346Flu1 growth in the presence of androgens still has to be established with future RNAi knockdown experiments. Previous reports showed that this growth suppressive effect of androgens was not due to increased apoptosis, but to G1 cell cycle arrest, accompanied by an increase in cdk inhibitors p21^{Waf/Cip1} and p27^{Kip} [10,15]. The authors suggested that androgen-induced down-regulation of c-Myc oncogene levels or up-regulation of the tumor suppressor GADD45 γ could take part in this process [11,20]. The mechanism by which androgens regulate c-Myc or GADD45 γ levels in those cells, or whether EHF plays a role in this process, are as yet undefined and deserve future attention.

A crucial question remains: is the AR pathway indeed required for PC346Flu1 growth or is the overexpressed AR just a bystander, possibly only relevant in the initial response to androgen-deprivation? The fact that expression of AR target genes was not significantly decreased in PC346Flu1, compared to parental PC346C, suggests that AR pathway may still be maintained in the absence of androgens. Previous AR knockdown experiments, using RNA interference technology, have shown induction of apoptosis and growth inhibition, not only in hormone-dependent cells but also, in multiple castration-resistant cells lines and xenografts [21,22,23,24,25,26]. Although similar experiments are necessary to conclusively relate the AR to the proliferation of PC346Flu1, the results above confirm the importance of the AR pathway in hormone-refractory growth.

Another hormone-resistant subline investigated in our study, PC346Flu2, was growth stimulated by both R1881 and the antiandrogen hydroxyflutamide. AR sequencing revealed the T877A mutation, well-known for its ability to broaden the AR activity to diverse non-androgenic ligands including flutamide [27,28]. Thus, the PC346Flu2 cell line replicates another common AR modification (activating mutation) detected in about 10% of hormone-refractory tumors. The detection of the T877A AR mutation also coincided with a similar gene expression response to both R1881 and flutamide in the microarray analysis, although the stimulatory effect of the latter was weaker. As expected, when directly compared to the parental PC346C, PC346Flu2 was the least divergent subline, which is in agreement with the hypothesis that the growth of both these cell lines is regulated by ligand-activated AR pathway. However, basal growth of PC346Flu2 in the absence of R1881 or flutamide is retarded but still 2-fold faster than the parental PC346C, indicating additional mechanisms may be involved in either activating the AR or alternative survival pathways. The control of AR function involves interaction with a number of co-factors that regulate AR transcriptional activity. Alterations in AR co-regulators, such as SRC1, TIF2, NCOR1 or NCOR2, have been described in hormone-refractory disease [29,30]. In fact, nuclear receptor interacting protein 1 (NRIP1), a repressor of AR transactivation [31,32], has been found to be down-regulated in PC346Flu2, and could represent a possible mechanism to adapt AR signaling to residual androgens levels in the medium. Another possibility is the production of androgens by the cancer cells themselves [33,34]. For our PC346 cell lines this is an improbable mechanism, as no hint of steroidogenic enzymes modulation was detected in the expression microarray analysis. As for PC346C, the AR pathway

seems to play an active role in PC346Flu2 proliferation, but only AR knockdown experiments can unequivocally show if it is also driving the basal growth of unstimulated PC346Flu2 cells.

In contrast, the PC346DCC cell line expresses very little AR and PSA and showed background levels of AR reporter activity, which was not up-regulated by R1881. This cell line exhibited fast growth that was insensitive to androgen depletion or antiandrogen treatment. Curiously, a novel mutation was detected in codon 311 of PC346DCC AR, which resulted in a Lys to Arg substitution. However, AR reporter assays showed no evidence of altered transactivation properties of this mutated receptor, which had a similar response as the wild-type receptor to R1881 and hydroxyflutamide (unpublished data). Furthermore, in a microarray analysis, PC346DCC did not show differences in gene expression in response to R1881 stimulation. Altogether, these results suggest that PC346DCC has bypassed the AR pathway and that alternative growth pathways guide survival and proliferation of these cells. Expression profiling of PC346DCC confirmed down-regulation of AR-target genes and three candidates were chosen for their potential involvement in AR pathway bypass: VAV3, TWIST1 and DKK3. These candidates were selected based on the consistent deregulation across the multiple prostate cancer metastasis databases analysed and potential pathological function. In this manner, VAV3 and TWIST1, found to be overexpressed in PC346DCC cells and metastasis datasets, are potential oncogenes, whereas the down-regulated DKK3 is a putative tumor suppressor.

VAV3 is a GTPase guanine nucleotide exchange factor that mediates receptor protein tyrosine kinase signaling [35,36]. It is activated by growth factor receptors, such as EGFR, PDGFR, IR and IGF1R, and interacts with respective downstream signaling molecules including Shc, Gbr2, PLC and PI3K [35,36,37]. VAV3 has been previously implicated in prostate cancer, where it has been detected in increased amounts and may cross-talk with the AR pathway, stimulating hormone-refractory cell growth [38,39,40]. Furthermore, a mouse model targeting constitutively active VAV3 expression to the prostate induced prostate cancer and inflammation, suggesting a direct role of VAV3 in prostate cancer development [41]. Surprisingly, in our prostate cancer patient cDNA panel, VAV3 expression was down-regulated during prostate cancer progression and in hormone-refractory samples. A possible explanation for this unexpected finding could lie on the multiple VAV3 splice variants. There are 3 major transcripts of VAV3: the full-length VAV3 alpha, the super-active VAV3 beta, and the short VAV3.1 variant [35,36,42]. The quantitative-PCR probes used in our study target the last 2 of the 27 exons in VAV3 gene, and it is possible that they capture preferentially the short C-terminal VAV3.1 transcript. This short VAV3.1 variant lacks guanine nucleotide exchange activity due to the truncation of N-terminal domains. It is expressed in many tissues and is the major variant in the prostate [36,42]. Due to the lack of the activation domains the VAV3.1 variant is not oncogenic and it has been proposed to function as a dominant negative of other VAV family members [36,42]. In this context, a decrease in the VAV3.1 variant could actually result in increased activity of oncogenic VAV proteins. Therefore, it is essential to characterize the different VAV3 variants during prostate cancer progression. At the moment, a genome-wide exon microarray analysis is ongoing on our prostate tissue panel used in the quantitative-PCR assays. Among the other

genes, VAV3 is well-covered by the microarrays used in this study, which will help us identify the major transcript variants in the prostate and how their balance is affected in the different stages of prostate cancer.

TWIST1 is a helix-loop-helix transcription factor, highly expressed in many types of human cancer, and involved in the processes of cancer cell survival, proliferation and migration [43,44,45,46,47]. In particular, TWIST1 appears to regulate metastasis by promoting an epithelial-mesenchymal transition through down-regulation of E-cadherin [48,49]. Recently, increased TWIST1 levels were also detected in prostate tumors, correlating with Gleason-grade and metastasis [48,49]. The function of TWIST1 in prostate cancer progression was further supported by the suppressive effect of TWIST1 inactivation on migration and invasion abilities of hormone-refractory prostate cancer cells [49]. All together, these results made it a good candidate for the bypass of the AR pathway in PC346DCC cells. Analysis of TWIST1 expression in our prostate tumor panel confirmed up-regulation in prostate cancer and metastasis, but the expression levels did not correlate with Gleason-score or progression to hormone-refractory disease. Basically, our results indicate that increased TWIST1 expression by itself is not a representative mechanism of hormone-refractory growth in clinical samples. However, like VAV3, TWIST1 was also shown to crosstalk with growth receptor signaling pathways, such as EGF and IGF1, suggesting that activation of these alternative pathways could be the effector mechanism in the progression to androgen independence [50,51]. Alternative survival and growth pathways bypassing the AR will be discussed in a separate section below.

The last candidate gene analysed, DKK3, belongs to the evolutionary conserved Dickkopf gene family, implicated in the modulation of Wnt/beta-catenin signaling [52]. DKKs play an important role in vertebrate development, bone formation, Alzheimer's disease and cancer. Down-regulation of DKK3 is frequently detected in multiple human cancers, including prostate tumors, which has been associated with promotor methylation [53,54,55]. In the prostate, DKK3 seems to play a role in acinar differentiation and malignant growth, by inducing apoptosis and inhibits prostate cancer cell proliferation [56,57]. In our human prostate cancer panel, DKK3 expression was significantly decreased in primary prostate tumors and metastasis, but did not associate with tumor progression nor hormone-refractory disease. These results suggest that DKK3 down-regulation is probably an early event in prostate carcinogenesis. In conclusion, activation of oncogenes and tumor suppressor down-regulation may be driving PC346DCC survival and proliferation, but TWIST1 and DKK3 by themselves do not appear to represent common mechanisms of hormone-refractory growth in clinical samples.

To follow alterations in the AR pathway during the development and progression of prostate cancer, the AR-regulated gene signature from PC346 cells was linked to seven microarray databases of normal prostate, primary tumor and metastatic cancer material (Chapter 4). One cluster consisted of AR up-regulated genes that were overexpressed in metastases and were involved in cell survival, proliferation, cytoskeletal remodeling and adhesion, all crucial functions in tumor progression and invasion. However, the major cluster consisted of AR up-regulated genes, which were often overexpressed in primary tumors but down-regulated in metastasis. This cluster is

enriched for genes involved in differentiation and secretory function of the prostate, functions that are redundant and disadvantageous for a rapidly propagating tumor.

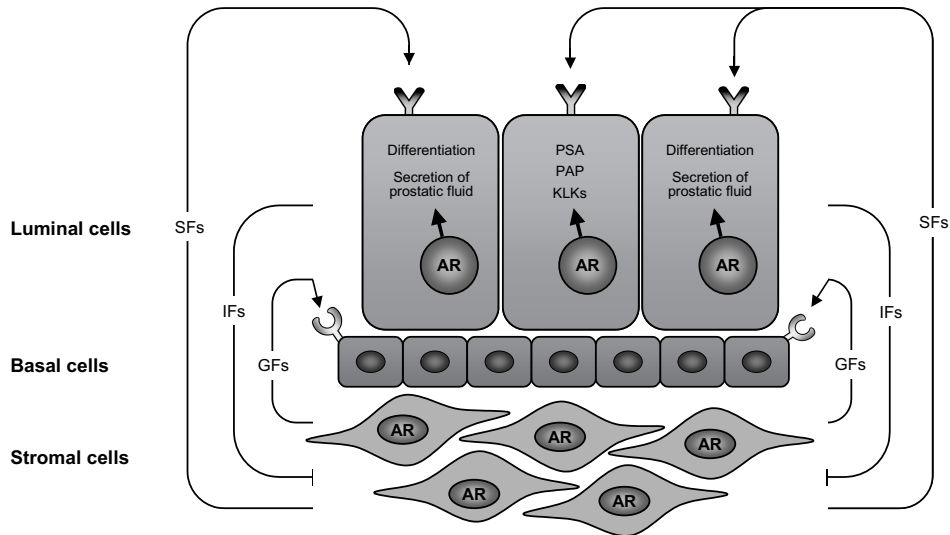


Figure 1 - Mechanism of AR function on different cell types in the healthy prostate. AR is expressed in prostate stromal cells and luminal epithelial cells, but not in basal cells. The basal cell compartment contains a self-renewal population responsible for restoring aged or injured cells, which will acquire AR expression as they commit to the luminal cell lineage. AR expression will further drive differentiation of luminal cells and maintain their function in the production and secretion of prostatic fluid components, including prostate specific antigen (PSA), prostate acid phosphatase (PAP) and several kallikreins (KLKs). Furthermore, androgens indirectly promote proliferation of basal cells through regulation of paracrine growth factors (GFs) expression by stromal cells. Stromal cells also produce survival factors (SFs) that inhibit apoptosis of luminal epithelial cells. To prevent the epithelial cells from proliferating indefinitely in the presence of androgens, a negative feedback signal, from the luminal to the stromal cells, regulates the production of stromal growth factors. (IFs): inhibitory factors.

The view of the AR pathway as a driving force for cancer growth and proliferation, may be over-simplistic as mounting evidence suggests that this pathway may have different functions in different stages of the disease. Previously, Hendriksen *et al.* also observed a partial down-regulation of the AR pathway in advanced disease, by using the androgen-response program from LNCaP cells to interrogate a set of prostate cancer xenografts and Lapointe's patient derived samples [58]. Two subsequent studies, using distinct bioinformatics approaches, further confirmed an attenuated androgen signaling signature in high-grade and metastatic prostate cancer [59,60]. Finally, Sterbis *et al.* showed that decreased tissue PSA mRNA was associated with increased risk of recurrence after radical prostatectomy [61]. This is not the case for PSA levels in serum, which can be explained by the fact that serum levels reflect the increasing tumor burden during progression, whereas tissue levels denote alterations in the tumor cell

microenvironment. Therefore, attenuation of the AR pathway in advanced stages of prostate cancer was observed in multiple studies and may reflect a real mechanism for progression rather than an artifact of the *in vitro* system used in the present study. This attenuation of the AR pathway in advanced stages of prostate cancer may reflect tumor dedifferentiation, but whether it is a cause or the result still has to be clarified.

Two recent studies support opposing roles of the AR in prostate cancer cells by showing that: (i) knockdown of the AR in epithelial hormone-refractory CWR22rv1 cells increased invasion in bone lesion assays and *in vivo* mouse models; (ii) whereas restoration of AR in AR-negative PC3 cells decreased invasion; (iii) mice lacking prostate epithelial AR have increased apoptosis in secretory luminal cells but increased proliferation of basal-intermediate cells; (iv) AR knockdown in both prostate stroma and epithelium of ARKO-TRAMP mouse models resulted in smaller primary prostate tumors than *wild-type* TRAMP littermates; (v) whereas targeted AR knockdown limited to prostate epithelial cells resulted in increased tumor growth compared to *wild-type* TRAMP mice [62,63]. Based on these results, the authors suggested that the AR might function both as tumor suppressor and proliferator in prostate cancer, depending on the cell type targeted. Thus, the AR may promote differentiation of luminal secretory cells, suppress growth of basal-intermediate cells and inhibit metastasis but, simultaneously, promote survival and proliferation of prostate tumor epithelium by regulating paracrine stromal factors (Fig. 1) [64].

Alternative survival and growth pathways in hormone-refractory prostate cancer

In addition to the androgen receptor, other pathways have been shown to stimulate prostate cancer growth. For example, EGF, IGF1, HGF, KGF, FGFs, IL6 and/or respective receptors are often overexpressed in prostate cancer, in particular in hormone-refractory samples [64]. These growth factors are normally secreted by stromal cells, some under androgen regulation, binding to receptors expressed on neighbouring epithelial cells. However, in hormone-refractory cells a shift has been reported from paracrine secretion to autocrine expression of these growth factors by epithelial cells [64]. Deregulation of growth factor pathways was further substantiated by the present study, where we observed variation not on the expression level of growth factors and receptors, but of multiple other members of these signaling cascades, among which the oncogenes VAV3 and TWIST1. The effect of peptide growth factors/cytokines on androgen independent proliferation of prostate cancer cells is mainly mediated via the Ras/MAPK, PI3K/AKT and STAT3 signaling cascades [65,66]. These signaling pathways may directly activate transcription of genes involved in cell survival, proliferation and migration, but may also indirectly activate the AR pathway in a ligand-independent manner (Fig. 2). In the absence of androgens, MAPK and AKT kinases may induce AR phosphorylation and activation, whereas STAT3 can bind ligand-free AR and facilitate its translocation to the nucleus. Both these mechanisms ultimately result in ligand-independent expression of AR target genes [65,66]. Thus cytokines and peptide growth factors may function as alternative survival/growth pathways, for example in the subgroup of AR negative prostate tumors, and/or as an adaptation of AR pathway by preserving AR activity under androgen ablation conditions. Recent reports have implicated Src, a member of the Src-family kinases, in the proliferation of hormone-refractory tumors. Src kinase was found to be overexpressed in prostate cancer, where

Src inhibitors decreased proliferation and invasion of cell lines and xenografts [67,68]. Src-family kinases are nonreceptor protein tyrosine kinases responsible for signal transduction in many cellular and oncogenic processes. Src kinases are activated upon binding to cell surface receptors, such as G-protein coupled receptors, growth factor receptors and integrins, or other intracellular nonreceptor protein kinases [67,69]. In turn, activated Src kinases signal via the MAPK, PI3K, STAT3 and FAK pathways (Fig. 2). Src kinases are also activators of VAV3 and TWIST1, either directly by phosphorylating and releasing inhibitory tyrosine Y173 of VAV3, or indirectly by activating STAT3, a transcription activator for TWIST1 [70,71]. These results link the Src pathway to growth factor pathways and to our candidate genes selected for hormone-refractory progression. Previous studies have shown that decreased AR activity in hormone-refractory disease correlated with increased Src activity, and that Src activation induced androgen-independent growth [60]. These results reveal the Src pathway as a potential therapeutic target in prostate cancer and justify future clinical trials with Src inhibitors in hormone-refractory disease.

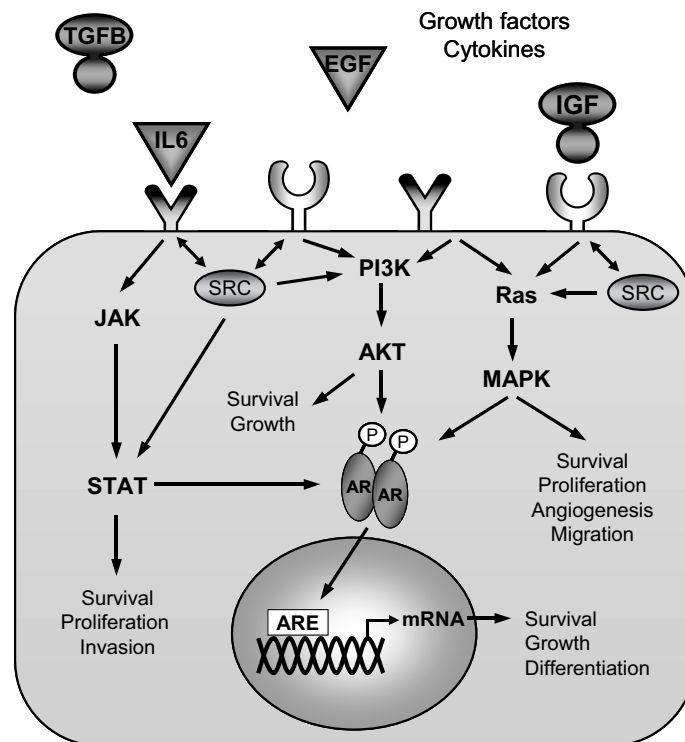


Figure 2 - AR pathway crosstalk. Growth factors and cytokines binding to membrane receptors on prostate cancer cells activate, among others, Ras/MAPK, PI3K/AKT and JAK/STAT signaling cascades. Intracellular kinases may then phosphorylate and activate the AR, leading to androgen-independent transcription of AR target genes. Furthermore, these pathways by themselves are also involved in survival, growth and invasion processes.

Hypothetical mechanism of prostate cancer progression

The results of the present study, combined with our current knowledge of prostate cancer disease, can be summarized in the mechanistic model proposed in Fig. 3. In this model, the AR pathway plays a crucial role in the normal prostate and initial stages of prostate malignancy. However, the AR has dual cellular functions, dependent on the cell type and context on which it is activated: on one hand it promotes survival and proliferation, on the other hand it induces cellular differentiation and maturation. In healthy settings, the AR maintains prostate function through a delicate balance between cell survival and differentiation. Malignant outgrowth is triggered by the switch from androgen-dependent survival to androgen-stimulated cellular proliferation. Possible candidates for initiating this process are gene fusions between androgen-regulated genes and ETS transcription factor family members [72,73,74]. The most frequent of these rearrangements is the TMPRSS2-ERG fusion, which can be detected in as much as the half of prostate tumors [75]. So far, multiple ETS family members (ETV1, ETV4, ETV5, ELK4 or FLI1) and 5' fusion partners (SLC45A3, ACSL3, HERV-K_22q11.3, HNRPA2B1, C15orf21, KLK2, CANT1, FLJ35294 and DDX5) have also been identified [72,73,74,76]. However, ectopic overexpression of ERG or ETV1 in prostate epithelial cells RPWE and PrEC had no effect on cell proliferation, anchorage-independent growth nor did it cause cell transformation. Instead, it made the epithelial cells invasive through Matrigel assays. Conversely, ERG or ETV1 knockdown in VCaP and LNCaP cells, respectively, significantly inhibited invasion without affecting proliferation [73,77]. Furthermore, prostate specific expression of ERG or ETV1 in mice induced prostatic intraepithelial neoplasia (PIN) but it did not progress into carcinoma [73,77]. In contrast, ETS translocations are not frequently found in association with PIN lesions in human prostate [78]. These results indicate that ERG or ETV1 overexpression alone is not sufficient to initiate neither prostate neoplasia nor human PIN. Tomlins *et al.* proposed that preceding genetic lesions deregulate cellular proliferation resulting in PIN, whereas ETS fusions drive the transition to carcinoma [79]. Recently, two independent transgenic mouse models revealed a cooperation between TMPRSS2:ERG and PTEN loss in the transition from prostatic intraepithelial neoplasia (PIN) to prostate adenocarcinoma [80,81]. In addition, these studies have shown that PTEN loss/down-regulation and ETS gene fusions co-occur in early disease, thus confirming that this mechanism may also be involved in prostate cancer initiation in humans. Neither TMPRSS2-ERG nor TMPRSS2-ETV1 fusions have been detected in PC346 cell lines, and it is unclear which mechanism drives androgen-sensitive growth of PC346C cells. Nevertheless, it is still possible that other less common fusion partners that we have not tested are involved.

At early stages, when tumors are well differentiated, AR signaling simultaneously stimulates tumor growth and maintains expression of genes involved in prostate function and secretion of prostatic fluid. As cancer progresses, the AR pathway is attenuated due to down-regulation of AR target genes involved in prostate cell differentiation and maturation. Hormonal therapy also plays a role in this AR pathway attenuation, which will eventually culminate in fast-growing, poorly-differentiated tumors. Nevertheless, AR knockdown experiments suggest that the AR pathway may remain vital for most hormone-refractory cells, as it induced apoptosis and inhibited growth of multiple castration-resistant cell lines and xenografts [21,22,23,24,25,26]. Upon

hormone therapy, androgen-refractory cells may resume growth by adaptations of the AR pathway and/or activation of alternative growth pathways (Fig. 3) [82]. Our cell line model represents two of these AR modifications: AR mutation (PC346Flu2) and AR overexpression (PC346Flu1), as well as AR pathway bypass through activation of oncogenes and tumor suppressor down-regulation (PC346DCC). During the preparation of this manuscript, a novel mechanism for androgen-receptor adaptation was discovered, implicating constitutively active truncated AR variants in hormone-refractory growth. These variants may be produced either by alternative splicing or by proteolytic cleavage mediated by calpain [83,84,85]. In either case, truncated AR, lacking the C-terminal LBD domain, is produced that exhibits constitutive activity independent of ligand. We have not yet investigated whether such truncated variants are present in the PC346 panel, and the possibility remains that such phenomenon could be responsible for PC346Flu1 or PC346Flu2 proliferation in the absence of androgens.

Prostate cancer progression markers

The last goal of this study was to identify markers for the diagnosis and/or prognosis of prostate cancer, or with potential value for targeted therapies. Currently, the most widely used cancer marker is prostate specific antigen (PSA). The serum PSA test is used not only in the detection of prostate cancer, but also in the follow up of tumor recurrences after therapy [86,87]. However, the PSA test is neither specific, as serum PSA levels may also be increased by other prostatic diseases, such as benign prostatic hyperplasia (BPH) or prostatitis, nor can it predict tumor progression [87,88,89].

In the present study, following expression microarray analysis, 6 candidate genes were selected for real-time PCR quantification in a distinct set of prostate cancer samples. This selection included 3 androgen-regulated genes, ACSL3, ENDOD1, MCCC2, and 3 genes unaffected by androgens, VAV3, TWIST1 and DKK3. All these genes showed deregulation in prostate cancer, but their diagnostic/prognostic value was limited due to high inter-individual variation and poor separation across the different disease states. The best separation between normal prostate tissue and prostate cancer samples was seen for the expression of the tumour suppressor DKK3, which showed a sensitivity of 63% and specificity of 95% (data not shown). Furthermore, DKK3 is a secreted protein, which facilitates quantification in serum, urine or prostatic fluid. But its down-regulation in cancer makes it technically less suitable as a diagnosis tool. On the other hand, VAV3 could be an interesting prognostic marker as its expression decreased stepwise during progression to invasive prostate cancer and hormone-refractory disease. Furthermore, low VAV3 expression associated with decreased metastasis-free survival. These were unexpected findings as VAV3 belongs to a family of oncoproteins and showed increased expression levels in metastatic prostate tumors across multiple public microarray databases. A possible explanation for this discrepancy was described above and could lie on the fact that VAV3 has multiple splice variants. Therefore, before VAV3 may be considered as a prognostic tool, one must first clarify the reason for such discrepancies and how the different splice variants contribute to prostate cancer progression. In conclusion, an optimal diagnostic marker must be simultaneously sensitive, specific for prostate cancer and detectable by non-invasive methods. On the other hand, an optimal prognostic marker should, at an earlier disease stage, be able to distinguish the indolent from the life threatening tumors, or to predict

the response to therapy. Of the six candidates analysed in the present study, DKK3 and VAV3 had the most potential as disease markers, but further optimisation and validation will be necessary to develop reproducible and robust assays. In addition, all the tested candidate genes showed deregulated expression patterns in prostate malignancy, thus providing important clues on the mechanisms of prostate cancer development and progression.

Therapeutical implications

Several findings made during the course of this study may have repercussions in our understanding of prostate cancer progression and in the way we treat hormone-refractory disease. In this sense, we showed that:

(i) AR modifications occurred in the vast majority of castration-resistant cell lines and xenografts subjected to androgen ablation and/or antiandrogen treatment. Selective pressure from hormonal treatment may enrich for AR amplification and AR mutations that are activated by non-androgenic compounds, such as antiandrogen flutamide (Chapters 2 and 3). These results suggest that the AR pathway plays an important role in prostate cancer proliferation but current hormonal therapy is not capable of efficiently shutting down AR signaling. The failure of these therapies is not caused only by the selection of activating AR mutations. Constitutively active AR variants originating from alternative splicing or proteolytic cleavage, ligand-independent AR activation by crosstalk with other intracellular signaling cascades, local androgens production by prostate tumor cells and alterations in AR co-regulators may all activate the AR under hormone blockade therapy (Fig. 3) [82]. Recently, new generation antiandrogens, MDV3100 and RD162, have been produced for the treatment of advanced prostate tumors. These new compounds induced significant responses in 40% of the castration-resistant patients, reaching 50% decline in PSA, and are now entering a phase III trial. But whether these effects can be maintained longer than the reported 3 months is still unknown [90]. Both MDV3100 and RD162 target the ligand-binding domain of the AR, and may not be efficient in blocking constitutive ligand-independent AR activity. Therefore, compounds capable of targeting the AR transactivation or DNA-binding domains might prove more efficient in blocking AR activity and deserve more attention in drug development.

(ii) Increased AR levels may result in a hyper-responsive receptor, active in the absence of ligand and/or sensitive to residual androgen levels. AR overexpression in PC346Flu1 cell line resulted in growth inhibition in the presence of physiological concentrations of ligand (Chapters 2 and 3). This androgenic repression phenomenon could be a consequence of AR induced cellular differentiation and a possible mechanism underlying hormonal therapy withdrawal responses observed in some patients.

(iii) AR pathway is attenuated in advanced metastatic prostate cancer, which may reflect the hormonal therapy given to disseminating tumors. This down-regulation is selective and includes genes involved in development and cellular differentiation, of which expression is less favourable during accelerated growth and invasion (Chapter 4). These results and the observed growth inhibitory effect of androgens on hyper-reactive hormone-refractory cells suggest intermittent hormone therapy, in cycles blocking growth and restoring androgen-regulation, as a potential treatment option to retard

tumor progression. The feasibility of intermittent hormone therapy is under investigation in multiple clinical trials [91]. Although final data from phase III trials are still due, in the past years over a dozen phase II trials, including more than 2000 patients, have evaluated the efficacy and safety of this treatment modality. Despite beneficial effects on quality of life and reduced morbidity, preliminary results show no evidence supporting a delay of the progression to hormone-refractory disease. Nevertheless, this does not exclude the possibility that intermittent therapy may delay progression of specific subgroups of tumors, in particular those exhibiting AR amplification/up-regulation. Furthermore, it is also possible that the study protocols still need further optimization, for example on the type of hormonal therapy offered, when to commence the treatment and the duration of the on- and off-periods in each cycle. Since cell line and xenograft studies show that the growth inhibitory effects are reached at higher androgen concentrations than those that stimulate growth, it is also important to optimize the extent of testosterone recovery in the off-treatment periods.

(iv) Activation of cytokine and peptide growth factors pathways is a possible mechanism of androgen-independent growth (Chapter 5). These pathways signal via Src kinase, MAPK, PI3K and STAT3 cascades, among others, which in turn may directly induce survival, proliferation and invasion processes, or phosphorylate and activate the AR or its coregulators (Fig. 2). Additionally, Src kinase is a key regulator of healthy bone turnover and appears to be involved in prostate cancer metastasis to the bone [92,93,94]. In this sense, Src, MAPK, PI3K or STAT3 inhibitors have the potential to target simultaneously both AR and alternative growth pathways, thus providing an interesting therapeutical approach for hormone-refractory prostate cancer. Inhibitors targeting these pathways, such as AZD6244 (ras/MAPK), AZD0530 (Src), perifosine (PI3K/AKT) or INCB18424 (JAK/STAT), are currently being tested in clinical trials on a variety of tumors [67,95,96,97]. The available data on prostate cancer trials is disappointing. A phase II trial of the Src inhibitor AZD0530 in patients with advanced hormone-refractory disease showed limited clinical efficacy [98]. Also, the AKT inhibitor perifosine had modest clinical activity in biochemically recurrent prostate cancer [96]. The same is true for Iressa (gefitinib), a selective tyrosine kinase inhibitor specific for epidermal growth factor receptor [99]. Nevertheless, most of these studies included a small number of patients with late hormone-refractory disease, and it remains to be tested how these drugs perform in earlier disease stages or together with androgen ablation therapy. Novel compounds with enhanced *in vitro* and *in vivo* potency are currently under development, which, in combination with hormonal therapies, may improve the treatment of advanced prostate cancer.

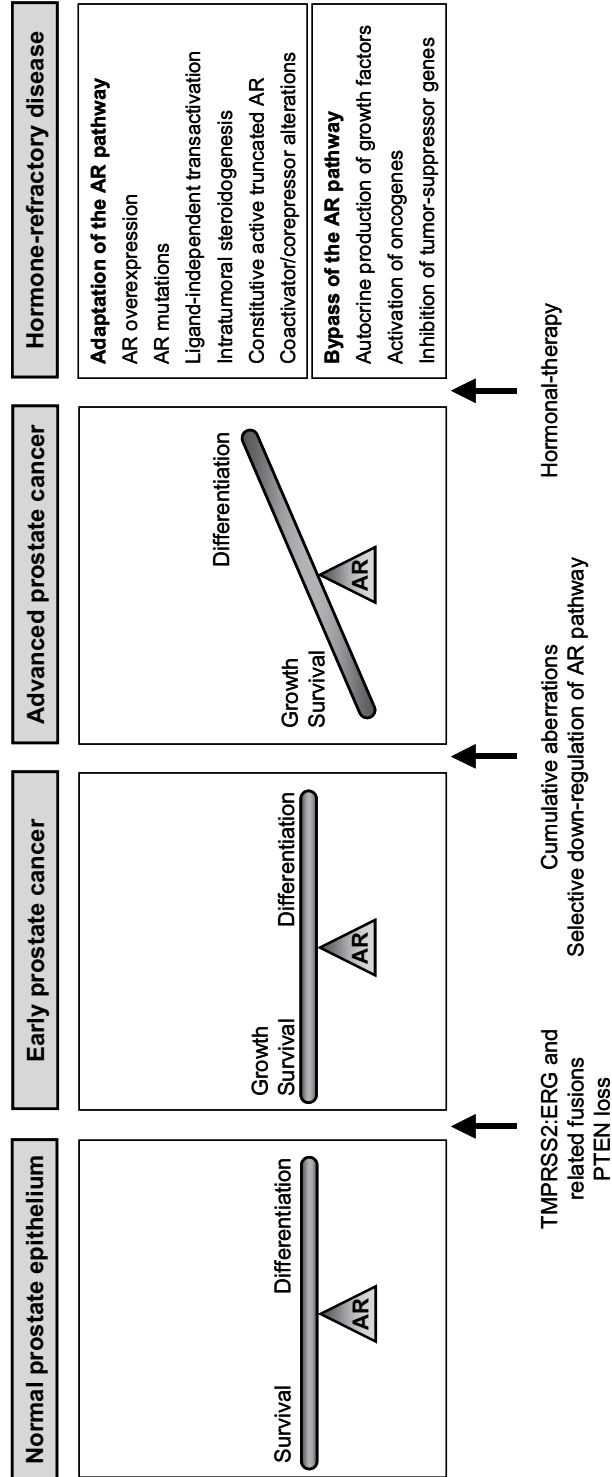


Figure 3 - Mechanistic model of prostate cancer progression. In normal prostate epithelium there is equilibrium between survival and differentiation functions of the AR. The switch from androgen-dependent survival to androgen-responsive proliferation marks the development of prostate cancer. Cooperation between TMPRSS2:ERG (or related fusions) and PTEN loss is a possible initiating event in prostate tumorigenesis. In advanced stages, the AR pathway is selectively modulated and the balance is tilted towards tumor growth. Hormonal-therapy is offered to patients with advanced invasive disease, but the tumors will eventually become resistant to androgen ablation/blockade by either adapting or bypassing the AR pathway.

REFERENCES

1. Huggins C, Hodges CV (2002) Studies on prostatic cancer: I. The effect of castration, of estrogen and of androgen injection on serum phosphatases in metastatic carcinoma of the prostate. 1941. *J Urol* 168: 9-12.
2. Sharifi N, Gulley JL, Dahut WL (2005) Androgen deprivation therapy for prostate cancer. *Jama* 294: 238-244.
3. Crawford ED, Eisenberger MA, McLeod DG, Spaulding JT, Benson R, et al. (1989) A controlled trial of leuprolide with and without flutamide in prostatic carcinoma. *N Engl J Med* 321: 419-424.
4. Eisenberger MA, Blumenstein BA, Crawford ED, Miller G, McLeod DG, et al. (1998) Bilateral orchiectomy with or without flutamide for metastatic prostate cancer. *N Engl J Med* 339: 1036-1042.
5. Brown RS, Edwards J, Dogan A, Payne H, Harland SJ, et al. (2002) Amplification of the androgen receptor gene in bone metastases from hormone-refractory prostate cancer. *J Pathol* 198: 237-244.
6. Koivisto P, Kononen J, Palmberg C, Tammela T, Hyytinen E, et al. (1997) Androgen receptor gene amplification: a possible molecular mechanism for androgen deprivation therapy failure in prostate cancer. *Cancer Res* 57: 314-319.
7. Linja MJ, Savinainen KJ, Saramaki OR, Tammela TL, Vessella RL, et al. (2001) Amplification and overexpression of androgen receptor gene in hormone-refractory prostate cancer. *Cancer Res* 61: 3550-3555.
8. Chen CD, Welsbie DS, Tran C, Baek SH, Chen R, et al. (2004) Molecular determinants of resistance to antiandrogen therapy. *Nat Med* 10: 33-39.
9. Culig Z, Hoffmann J, Erdel M, Eder IE, Hobisch A, et al. (1999) Switch from antagonist to agonist of the androgen receptor bicalutamide is associated with prostate tumour progression in a new model system. *Br J Cancer* 81: 242-251.
10. Kokontis JM, Hay N, Liao S (1998) Progression of LNCaP prostate tumor cells during androgen deprivation: hormone-independent growth, repression of proliferation by androgen, and role for p27Kip1 in androgen-induced cell cycle arrest. *Mol Endocrinol* 12: 941-953.
11. Kokontis J, Takakura K, Hay N, Liao S (1994) Increased androgen receptor activity and altered c-myc expression in prostate cancer cells after long-term androgen deprivation. *Cancer Res* 54: 1566-1573.
12. Dehm SM, Tindall DJ (2006) Ligand-independent androgen receptor activity is activation function-2-independent and resistant to antiandrogens in androgen refractory prostate cancer cells. *J Biol Chem* 281: 27882-27893.
13. Shi XB, Ma AH, Tepper CG, Xia L, Gregg JP, et al. (2004) Molecular alterations associated with LNCaP cell progression to androgen independence. *Prostate* 60: 257-271.
14. Jenster G (1999) The role of the androgen receptor in the development and progression of prostate cancer. *Semin Oncol* 26: 407-421.
15. Tararova ND, Narizhneva N, Krivokrisenko V, Gudkov AV, Gurova KV (2007) Prostate cancer cells tolerate a narrow range of androgen receptor expression and activity. *Prostate* 67: 1801-1815.
16. Kas K, Finger E, Grall F, Gu X, Akbarali Y, et al. (2000) ESE-3, a novel member of an epithelium-specific ets transcription factor subfamily, demonstrates different target gene specificity from ESE-1. *J Biol Chem* 275: 2986-2998.
17. Cangemi R, Mensah A, Albertini V, Jain A, Mello-Grand M, et al. (2008) Reduced expression and tumor suppressor function of the ETS transcription factor ESE-3 in prostate cancer. *Oncogene* 27: 2877-2885.
18. Park C, Lee I, Kang WK (2006) Influence of small interfering RNA corresponding to ets homologous factor on senescence-associated modulation of prostate carcinogenesis. *Mol Cancer Ther* 5: 3191-3196.
19. Kleinbaum LA, Duggan C, Ferreira E, Coffey GP, Buttice G, et al. (1999) Human chromosomal localization, tissue/tumor expression, and regulatory function of the ets family gene EHF. *Biochem Biophys Res Commun* 264: 119-126.

20. Jiang F, Wang Z (2004) Gadd45gamma is androgen-responsive and growth-inhibitory in prostate cancer cells. *Mol Cell Endocrinol* 213: 121-129.
21. Compagno D, Merle C, Morin A, Gilbert C, Mathieu JR, et al. (2007) SIRNA-directed in vivo silencing of androgen receptor inhibits the growth of castration-resistant prostate carcinomas. *PLoS ONE* 2: e1006.
22. Liao X, Tang S, Thrasher JB, Griebeling TL, Li B (2005) Small-interfering RNA-induced androgen receptor silencing leads to apoptotic cell death in prostate cancer. *Mol Cancer Ther* 4: 505-515.
23. Haag P, Bektic J, Bartsch G, Klocker H, Eder IE (2005) Androgen receptor down regulation by small interference RNA induces cell growth inhibition in androgen sensitive as well as in androgen independent prostate cancer cells. *J Steroid Biochem Mol Biol* 96: 251-258.
24. Cheng H, Snoek R, Ghaidi F, Cox ME, Rennie PS (2006) Short hairpin RNA knockdown of the androgen receptor attenuates ligand-independent activation and delays tumor progression. *Cancer Res* 66: 10613-10620.
25. Furutani T, Takeyama K, Koutoku H, Ito S, Taniguchi N, et al. (2005) A role of androgen receptor protein in cell growth of an androgen-independent prostate cancer cell line. *Biosci Biotechnol Biochem* 69: 2236-2239.
26. Snoek R, Cheng H, Margiotti K, Wafa LA, Wong CA, et al. (2009) In vivo knockdown of the androgen receptor results in growth inhibition and regression of well-established, castration-resistant prostate tumors. *Clin Cancer Res* 15: 39-47.
27. Veldscholte J, Ris-Stalpers C, Kuiper GG, Jenster G, Berrevoets C, et al. (1990) A mutation in the ligand binding domain of the androgen receptor of human LNCaP cells affects steroid binding characteristics and response to anti-androgens. *Biochem Biophys Res Commun* 173: 534-540.
28. Veldscholte J, Berrevoets CA, Ris-Stalpers C, Kuiper GG, Jenster G, et al. (1992) The androgen receptor in LNCaP cells contains a mutation in the ligand binding domain which affects steroid binding characteristics and response to antiandrogens. *J Steroid Biochem Mol Biol* 41: 665-669.
29. Brooke GN, Parker MG, Bevan CL (2008) Mechanisms of androgen receptor activation in advanced prostate cancer: differential co-activator recruitment and gene expression. *Oncogene* 27: 2941-2950.
30. Chmelar R, Buchanan G, Need EF, Tilley W, Greenberg NM (2007) Androgen receptor coregulators and their involvement in the development and progression of prostate cancer. *Int J Cancer* 120: 719-733.
31. Carascossa S, Gobinet J, Georget V, Lucas A, Badia E, et al. (2006) Receptor-interacting protein 140 is a repressor of the androgen receptor activity. *Mol Endocrinol* 20: 1506-1518.
32. Augereau P, Badia E, Balaguer P, Carascossa S, Castet A, et al. (2006) Negative regulation of hormone signaling by RIP140. *J Steroid Biochem Mol Biol* 102: 51-59.
33. Montgomery RB, Mostaghel EA, Vessella R, Hess DL, Kalhorn TF, et al. (2008) Maintenance of intratumoral androgens in metastatic prostate cancer: a mechanism for castration-resistant tumor growth. *Cancer Res* 68: 4447-4454.
34. Stanbrough M, Bubley GJ, Ross K, Golub TR, Rubin MA, et al. (2006) Increased expression of genes converting adrenal androgens to testosterone in androgen-independent prostate cancer. *Cancer Res* 66: 2815-2825.
35. Movilla N, Bustelo XR (1999) Biological and regulatory properties of Vav-3, a new member of the Vav family of oncoproteins. *Mol Cell Biol* 19: 7870-7885.
36. Zeng L, Sachdev P, Yan L, Chan JL, Trenkle T, et al. (2000) Vav3 mediates receptor protein tyrosine kinase signaling, regulates GTPase activity, modulates cell morphology, and induces cell transformation. *Mol Cell Biol* 20: 9212-9224.
37. Moores SL, Selfors LM, Fredericks J, Breit T, Fujikawa K, et al. (2000) Vav family proteins couple to diverse cell surface receptors. *Mol Cell Biol* 20: 6364-6373.
38. Dong Z, Liu Y, Lu S, Wang A, Lee K, et al. (2006) Vav3 oncogene is over-expressed and regulates cell growth and androgen receptor activity in human prostate cancer. *Mol Endocrinol* 20: 2315-2325.

39. Lyons LS, Rao S, Balkan W, Faysal J, Maiorino CA, et al. (2008) Ligand-independent activation of androgen receptors by Rho GTPase signaling in prostate cancer. *Mol Endocrinol* 22: 597-608.
40. Lyons LS, Burnstein KL (2006) Vav3, a Rho GTPase guanine nucleotide exchange factor, increases during progression to androgen independence in prostate cancer cells and potentiates androgen receptor transcriptional activity. *Mol Endocrinol* 20: 1061-1072.
41. Liu Y, Mo JQ, Hu Q, Boivin G, Levin L, et al. (2008) Targeted overexpression of vav3 oncogene in prostatic epithelium induces nonbacterial prostatitis and prostate cancer. *Cancer Res* 68: 6396-6406.
42. Trenkle T, McClelland M, Adlkofer K, Welsh J (2000) Major transcript variants of VAV3, a new member of the VAV family of guanine nucleotide exchange factors. *Gene* 245: 139-149.
43. Wallerand H, Robert G, Pasticier G, Ravaud A, Ballanger P, et al. (2009) The epithelial-mesenchymal transition-inducing factor TWIST is an attractive target in advanced and/or metastatic bladder and prostate cancers(). *Urol Oncol*.
44. Puisieux A, Valsesia-Wittmann S, Ansieau S (2006) A twist for survival and cancer progression. *Br J Cancer* 94: 13-17.
45. Maestro R, Dei Tos AP, Hamamori Y, Krasnokutsky S, Sartorelli V, et al. (1999) Twist is a potential oncogene that inhibits apoptosis. *Genes Dev* 13: 2207-2217.
46. Cheng GZ, Chan J, Wang Q, Zhang W, Sun CD, et al. (2007) Twist transcriptionally up-regulates AKT2 in breast cancer cells leading to increased migration, invasion, and resistance to paclitaxel. *Cancer Res* 67: 1979-1987.
47. Yang J, Mani SA, Donaher JL, Ramaswamy S, Itzykson RA, et al. (2004) Twist, a master regulator of morphogenesis, plays an essential role in tumor metastasis. *Cell* 117: 927-939.
48. uen HF, Chua CW, Chan YP, Wong YC, Wang X, et al. (2007) Significance of TWIST and E-cadherin expression in the metastatic progression of prostatic cancer. *Histopathology* 50: 648-658.
49. Kwok WK, Ling MT, Lee TW, Lau TC, Zhou C, et al. (2005) Up-regulation of TWIST in prostate cancer and its implication as a therapeutic target. *Cancer Res* 65: 5153-5162.
50. Lo HW, Hsu SC, Xia W, Cao X, Shih JY, et al. (2007) Epidermal growth factor receptor cooperates with signal transducer and activator of transcription 3 to induce epithelial-mesenchymal transition in cancer cells via up-regulation of TWIST gene expression. *Cancer Res* 67: 9066-9076.
51. Dupont J, Fernandez AM, Glackin CA, Helman L, LeRoith D (2001) Insulin-like growth factor 1 (IGF-1)-induced twist expression is involved in the anti-apoptotic effects of the IGF-1 receptor. *J Biol Chem* 276: 26699-26707.
52. Niehrs C (2006) Function and biological roles of the Dickkopf family of Wnt modulators. *Oncogene* 25: 7469-7481.
53. Hsieh SY, Hsieh PS, Chiu CT, Chen WY (2004) Dickkopf-3/REIC functions as a suppressor gene of tumor growth. *Oncogene* 23: 9183-9189.
54. Zenzmaier C, Untergasser G, Hermann M, Dirnhofer S, Sampson N, et al. (2008) Dysregulation of Dkk-3 expression in benign and malignant prostatic tissue. *Prostate* 68: 540-547.
55. Lodygin D, Epanchintsev A, Menssen A, Diebold J, Hermeking H (2005) Functional epigenomics identifies genes frequently silenced in prostate cancer. *Cancer Res* 65: 4218-4227.
56. Kawano Y, Kitaoka M, Hamada Y, Walker MM, Waxman J, et al. (2006) Regulation of prostate cell growth and morphogenesis by Dickkopf-3. *Oncogene* 25: 6528-6537.
57. Abarzua F, Sakaguchi M, Takaishi M, Nasu Y, Kurose K, et al. (2005) Adenovirus-mediated overexpression of REIC/Dkk-3 selectively induces apoptosis in human prostate cancer cells through activation of c-Jun-NH2-kinase. *Cancer Res* 65: 9617-9622.
58. Hendriksen PJ, Dits NF, Kokame K, Veldhoven A, van Weerden WM, et al. (2006) Evolution of the androgen receptor pathway during progression of prostate cancer. *Cancer Res* 66: 5012-5020.
59. Tomlins SA, Mehra R, Rhodes DR, Cao X, Wang L, et al. (2007) Integrative molecular concept modeling of prostate cancer progression. *Nat Genet* 39: 41-51.

60. Mendiratta P, Mostaghel E, Guinney J, Tewari AK, Porrello A, et al. (2009) Genomic Strategy for Targeting Therapy in Castration-Resistant Prostate Cancer. *J Clin Oncol*.
61. Sterbis JR, Gao C, Furusato B, Chen Y, Shaheduzzaman S, et al. (2008) Higher expression of the androgen-regulated gene PSA/HK3 mRNA in prostate cancer tissues predicts biochemical recurrence-free survival. *Clin Cancer Res* 14: 758-763.
62. Niu Y, Altuwaijri S, Lai KP, Wu CT, Ricke WA, et al. (2008) Androgen receptor is a tumor suppressor and proliferator in prostate cancer. *Proc Natl Acad Sci U S A* 105: 12182-12187.
63. Niu Y, Altuwaijri S, Yeh S, Lai KP, Yu S, et al. (2008) Targeting the stromal androgen receptor in primary prostate tumors at earlier stages. *Proc Natl Acad Sci U S A* 105: 12188-12193.
64. Berry PA, Maitland NJ, Collins AT (2008) Androgen receptor signalling in prostate: effects of stromal factors on normal and cancer stem cells. *Mol Cell Endocrinol* 288: 30-37.
65. Wang Y, Kreisberg JI, Ghosh PM (2007) Cross-talk between the androgen receptor and the phosphatidylinositol 3-kinase/Akt pathway in prostate cancer. *Curr Cancer Drug Targets* 7: 591-604.
66. Culig Z (2004) Androgen receptor cross-talk with cell signalling pathways. *Growth Factors* 22: 179-184.
67. Fizazi K (2007) The role of Src in prostate cancer. *Ann Oncol* 18: 1765-1773.
68. Asim M, Siddiqui IA, Hafeez BB, Baniahmad A, Mukhtar H (2008) Src kinase potentiates androgen receptor transactivation function and invasion of androgen-independent prostate cancer C4-2 cells. *Oncogene* 27: 3596-3604.
69. Tatarov O, Edwards J (2007) The role of src family kinases in prostate cancer. *Translational Oncogenomics* 2: 85-95.
70. Colomba A, Courilleau D, Ramel D, Billadeau DD, Espinos E, et al. (2008) Activation of Rac1 and the exchange factor Vav3 are involved in NPM-ALK signaling in anaplastic large cell lymphomas. *Oncogene* 27: 2728-2736.
71. Cheng GZ, Zhang WZ, Sun M, Wang Q, Coppola D, et al. (2008) Twist is transcriptionally induced by activation of STAT3 and mediates STAT3 oncogenic function. *J Biol Chem* 283: 14665-14673.
72. Han B, Mehra R, Dhanasekaran SM, Yu J, Menon A, et al. (2008) A fluorescence in situ hybridization screen for E26 transformation-specific aberrations: identification of DDX5-ETV4 fusion protein in prostate cancer. *Cancer Res* 68: 7629-7637.
73. Tomlins SA, Laxman B, Dhanasekaran SM, Helgeson BE, Cao X, et al. (2007) Distinct classes of chromosomal rearrangements create oncogenic ETS gene fusions in prostate cancer. *Nature* 448: 595-599.
74. Attard G, Clark J, Ambrosine L, Mills IG, Fisher G, et al. (2008) Heterogeneity and clinical significance of ETV1 translocations in human prostate cancer. *Br J Cancer* 99: 314-320.
75. Tomlins SA, Rhodes DR, Perner S, Dhanasekaran SM, Mehra R, et al. (2005) Recurrent fusion of TMPRSS2 and ETS transcription factor genes in prostate cancer. *Science* 310: 644-648.
76. Maher CA, Kumar-Sinha C, Cao X, Kalyana-Sundaram S, Han B, et al. (2009) Transcriptome sequencing to detect gene fusions in cancer. *Nature* 458: 97-101.
77. Tomlins SA, Laxman B, Varambally S, Cao X, Yu J, et al. (2008) Role of the TMPRSS2-ERG gene fusion in prostate cancer. *Neoplasia* 10: 177-188.
78. Kumar-Sinha C, Tomlins SA, Chinnaiyan AM (2008) Recurrent gene fusions in prostate cancer. *Nat Rev Cancer* 8: 497-511.
79. Carver BS, Tran J, Chen Z, Carracedo-Perez A, Alimonti A, et al. (2009) ETS rearrangements and prostate cancer initiation. *Nature* 457: E1; discussion E2-3.
80. King JC, Xu J, Wongvipat J, Hieronymus H, Carver BS, et al. (2009) Cooperativity of TMPRSS2-ERG with PI3-kinase pathway activation in prostate oncogenesis. *Nat Genet* 41: 524-526.
81. Carver BS, Tran J, Gopalan A, Chen Z, Shaikh S, et al. (2009) Aberrant ERG expression cooperates with loss of PTEN to promote cancer progression in the prostate. *Nat Genet* 41: 619-624.
82. Devlin HL, Mudryj M (2009) Progression of prostate cancer: multiple pathways to androgen independence. *Cancer Lett* 274: 177-186.

83. Hu R, Dunn TA, Wei S, Isharwal S, Veltri RW, et al. (2009) Ligand-independent androgen receptor variants derived from splicing of cryptic exons signify hormone-refractory prostate cancer. *Cancer Res* 69: 16-22.
84. Ceraline J, Cruchant MD, Erdmann E, Erbs P, Kurtz JE, et al. (2004) Constitutive activation of the androgen receptor by a point mutation in the hinge region: a new mechanism for androgen-independent growth in prostate cancer. *Int J Cancer* 108: 152-157.
85. Libertini SJ, Tepper CG, Rodriguez V, Asmuth DM, Kung HJ, et al. (2007) Evidence for calpain-mediated androgen receptor cleavage as a mechanism for androgen independence. *Cancer Res* 67: 9001-9005.
86. Frydenberg M, Stricker PD, Kaye KW (1997) Prostate cancer diagnosis and management. *Lancet* 349: 1681-1687.
87. Lilja H, Ulmert D, Vickers AJ (2008) Prostate-specific antigen and prostate cancer: prediction, detection and monitoring. *Nat Rev Cancer* 8: 268-278.
88. Schröder FH, Hugosson J, Roobol MJ, Tammela TL, Ciatto S, et al. (2009) Screening and prostate-cancer mortality in a randomized European study. *N Engl J Med* 360: 1320-1328.
89. Andriole GL, Grubb RL, 3rd, Buys SS, Chia D, Church TR, et al. (2009) Mortality results from a randomized prostate-cancer screening trial. *N Engl J Med* 360: 1310-1319.
90. Tran C, Ouk S, Clegg NJ, Chen Y, Watson PA, et al. (2009) Development of a Second-Generation Antiandrogen for Treatment of Advanced Prostate Cancer. *Science*.
91. Tunn U (2008) Can intermittent hormone therapy fulfil its promise? *Eur Urol Suppl* 7: 752-757.
92. Saad F (2009) Src as a therapeutic target in men with prostate cancer and bone metastases. *BJU Int* 103: 434-440.
93. Araujo J, Logothetis C (2009) Targeting Src signaling in metastatic bone disease. *Int J Cancer* 124: 1-6.
94. Horne WC, Sanjay A, Bruzzaniti A, Baron R (2005) The role(s) of Src kinase and Cbl proteins in the regulation of osteoclast differentiation and function. *Immunol Rev* 208: 106-125.
95. Wong KK (2009) Recent developments in anti-cancer agents targeting the Ras/Raf/MEK/ERK pathway. *Recent Pat Anticancer Drug Discov* 4: 28-35.
96. Chee KG, Longmate J, Quinn DI, Chatta G, Pinski J, et al. (2007) The AKT inhibitor perifosine in biochemically recurrent prostate cancer: a phase II California/Pittsburgh cancer consortium trial. *Clin Genitourin Cancer* 5: 433-437.
97. Pardanani A (2008) JAK2 inhibitor therapy in myeloproliferative disorders: rationale, preclinical studies and ongoing clinical trials. *Leukemia* 22: 23-30.
98. Lara PN, Jr., Longmate J, Evans CP, Quinn DI, Twardowski P, et al. (2009) A phase II trial of the Src-kinase inhibitor AZD0530 in patients with advanced castration-resistant prostate cancer: a California Cancer Consortium study. *Anticancer Drugs* 20: 179-184.
99. Curigliano G, De Braud F, Teresa Sandri M, Renne G, Zorzino L, et al. (2007) Gefitinib combined with endocrine manipulation in patients with hormone-refractory prostate cancer: quality of life and surrogate markers of activity. *Anticancer Drugs* 18: 949-954.

SUMMARY

SAMENVATTING

SUMMARY

Prostate cancer is the most diagnosed male cancer in the western society. In most of the cases it has a benevolent course and these patients rather die with the prostate tumor than from the disease. However, once the tumor has escaped the prostate and metastasized, no curative treatment is available and palliative hormonal-therapy is often offered. The aim of the present study was to address the following critical questions in this field of research: (i) How do we distinguish the benevolent tumors from those with an aggressive outcome? (ii) What is the role of the AR pathway in prostate cancer progression? (iii) What other survival and growth pathways are involved in hormone-refractory proliferation?

Basic and translational prostate cancer research relies on diverse model systems to investigate disease mechanisms, identify diagnostic/prognostic markers and test novel therapies. In **Chapter 2** we reviewed *in vivo* and *in vitro* models for human prostate cancer, with particular focus on the PC346 panel used throughout this study. Thanks to a unique combination of primary tumor origin, *wild-type* AR expression, PSA secretion and androgen-responsive growth, the PC346C cell line is a predilect model to replicate hormone-naïve prostate cancer. Three hormone-refractory sublines were derived *in vitro* from the androgen-responsive PC346C, upon long-term hormonal manipulations: PC346DCC (androgen ablation), PC346Flu1 and PC346Flu2 (supplemented with antiandrogen flutamide).

In **Chapter 3** we further characterized the AR status and hormone response of these castration-resistant sublines, compared to the parental PC346C cells. The PC346DCC subline was shown to express background levels of AR and PSA and was insensitive to hormonal stimulations, suggesting it may have bypassed the AR pathway. In turn, PC346Flu1 overexpressed a *wild-type* AR, being hypersensitive to and growth inhibited by R1881. Finally, the T877A AR mutation was identified in PC346Flu2. This mutation is known to promote proliferation in the presence of non-androgenic ligands, including the antiandrogen flutamide, and explains the stimulatory effect of both R1881 and hydroxyflutamide on PC346Flu2 cells. Herein, we showed that long-term hormonal manipulations selected for AR modifications that guide hormone-refractory growth.

The role of the AR pathway in prostate cancer progression was addressed in **Chapter 4**. To begin with, the AR-regulated gene signature of PC346 cell lines was established using expression microarray analysis. Consistent with the physiological role of the AR pathway in prostate development, maturation and function, the androgen-regulated genes identified in PC346 cells are involved in the processes of transcription regulation, intracellular signal transduction, differentiation and regulation of cell proliferation and cell death. Furthermore, R1881 also induced genes associated with the metabolism of proteins, carbohydrates and lipids that contribute to the production and secretion of prostatic fluid. Subsequently, this AR target signature was linked to previous prostate cancer microarray studies, to explore how the AR pathway is modulated during the disease development and progression. This approach showed a consistent attenuation of the AR pathway in late stage metastatic disease, which appeared to be selective for genes involved in cellular differentiation and maintenance of secretory function. These findings, together with the growth inhibitory effect of androgens on

PC3436Flu1, question the current over-simplistic view of the AR pathway as the mechanism of prostate cancer proliferation.

Besides the AR, alternative survival and growth pathways were investigated, by profiling differential gene expression between hormone-naive PC346C cells and derivative hormone-refractory sublines (**Chapter 5**). Deregulation of growth factor signaling was detected in PC346DCC, the subline believed to have bypassed AR pathway. In addition, the tumor suppressor DKK3, and the VAV3 and TWIST1 oncogenes were evaluated for their role in prostate cancer progression and as potential prognostic markers.

Finally, in **Chapter 6** we summarize the findings of this study, integrating with the current knowledge in the field, to propose a mechanistic model for prostate cancer progression and potential therapeutical strategies for hormone-refractory disease.

SAMENVATTING

Prostaatcancer is de meest voorkomende vorm van kanker bij mannen in de westerse samenleving. In de meeste gevallen is sprake van een gunstig ziekteverloop en overlijden deze patiënten niet als gevolg van de prostaattumor. Wanneer de tumor is uitgezaaid is er geen genezende behandeling mogelijk, en wordt palliatieve hormonale therapie vaak aangeboden. Het doel van de huidige studie is meer inzicht te krijgen in enkele voor dit onderzoeksgebied essentiële vraagstellingen: (i) Hoe identificeren we de tumoren met een gunstig verloop van tumoren met een agressief ziekteverloop? (ii) Wat is de rol van de androgeenreceptor (AR) cascade in de progressie van prostaatcancer? (iii) Welke andere overlevings- en groeicascades zijn betrokken bij hormoon-refractaire proliferatie?

Basaal en translationeel prostaatcancer onderzoek heeft verschillende modelsystemen nodig voor het bestuderen van de ziektemechanismen, het zoeken naar diagnostische en prognostische merkstoffen en de ontwikkeling van nieuwe behandelingen. In **Hoofdstuk 2** geven we een overzicht van *in vivo* en *in vitro* modellen voor humane prostaatcancer, met de focus op het PC346 panel gebruikt in onze studie. De PC346C cellijn is afkomstig van een tumor uit de prostaat, vertoont *wild-type* AR expressie en prostaat specifiek antigeen (PSA) secretie, en is afhankelijk van androgeen voor optimale groei. Dankzij deze unieke combinatie is PC346C een bijzonder geschikt model om de hormoon-gevoelige fase van prostaatcancer te vertegenwoordigen. Drie androgeen-onafhankelijke sublijnen zijn afgeleid van de androgeen-gevoelige PC346C cellen, na langdurige *in vitro* hormoonbehandelingen: PC346DCC (androgeen ablatie), PC346Flu1 and PC346Flu2 (aangevuld met het antiandrogeen flutamide).

In **Hoofdstuk 3** hebben we de status van de AR cascade en de hormoon-gevoeligheid van deze androgeen-onafhankelijke cellijnen gekarakteriseerd en vergeleken met de oorspronkelijke PC346C cellen. De drie gegenereerde PC346 sublijnen hebben allen een uniek fenotype. De PC346DCC brengt vrijwel geen AR of PSA meer tot expressie en groeit androgeen-onafhankelijk, een aanwijzing dat de AR cascade mogelijk is omzeild. Daarentegen, vertoont PC346Flu1 over-expressie van *wild-type* AR en is supergevoelig geworden voor androgenen. Ten slotte, werd de T877A AR mutatie in PC346Flu2 cellen aangetroffen. Deze gemuteerde AR wordt ook geactiveerd door antiandrogenen, zoals het antiandrogeen flutamide, en verklaart de groei stimulerende uitwerking van zowel R1881 als flutamide op PC346Flu2 cellen. Hierbij hebben we aangetoond dat langdurige hormonale behandelingen selecteerde voor AR afwijkingen die leiden tot androgeen-onafhankelijke groei.

De rol van de AR cascade in progressie van prostaatcancer wordt in **Hoofdstuk 4** beschreven. Om te beginnen, is het AR-gereguleerd genexpressie profiel van PC346 cellijnen vastgesteld door middel van de microarray technologie. De androgeen-gereguleerde genen geïdentificeerd in PC346 cellen weerspiegelen de fysiologische rol van de AR cascade in de ontwikkeling, rijping en functie van de prostaat. Het merendeel van deze genen is betrokken bij de processen van transcriptie regulatie, intracellulaire signaal transductie, differentiatie en regulering van celproliferatie en celdood. Bovendien, induceert R1881 ook genen betrokken bij het metabolisme van eiwitten, koolhydraten en vetten die bijdragen aan de productie en secretie van de prostaatvloeistof. Vervolgens, is deze AR-gereguleerde signatuur gekoppeld aan eerder

gepubliceerde prostaatkanker microarray studies, om na te gaan hoe de AR cascade wordt gemoduleerd tijdens de ontwikkeling en progressie van deze ziekte. Deze aanpak liet een consistente afname van de AR cascade activiteit zien bij gemetastaseerde ziekte. Deze afname leek selectief voor genen die betrokken zijn bij cellulaire differentiatie en het onderhoud van de secretiefunctie. Deze bevindingen, samen met het groeiremmende effect van androgenen op PC3436Flu1, trekken het huidige oversimplistische inzicht van de AR cascade als het mechanisme van prostaatkanker proliferatie in twijfel.

Behalve de AR, zijn alternatieve overlevings- en groeicascades onderzocht door de differentiële genexpressie tussen hormoon-naïeve PC346C cellen en hormoon-refractaire sublijnen te analyseren (**Hoofdstuk 5**). Deregulering van groeifactorcascades werd ontdekt in PC346DCC, de sublijn die de AR cascade omzeilde. Verder, zijn het tumorsuppressorgen DKK3 en het oncogenen VAV3 en TWIST1 beoordeeld op hun rol in de progressie van prostaatkanker en als potentiële prognostische merkstoffen.

Tenslotte, worden in **Hoofdstuk 6** de bevindingen van deze studie besproken en geïntegreerd in de huidige kennis op dit gebied. Hierbij, stellen we een mechanistisch model voor prostaatkanker progressie en potentiële therapeutische strategieën voor.

ACKNOWLEDGEMENTS

CURRICULUM VITAE

LIST OF PUBLICATIONS

ACKNOWLEDGEMENTS

It seems like such a long time ago that I first set my feet in this green, flat and rainy land called the Netherlands. My first impression was that it was warmer than I expected... not warm as in Portugal, of course, but where was all the snow and the people ice-skating in the canals? I must admit I was rather disappointed, but the people I came across during my internship in Utrecht and the liberal Dutch culture captivated me and prompted my return to the land of the tulips to start my PhD!

First of all, I would like to acknowledge my promotor Chris and co-promotor Guido. Thank you for believing in me and giving me the opportunity to get my PhD in this project. Guido, your enthusiasm for research is contagious! I learned a lot from our discussions and working with you was an enriching experience, which will guide me through my future career.

This thesis would not be here without the prostate cancer models developed by Wytse van Weerden. Thank you Wytse for introducing me to the PC346 panel and for the useful discussions when writing the articles and this thesis.

Further, I would like to thank all my colleagues in the AIO room: Leonie, Dennis, Karin, Gert-Jan, Peter, Richard, Marieke, Flip and Rogier. We had many constructive (and other less educational) exchanges of ideas! It may have not been the quietest room from the JN1, but was for sure the most fun! I will never forget the “appelflap eating meetings”!

To the colleagues from the Urology lab: Natasja, Wilma, Sigrun, Laura, Angelique, Joke, Eddy, Charlie, Delshad, Rajesh, Robert, Corrina, Denie and Suzanne. With you I learned a lot, worked a lot and laughed a lot! In particular, I would like to thank Natasja for teaching me the microarray procedures and for the TaqMan PCRs; Sigrun, for assistance with the PC346 cell line models; Corrina, Denie and Suzanne, for performing the mouse experiments.

Since my bitter-sweat experience with computers, I’m also very thankful to the bioinformatics guys, Antoine and Don, for their assistance with the software for the microarray analysis and for fixing the numerous crashes and meltdowns of my digital work-horse!

Furthermore, I would like to thank Jan Trapman and the colleagues from the department of Pathology. In particular, Karin, for the CGH array data and AR sequencing, and Marcel, for all the work on the AR transgenic mice project, which unfortunately had to be stopped.

Wilfred and Christel from the Erasmus Centre for Biomics I thank for providing the microarrays, equipment and technical support for the expression profiling.

Outside the lab, a huge network of family and friends has given me all the support and necessary distraction to keep my mental sanity through the difficult times! I would need another book to name you all personally, so I will focus on the ones that have been the closest to me in the latest years.

To start with, I want to thank those who first welcomed me in the Netherlands. Henry and Kiona, you were my first Dutch friends, introduced me to the Dutch cuisine, carnival and music! Thank you for being my safe haven when I missed my home and family!

Also many thanks to the Portuguese bunch, Carla, Sónia, Ana and respective (Dutch!) partners. I can't wait to share a table full of Portuguese delicacies in our next dinner!

Niels, when Tom first introduced you, I could never imagine we would become such good friends. You also gave a hand in the completion of my thesis as our personal computer helpdesk!

With Tom I also started a relationship with my new Dutch family: Corry, Ellis, Hannie, Hans, Gerda, Walter, Els, Ton, Jaqueline, Willem, Dennis, Eveline, Jaap, Rick and Jolanda. Thank you for taking me in the family and always making me feel so welcome. There are no words to explain how important this is for me here, so far from my own Portuguese family. Thank you! Special thanks to Corry for all the "oma dagen" with Ruben. Without your help it would be even more difficult to combine family with my work in Leiden and the writing of this thesis.

To my friends in Portugal: Marta, Manela, Isabel, Patrícia, Tiaguinho e Vanda, desculpem ter desleixado um pouco a nossa amizade, mas espero agora ter mais tempo para telefonar, trocar mails e combinar um cafézinho para por os cochichos em ordem! Obrigada pelo vosso apoio!

To my family in Portugal: um grande beijo para toda a minha familia, em especial às minhas priminhas Marta e Patrícia, que agora já estão grandes, mas que na minha memória ainda são as meninas de à 7 anos atrás...

Querida mãe, querido pai, queridos manos Nelson e Paulo, eu sei que não foi fácil deixar-me partir atrás dos meus sonhos. Foi longo e difícil o caminho percorrido para chegar onde estou hoje. Sou feliz e o que atingi hoje nunca teria sido possível sem o vosso apoio, carinho e palavras de coragem trocadas nas muitas horas que passámos ao telefone. Tão longe e tão perto... O amor não se agradece com palavras, por isso vos dedico este livro, o culminar do nosso sacrifício e o começo de uma vida nova... Amo-vos muito!

Finally, Tom and Ruben. Of all what I ever reached, you are my biggest achievement! My little Ruben, with you I rediscovered how to look at the world as if I see it all for the first time! I can't explain to you the meaning of this day but to you it will be the day when mama got a lot more time to play and read you stories! My dear Tom, where would I be without you? You brought my life into balance and now I have all that I ever wished for: my own family and a career. Thank you for all the support, care and patience of the last years. I have neglected you and Ruben, arriving late for dinner and spending weekends behind the computer. It is fair to say that this book came from my sweat and tears but also from yours. But after the storm, here comes the sun! I love you!

Rute Marques

CURRICULUM VITAE

Name: Rute Barbosa Marques

Date of birth: 5 January 1978

Place of birth: Espinho, Portugal

1990-1996: High School “Escola Secundaria Dr. Manuel Lorangeira”
Espinho, Portugal

1996-2001: Degree in Biochemistry - Applied Biochemistry
Faculty of Science, University of Porto, Portugal

2001: Internship in Department of Comparative Endocrinology
University of Utrecht, The Netherlands
Title: “Identification of domains responsible for receptor selectivity in the promiscuous luteinizing hormone of the African catfish: a structure function study”

2002-2006: PhD student in the Department of Urology
Erasmus Medical Center, Rotterdam, The Netherlands
Title: “The Role of the Androgen Receptor Pathway in Prostate Cancer Progression”

2007-present: Postdoc in the Department of Rheumatology
Leiden University Medical Center, Leiden, The Netherlands
Title: “Genetic susceptibility in rheumatoid arthritis: from genetic variant to biological function in autoimmunity”

LIST OF PUBLICATIONS

Marques RB, Dits NF, Erkens-Schulze S, van Ijcken WFJ, van Weerden WM, Jenster G. Gene expression profile of the androgen receptor pathway in androgen-responsive versus hormone-refractory PC346 prostate cancer cells. (submitted)

Marques RB, Dits NF, Erkens-Schulze S, van Weerden WM, Jenster G. Bypassing the androgen receptor pathway in PC346 hormone-refractory prostate cancer cells. (submitted)

Daha NA, Kurreeman FA, **Marques RB**, Stoeken-Rijsbergen G, Verduijn W, Huizinga TW, Toes RE. Confirmation of STAT4, IL2/IL21 and CTLA4 polymorphisms in rheumatoid arthritis. *Arthritis Rheum.* 2009. 60(5):1255-1260

Thabet MM, Huizinga TW, **Marques RB**, Stoeken-Rijsbergen G, Bakker AM, Kurreeman FA, White S, Toes RE, van der Helm-van Mil AH. The contribution of Fc gamma receptor IIIA gene 158V/F polymorphism and copy number variation to the risk of ACPA positive rheumatoid arthritis. *Ann Rheum Dis.* 19 Nov 2008. (in press)

Vischer HF, Granneman JC, Koelink PJ, **Marques RB**, Bogerd J. Identification of a luteinizing hormone-selective determinant in the exodomain of a follicle-stimulating hormone receptor. *Gen Comp Endocrinol.* 2008. 156(3):490-498

Kurreeman FA, Padyukov L, **Marques RB**, Schrodi SJ, Seddighzadeh M, Stoeken-Rijsbergen G, van der Helm-van Mil AH, Allaart CF, Verduyn W, Houwing-Duistermaat J, Alfredsson L, Begovich AB, Klareskog L, Huizinga TW, Toes RE. A candidate gene approach identifies the TRAF1/C5 region as a risk factor for rheumatoid arthritis. *PLoS Med.* 2007. 4(9):e278

Marques RB, van Weerden WM, Erkens-Schulze S, de Ridder CM, Bangma CH, Trapman J, Jenster G. The human PC346 xenograft and cell line panel: a model system for prostate cancer progression. *Eur Urol.* 2006. 49(2):245-257

Marques RB, Erkens-Schulze S, de Ridder CM, Hermans KG, Waltering K, Visakorpi T, Trapman J, Romijn JC, van Weerden WM, Jenster G. Androgen receptor modifications in prostate cancer cells upon long-term androgen ablation and antiandrogen treatment. *Int J Cancer.* 2005.117(2):221-229

Vischer HF, **Marques RB**, Granneman JC, Linskens MH, Schulz RW, Bogerd J. Receptor-selective determinants in catfish gonadotropin seat-belt loops. *Mol Cell Endocrinol.* 2004. 224(1-2):55-63

